CHALMERS
UNIVERSITY OF TECHNOLOGY

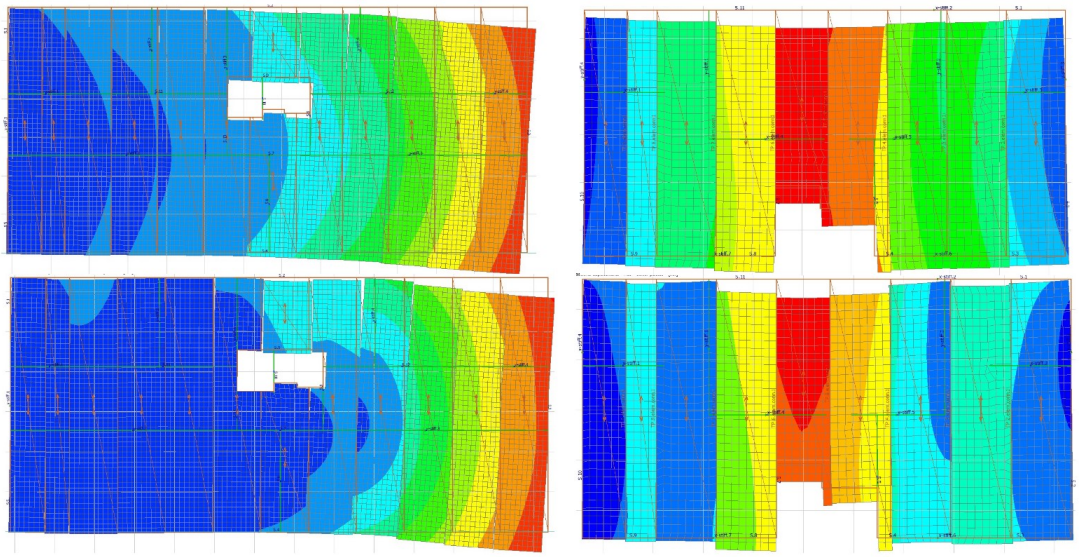

Diaphragm action in modern medium-rise timber/hybrid structures

A finite element parametric study of diaphragm response in modern timber/hybrid structures

Master's thesis in the Master's Programme Structural Engineering and Building Technology

Emil Thornadtsson

Department of Architecture and Civil Engineering
CHALMERS UNIVERSITY OF TECHNOLOGY
Master's thesis ACEX30
Gothenburg, Sweden 2023

Master's thesis ACEX30

Diaphragm action in modern medium-rise timber/hybrid buildings

A finite element parametric study examining diaphragm response under stiffness variations of the later load-resisting structures and the structural joints.

Emil Thornadtsson

CHALMERS
UNIVERSITY OF TECHNOLOGY

Department of Architecture and Civil Engineering
Division of Structural Engineering
Group for Light-Weight Structures
Chalmers University of Technology
Gothenburg, Sweden 2023

Diaphragm action in modern medium-rise timber/hybrid buildings
A parametric study of diaphragm response in modern timber buildings

Emil Thornadtsson

Examiner: Associate Professor Robert Jockwer, Department of Architecture and Civil Engineering

Department of Architecture and Civil Engineering
Division of Structural Engineering
Group for Light-Weight Structures
Chalmers University of Technology
SE-412 96 Gothenburg
Telephone +46 31 772 1000

Department of Architecture and Civil Engineering
Gothenburg, Sweden 2023

A parametric stiffness study of diaphragm response in modern timber buildings.
Finite element study of a variety of floor structures in-plane response with extensive stiffness variations of the lateral load-resisting structures.
EMIL THORNADTSSON
Department of Architecture and Civil Engineering
Chalmers University of Technology

Abstract

In the design of the structural system of a structure, the knowledge of how the diaphragm distributes the horizontal actions is of essential importance. A diaphragm can be classified as, rigid, semi-rigid, or flexural, where the classification is governed by the structural response of the diaphragm. Furthermore, a rigid diaphragm is characterized by a stiffness distribution of horizontal actions to the later load-resisting structures, a flexible diaphragm is characterized by the horizontal actions distributed by tributary area to the later load-resisting structures, and the semi-rigid classification is characterized by the diaphragm response is a combination of the rigid and flexural response.

The classification of the diaphragm, however, is not intuitive in timber structures as there is a variety of variables that influence the response of a timber diaphragm, e.g, of timber products, timber connections, etc., and the guidance provided by today's building regulations is insufficient. Furthermore, guidance in literature is often in unquantified terms such as - the diaphragm can be considered rigid if the diaphragm is a lot stiffer than the shear walls, and vice versa for a flexural response.

Hence, this project's aim is to determine stiffness relation boundaries for a variety of commonly used timber/TCC diaphragm types, where the influence of stiffness variations of the structural joints of adjoining element/panels are taken into respect, and the LLRS, that quantifies if the diaphragm response is flexible, semi-rigid or rigid. To obtain the aim was a finite element parametric study executed, examining the diaphragm response under extensive stiffness variations of the later load-resisting structures. The parametric study was performed in the software FEM-Design, by a coded C-sharp script that looped analysis with stiffness increment of the LLRS or the structural joint o a diaphragm.

Obtained results from the parametric study showed that the stiffness of structural joints in timber diaphragm has a great impact on the overall response and cannot be neglected in diaphragm analysis. Stiffness relations of the diaphragms and LLRS to classify the diaphragm response were obtained for the structural floor plan of Object 1, however, for the structural floor plan of Object 2 were no correlations of stiffness relations found. Finally, the obtained stiffness relations of the structural floor plan of Object 1 need further studies to be confirmed.

Keywords: diaphragm, diaphragm action, in-plane stiffness, parametric stiffness study, stabilization, horizontal load distribution.

Acknowledgements

This dissertation is the closure of a six-year academic journey spread over a total span of ten years. Throughout this journey, Sissy - my wife - has supported me and in the latter years, carried a great deal of the parenting of our boys Algot and Loui, and made this journey possible for me which I'm eternally grateful for.

A special thanks to my dear friend Johan Pyykkö who always took his time to discuss questions, that added substantial additions to this project with his knowledge in the field.

I would also like to show appreciation to Stiba AB for the opportunity of this Master's thesis.

Emil Thornadtsson, Gothenburg, June 2023

Contents

List of Figures

List of Tables

1
Introduction

The introduction chapter describes the project with a brief background presentation, followed by the aim of the project, where the purpose of the rapport is described. Furthermore, objectives state actions that have to be taken in order to reach the aim of the thesis, and a more in-depth explanation of steps to reach the aim of the study are given in the method chapter. Lastly stating the limitations of the project.

1.1 Background

Sweden has a long history of building timber structures, however, mainly single-family or terraced houses where the structures usually consist of an entrance floor and a second-storey timber joist floor. These types of structures are usually uncomplicated in regard to structural design. A reason that timber structures haven't been built to a larger extent in Sweden, is that previous Swedish building regulations limited timber houses to two storeys. Regulations were created in the late 19th century after a severe city fire in Sundsvall and were removed, over a hundred years later, in 1994. Due to the previous regulations, Sweden has a certain lack of experience in building medium-rise or higher timber structures. However, with the removed regulation in combination with a global extensive ambition for a more sustainable and renewable building, timber as a structural material is a topic of interest for multi-residential structures.

Moreover, using timber as structural material comes with great complexities, such as anisotropic material properties, thus different properties in different directions to the grain. Timber is, in general, light in comparison to its strength, which can cause problems with vibration, stability, acoustics, etc. Also, when building with elements of timber, it is, inevitable, that the structural joints must, carefully, be designed. Despite some complexities, with properly selected wood products, such as engineered wood products (EWP), timber as a structural material is adequate for mid-rise, or even high-rise timber/hybrid structures.

Diaphragm response can be divided into rigid, semi-rigid, and flexible, where the stiffness relation of the diaphragm and lateral load-resisting structures (LLRS) governs the classification. However, the classification is not intuitive for timber/hybrid structures and guidance is insufficient in the building regulations, i.e. Eurocodes, of today. Giving boundaries for the classification is complex in timber structures, and literature in the field often gives a rough description of the classification of

diaphragms; if the diaphragm lot stiffer than the stabilization units the response is rigid, and a flexible response is obtained if the LLRS is greatly stiffer than the diaphragm, and in an undefined, intermediate stiffness relation is the semi-rigid response. Furthermore, the in-plane stiffness of a timber diaphragm varies between different types of timber/hybrid structural floors. Therefore, if analyzing the horizontal load distributed to a stabilization unit in a structural floor plan with two different types of floor structures, reaction forces can vary in a non-negligible magnitude (Robert Kliger et al., 2022).

Therefore, a finite element (FE) parametric study of the diaphragm response is executed, where the diaphragm response of commonly used structural floor types, in up to mid-rise timber structures, is analyzed to study if boundaries of the diaphragm classification can be obtained. Furthermore, more detailed knowledge of the diaphragm action is valuable in many ways. Good early estimation in a project on what is doable or how to make it doable can save time and money for a client. It can also contribute to the development of a better structural design in timber structures which can include e.g. a more adaptable design, efficient design, optimized structure, etc.

1.2 Aim

This project's aim is to determine stiffness relation boundaries of a variety of commonly used timber/TCC diaphragm types, where the influence of stiffness variations of the structural joints of adjoining panels are taken into respect, and the LLRS that classify if the diaphragm response is rigid, semi-rigid or flexible. Also, the obtained results from the study are presented in figures with timber shear wall references to ease the assessment of, or to generalize, a diaphragm response in an early project phase.

1.3 Objectives

To achieve the aim, a numerical parametric study will be executed on two different structural floor plans, with four different types of structural floors(diaphragms), with an extensive stiffness variation of the LLRS and, when applicable, stiffness variations of the structural joints connecting elements. This will be carried out by programming a script in the code language C-Sharp (C#), that interacts with the API of the FE software FEM-Design, which runs analyses that perform an increment to the stiffness of choice in each loop of the analysis. The resulting horizontal reaction force and stiffness magnitude of the LLRS and/or the stiffness of the structural joints are collected from each loop of the analyses. The collected data are examined with the objective to find stiffness relations that set boundaries to the classification of rigid, semi-rigid, and flexible response of the diaphragm. Moreover, the diaphragm response is also set in relation to the stiffness of several timber walls, to examine if a diaphragm classification can be generalized against a certain type of timber wall.

1.4 Method

The project is initiated by a literature study, where the first phase of the literature study is to familiarize with the topic of stabilization and give emphasis to timber structures. However, the literature study is an ongoing process during the project that will be resumed during the project when needed in different phases.

After the initiation phase, applicable standards of the Eurocode standards are identified, with the Swedish national annex to the Eurocode, EKS12, to examine what is given about the subject in the regulations.

Thereafter, with the gained theory of the literature study, the necessary parameters to run the FE parametric study and to compare/verify the obtained FE results e.g. the shear stiffness of structural joints, shear stiffness of the different LLRS, stiffness distribution of horizontal actions, etc., are analytically obtained.

Subsequently, the numerical models are created in the software FEM-Design, and the FE models are verified by a convergence study and by comparing the FE results with analytically obtained results. Furthermore, Coding a script in C#, which interacts with the FEM-Design API module, enables to run the parametric study of extensive stiffness variations, by looping analysis with stiffness increment, of each model.

Lastly, obtained data from the parametric study are summarized, and results are studied and discussed with the aim to conclude limits/ranges of the stiffness relation of diaphragm and LLRS that facilitate the classification of the expected response of rigid, semi-rigid, or flexible diaphragm. If limits are concluded, recommendations are derived that can be used to ease the interpretation of the expected response by the diaphragm. Also, at the end of the thesis, the need for further studies to better in-depth knowledge in the field will be discussed.

1.5 Limitations

The main limitations of this study are stated in below bullet list:

- Structural floor types are analyzed with isolated analyzes of the in-plane resisting material, no effects of e.g, chords, joists, or other similar elements that may influence the stiffness are included.
- Only structural joints that connect floor elements/panels of the diaphragm, which may influence the diaphragm stiffness will be analyzed.
- Local effects of imperfections are ignored, e.g. buckling.
- Studies by numerical analyses are performed for two different structural floor plans, which are considered to give an insight into how the diaphragm and stabilization units interact. It will, however, not cover all cases of design situations, and the given guidance does not override the real design in practice.
- No global effects will be considered, such as uplifting of elements and/or tilting of the structure, etc.
- Diaphragms will be analyzed for the horizontal actions by wind and unintended inclination. This study does not consider analysis of how e.g. extensive transverse point load(s) or other forces may influence the diaphragm's overall response.

2

Theory

The following sections cover the needed theory in the matter of achieving the aim of the project. Such as timber products, structural systems, horizontal actions on a structure, and today's standards are briefly described,

2.1 Timber

Timber has been used as a building material since ancient times with the same purpose as now, protecting against unwanted weather conditions such as rain, wind, and cold. Already at this era were timber frame techniques used with logs as the primary structural element (Thelandersson, 2003), and timber buildings in Europe were built up to sizes of 5.5-7m wide and 20-45m in length. Moreover, Borgund church, located in Lærdal municipality Norway, is one of the oldest extant timber structures in Scandinavia, which is a region with long culture of timber houses mainly of the availability of wood, and was built about 900 years ago in the 12th century.

Despite that today's modern houses have considerable requirements e.g., thermal insulation, fire protection, and acoustics, are today's modern timber structures commonly built using the same base technique of frames. A timber skeleton of joists and studs, covered with fastened sheathing panels according to (Thelandersson, 2003). This technique, with adaptations for today's requirements, is adequate for a variety type of structures, such as single-family houses, multi-residential houses, and commercial buildings up to 5-6 storey. Furthermore, sheathing panels can be wood-based panels, such as particleboard, fiberboard, plywood, or oriented strand boards (OSB). Mentioned wood-based boards are so-called *engineered wood products* (EWP), which are further discussed in Chapter 2.1.1. In combination with wood-based panels are gypsum panels widely used, first and foremost for fire resistance but also for aesthetic cause, with gypsum boards providing a different structure on the surface, compared to wood-based panels. Sheathed studs and joists can be of multi-structural use, as it is feasible to transfer lateral and vertical loads, also known as shear walls and diaphragm respectively.

Latterly, new types of EWP products such as *cross laminated timber* (CLT) and *timber concrete composite* (TCC) floors, are used in modern timber/hybrid structures. These products are not only beneficial in terms of acoustics, fire, and some cases thermal insulation but also allow for larger normal forces and longer spans due

to the efficient use of material properties and thus allow for a more flexible design (Gustafsson, 2019). Moreover, it is feasible to build higher structures and longer spans with TCC and CLT, compared with framed structures in modern timber/hybrid buildings.

2.1.1 Engineered wood products - EWP

When producing sawn timber, achievable sizes, cross-section and length, and strength classes are governed by the size, diameter and straightness, and quality of the log. Spiral grain, knots, and compression wood, etc. are effects that may influence the strength properties of the sawn timber. Moreover, due to the log's circular shape and arrangement of annual rings, etc, is it inevitable to avoid residuals of the log when sawing structural timber. Also, the Swedish sawmill industry can typically manage logs with a length of 5.5 meters and a diameter of up to 40cm (Robert Kliger et al., 2022). Hence, sawn timber in Sweden can at best be 245 millimeters in height and 5.5 meters long.

However, to avoid extensive residuals, overcome size limitations, and more efficient use of a log, *engineered wood products* EWP, come to use. EWP are invented wood products that optimize the usage of timber (Blaß & Sandhaas, 2017), shown in figure 2.1 is a timeline of when most commonly used EWP's were invented. As seen in the figure is that glulam was invented already in the late 19th century and CLT (X-Lam in the figure) was invented about 100 years later in the year 2000, both products are sawn timber boards glued together. Moreover, several panel/board types also exist in the EWP family, such as plywood, particleboard, medium-density fibreboard (MDF), and OSB which were invented throughout the 20th century. Lastly, in this study, the applicable EWP products plywood, particleboard, OSB, I-joist, and CLT, are further analyzed.

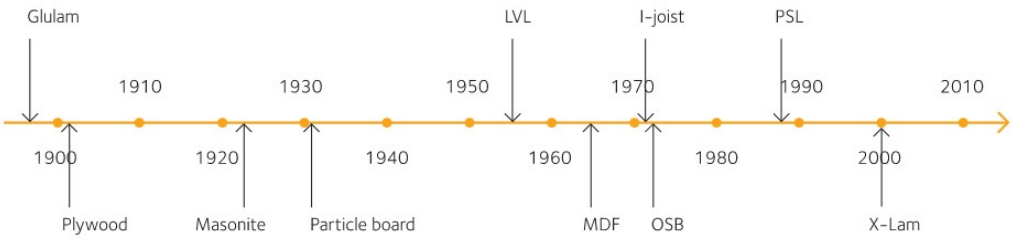

Figure 2.1: Timeline of EWP products. LVL - Laminated veneer lumber, PSL - Parallel-strand lumber. Copyright 2022 by Swedish Wood

2.1.1.1 Plywood

Plywood is a veneer-based panel EWP and is one of the very first invented EWPs, seen in Figure 2.1. Veneers are made by peeling rotating logs with a knife, which is schematically illustrated in figure 2.2.

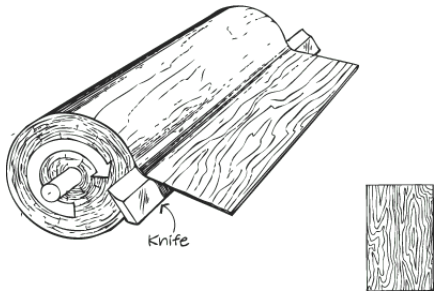

Figure 2.2: Schematic illustration of veneer peeling. Copyright 2014 by Architectural Woodwork Standards.

Plywood consists of at least three layers of veneers bonded with adhesives, where the adjoining layers are perpendicular to each other. The normal size for plywood panels with structural purposes is 1200x2400 mm and 900x2400 mm (in Sweden), with the outer layers of veneers grain direction in the long direction (Robert Kliger et al., 2022). Hence, plywood has uni-axial strength properties with the highest stiffness in its longitudinal direction. Thicker plywood boards normally have more than three layers of veneers, however, the number of layers is always kept odd to ensure that the outer veneers have the same grain direction, shown in Figure 2.3. Plywood is suitable as a sheathing material on framed studs and joists in regard to stabilization and diaphragm.

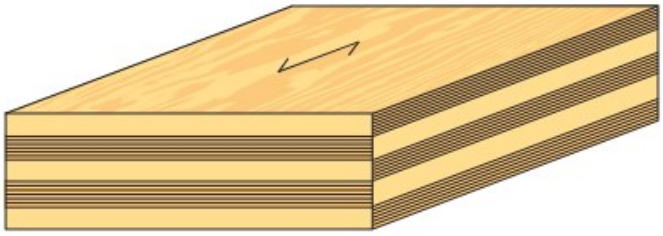

Figure 2.3: Plywood of five layers. Copyright 2022 by Swedish Wood.

2.1.1.2 Oriented strand board - OSB

OSB is a product made of strands with a size of approximately 0.8 mm in thickness, 13 mm in width, and a length of 100 mm. OSB is produced of strands mixed in adhesives, that bond under a process of heating and pressure. The outer strands are oriented parallel to the long axis of the board, and strands in the mid-region of the thickness are irregularly oriented and together produce an optimal product according to (Robert Kliger et al., 2022). Likewise, to plywood, the OSB's normal size is 1200x2400mm and 900x2400mm (in Sweden). The size of strands allows for the use of residuals from logs or smaller logs. OSB is often used as a sheathing material for framed walls.

2.1.1.3 Particleboard

Particleboards are made of timber chips in the size range of 10-15 mm long 2-2.5 mm wide and 0.2-0.5 mm thick. The chips are bonded together with adhesives un-

der pressure and heating (150-240°C) and a particle board is schematic illustrated in Figure 2.4. Particleboards are sensitive to moisture that influence strength and stiffness of the boards. Typically are particleboards used is in floor structures (Robert Kliger et al., 2022).

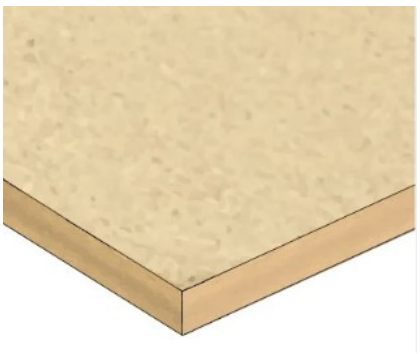

Figure 2.4: Particleboard. Copyright 2022 by Swedish Wood.

2.1.1.4 I-Joist

I-joist are glued composite timber/EWP members, often in the shapes of I-beams or box girders, shown in Figure 2.5. Typically for I-joists, differs the material of use between the web and flange, nonetheless, web and flange can be of the same material. Common material choices for the web are OSB, plywood, or particleboards and in regard to flanges finger-jointed sawn lumber, laminated veneer, or glulam (Blaß & Sandhaas, 2017). In addition mentions (Robert Kliger et al., 2022) the importance of quality controls for I-joist products e.g., verification of bonding (with adhesives) between web and flange and to ensure no extensive local defects in flanges timber members. However, this comes with difficulties to perform adequately and requires industrialized techniques. When designing I-joist, full composite action is assumed, thus linear strain and Hook's law applies. I-beams are most frequently used to floor and roof structures.

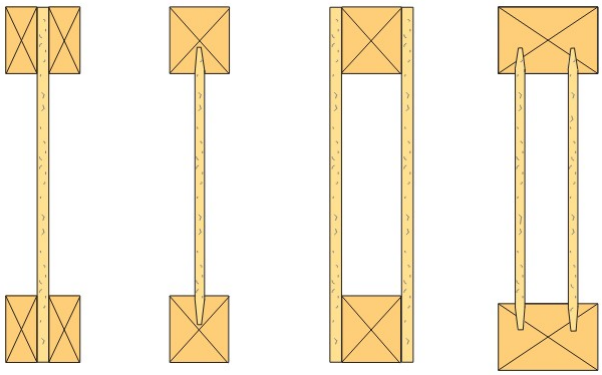

Figure 2.5: Common sections of I-Joist, where the first two from left hand side are types of I-beams and the latter two are I-box types. Copyright 2022 by Swedish Wood.

2.1.1.5 Cross laminated timber - CLT

Cross-laminated timber is one of the latest EWPs, and started to be used commercially about the year 2000, seen in Figure 2.1. CLT is made by layers of sawn timber boards that are bonded together with adhesives, where adjoining layers of grain direction are oriented in the perpendicular direction (Blaß & Sandhaas, 2017). Like plywood, is CLT built up with an odd number of layers of 3, illustrated in Figure 2.6, 5 and 7 (or even more), etc. However, more than seven layers are rarely produced, and instead, are producers laboring with varying thicknesses of the layers to improve the strength properties. The outer top and bottom layers fiber direction are oriented in the same direction to optimize stiffness and strength properties. The good strength and stiffness properties, especially in respect to its weight, of CLT, allows timber to contend as the main structural material of use for high-rise buildings which earlier weren't structurally doable for timber(Robert Kliger et al., 2022).

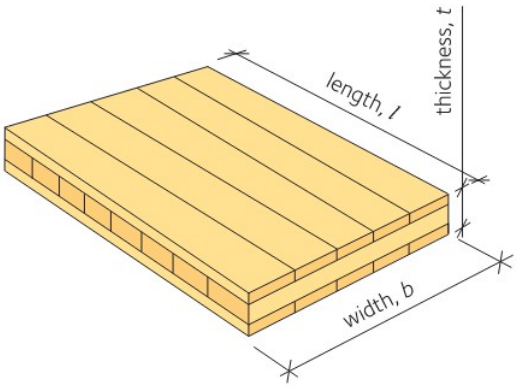

Figure 2.6: Three-layer CLT panel. Copyright 2022 by Swedish Wood.

2.1.2 Timber concrete composite - TCC

By combining materials, can the strength of each material be utilized to a great degree. In regard to TCC, is it favourable to use concrete in the compression zone and timber in the tension zone, to benefit the greatest of the materials. In consequence, a product that has high stiffness in relation to its self-weight is obtained (Blaß & Sandhaas, 2017). Figure 2.7, is a common TCC built-up illustrated, that comprises a thinner concrete slab on top of glulam beams with screws that act as shear connectors. As a result, with increased stiffness and added mass, compared with timber composite floor, TCC performs better in regard to deflection, vibration, and acoustics. Additionally, the use of concrete slabs instead of timber panels increases the in-plane stiffness of the diaphragm, which can be useful in regard to rigid diaphragm response.

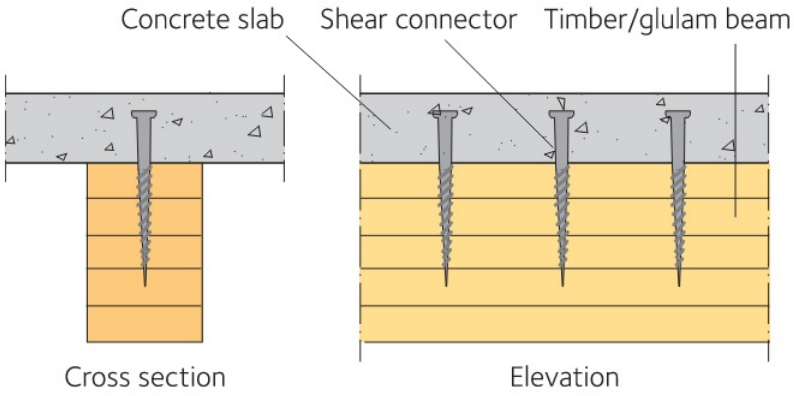

Figure 2.7: TCC section and elevation. Copyright 2022 by Swedish Wood.

2.2 Eurocode standards

Regulations for civil engineering in Sweden follow the European standards Eurocode. This section gives a brief introduction to the Eurocodes and briefly describes how to achieve a satisfied safety of design by using the so-called partial factory method.

2.2.1 Eurocodes built-up

Eurocode standards are built-up of ten main categories of EN 1990 Basis of structural design, EN 1991 Actions on structures, EN 1992 Design of concrete structures, EN 1993 Design of steel structures, EN 1994 Design of composite steel and concrete structures, EN 1995 Design of timber structures, EN 1996 Design of masonry structures, EN 1997 Geotechnical design and EN 1998 design of structures for earthquake resistance (About the EN Eurocodes, 2023). How they are linked to each other are shown in Figure 2.8.

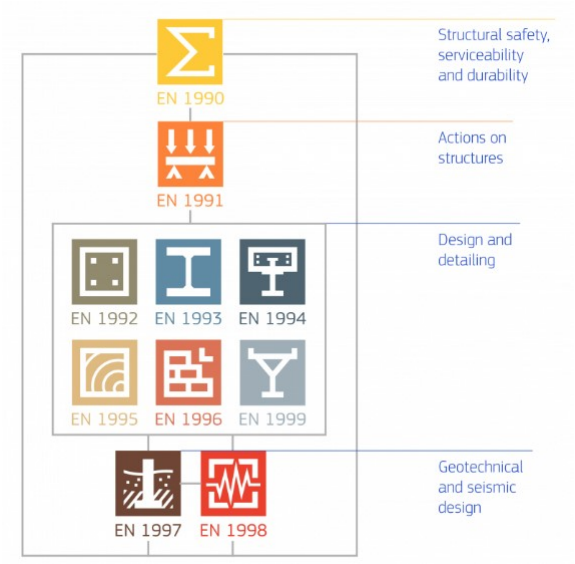

Figure 2.8: Eurocode built-up tree (About, 2023).
Copyright European comission

Moreover, for this study are the Eurocode standards EN 1990, EN 1991, EN 1992, and EN 1995 applicable. Relevant guidance of these standards will be further analyzed continuously in the project.

2.2.2 Satisfied safety of design

Eurocode EN-1990 (European Standard, 2010a) set the essential demands on a structure in the way of safety, serviceability, and durability. Also, it describes the basis of design and verification. Further, Eurocode EN-1990 state that a structure in its intended service time, shall be designed to have a satisfied reliability to resist all possible types of actions that may occur on the structure from erection to the end of design life. Moreover, proper reliability in design is fulfilled by Eurocode EN-1990 if a structure is designed by the use of the so-called partial factor method in combination with the recommended values of partial factors.

2.2.3 Design load effect and design resistance

Eurocode (European Standard, 2010a) distinguishes between what is to be designed in the ultimate limit state, for example, loss of equilibrium (EQU), structural failure (STR), fatigue failure (FAT), etc, where each type of design has its approach to obtaining the design effect. For this study, however, the design effect will be executed in accordance with STR (set B) limit state. When designing a structure accordingly with STR, sufficient safety of design is verified if the design resistance, R_d, is greater than design load effect, E_d, shown in Equation 2.1

$$E_d \leq R_d \tag{2.1}$$

Moreover, equations to obtain the design effect, E_d, is defined in (European Standard, 2010a) (c.h 6.5.3). Generally, the design effect are considering a combination

of actions in regard to a leading variable action and accompanying variable action. To obtain the design effect, E_d, in an STR analysis shall the less favourable of equations 6.10a and 6.10b in EN 1990 be used, which are defined in Equations 2.2 and 2.3. Where $\gamma_{i,j}$ is a partial safety factor of the load, G_i is the self-weight, P pre- or post-tensioned), Q_i is the variable load(s), and ψ is a partial factor for load combination

$$\begin{cases} \sum_{j\geq 1} \gamma_{G,j} G_{k,j} \text{"} + \text{"} \gamma_p P \text{"} + \text{"} \gamma_{Q,1} \psi_{0,1} Q_{k,1} \text{"} + \text{"} \sum_{j>1} \gamma_{Q,i} \psi_{0,i} Q_{k,i} & (2.2) \\ \sum_{j\geq 1} \zeta_j \gamma_{G,j} G_{k,j} \text{"} + \text{"} \gamma_p P \text{"} + \text{"} \gamma_{Q,1} Q_{k,1} \text{"} + \text{"} \sum_{j>1} \gamma_{Q,i} \psi_{0,i} Q_{k,i} & (2.3) \end{cases}$$

where:

" + "	to be combined with
$\sum$	the combined effect of
ζ	reduction factor for unfavourable permanent actions

However, Eurocode allows for national choice of equation 6.10a in regard to purely analyze permanent action. This option is adopted by the Swedish annex EKS12 (Boverket, 2022) and, hence, shall analyses with equation 6.10a be based on permanent actions only. Equation 2.2/6.10a and 2.3/6.10b with the Swedish adoption are summarized in EKS12 in table B-3:

Table 2.1: Load combination of STR design values of actions, (Boverket, 2022) table B-3

Persistent and transient d.s[1]	Permanent actions		Leading variable action	Accompanying variable actions
	Unfavourable	Favourable		
Eq. 6.10a	$\gamma_d 1.35 G_{kj,sup}$	$1.00 G_{kj.inf}$	-	-
	$\gamma_d 1.35 P_k$	$1.00 P_k$		
Eq. 6.10b	$\gamma_d 0.89\, 1.35 G_{kj,sup}$	$1.00 G_{kj.inf}$	Unfavourable: $\gamma_d 1.5 Q_{k,1}$ Favourable: 0	Unfavourable: $\gamma_d 1.5 \psi_{0,i} Q_{k,1}$ Favourable: 0
	$\gamma_d 1.35 P_k$	$1.00 P_k$		

[1] design situations.

2.2.4 Revised upcoming Eurocodes

Today's version of the Eurocode EN 1995 (European Standard, 2004), which is the standard that covers timber design, has insufficient guidance on how to classify a timber diaphragm, also is no guidance given on how to analytically obtain in-plane deformation of a timber diaphragm. However, the Eurocodes are ongoing a revision of EN 1995, unpublished at the time of this report and in a working draft version of the EN 1995 (European Standard, 2022), gives some guidance is given, i.e. how to obtain in-plane deformations of sheathed joist floor.

2.3 Structural stability

For a structure to be stable, it must be designed to safely transfer both vertical and horizontal actions to the foundation without overturning, sliding, or internal structural failure. Lateral stability and the transfer of horizontal loads to the foundation can be realized by different structural systems. This study analyses the diaphragm response on a local storey level of the structure. Therefore, global stability phenomena such as overturning and sliding, which undoubtedly must be controlled in regard to overall stability design, will not be further discussed in this study.

2.3.1 Basis of stabilization

To ensure the horizontal stability of a structure, the choice of structural system needs to be designed in such a way that internal forces are created when the structure deforms due to being subjected to horizontal action. At the time of action duration ends, the internal forces bring the structure back to its initial state. Furthermore, a structure that is vertically stable, see Figure 2.9 a), can still be horizontally unstable. When the structure is subjected to horizontal load, shown in the b) illustration, the structure lacks the ability to generate internal forces which leads to extensive deformation, shown in the c) illustration, that at a certain point will lead to structural failure. (Robert Kliger et al., 2022)

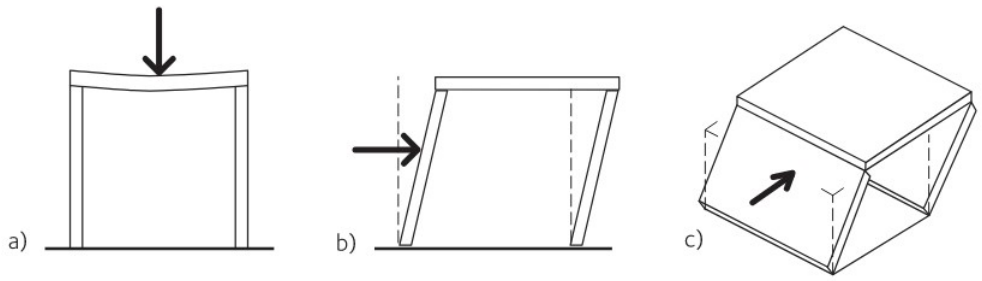

Figure 2.9: a) Vertical stable structure, b) and c) subjected to horizontal load, created extensive deformations. Copyright 2022 by Swedish Wood.

To provide horizontal stability in a structure, or local stability of a storey in a structure, mainly three options of bracing are plausible (Robert Kliger et al., 2022). Through diagonal bracing(alternatively with crossing ties), by shear walls, or rigidly connected frame which are illustrated in Figure 2.10. There are more alternatives to stabilizing a structure, however, the discussed methods in Figures 2.9 and 2.10 are the common ways to stabilize timber residential structures up to medium-rise.

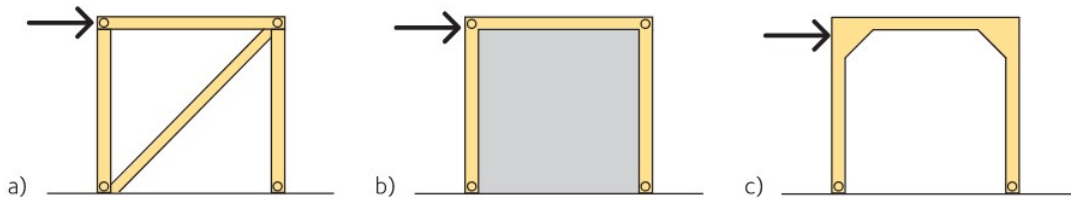

Figure 2.10: Alternatives of stabilization a) diagonal bracing b) b) shear wall and c) rigid frame connection. Copyright 2022 by Swedish Wood.

2.3.2 Structural system

Lateral actions usually impose over a surface e.g., wind actions impose on the facade, seismic action (mass distributed although), and unintended inclination are typically actions that impose directly on horizontal elements in a structure, for example, the structural floor, etc. Therefore, it isn't sufficient to only introduce lateral stabilization units in a structure to obtain horizontal stability, a structure must also comprise elements with the ability to distribute horizontal action to lateral stability units, this overall refers to a structural system and is schematically illustrated in Figure 2.11 (Robert Kliger et al., 2022).

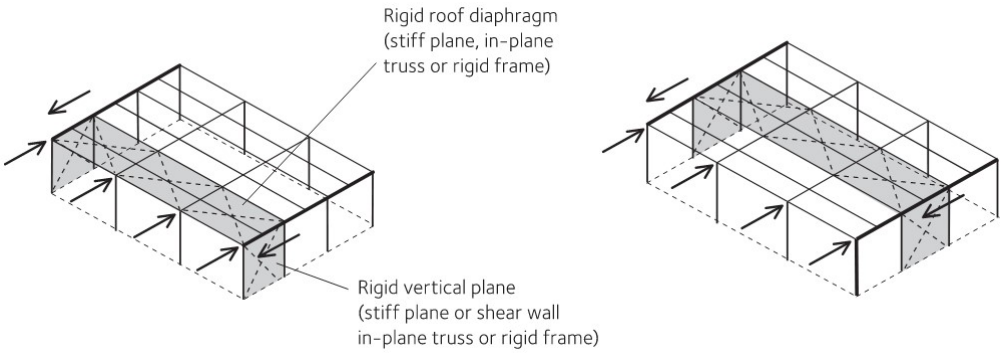

Figure 2.11: Wind action imposing on the long side of the structure. Whereas, the LHS figure illustrates a secondary framing that distributes lateral forces to lateral stabilization units on the gable. RHS, in addition to LHS, the secondary system can be in any place on the roof. Copyright 2022 by Swedish Wood.

Moreover, horizontal actions can act in any direction and thus, bracing must be adequately designed to resist the horizontal action in any direction of the structure. The basis in the design of stabilization of a structure diverges in whether rigid diaphragm action can be obtained or not (Blaß & Sandhaas, 2017). In the case of present rigid diaphragm action, a minimum of three lateral load-resisting structures that, at any point, do not intersect with each other or that all three are parallel aligned, shown in Figure 2.12 a), b). Structures that lack diaphragm action, however, require not less than four later-resisting structures where a maximum of two walls can intersect at the same point and no more than two walls can be parallel to each other, shown in Figure 2.12 c), d).

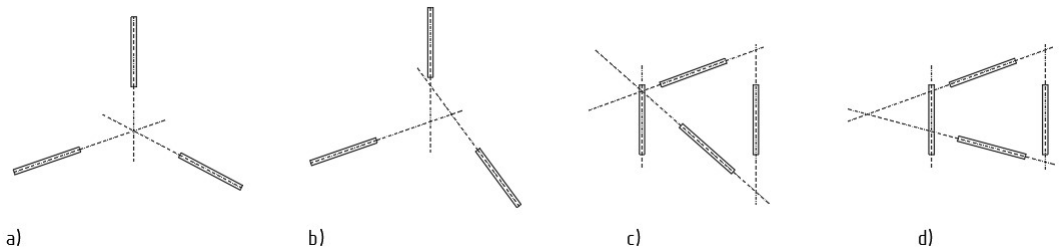

Figure 2.12: Minimum requirement to obtain stability with and without diaphragm a) Three walls, diaphragm present; not stable. b) Three walls, diaphragm present; stable. c) Four walls, diaphragm absence; not stable. d) Four walls, diaphragm absence; stable

2.3.3 Diaphragm

Diaphragm refers to an in-plane element, structural floors, and roofs, designed to transmit and distribute horizontal forces to lateral supporting units in a structure. Diaphragms are common in residential and commercial buildings, where span lengths are regularly not too long. Contrarily, factories, sports halls, and industrial are typically designed with elements that lack the ability of diaphragm action, eg., trusses, and rigid frames. Moreover, diaphragms are categorized into three categories; flexible, semi-rigid, and rigid (Robert Kliger et al., 2022). The categorization is governed by the stiffness relation of the diaphragm and the LLRS, and it is of essential importance to categorize the diaphragm properly as the structural behavior and horizontal load distribution to the LLRS can vary significantly between rigid, semi-rigid, and flexural diaphragms.

2.3.3.1 Rigid Diaphragm

A diaphragm is considered to be rigid if the stiffness of the diaphragm is significantly stiffer than the LLRS. Horizontal loads are then distributed to the LLRS in proportion to the stiffness of the LLRS, this is often referred to as the so-called diaphragm action, which is illustrated in Figures 2.13a and 2.13b.

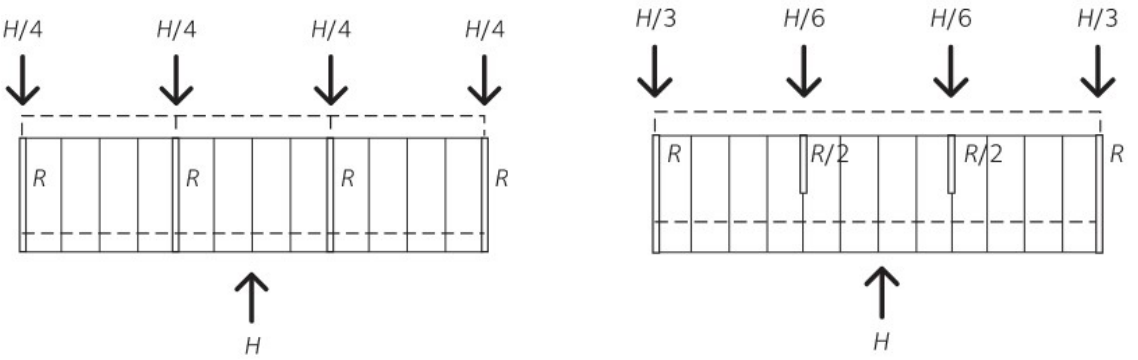

(a) Rigid diaphragm, constant stiffness in all shear walls

(b) Rigid diaphragm, vary stiffness in shear walls

Figure 2.13: Horizontal loads distribution with a rigid diaphragm. Copyright 2022 by Swedish Wood.

Additionally, previously discussed LLRS in Figures 2.13a and 2.13b are simplified arranged examples with the rotational center (R.C) coincide with the shear center (S.C). However, most often in real design cases, doesn't S.C and the R.C, which placement is governed by the stiffness arrangement of LLRS, coincide on the structural floor plan. The eccentricity between S.C and R.C multiplied with the magnitude of resultant horizontal force together create a torsional moment in the diaphragm, illustrated in Figure 2.14 (Robert Kliger et al., 2022). Thus, in addition to translation, must also the rotation, and how it influences the horizontal load distribution, be taken into account in the design of a rigid diaphragm.

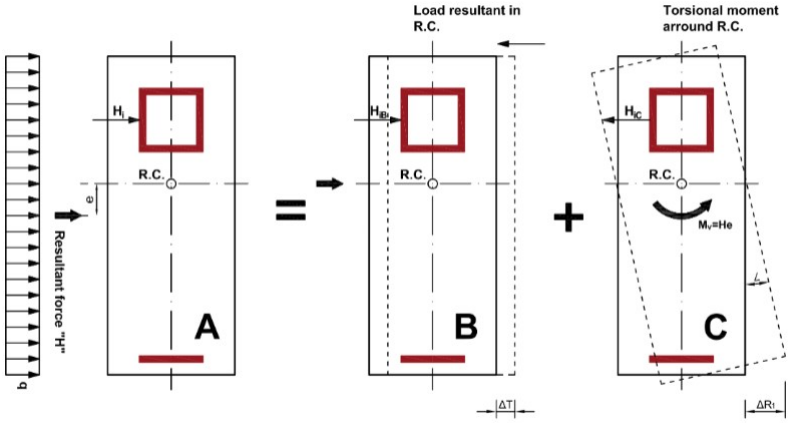

Figure 2.14: Structural behavior of a rigid diaphragm where rotational center R.C and shear center (resultant force H) doesn't coincide. (Ignasi Fernandez, Associate Professor at Structural Engineering Chalmers, September 2021)

2.3.3.2 Flexible Diaphragm

In a reverse situation to the rigid diaphragm with LLRS significantly (infinitely in analytical models) stiffer in relation to the floor/roof stiffness, the diaphragm is

considered as flexible. A flexible diaphragm lacks the so-called diaphragm action, consequently, the load distribution to the LLRS is rather straightforward as horizontal loads are distributed in accordance to tributary areas, which are illustrated in Figure 2.15a. Thus, simplified analytical models of flexible diaphragms assume that the diaphragm deforms while the LLRS remains undeformed, as a consequence, flexible diaphragms are not considered to have the ability to rotate(torsion) (Robert Kliger et al., 2022).

2.3.3.3 Semi-rigid Diaphragm

Previously discussed approaches of diaphragms, rigid or flexible, are often good enough approaches to describe the force distribution in a structure, however, in reality, there are no infinitely stiff floors/roofs or LLRS. There is an intermediate stage where the structural behavior is described by a continuous beam on a flexible support, which is known as a semi-rigid diaphragm. Thus, in a semi-rigid approach, it is assumed that both the diaphragm and LLRS are flexible and deflect, as illustrated in Figure 2.15b.
Moreover, there are no predefined stiffness relations that define a semi-rigid diaphragm (Robert Kliger et al., 2022). A semi-rigid diaphragm design is more comprehensive compared to the design of a rigid or flexible diaphragm and requires advanced computational models such as a finite element (FE) model. An advanced model is more time-consuming, and not always plausible in the manner of project conditions.

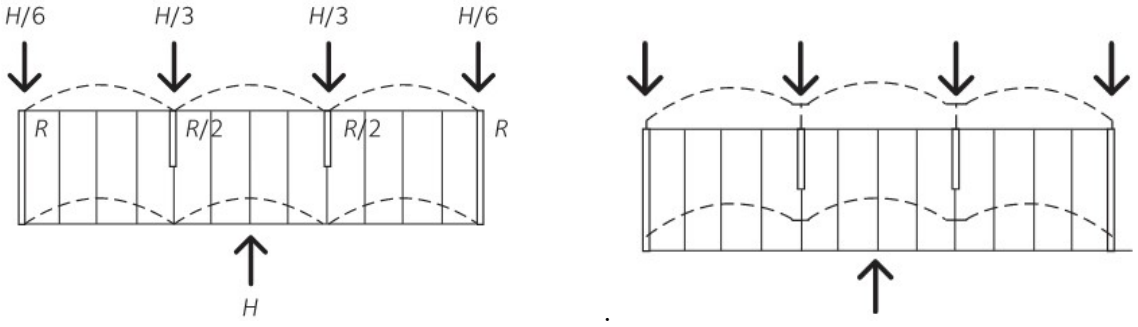

(a) Flexible diaphragm

(b) Semi-rigid diaphragm

Figure 2.15: Horizontal loads distribution with a flexural and semi-rigid diaphragm. Copyright 2022 by Swedish Wood.

2.3.3.4 Limited guidance in diaphragm classification

Eurocode EN 1995 (European Standard, 2004) provides a simplified method of diaphragm design in section 9.2.3.1. The simplification applies to designing a simply supported diaphragm as a deep beam. However, simply supported diaphragm is often not applicable in practise, and no guidance on how to obtain in-plane deformations or diaphragm stiffness is given.

(Robert Kliger et al., 2022) says that in the case of densely placed shear walls, the diaphragm can be considered rigid, and the opposite, a flexible diaphragm if shear walls are sparsely placed. Though, no further details are given by (Robert Kliger et al., 2022).

Moreover, (Blaß & Sandhaas, 2017) state a, somewhat, more refined detailing of how to determine if a diaphragm can be considered rigid or flexible, by saying that if the ratio between diaphragm width, b, and the span l is around one (1) between internal walls, the diaphragm can be considered to be rigid. Additionally, (Blaß & Sandhaas, 2017) also say that a safe approach to distributing the horizontal loads in a statically indeterminate system is, if the diaphragm is considered flexible, intermediate supports are continuous with a tributary area of $0.5 \cdot (l_1 + l_2)$, where l_1 and l_2 is the two adjacent span lengths, and the tributary area to the supports of the diaphragm is seen as simply supported, $0.5 \cdot l$ as tributary area.

2.3.4 Lateral load resisting structures

There are variants of lateral load-resisting structures (LLRS), such as rigid frames, trusses, diagonal or cross bracing, shear walls, etc. Whereas the latter two are the most frequently used in low to medium-rise residential timber structures. LLRS functions are to transmit horizontal actions obtained from the diaphragm to the foundations. A multi-story structure accumulates the horizontal action from each storey from the top to the bottom of the structure to the LLRS. Lateral stability in a multi-residential timber building with shear walls is illustrated in Figure 2.16.

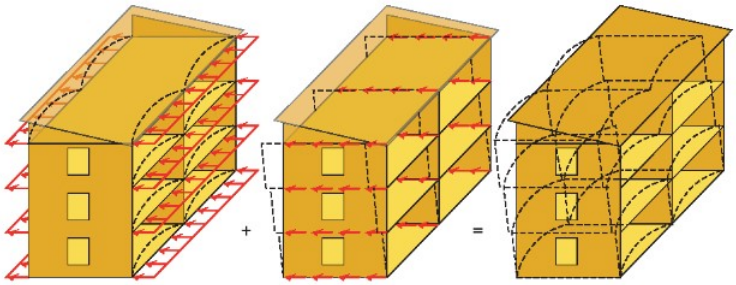

Figure 2.16: Multi-storey timber structure with shear walls.
Copyright 2022 by Swedish Wood.

Shear walls are structurally similar to diaphragms with in-plane actions and are also referred to by some as *vertical diaphragms*. In the field of timber construction are there mainly two types of shear walls, framed timber sheathed with a strength-graded wood-based panel, shown in Figure 2.17a, and solid timber CLT, shown in Figure 2.17b (Robert Kliger et al., 2022). In the design of shear walls, is the structural design model seen as cantilever beams with a point load at the top end of the beam, where the lower altitude, the floor, should be considered as a rigid connection of the cantilever and the upper floor is where the point load is addressed to the cantilever.

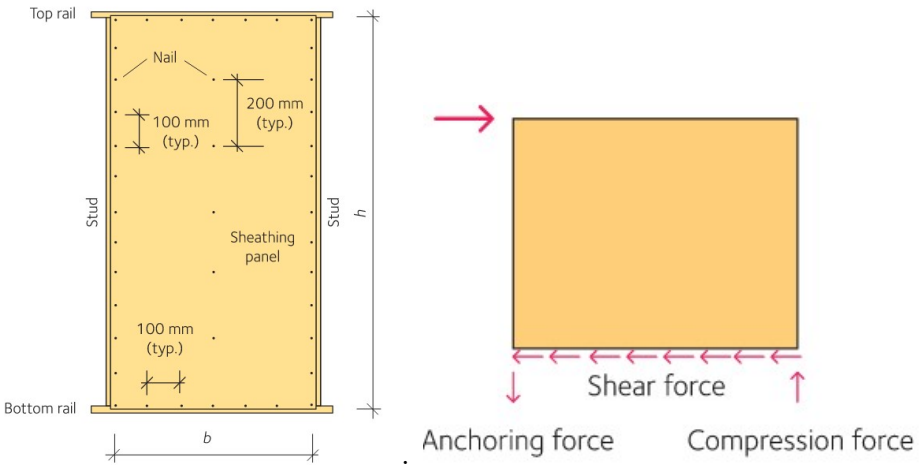

(a) Framed stud wall with wood-based sheathing

(b) Solid timber wall

Figure 2.17: Two types of shear walls in timber structures. Copyright 2022 by Swedish Wood.

The in-plane stiffness of the sheathing material is often relatively stiff with respect to in-plane deformations. However, nails or screws used to fasten the sheathing to the timber, illustrated in Figure 2.17a, and the overall in-plane stiffness of the shear wall is influenced by the sheathing-to-framing joints according to (Robert Kliger et al., 2022). The racking resistance of the sheathing-to-framing joint can be evaluated in both elastic or plastic models, whereas the latter is the most common approach. Lastly, (Robert Kliger et al., 2022) mention that other sheathing materials than wood-based can be used, such as gypsum or cement boards, however, plasticity models may not be applicable and more brittle failure in connections can be obtained.
Multi-story timber structures with sheathed framed timber systems have their limitations in 5-6 stories. In order to build higher multi-story structures must higher-strength timber products, such as solid CLT elements, be used (Thelandersson, 2003). The thickness of a CLT element is optional (to a certain degree) and thus, can the CLT elements be adopted to resist loads obtained in high-rise buildings, with the example of 20-story culture and hotel structure, *Sara Kulturhus*, built in the city Skellefteå.

2.4 Finite element method

The finite element method is a numerical solving method, where differential equations are approximately solved. The finite element method discretizes a region into finite elements, shown in Figure 2.18. Where the elements differential equation are solved at the element nodes, by the so-called approximation function, which can be of any polynomial order. With the finite element method, can analyses of larger regions where variables change in non-linear behavior over the region be solved by linear equations between the finite elements (Ottosen & Petersson, 1992). Moreover, the finite element collected together are often called *finite element mesh* and the size of the element mesh, combined with the polynomial of the approximation function governs how good your approximation is. However, if a too dense element mesh size is chosen or too high order of approximation polynomial, the finite element model becomes computationally heavy with the increased number of differential equations to solve.

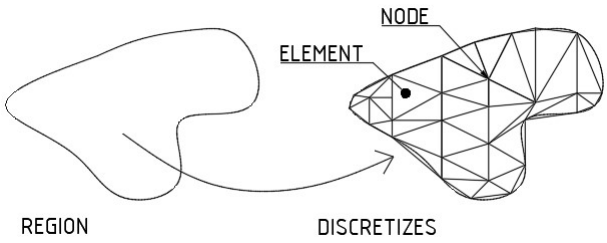

Figure 2.18: Region discretized into triangular finite elements.

2.5 Horizontal actions

A structure is not only subjected to vertical loads but also horizontal loads are exerted on a structure. Examples of horizontal loads are wind load, unintended inclination, and seismic actions. However, seismic actions are not relevant to the Swedish environment and are thus excluded from the Swedish design requirements (Boverket. 2022).

2.5.1 Wind load

A structure that is exerted to wind load, blocks the wind and thus, the wind's kinetic energy is converted to potential energy of pressure and suction (Schodek & Bechthold, 2014). Wind load acts on the façade as pressure or suction, structures however, always have seepage in their envelope that impose pressure on interior surfaces, illustrade in figure 2.19.

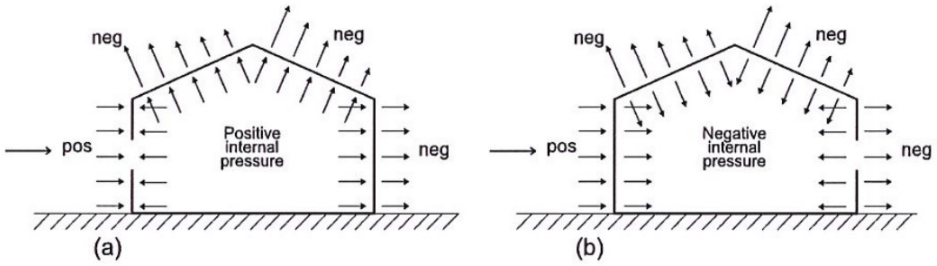

Figure 2.19: Pressure and on surfaces due to wind load. Copyright 2005 by Eurocode.

Wind action described in Eurocode 1991-1-4 (European Standard, 2010c) is the maximum influence of turbulent wind on a structure, simplified to pressure and forces, and the wind flows around a structure are illustrated in Figure 2.20.

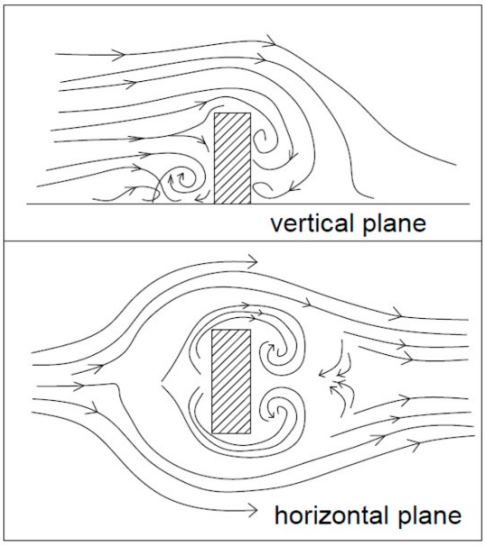

Figure 2.20: Wind flows around a structure. Copyright 1985 by Hosker.

2.5.2 Unintended inclination

In the design, vertical structural elements are assumed to be mounted geometrically vertically perfect, this assumption undoubtedly deviates from reality at times. Geometrical imperfections induce a horizontal load that must be accounted for in the design of a structure which is illustrated in Figure 2.21. However, eventual deviations of cross-sectional measures are included in the material partial coefficient. Eurocode EN 1992 (European Standard, 2010b) states that geometrical imperfections shall be taken into consideration for structural elements subjected to axial loads, and elements subjected to vertical loads. Additionally, Eurocode EN 1992 distinguishes the effect of inclination due to what kind of structural element or part that are designed, e.g., cantilevered column, pinned column, bracing system, diaphragm, and, roof diaphragm, also seen in Figure 2.21.

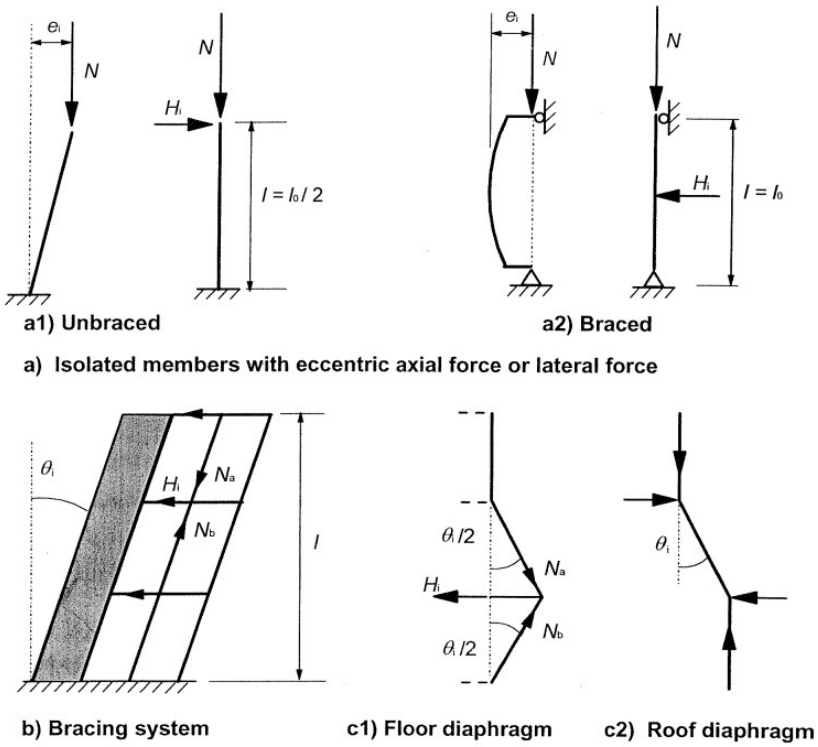

Figure 2.21: Wind flows around a structure. Copyright 2010 by Eurocode.

3
Methods

This chapter introduces the studied objects with associated structural floor plans, types of structural floor types, and, when applicable, structural joints in the floor types. Furthermore, analytical and numerical models are introduced and how the numerical model and parametric study are executed are presented.

3.1 Studied objects

The diaphragm load distribution is studied of two different structural floor plans, of *Object* 1 and *Object* 2. The main difference between the two analyzed structural floor plans, is that the rotational center on *Object* 2 deviates from the shear center to force a rotational moment in the diaphragm, on *Object* 1 is the rotational center close to coinciding with the shear center.

3.1.1 Object 1

Object 1 is a multi-residential building with 6 stories, built in the area of Gothenburg, Sweden. The structure is about $20m$ high, with outer geometries of approximately $20m$ in length and $10m$ wide, and comprises three apartments with a balcony to each apartment and a staircase.

3.1.1.1 Structural floor plan

The diaphragm is considered to be continuous over the whole structural floor plan, with shafts for the elevator and staircase, and the structural floor plan is shown in Figure 3.1. Furthermore, and the darker inclined hatch pattern indicates walls that contribute to the LLRS of the structure, and the lighter inclined hatch walls, are walls that purely provide vertical resistance. A coordinate system is introduced at the bottom left corner as an origin point for discussions and calculations.

Furthermore, the arrangement of shear walls in object one is oriented such way that the rotational center and shear center are closely oriented, and thus, a smaller eccentricity is obtained that induces a torsional moment if a rigid diaphragm is present. Balconies will not be considered in the diaphragm analysis.

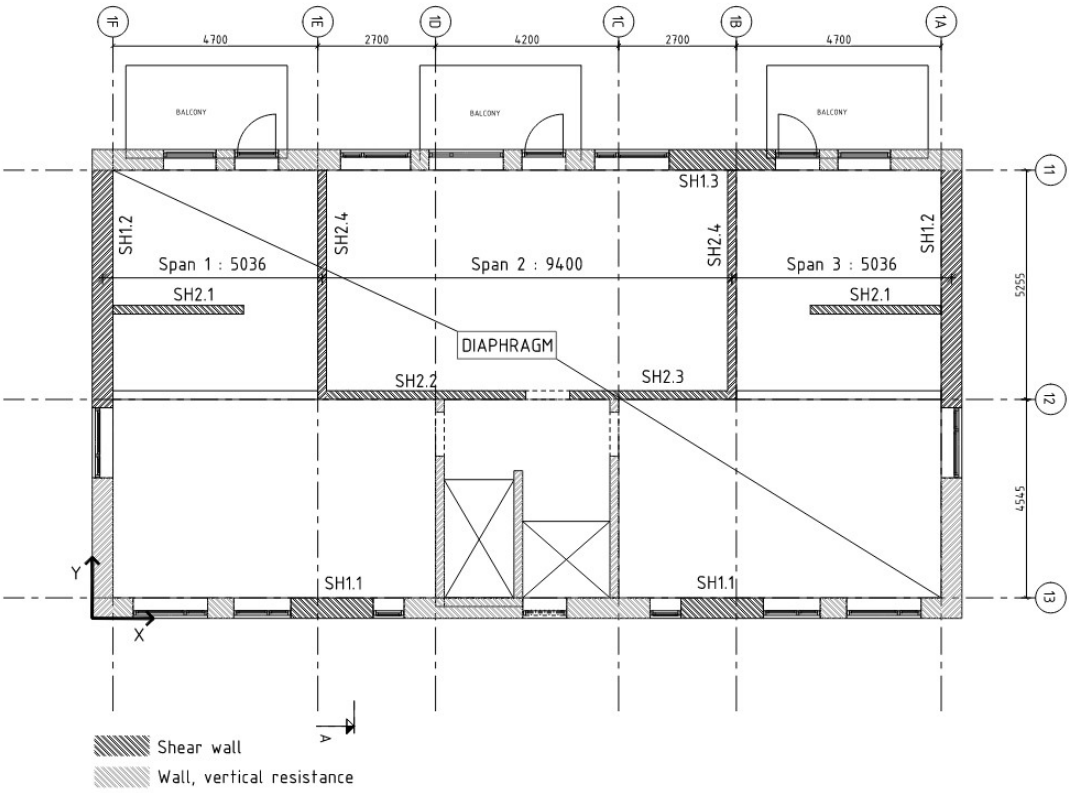

Figure 3.1: Structural plan of Object 1.

3.1.1.2 Shear walls

Shear walls are enumerated with SH, followed by two numbers I.J, where I is one (1) for exterior walls and two (2) for interior walls, furthermore, J is the numbering for unique lengths of the walls. Geometrical length and the stiffness direction of the walls are compiled in Table 3.1.

Table 3.1: Shear wall properties of Object 1

Wall number	Length $[m]$	Stiff. Direction
SH1.1	1.8	X
SH1.2	5.4	Y
SH1.3	2.4	X
SH2.1	3.0	X
SH2.2	4.6	X
SH2.3	3.6	X
SH2.4	5.2	Y

3.1.2 Object 2

Object 2 is a multi-residential building with 5 stories, in the area of Vänersborg, Sweden. The structure is about $17.5m$ high with outer geometries of approximately $27m$ in length and $13m$ wide and comprises four apartments and a staircase.

3.1.2.1 Structural floor plan

Similar to Object 1 is the diaphragm of Object 2 considered to be continuous over the structural floor plan, with shafts for the elevator and staircase, illustrated in Figure 3.2. The darker inclined hatch pattern indicates walls that contribute to the stabilization of the structure, and the lighter inclined hatch are walls that purely provide to vertical resistance, and a coordinate system is introduced at the bottom left corner to simplify further discussions and calculations.

In contrast to the structural floor plan of Object 1, the orientation of shear walls in Object 2 is such, that the shear center and rotational center deviate in the placement, the largest eccentricity is obtained in the X-direction and some eccentricity in the Y-direction. Additionally, the right part of the structure from SH2.7 to grid line 2 lacks lateral resistance in the Y-direction and thus, acts as a cantilever for horizontal actions. The cantilever span is a modification from the real structural floor plan.

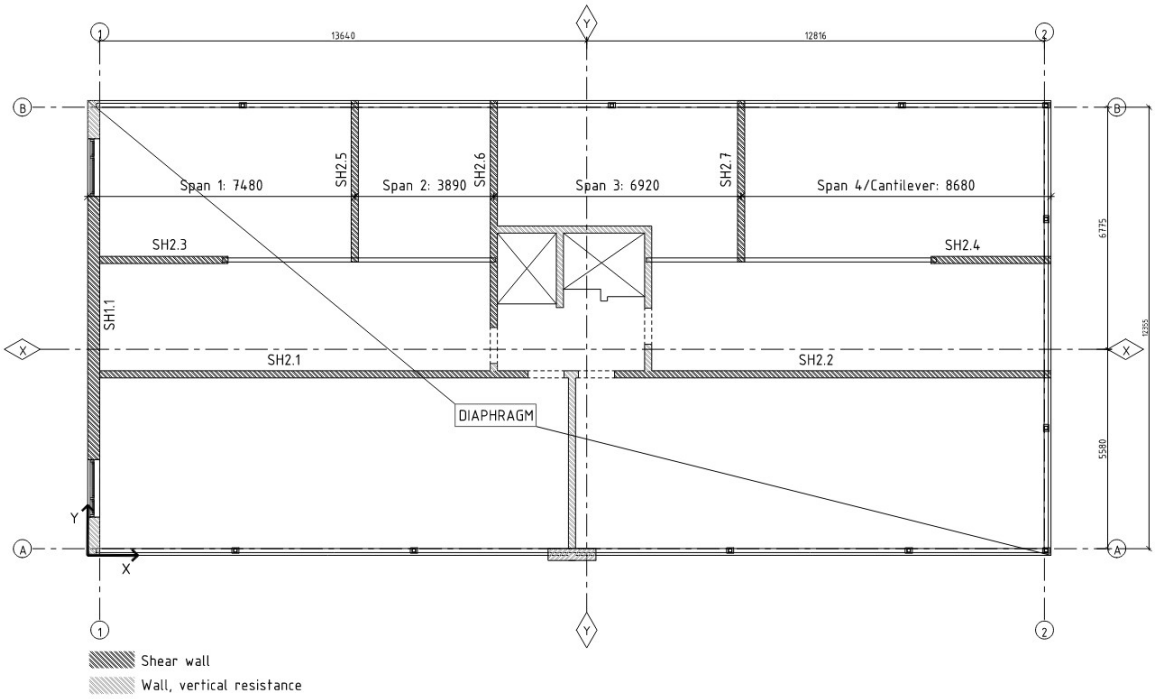

Figure 3.2: Structural plan of Object 2.

3.1.2.2 Shear walls

Shear walls on Object 2 are enumerated in the same analogy as for Object 1, see chapter 3.1.1.2, and geometrical length and the stiffness direction of the walls are compiled in Table 3.2.

Table 3.2: Shear wall properties of Object 2

Wall number	Length $[m]$	Stiff. Direction
SH1.1	7.3	Y
SH2.1	12.0	X
SH2.2	12.2	X
SH2.3	3.6	X
SH2.4	3.4	X
SH2.5	4.5	Y
SH2.6	6.4	Y
SH2.7	4.5	Y

3.1.3 Floor/roof diaphragms

Object 1 and Object 2 are analyzed with four different types of structural floors, and the structural floors are shown in Figure 3.3. Moreover, in the FE parametric study, materials that provide the in-plane stiffness are isolated analyzed.

- Type 1 - is a joist floor with particleboard sheathing that contributes to the in-plane stiffness, the particle board is assumed to be glue screwed to the joist, which is assumed to have full interaction between the boards.

- Type 2 - I-joist structural floor/roof solution, sheathed with plywood boards that provide the in-plane stiffness of the diaphragm. I-joist is commonly delivered in panels with a width of $2.4m$, hence, the panels of $2.4m$ are assumed to be glue screwed with full interaction, with structural joints that connect adjacent panels that can influence the diaphragm.

- Type 3 - CLT floor with a technical solution for installations and sound on top of it. The in-plane stiffness is purely provided by the CLT panels. The width of the CLT panels is producer dependent but is usually up to $2.5-3.0m$ wide. The influence of structural joints connecting CLT elements must also be considered to examine how they may influence the diaphragm response.

- Type 4 - Timber concrete composite floor, with the concrete slab on top of timber/glulam joists, with the concrete slab providing with the in-plane stiffness. This type of TCC is commonly produced in widths of $2.4m$ and longitudinal joints that are grouted on-site.

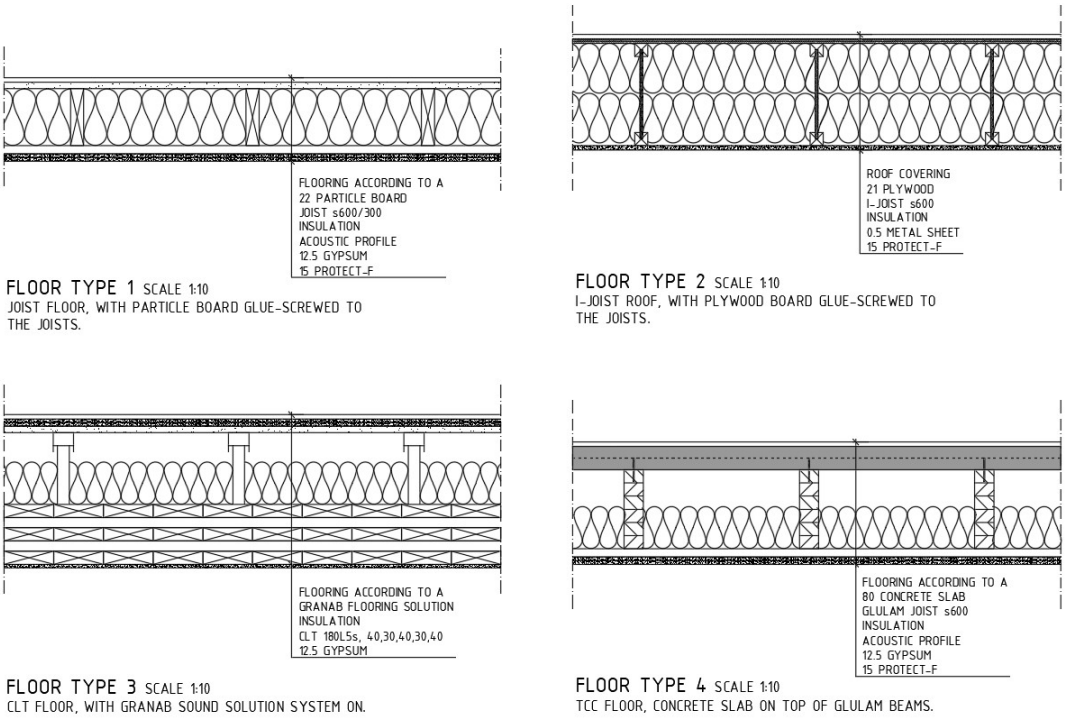

Figure 3.3: The Floor setups 1-4 for the study.

3.1.3.1 Structural joints in floor types

The floor types 2-4, see section 3.1.3, is mounted panel/element-wise, and thus, structural joints that connect adjacent elements with their in-plane stiffness to consider in the study. Floor type 2, panels of I-joist, with plywood boards on top, is commonly connected in accordance to Figure 3.4, which are two alternatives of screws connecting adjacent panels. the study will analyze connections of a screw diameter of $d = 4.0mm$ and with the spacing of s330, s220, s100, and infinitely stiff.

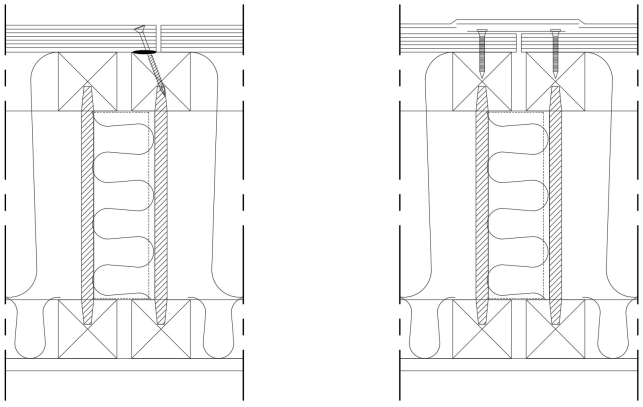

Figure 3.4: I-Joist longitudinal panel joint.LHS; smaller cantilever of the sheathing panel that is screwed to the adjacent I-joist. RHS; steel plate on top of the sheathing material that is screwed to both adjacent I-joist panels.

Furthermore, the CLT floor, floor type 3, are joints usually design to transmit shear force in screw connections of lap joints or butt joints shown in Figure 3.5. Although, alternative b) is widely used, and the structural joint of use in this study, as it can transmit vertical shear forces between the elements and thus prevent panels from unevenly deforming and create thresholds between the elements that might appear with joint type a). The analysis examines connections with a screw diameter of $d = 6.5mm$ and with the spacing of s350,s250, s100, and infinitely stiff.

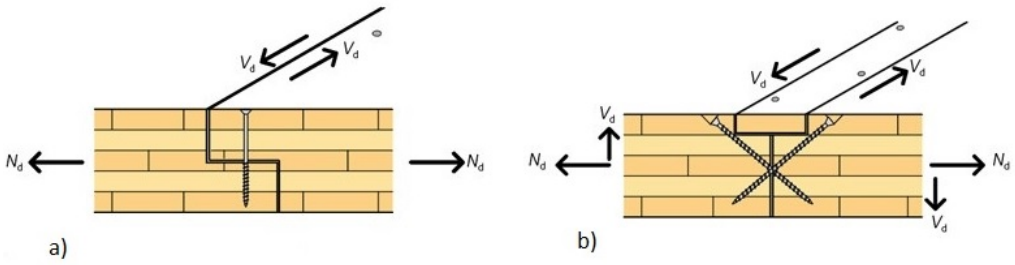

Figure 3.5: CLT joints. a) so-called lap joint with vertical screws. b) cross-screwed butt joint. Copyright 2019 by Swedish Wood.

Lastly, longitudinal structural joints connecting adjacent TCC elements, floor type 4, transmitting horizontal loads through grouted joints and with mechanical fastening. The joints are pre-engineered such that it eases the grouting, see Figure 3.6a, and an overview of the connection is shown in Figure 3.6b. The TCC diaphragms are analyzed with the stiffness of structural joints set to infinity and to analytical values obtained in the study.

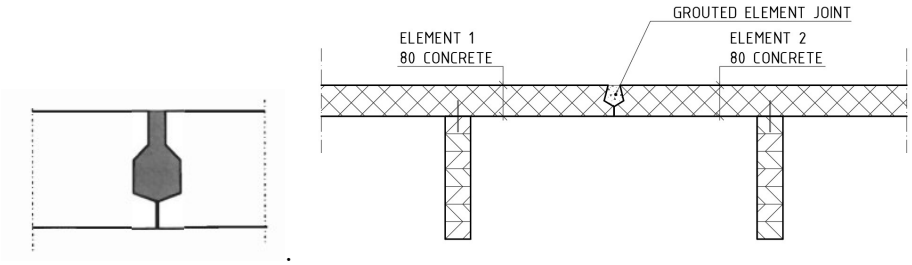

(a) Grouted connection in-zoomed. **(b)** Solid timber wall

Figure 3.6: Grouted connection between two adjacent concrete slabs.

3.1.4 Shear wall references

Shear walls shown in Figure 3.7 are used as stiffness references in the study. Stiffness reference lines are added to the plotted graphs obtained by the finite element parametric study, to examine if a geometrical correlation can be observed between the diaphragms and the reference shear walls. Shear wall Type 1 (with or without

45mm installation gap) and Type 2 are sheathed external and internal stud walls, and Type 3 is CLT wall elements that are insulated if used as external walls.

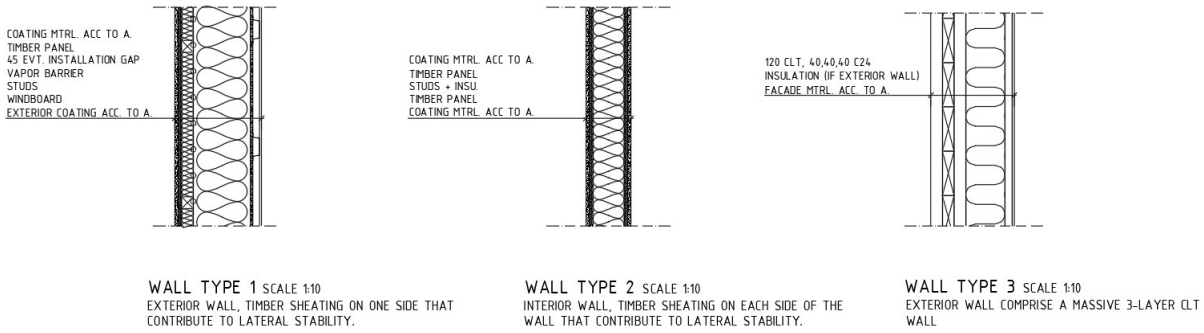

Figure 3.7: Reference shear wall type.

3.1.5 Storey height

In order to obtain the acting wind load per meter acting on the diaphragm must the storey height be known. Figure 3.8 below, is a part of section A for *Object* 1 (location on floor plan seen in Figure 3.1), that shows the tributary storey height of $2.9m$. For simplicity in the study, the same storey height of $2.9m$ is to be used for *Object* 2 as for *Object* 1.

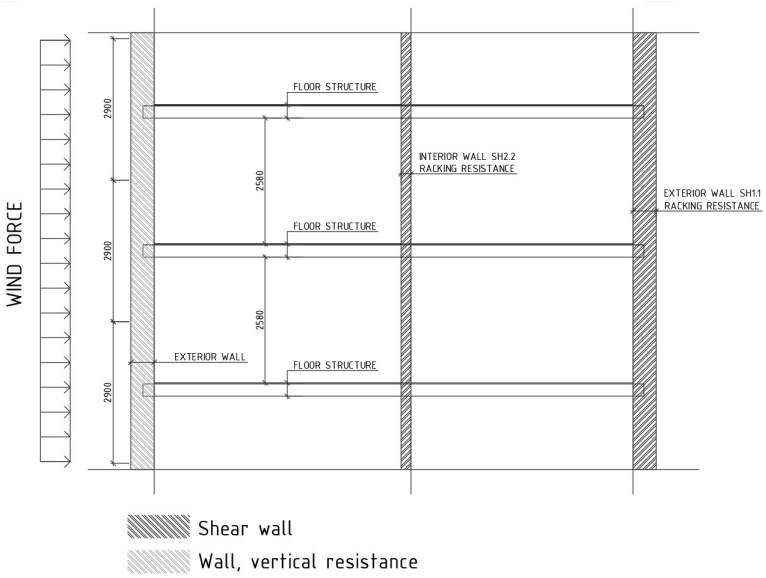

Figure 3.8: A part of the section A of *Object* 1

3.2 Load effects

In the design of a diaphragm are the horizontal actions from wind load and unintended inclination considered. This section guides on how to obtain the characteristic load for each action in accordance with Eurocode.

3.2.1 Wind load

Eurocode 1991-1-4 (European Standard, 2010c) guidance on how to calculate the wind load acting on a structure, and starts with how to obtain the peak velocity pressure, q_p, which is presented in chapter 4.5 in Eurocode 1991-1-4. However, the Swedish annex, EKS 12, makes a national choice in how to obtain the peak velocity pressure, Equation 3.1, and is derived in this chapter starting with exposure factor, $c_e(z)$ in Equation and 3.2:

$$q_p(z) = c_e(z) \cdot q_b \, [kN/m^2] \tag{3.1}$$

$$c_e(z) = \left[k_r \cdot ln\left(\frac{z}{z_0}\right)\right]^2 \cdot \left[1 + \frac{7}{ln\left(\frac{z}{z_0}\right)}\right] \tag{3.2}$$

where:

k_r	terrain factor depending on the roughness length z_0.
z	height of the building.
z_0	roughness length, which depends on the terrain category, see table 3.3.
q_b	basic velocity pressure, derived in equation 3.4
$c_e(z)$	exposure factor

The peak factor, k_p can be set to 3.0 in the design of structures where the dynamics effects of the structure can be neglected, which is suitable for this study, and in-depth analysis of k_p applies only to tall and slender structures. The terrain factor, k_r, depends on the surroundings of the structure and is calculated according to the Equation 3.3:

$$k_r = 0.19 \cdot \left(\frac{z_0}{z_{0,||}}\right)^{0.07} \tag{3.3}$$

where:

$z_{0,\|\|}$	are set to $0.05m$(terrain type II).
z_0	depends on the surrounding terrain in accordance to table 3.3.$[m]$

Table 3.3: Terrain categories and terrain parameters from Eurocode (European Standard, 2010c

Terrain category		z_0 m	z_{min} m
0	Sea or coastal area exposed to the open sea	0.003	1
I	Lakes or flat and horizontal area with negligible vegetation and without obstacles	0.01	1
II	Area with low vegetation such as grass and isolated obstacles (trees, buildings) with separations of at least 20 obstacle heights	0.05	2
III	Area with regular cover of vegetation or buildings or with isolated obstacles with separations of maximum 20 obstacle heights (such as villages, suburban terrain, permanent forest)	0.3	5
IV	Area in which at least 15 % of the surface is covered with buildings and their average height exceeds 15 m	1.0	10
NOTE:	The terrain categories are illustrated in A.1.		

Furthermore, the basic velocity pressure, q_b, is derived in Equation 3.4:

$$q_b = \frac{1}{2} \cdot \rho \cdot v_b^2 \tag{3.4}$$

where:

ρ is the air density, recommended value $1.25 kg/m^3$.
v_b basic wind velocity. m/s

Swedish maps providing the country's basic wind velocity, v_b, is given in the national annex, EKS12 in figure C-4; the basic wind velocity varies between 21-26 m/s in Sweden.
Eurocode continuous with how to obtain the external wind load acting on a structure, presented in chapter 5 of Eurocode 1991-1-4, and state the following Equation 3.5:

$$F_{w,e} = c_s c_d \cdot \sum_{surfaces} w_e \cdot A_{ref} \tag{3.5}$$

where:

$c_s c_d$ is a structural factor, set to 1.0 for analysed structures
w_e external pressure on a surface
A_{ref} reference surface area.

The external pressure is obtained according to Equation 3.6:

$$w_e = q_p(z) \cdot c_{pe} \tag{3.6}$$

where:

$q_p(z)$ is the peak velocity pressure, derived in Equation 3.1.
c_{pe} the external pressure coefficient.

Moreover, Eurocode state that the windward and leeward zones are denoted as zone D and zone E respectively.

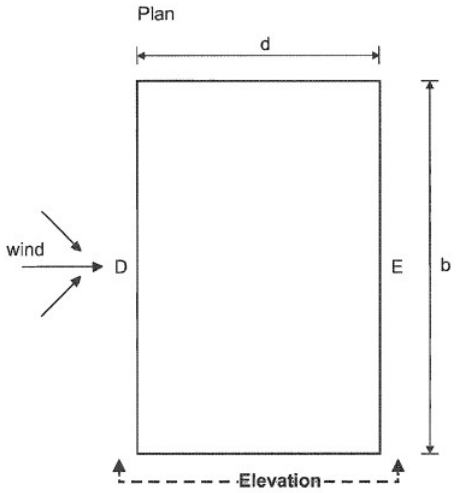

Figure 3.9: Zones for pressure coefficients c_{pe}. Copyright Eurocode 2010

Table 3.4 states the external pressure coefficient, c_{pe} for each zone in respect to the ratio of the height of the building, h, and cross sides length, d. For structures with a geometry ratio in intermediate ranges to the presented values in the table are interpolation allowed and, finally, coefficient $c_{pe,10}$ shall be used in the design of a diaphragm ($c_{pe,1}$ is for local effects in facade and roofs)

Table 3.4: Values of c_{pe} given in Eurocode 1991-1-4

Zone	D		E	
h/d	$c_{pe,10}$	$c_{pe,1}$	$c_{pe,10}$	$c_{pe,1}$
5	+0.8	+1.0	-0.7	
1	+0.8	+1.0	-0.5	
≤ 0.25	+0.7	+1.0	-0.3	

3.2.2 Unintended inclination

In the design of a diaphragm shall the load effect of unintended inclinations be taken into account, and Eurocode 1992-1-1 (European Standard, 2010b) chapter 5.2 gives guidance in how to obtain the load effect on a diaphragm and is derived in Equation 3.7:

$$H_i = \theta_i(N_b + N_a)/2 \tag{3.7}$$

where:

θ_i the imperfections represented in angle.
N_a is the normal force from the above structure, Shown in Figure 2.21
N_b is the normal force in the underlying load-carrying structure, Shown in Figure 2.21

And the represented angle θ_i is obtained by Equation 3.8:

$$\theta_i = \theta_0 \cdot \alpha_h \cdot \alpha_m \tag{3.8}$$

θ_0 basic value and set to 1/200.
α_h reduction factor for length or height, see Equation 3.9
α_m reduction factor, based on the number of contributing members, see Equation 3.10

$$\alpha_h = 2/\sqrt{l};\ 2/3 \leq \alpha_h \leq 1 \tag{3.9}$$

$$\alpha_m = \sqrt{0.5 \cdot (1 + 1/m)} \tag{3.10}$$

where:

l is the actual storey height (in regard to diaphragm design).
m total number of vertical load-carrying elements on the analyzed storey.

3.3 Analytical analysis

Analytical models to obtain the necessary stiffness properties to execute the numerical parametric study, furthermore, analytical models to perform convergence study and reference values are presented in this chapter.

3.3.1 Shear stiffness of timer to timber joints

Timber floor structures with in-plane structural joints, connected with screws shown in Figures 3.4 and 3.5, must the shear stiffness of the structural joint be known for a diaphragm analysis. Eurocode EN 1995-1-1 chapter 7.1 (European Standard, 2004) states how the shear stiffness of a structural joint can be obtained, which Eurocode name as the *slip modulus* and denotes it as K_{ser}. Moreover, the subscript, *ser*, stands for stiffness in service limit state and to obtain the ultimate limit state stiffness, K_u, shall the service limit state stiffness be multiplied with a correction factor of 2/3, hence, the ultimate limit state shear stiffness/slip modulus of a fastener is obtained by Equation 3.11:

$$K_u = \frac{2}{3} \cdot K_{ser} \tag{3.11}$$

where Eurocode 1995-1-1 state the Equations 3.12 and 3.13 shown in Table 3.5 to obtain K_{ser}:

Table 3.5: Equations for K_{ser} provided by Eurocode 1995-1-1

Fastener type	$K_{ser}[N/mm]$
Dowels Bolts with or without clearance* Screws Nails(with pre-drilling)	$\rho_m^{1.5} \cdot d/23$(3.12)
Nails (without pre-drilling)	$\rho_m^{1.5} \cdot d^{0.8}/30$(3.13)
*The clearance should be added separately to the deformation.	

where:

ρ_m is the mean density of the two connected timber elements. If the members have different densities shall the mean density be calculated as follows: $\rho_m = \sqrt{\rho_{m.1}\rho_{m.2}}$ in $[kg/m^3]$

d is the diameter of the fastener $[mm]$

3.3.2 Shear stiffness of grouted concrete joints

Guidance on how to obtain the shear stiffness of a concrete grouted joint isn't covered by the Eurocodes, however, (Elliott, 2019) gives an option on how to obtain the shear stiffness, K_s, of a grouted joint, originating from hollow core samples, according to Equations 3.14-3.19.

$$K_s = \frac{V}{\delta_s} \tag{3.14}$$

$$\delta_s = \frac{\ln(\delta_{t.max}/\delta_{ti})}{\beta} \tag{3.15}$$

$\delta_{t.max}$ According to equation 3.16 and $\leq 0.5[mm]$.

δ_{ti} is presented in Table 3.6.

β conservatively set to 3.0.

V Shear force in the examined joint

δ_s Deflection in joint due to shear forces

Table 3.6: Initial crack widths in prefabricated concrete elements with grouted joints (Elliott, 2019)

Age of precast unit when joint is filled (days)	Width of precast unit (mm)	Width of longitudinal joint (mm)	Initial crack width δ_{ti}(mm)
<7	1200	25	0.215
	1200	50	0.230
	600	25	0.115
	600	50	0.130
28	1200	25	0.135
	1200	50	0.150
	600	25	0.075
	600	50	0.090
>90	1200	25	0.095
	1200	50	0.110
	600	25	0.055
	600	50	0.070

$$\delta_t = l_s + \delta_{ti} \tag{3.16}$$

where l_s is the elastic elongation calculated according to Equation 3.17:

$$l_s = \frac{T_b \cdot L_s}{A_{sh.prov} \cdot E_s}[mm] \tag{3.17}$$

E_s is the Young's modulus of chosen steel/rebar and T_b is the tension force in the diaphragm in accordance with deep beam theory, see figure 3.10, and calculated in accordance to Equation 3.18:

$$T_b = M_b/z \tag{3.18}$$

where:

M_b is the diaphragm moment. $[kNm]$
z is the lever arm. $[m]$

Furthermore, the value of the lever arm, z, depends on the aspect ratio (Elliott, 2019) and is given in table 3.7:

Table 3.7: Values of z depending on the aspect ratio of the floor diaphragm.

B/L	z/B
< 0.5	0.9
$0.5 < 1.0$	0.8

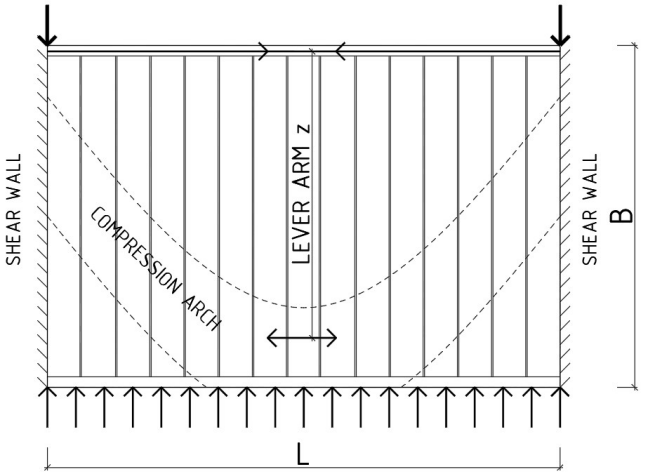

Figure 3.10: Forces according to deep beam analogy.

Moreover, L_s is the characteristic length, $[mm]$, of the tie bar, and is obtained by the least of the two expressions given in Equation 3.19:

$$L_s = min \begin{cases} 30\Phi \cdot A_{sh.calc}/A_{sh.prov} \\ 0.8 \cdot W \end{cases} \tag{3.19}$$

where:

Φ	is the tension bar diameter $[mm]$.
$A_{sh.calc}$	is the calculated required reinforcement area $[mm^2]$.
$A_{sh.prov}$	actual provided reinforcement area $[mm^2]$.
W	width of precast element $[mm]$.

3.3.3 Shear wall stiffness

The shear stiffness for timber walls is calculated in linear Euler theory, however, the stiffness of sheathed stud walls is also influenced by the nail design. Equations 3.20-3.24 guidance in how to obtain shear wall stiffness of the shear wall types stated in chapter 3.1.4, furthermore, description of the notations in the equations and visualization of the response is shown in Figure 3.11.

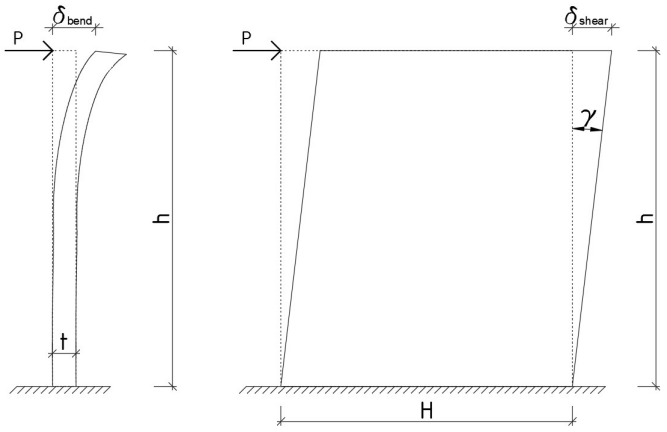

Figure 3.11: Bending and shear deflection of a cantilever wall (beam) subjected to point load, P, at the top

$$\delta_{bending} = \frac{P \cdot h^3}{3 \cdot E_m \cdot I} \tag{3.20}$$

$$\delta_{shear} = \frac{P \cdot h}{A \cdot G} \tag{3.21}$$

$$\delta_{tot.e} = \delta_{bending} + \delta_{shear} = \underbrace{\frac{P \cdot h^3}{3 \cdot E \cdot I}}_{\text{Bending contribution}} + \underbrace{\frac{P \cdot h}{A \cdot G}}_{\text{Shear contribution}} \tag{3.22}$$

where:

P	Point load acting on the top end of the cantilever.
h	is the height of the wall segment.
E	Young's-Modulus of studied material.
I	is the moment of inertia.
A	shear area of analysed web, $H \cdot t$.
G	the material shear modulus.

Moreover, by analyzing the stiffness of sheathed stud walls, (Källsner & Girhammar, 2009) present a model, shown in Equation 3.23, of how to obtain deflections in the nails of the sheathing material.

$$\delta_{nails} = 4.5 \cdot \frac{s}{H} \frac{P}{K_u} \tag{3.23}$$

where:

s	spacing of the nails at the periphery of the sheathing board.
k_u	The slip-modulus of the fastening screws/nails.

Hence, the stiffness of a cantilever subjected to a point load at its end is obtained by Equation 3.24, note that the term of Equation 3.23 is removed for solid shear walls.

$$k_{cant} = \frac{P}{\delta_{tot}} = \frac{P}{\left(\frac{P \cdot h^3}{3 \cdot E_m \cdot I} + \frac{P \cdot h}{A \cdot G} + 4.5 \cdot \frac{s}{H} \frac{P}{K_u}\right)} = \frac{1}{\left(\frac{h^3}{3 \cdot E_m \cdot I} + \frac{h}{A \cdot G} + 4.5 \cdot \frac{s}{H} \frac{1}{K_u}\right)} \tag{3.24}$$

3.3.4 Stiffness distribution of horizontal actions

With a rigid diaphragm are the horizontal actions distributed to the shear wall in respect of their relative stiffness, furthermore, the stiffness arrangement of LLRS governs where the R.C is located. If the location of the resultant of horizontal(S.C), H in Figure 3.12, deviates from the R.C, a torsional moment in the diaphragm is induced with the magnitude of $e \cdot H[kNm]$. Thus, when the horizontal loads are stiffness distributed with a rigid diaphragm to the LLRS, must both translation and rotation be taken into consideration.
The location of the rotation center in the x and y direction are found with Equations 3.25 and 3.26 respectively.

$$x = \frac{\sum(x_i \cdot S_{yi})}{\sum(S_{yi})} \tag{3.25}$$

$$y = \frac{\sum(y_i \cdot S_{xi})}{\sum(S_{xi})} \tag{3.26}$$

where:

x_i	Geometrical center of the i-th wall member in the x-direction.
y_i	Geometrical center of the i-th wall member in the y-direction.
$S_x i$	Stiffness of the i-th wall member in the x-direction.
$S_y i$	Stiffness of the i-th wall member in the y-direction

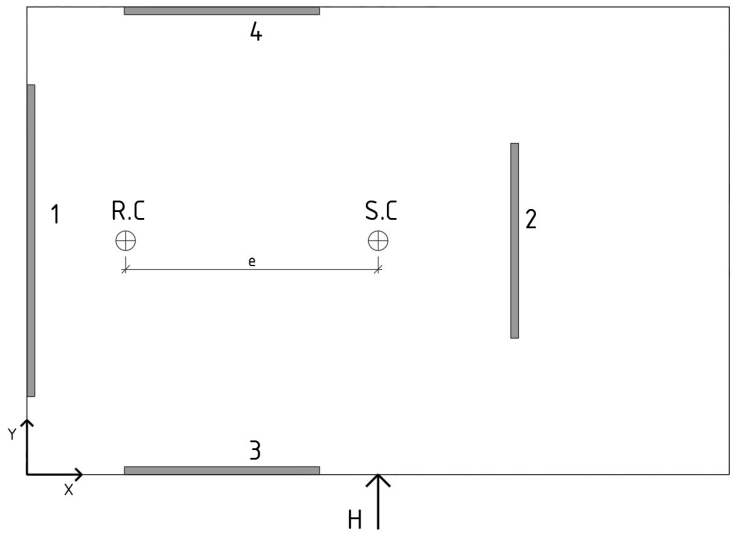

Figure 3.12: R.C and S.C deviate, thus a leverarm, e, from shear center to rotation center induces a torsional moment in the diaphragm

Furthermore, the horizontal load distribution for pure translation, see Figure 2.14, to the bracing units, is for the i-th member in the x or y direction presented by

Equations 3.27 and 3.28 respectively.

$$H_{xi} = H_x \cdot \frac{S_{xi}}{\sum S_{xi}} \tag{3.27}$$

$$H_{yi} = H_y \cdot \frac{S_{yi}}{\sum S_{yi}} \tag{3.28}$$

In structural floor plans where the R.C and the S.C don't coincide, the torsional moment is calculated according to the Equation 3.29, where e is the eccentricity of the rotational center and shear center and H is the resultant horizontal force, see Figure 3.12.

$$T = H \cdot e \tag{3.29}$$

The influence of the diaphragm rotation to the shear walls with stiffness in x and y directions are obtained in the Equations 3.30 and 3.31 respectively.

$$H_{i.x} = T \cdot \frac{S_{xi} \cdot y_i}{S_T} \tag{3.30}$$

$$H_{i.y} = T \cdot \frac{S_{yi} \cdot x_i}{S_T} \tag{3.31}$$

where:

x_i and y_i is the distance from R.C to the geometrical center of i-th wall member in the x and y direction respectively, see Figure 3.13.

The total torsional stiffness in the system, S_T, is obtained by Equation 3.32.

$$S_T = \sum (S_{xi} \cdot y_i^2) + \sum (S_{yi} \cdot x_i^2) \tag{3.32}$$

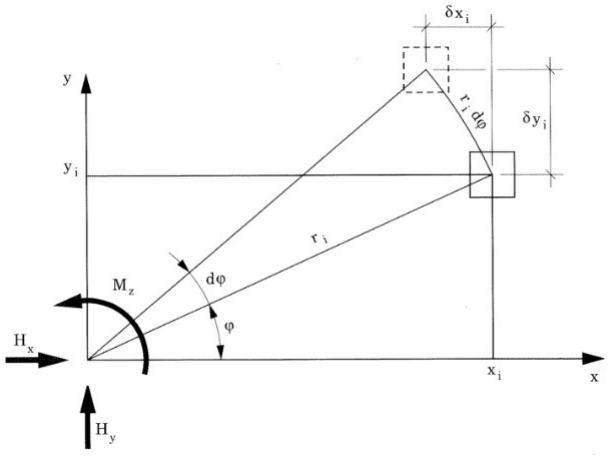

Figure 3.13: Distance from R.C to geometrical center of a shear wall. Reproduced (Björn Engström, n.d.)

The total distribution of horizontal loads to the LLRS with the stiffness in the x or y direction is the summation of the influence of translation and rotation, shown in Equations 3.33 and 3.34.

$$H_{i.x} = H_x \cdot \frac{S_{xi}}{\sum S_{xi}} + T \cdot \frac{S_{xi} \cdot y_i}{S_T} \tag{3.33}$$

$$H_{i.y} = H_y \cdot \frac{S_{yi}}{\sum S_{yi}} + T \cdot \frac{S_{yi} \cdot x_i}{S_T} \tag{3.34}$$

3.4 Numerical analysis

The numerical analysis is performed in the finite element software, FEM-Design 22 version 22.00.001, developed by StruSoft. The FEM-Design application programming interface (API) module allows to run the FE software by, for instance, coding and the coding language C#. Moreover, there are other methods to run FEM-Design through its API module, but in this study is the C# code language used to control the input data and export data for the parametric analysis.

3.4.1 Model overview

General overviews of the two models' structural floor plans are shown in Figures 3.14, and 3.15, to introduce the global orientation of the model and obtain an overview. Both structural floor plans are oriented with the long facade facing the global y-direction of the model, and the gable side of the structure in the global x-direction. Furthermore, at the bottom left corner is the global coordinate system of the model found, whereas the green arrow illustrates the global x-direction and the red arrow is the global y-direction. All components in the software, such as supports, shells, etc., have a local coordinate system, also seen in the figures as smaller green and red arrows, which will be further discussed in the upcoming sections.

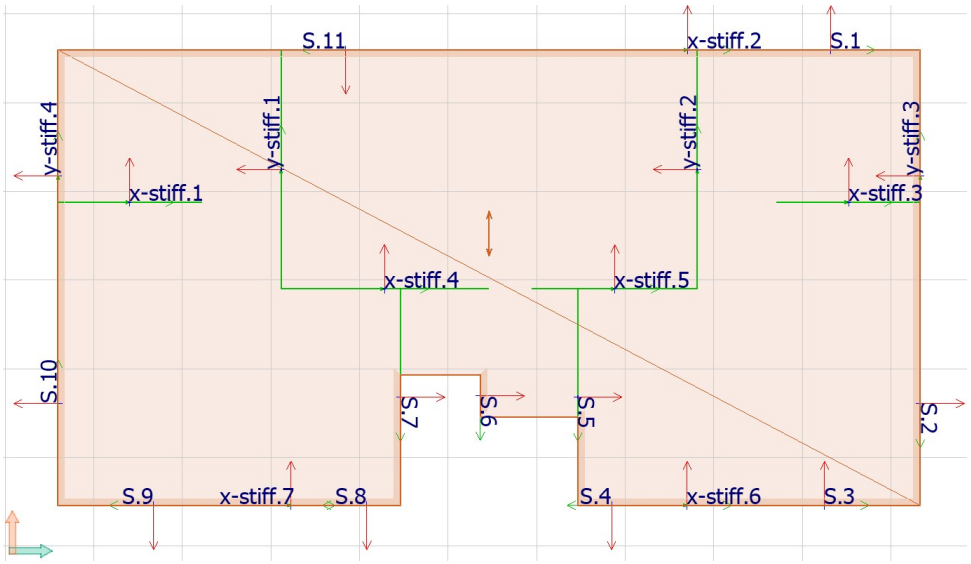

Figure 3.14: Overview of the FE model of the structural floor plan 1 with solid particleboard shell element.

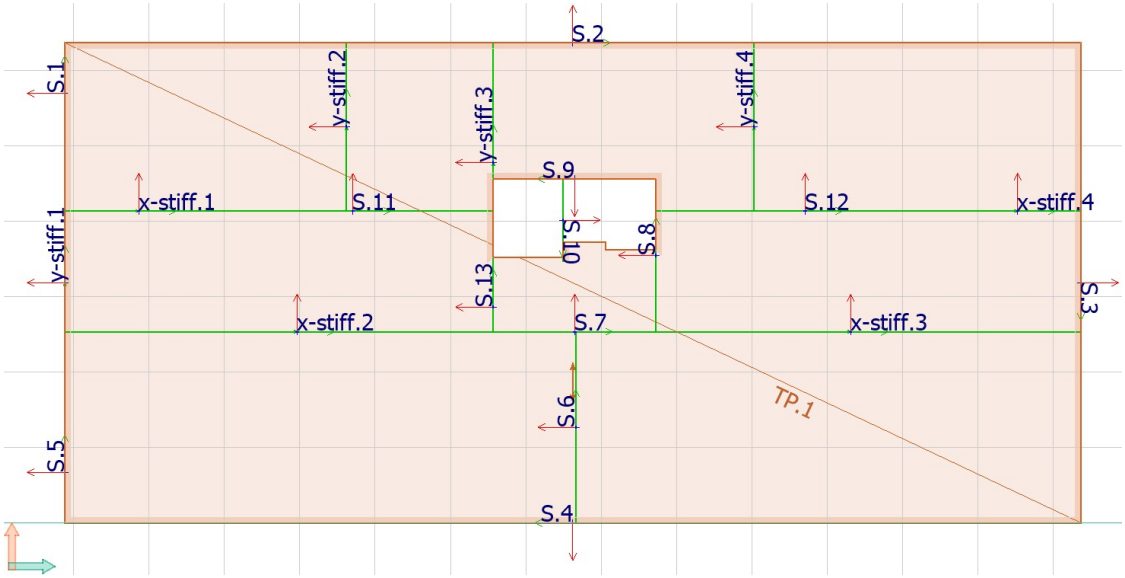

Figure 3.15: Overview of the FE model of the structural floor plan 2 with solid particleboard shell element.

3.4.2 Boundary conditions

Boundary conditions apply for the constraints and loads in the models, and the constraints, are defined in the model, either through 'line supports' or when analyzing panels-wise diaphragms, stiffness of the structural joints between the panels are defined in the FE model as 'edge connections'. Furthermore, boundary conditions of horizontal loads are applied as 'line loads'.

3.4.2.1 Line supports

The load-bearing walls are simulated in the models as so-called 'line supports', which are divided into three analytical IDs in the models, 's', 'x-stiff, and 'y-stiff', seen in Figures 3.14, 3.15. Line supports with the ID 's' are simulating load-bearing walls that only carry the vertical load and do not contribute to the lateral load-resisting system. Moreover, line supports denoted with the ID 'x-stiff' or 'y-stiff' simulate load-carrying walls that carry vertical loads and provide to the lateral load-resisting system in the global x-direction and global y-direction, respectively. IDs to the line support simplifies in the coding process to identify which of the supports provides to the lateral load-resisting system, and in which global direction it provides.

The line supports stiffness properties are defined in a local coordinate system, x', y', and z', in the unit of $kN/m/m$, see Figure 3.16, where x' is the direction parallel to the propagation line of the line support(green arrow), y' is in-plane perpendicular to the x'-direction (red arrow), and the z'-direction is out-of-plane perpendicular to the x' and y' plane. Moreover, motion stiffness for all line supports is set to zero, the z'-direction set to infinitely stiff, and the opposite stiffness properties are set to the y'-direction with zero stiffness, lastly, the x'-direction is the direction where shear walls have its stiff direction and thus, are stiffness set in varying ranges in the x'-direction, for the line support denoted *y-stiff* and *x-stiff*, with the help of the script and the type of parametric study.

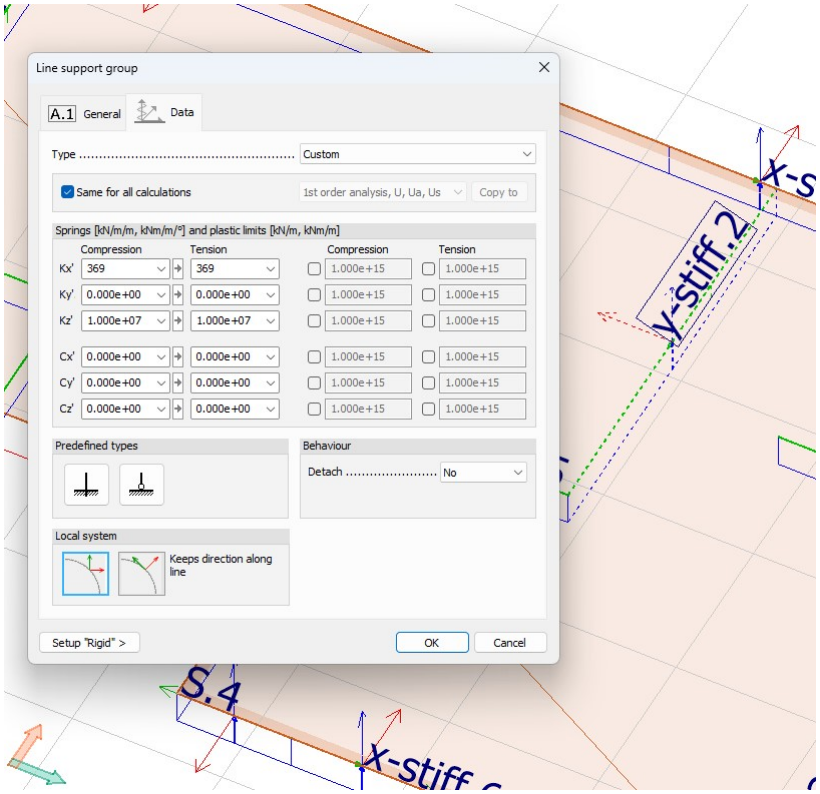

Figure 3.16: Example of stiffness properties of line support 'y-stiff.2'. The local coordinate system of the line support is found below the 'y'.

3.4.2.2 Edge connections

The structural floor types 2-4, see Chapter 3.1.3, are mounted panels-wise with structural joints, which are modeled in FEM-Design by modeling the actual panels, FEM-Design then allows controlling the stiffness values of, what FEM-Design calls, the *edge connection* between the adjacent panels. Edge connections are given in the unit of $kN/m/m$ and Figure 3.17 shows the stiffness properties options of the edge connection with a darker hatched area parallel to the edge of the panel, with a hatch dash-pattern in 45°. In similarity to line support, edge connection has a local coordinate system, and the local coordinate system's axes are oriented in the same manner as for the line supports (see Chapter 3.4.2.1). Stiffness values of structural joints will be implemented to the x' and y' axis of the edge connection in the parametric study.

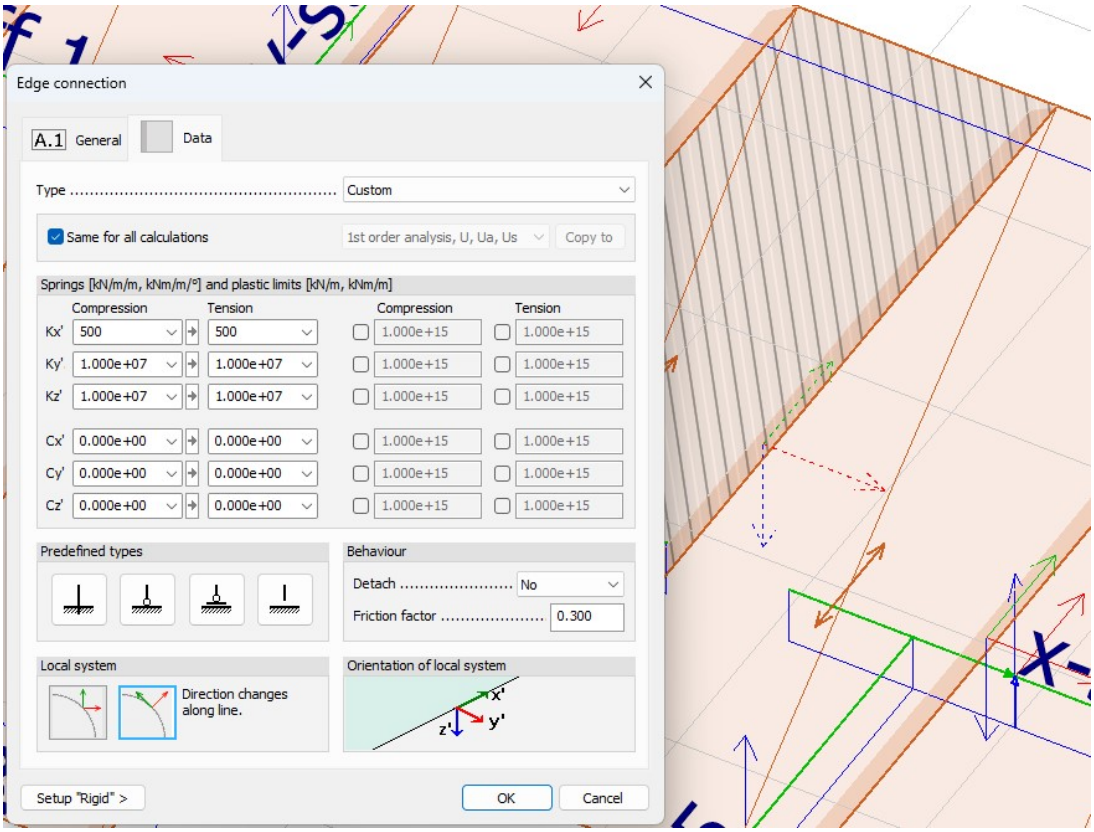

Figure 3.17: Edge connection properties of a structural joint of adjacent panels in FEM-Design.

Additionally, to manage the script code to be able to identify which edge connections the stiffness properties are to be changed for, the ID of the desired edge connections are set to 'elem.conn', shown in Figure 3.18.

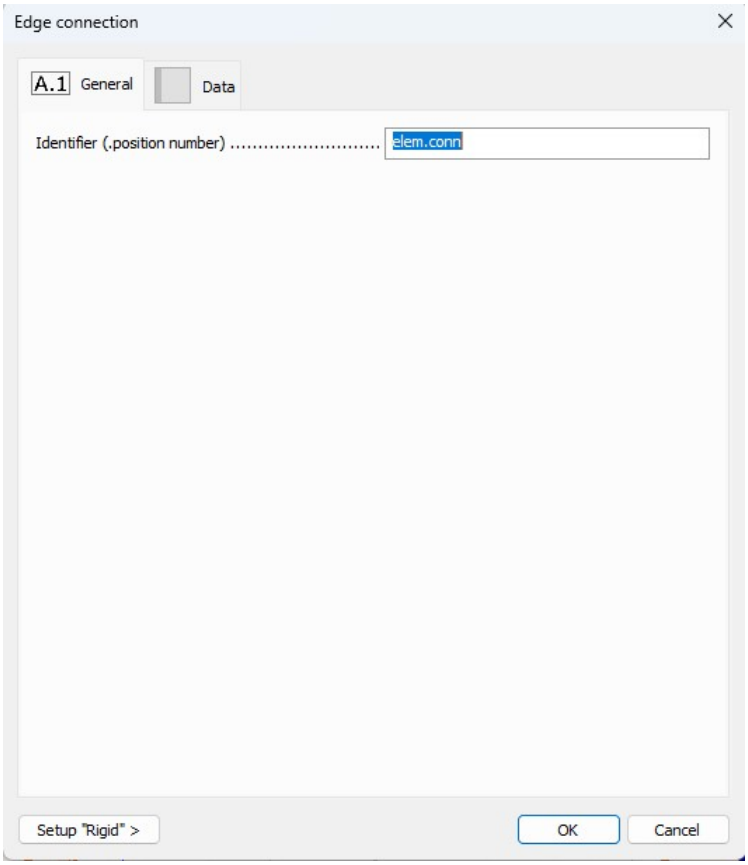

Figure 3.18: Defining ID of edge connection in FEM-Design

3.4.2.3 Horizontal Loads

The horizontal loads are defined to act in the global negative y-direction and applied to the shell boundary facing the positive y-direction as a line load along the diaphragms propagation in the x-direction, see Figure 3.19. The horizontal loads are divided into self-weight and wind loads and given in characteristic magnitude. FEM-Design then combines the load cases into design load combinations in accordance with Eurocodes.

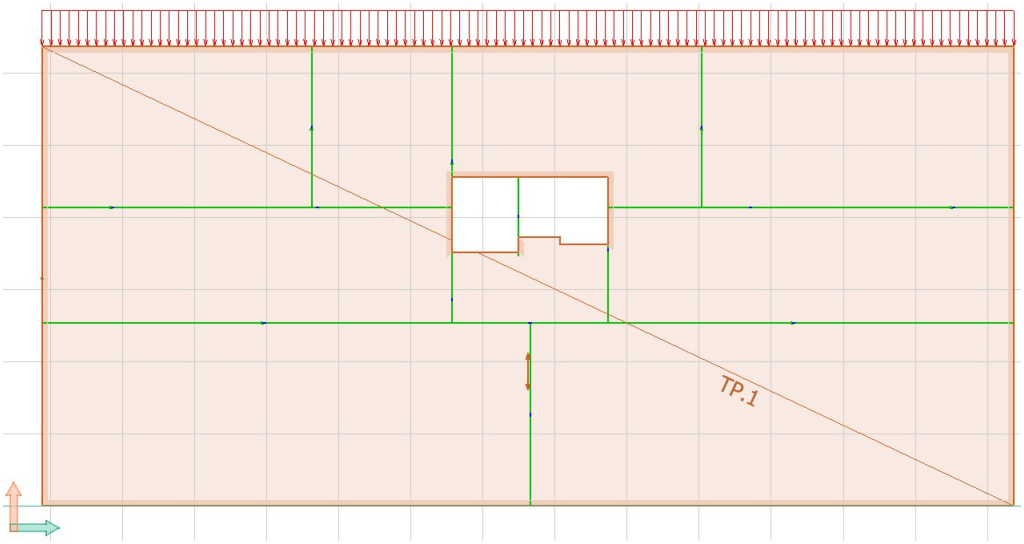

Figure 3.19: Horizontal actions acting in the global negative y-direction, introduced at the shell boundary facing the positive y-axis.

3.4.3 Shell elements stiffness

FEM-Design has a predefined library of mechanical properties for numerous materials and structural elements, where predefined stiffness properties of particleboard type 5, plywood Moelven K20/70 oputsad, CLT 180-5s, and concrete c25/30 are given and used in the study. Stiffness properties of the timber products; particleboard, plywood Moelven and Martinsson 180-5s are shown in Figures 3.20-3.22, which are confirmed with producer's technical approvals of the products, and the concrete strength c25/30 material data in FEM-Design were confirmed against values given in the Eurocode EN 1992-1-1. Moreover, the FE models are purely modeled with shell elements for simulating the diaphragms, thus, no stiffness contributes from joists, chords, etc.

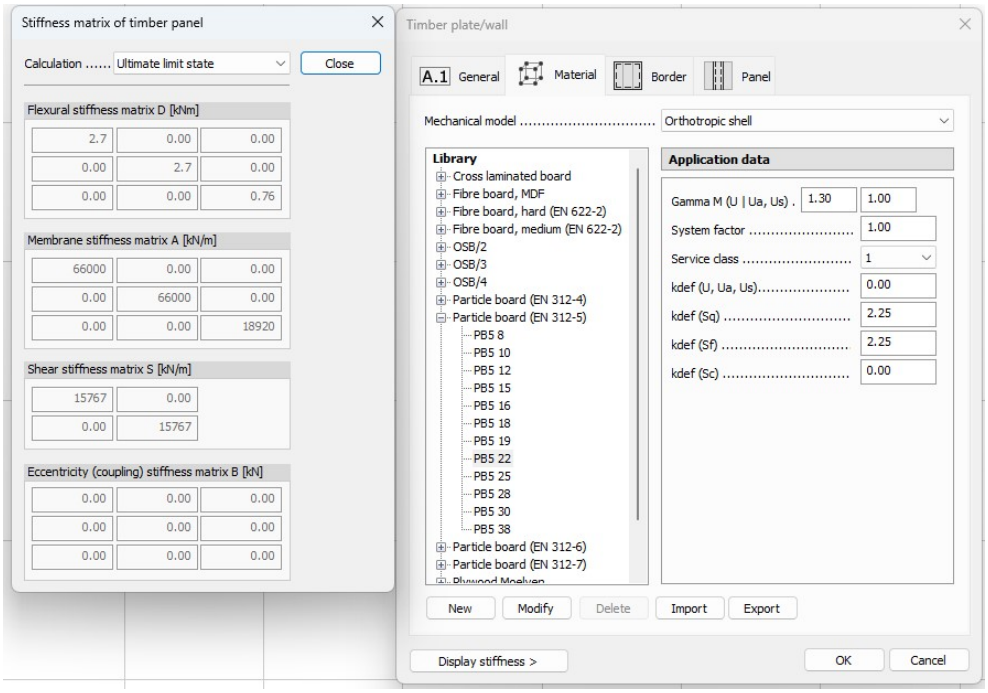

Figure 3.20: FEM-Design particleboard type 5 properties.

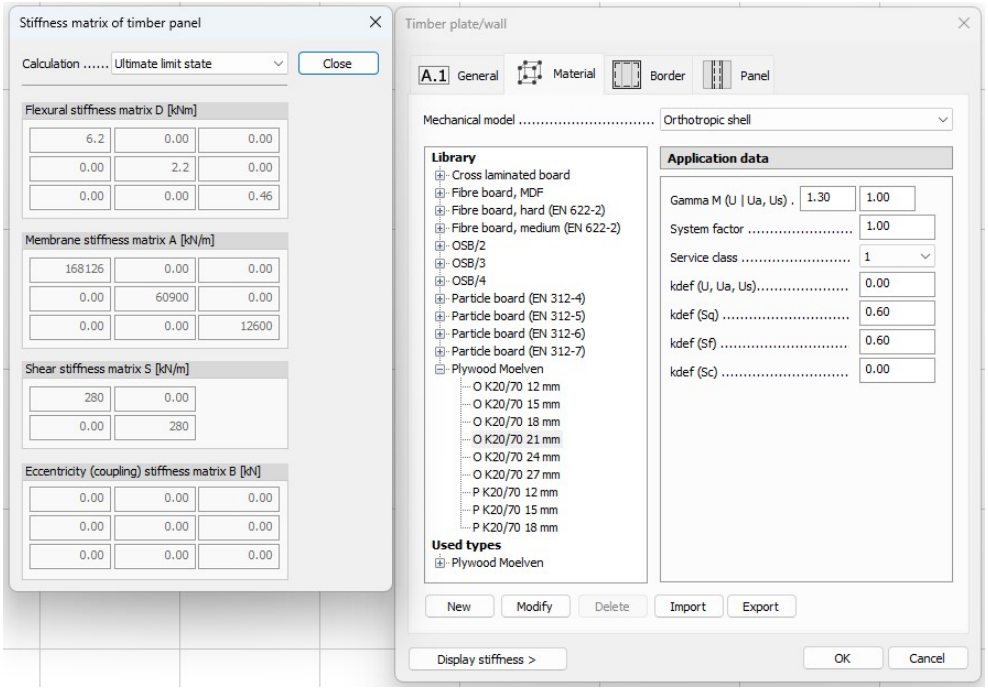

Figure 3.21: FEM-Design plywood O K20/70 board by Moelven.

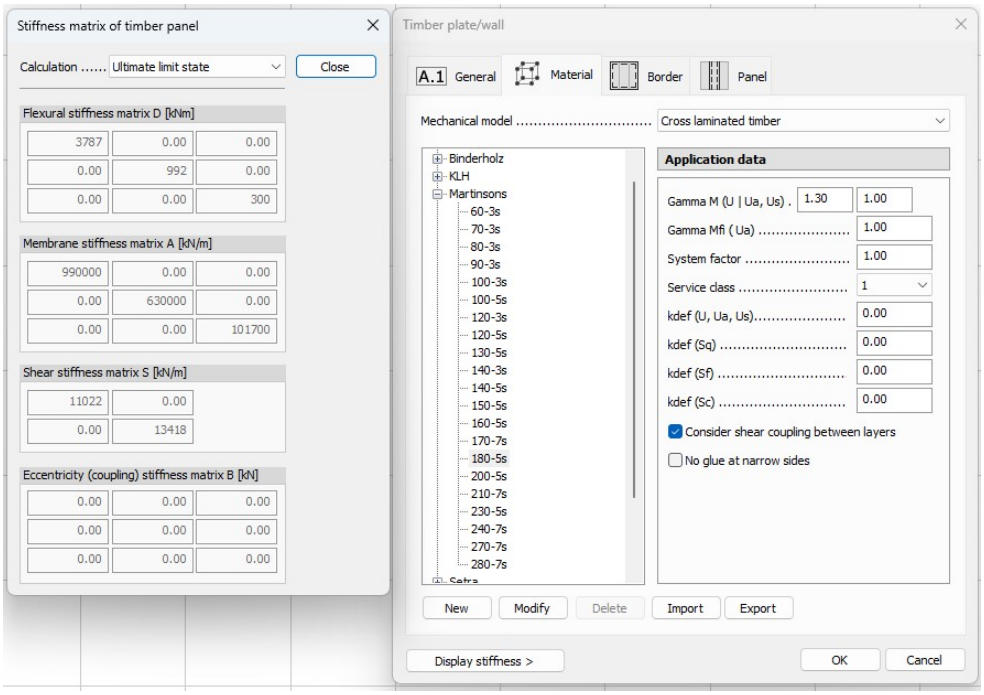

Figure 3.22: FEM-Design CLT 180-5s board stiffness properties.

3.4.4 Mesh size

The mesh element size may govern if the obtained results in a FE model are close enough to the real structural behavior and force flow in a structure - without the model getting too computationally heavy. The finer choice of mesh size in a model, the more computationally heavy the model will become as the number of differential equations to solve increases. A feature in the FEM-Design software is to let the software calculates a recommended average mesh element size, and recommended element sizes are presented in Table 3.8, which are the mesh size of use in the study.

Table 3.8: Mesh sizes used in the analysis

Model	Material	Mesh size $[m]$
Floor plan 1	Particle board	0.66
	Plywood panels	0.32
	CLT panels	0.33
	Precast concrete panels	0.33
Floor plan 2	Particle board	0.56
	Plywood panels	0.25
	CLT panels	0.25
	Precast concrete panels	0.25

3.4.5 Model verification

To ensure the models' correctness, a convergence study was made for each floor plan and each floor type. The convergence study is presented in Tables 3.9 and 3.10 for

floor plan 1 and floor plan 2 respectively. Mesh size marked with * in each floor type is the mesh size of use in the parametric study. In addition to the convergence study, are the FE models verified by comparing the resulting horizontal supports reaction between the FE model and hand calculations.

3.4.5.1 Convergence study

Observing the results of the convergence study of structural floor plan 1 in Table 3.9, is the largest difference, in percentage, of deflection in δ_1 between the used mesh, marked with *, and the finest mesh size of $0.10m$ obtained at the TCC floor type and resulted in a difference of 1.1% or $0.002mm$. Furthermore, the largest actual deflection is obtained for the plywood floor type with a difference of $0.0078mm$ between the used mesh and the finest mesh size of $0.10m$. Both deviations are considered to be small differences. Additionally, the same order of differences is obtained for δ_2. Thus, for all floor types, there is no need to use a finer mesh than the size recommended by the FEM-Design software. In regard to the reaction forces, R_1, R_2, R_3, and R_4(which are the support reactions of the supports *y-stiff.1* to *y-stiff.4*, see Figure 3.14), no deviations were observed between the analyzed mesh sizes. However, it could be argued to use a more sparse mesh size for the as the difference in δ_1 and δ_2 between these mesh sizes also is considered to be small, but with the FE models being local to one storey the computational time gain is neglectable.

Table 3.9: Convergence control floor plan 1, Mesh size in $[m]$, δ in $[mm]$ and R_i in $[kN]$

Model	Mesh size	δ_1	δ_2	R_1	R_2	R_3	R_4
Particle board	0.10	0.9095	0.3872	48.7	48.6	10.3	10.2
	0.30	0.9057	0.3860	48.8	48.5	10.3	10.2
	0.66*	0.9033	0.3803	48.8	48.6	10.3	10.1
	1.00	0.8938	0.3757	48.7	48.4	10.4	10.2
Plywood	0.10	0.8278	0.3365	44.2	45.8	14.5	13.3
	0.32*	0.8200	0.3337	44.2	45.8	14.5	13.3
	0.64	0.8026	0.3260	44.3	45.8	14.4	13.2
	1.00	0.8199	0.3397	44.4	45.1	14.9	13.4
CLT	0.10	0.1197	0.0549	43.8	45.2	15.1	13.7
	0.33*	0.1204	0.0547	43.2	45.4	15.1	14.1
	0.66	0.1297	0.0543	42.8	45.6	15.1	14.3
	1.00	0.1284	0.0545	43.1	45.1	15.4	14.2
TCC	0.10	0.0182	0.0094	43.1	45.8	15.1	13.8
	0.33*	0.0184	0.0094	42.2	46.2	15.1	14.3
	0.66	0.0187	0.0094	41.4	46.4	15.2	14.8
	1.00	0.0195	0.0099	41.7	45.6	15.8	14.7

Continuing, by studying the results obtained in the convergence study of structural floor plan 2, Table 3.10, the largest difference of deflection, in percentage, in δ_1

and δ_2 between the used mesh, marked with *, and the finest mesh size of $0.10m$ obtained with the particleboard floor type and resulted in a difference of 1.7%/0.9% or $0.003mm/0.014mm$ respectively. The deflection deviations between the two mesh sizes are considered small. In regard to the reaction forces, R_1, R_2, R_3, and R_4(which are the support reactions of the supports *y-stiff.1* to *y-stiff.4*, see figure 3.15), no deviations were observed between the analyzed mesh sizes. Therefore, the conclusion of the floor plan 2 convergence study is in line with the convergence study of floor plan 1, recommended mesh size of FEM-Design software is fine to use, however, a sparse mesh could have been used but the computational time gain ended up being neglectable.

Table 3.10: Convergence control floor plan 2, Mesh size in $[m]$, δ in $[mm]$ and R_i in $[kN]$

Model	Mesh size	δ_1	δ_2	R_1	R_2	R_3	R_4
Particle board	0.10	0.6429	3.4976	18.2	31.6	36.2	86.0
	0.30	0.6416	3.4921	18.2	31.6	36.2	86.0
	0.56*	0.6397	3.4833	18.3	31.6	36.1	86.0
	1.00	0.6368	3.4663	18.3	31.7	36.0	86.1
Plywood	0.10	0.5312	3.9370	18.7	31.1	35.0	87.2
	0.25*	0.5304	3.9324	18.7	31.2	34.9	87.2
	0.50	0.5282	3.9241	18.7	31.2	34.8	87.3
	1.00	0.5272	3.9089	18.7	31.2	34.8	87.3
CLT	0.10	0.0871	0.4858	16.8	32.1	37.9	85.2
	0.25*	0.0870	0.4855	16.8	32.1	37.9	85.2
	0.50	0.0868	0.4849	16.8	32.1	37.8	85.2
	1.00	0.0864	0.4835	16.9	32.1	37.8	85.2
TCC	0.10	0.0151	0.0859	19.0	30.4	36.1	86.6
	0.25*	0.0151	0.0859	19.0	30.4	36.1	86.6
	0.50	0.0151	0.0859	19.0	30.4	36.1	86.6
	1.00	0.0151	0.0858	19.0	30.4	36.1	86.6

3.4.5.2 Comparison of horizontal support reactions

Hand calculations with stiffness distribution theory are compared with the FE models. To ensure that stiffness distribution was obtained in the FE models, the line supports stiffness of *x-stiff* and *y-stiff* members was set to the value of $20kN/m/m$, which is a low stiffness value that the shear walls to force a stiffness distribution of the diaphragm in the FE-model. Derivations of the analytical shear wall stiffness are found in Appendix B.

The resulting horizontal reaction forces for floor plan 1 are presented in Table 3.11, and seen is that the hand calculations and FE model deviate under one percent and thus seen as proper a proper model. Derivations of analytical calculations are found in Appendix A.

Table 3.11: Floor plan 1 - Comparison of resulting horizontal reaction forces of supports in the global y-direction between hand calculations and FE model with stiffness distribution of the horizontal loads.

Analysis	*y-siff.1*	*y-siff.2*	*y-siff.3*	*y-siff.4*
Hand calc.	28.88	28.96	30.02	30.02
FEM	28.74	28.74	30.16	30.15
Difference %	0.48	0.76	0.47	0.43

Furthermore, the resulting horizontal reaction forces of structural floor plan 2, with the same stiffness properties as in the structural floor 1 analysis, are presented in Table 3.12, and observed is that the hand calculations and FE model deviate under one percent for all supports except *y-stiff.1* where it deviates 5.59%, however, the deviation is only $0.3kN$ in force. The deviation is considered small, as small force deviations for *y-stiff.1* will result in a high percentage of deviations as the resultant reaction force is small in comparison to the other supports. Therefore, the FEM and analytical models are considered to be in good agreement. For the derivation of the hand calculations see Appendix A

Table 3.12: Floor plan 2 - Comparison of resulting horizontal reaction forces of supports in the global y-direction between hand calculations and FE model with stiffness distribution of the horizontal loads.

Analysis	*y-siff.1*	*y-siff.2*	*y-siff.3*	*y-siff.4*
Hand calc.	4.83	30.98	64.84	71.51
FEM	5.10	30.93	64.67	71.20
Difference %	5.59	0.16	0.26	0.42

3.4.6 Parametric analyzes with C# script

The FE parametric study is executed by a created C# script that connects to the FEM-Design through its API module and runs analyzes of the created FE models, with parametric control of the stiffness of the model's line supports or shell elements edge connection. The script is structured such that it reads and scans through an exported XML file of the FE model, and identifies line supports and/or edge connections of interest for the user to be analyzed, if requested parts do not match the model, the run is terminated. Furthermore, if the requested parts correspond to the model, the script continues with setting the stiffness properties of choice to the examined line supports and/or edge connections and runs an analysis. The stiffness increment is balanced for each studied floor type on Object 1 and Object 2 to run the analysis to such an extent that the variation in the change of support reaction approaches zero for at least one(if structural joints are present) type och each structural floor. Subsequently, results from the analysis are exported by the script and the script loop a new analysis, with different shear stiffness settings of choice until it reaches the last loop of the analysis and then terminates the run, a flow sheet of the description of the script is shown in Figure 3.23. The C# code is found in the Appendix F

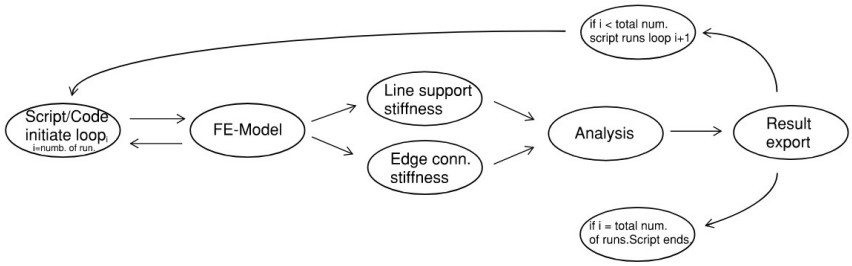

Figure 3.23: Flow sheet of the C# script and FEM-Design interaction.

4

Results

4.1 Shear wall stiffness

Shear wall stiffness for wall types in 3.1.4, where types one and two are analyzed with OSB and plywood board as a sheathing material are presented in table 4.1. Sheathing types marked with * in the table are walls of type 1 without the installation space, thus the sheathing material is directly fastened to the studs. Full derivations of calculations are found in the Appendix B

Table 4.1: Shear wall stiffness of wall types 1 and 2 in object 1.

Wall type	Sheathing	Stiffness $(kN/m/m)$	Stiffness $(kN/0.9m/m)$
Type 1	OSB	125	88
	OSB*	369	260
	Plywood	172	145
	Plywood*	505	427
Type 2	OSB	738	520
	Plywood	1009	854

Furthermore, the shear stiffness of CLT wall segments of Object 1 and Object 2 are shown in Table 4.2, and the derivation of calculations is found in the Appendix B.

Table 4.2: Shear wall stiffness of wall types 3 and 4 for objects 1 and 2.

Object 1			Object 2		
Wall ID	CLT type	Stiffness kN/m	Wall ID	CLT type	Stiffness kN/m
$SH_{1.1}$	CLT60-C3s	12247	$SH_{1.1}$	CLT60-C3s	84120
	CLT100-C3s	19469		CLT100-C3s	139504
	CLT120-C5s	24495		CLT120-C5s	168240
	CLT160-C5s	34332		CLT160-C5s	225445
$SH_{1.2}$	CLT60-C3s	59997	$SH_{2.1}$	CLT60-C3s	142305
	CLT100-C3s	99123		CLT100-C3s	236725
	CLT120-C5s	119993		CLT120-C5s	284610
	CLT160-C5s	161410		CLT160-C5s	380202
$SH_{1.3}$	CLT60-C3s	20179	$SH_{2.2}$	CLT60-C3s	14757
	CLT100-C3s	32537		CLT100-C3s	240819
	CLT120-C5s	40359		CLT120-C5s	289514
	CLT160-C5s	55687		CLT160-C5s	386730
$SH_{2.1}$	CLT60-C3s	28314	$SH_{2.3}$	CLT60-C3s	36398
	CLT100-C3s	46075		CLT100-C3s	59591
	CLT120-C5s	56628		CLT120-C5s	72796
	CLT160-C5s	77375		CLT160-C5s	98841
$SH_{2.2}$	CLT60-C3s	49624	$SH_{2.4}$	CLT60-C3s	33715
	CLT100-C3s	81745		CLT100-C3s	55101
	CLT120-C5s	99248		CLT120-C5s	67429
	CLT160-C5s	133906		CLT160-C5s	91721
$SH_{2.3}$	CLT60-C3s	36398	$SH_{2.5}$	CLT60-C3s	48315
	CLT100-C3s	59591		CLT100-C3s	79552
	CLT120-C5s	72796		CLT120-C5s	96631
	CLT160-C5s	98841		CLT160-C5s	130437
$SH_{2.4}$	CLT 60-C3s	57418	$SH_{2.6}$	CLT60-C3s	72766
	CLT 100-C3s	94804		CLT100-C3s	120505
	CLT 120-C5s	114837		CLT120-C5s	145531
	CLT 160-C5s	154572		CLT160-C5s	195293
			$SH_{2.7}$	CLT 60-C3s	48315
				CLT 100-C3s	79552
				CLT 120-C5s	96631
				CLT 160-C5s	130437

4.2 Edge connection stiffness

Floor types, two, three, and four are mounted panel-wise and connected to adjacent panels. In the sub-sections of this section is the stiffness of different connections presented.

4.2.1 I-Joist

Structural floor type 2, I-joist, are panel-wise mounted diaphragms, thus, structural joints with a screw connection for both panels to a shared joist, connection will obtain double deflection and thus halved stiffness, see Figure 3.4. Table 4.3 present obtained shear stiffness values with a screw diameter of $d = 4.0mm$ and the full derivation of calculations is obtained in the Appendix C.

Table 4.3: Edge connection stiffness of screwed, with a diameter of $d = 4.0mm$, I-Joist panels.

Screw connection Plywood - C24	Stiffness (kN/m)	Stiffness $(kN/m/m)$
One screw pair	335	-
Screws $s = 330mm$	-	1000
Screws $s = 220mm$	-	1500
Screw $s = 100mm$	-	3350

4.2.2 CLT

The resulting shear stiffness of the structural joint between two adjacent CLT panels, with cross screwed pairs, see Figure 3.5 b), of the diameter $d = 6.5mm$ are presented in Table 4.4. Derivations of calculations are seen in Appendix C.

Table 4.4: Edge connection stiffness of cross-screwed CLT butt joints, screw diameter of $d = 6.5mm$.

Screw connection CLT - CLT	Stiffness (kN/m)	Stiffness $(kN/m/m)$
One screw	1220	-
Cross pair $s = 350mm$	-	6970
Cross pair $s = 250mm$	-	9755
Cross pair $s = 100mm$	-	24390

4.2.3 TCC

Stiffness calculations of the grouted joints are performed for the worst case of in each structural floor plan with a conservatively low area of reinforcement in the tie chord, resulting stiffness is stated in Table 4.5 and derivations of calculations are found in the Appendix C.

Table 4.5: Stiffness of grouted structural joints of TCC panels

Grouted connection TCC - TCC	Span	Stiffness (kN/m)	Unit meter stiffness of joint ($kN/m/m$)
Object 1	Mid	504098	60735
Object 2	Cantilever	314792	25593

4.3 Object 1

Results obtained from the parametric study of Object 1 with the different structural floors are presented in this chapter. Common for upcoming figures are, obtained horizontal reaction force of line supports *y-stiff.2* and *y-stiff.4* in relation to the shear wall stiffness are presented collected in the figures, for each structural floor with dashed and solid colored lines, respectively. Furthermore, vertical stiffness reference lines are shown in the figures, where each line stiffness reference is stated either in the figures or on the legend of the figures. Design horizontal action on Object 1 is $6.047kN/m$ and derived in Appendix D

Wall stiffness references of Object 1 are calculated with a shear wall length of $5.4m$, multiplied by the obtained shear wall stiffness given in Chapter 4.1. Furthermore, to present the line support stiffness from the FE model in unit kN/m on the x-axis of the figures, the line support stiffness, $kN/m/m$, from FE analysis is multiplied by the length of $5.4m$ and results in stiffness of the shear walls with the stiff direction in the global y-direction. The FE analyses of stiffness increment on edge connections are the edge connection stiffness defined as, $kN/m/m$, which is multiplied by the total depth of the diaphragm, $10.3m$, to obtain the reference in kN/m on the x-axis of figures. Lastly, diaphragm stiffness is presented in each subchapter, diaphragm stiffness, of specific floor diaphragm.

4.3.1 Particleboard diaphragm

Results obtained for object 1 with particleboards are presented in this section.

4.3.1.1 Diaphragm stiffness

Stiffness properties of the diaphragm obtained numerically is presented in table 4.6.

Table 4.6: Diaphragm stiffness of Object 1 with the floor type of particleboards.

Type of analysis	Span	Deflection (mm)	Stiffness (kN/m)
FEM	1	0.39	78146
	2	0.79	71952
	3	0.39	78146

4.3.1.2 Stiffness increment of line supports

The resulting horizontal load distribution to the supports, in relation to the stiffness of the line supports (shear walls) is presented in Figure 4.1. For particleboard analysis are obtained support reaction of the line support *Y-stiff.1-4* shown.

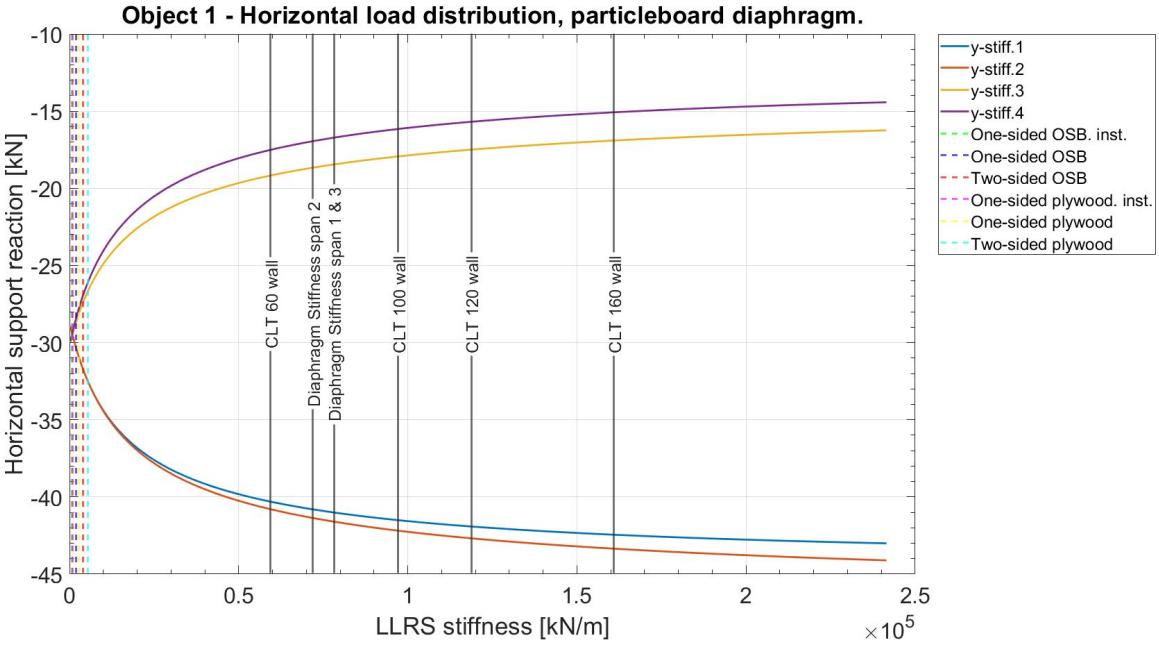

Figure 4.1: Object 1, horizontal load distribution of particleboard diaphragm type with an increment of the line support stiffness.

Moreover, Figure 4.2 presents a closer view of wall stiffness up to $15000kN/m$, to ease the interpretation of the horizontal load distribution in the stiffness range of the sheathed framed stud wall types.

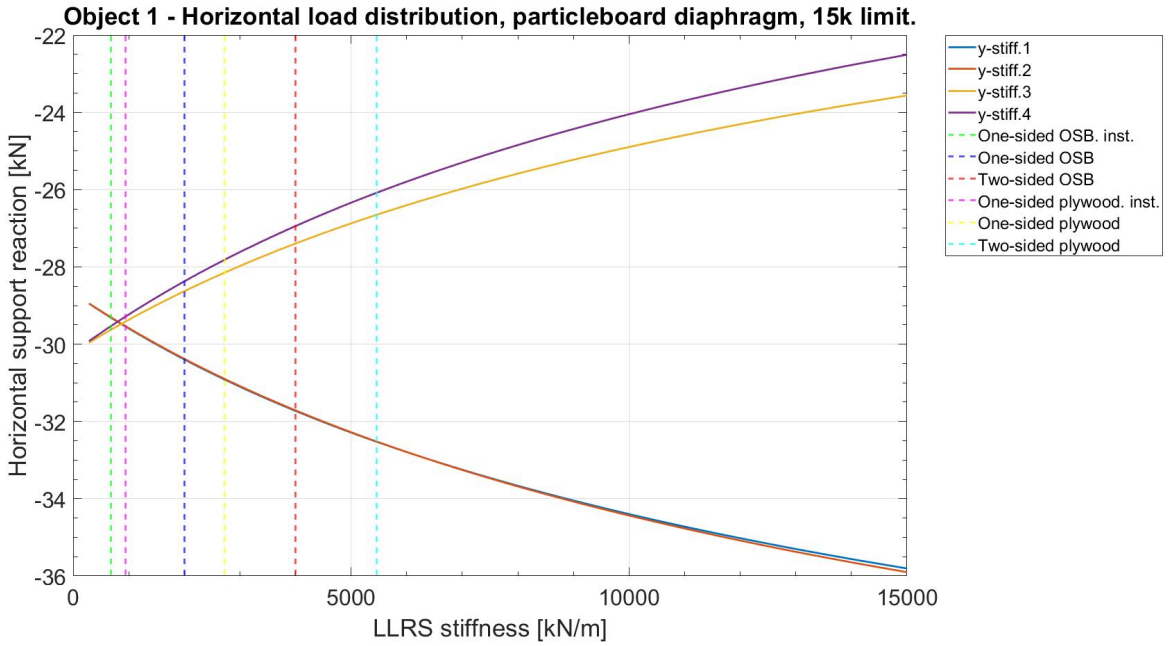

Figure 4.2: Object 1, horizontal load distribution of particleboard diaphragm type with an increment of the line support stiffness. Shear walls stiffness limited to 15k

4.3.2 Plywood panels diaphragm

The plywood diaphragm is analyzed either with an increment of line supports or edge connections. Results obtained from the parametric stiffness study of the plywood diaphragm, with the structural edge connections stated in section 3.1.3.1, are presented in this section.

4.3.2.1 Diaphragm stiffness

Table 4.7 presents obtained diaphragm stiffness of the panel-wise plywood board diaphragm, for the four different edge connection stiffness types in Chapter 3.1.3.1, with the stiffness presented in Section 4.2.1. Additionally, the line support stiffness was set to infinitely stiff when the diaphragm stiffness was evaluated.

Table 4.7: Diaphragm stiffness of Object 1 with the floor type of plywood boards with a variation of the edge connection stiffness.

Type of analysis	Span	Deflection (mm)	Stiffness (kN/m)
FEM - inf.	1	0.3338	91312
	2	0.8200	69317
	3	0.3289	92672
FEM - s100	1	0.7692	39626
	2	1.8611	30541
	3	0.9080	33568
FEM - s220	1	1.0986	27744
	2	3.0454	18664
	3	1.4073	21658
FEM - s330	1	1.3667	22302
	2	4.1172	13805
	3	1.8023	16912

4.3.2.2 Stiffness increment of line supports

Results from the analyses of the panel-wise plywood board diaphragm, with the four different structural joints, with stiffness increment of line supports are shown in Figure 4.3. Full reports of all analyses can be found in Appendix E.

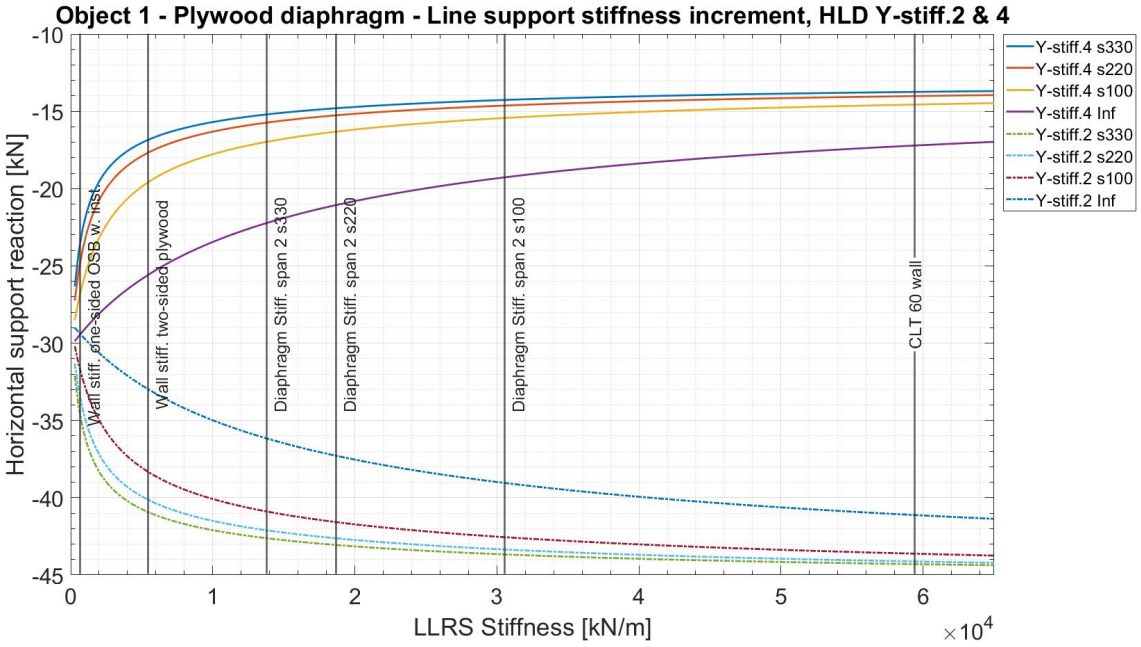

Figure 4.3: Object 1, horizontal load distribution to the line supports y-stiff.2 & 4 of plywood board diaphragm type with varying edge connection stiffness as a function of incremented line support stiffness.

4.3.2.3 Stiffness increment of edge connections

Results obtained from plywood board diaphragm floor type are analyzed in three runs where the lines support stiffness set to the fixed values of; $100kN/m/m$ $500kN/m/m$, and $1000kN/m$ respectively in the three analyses, while the edge connection stiffness is incremented for each loop in the analyses, with obtained results shown in Figure 4.4 and full reports of all analyses can be found in the Appendix E

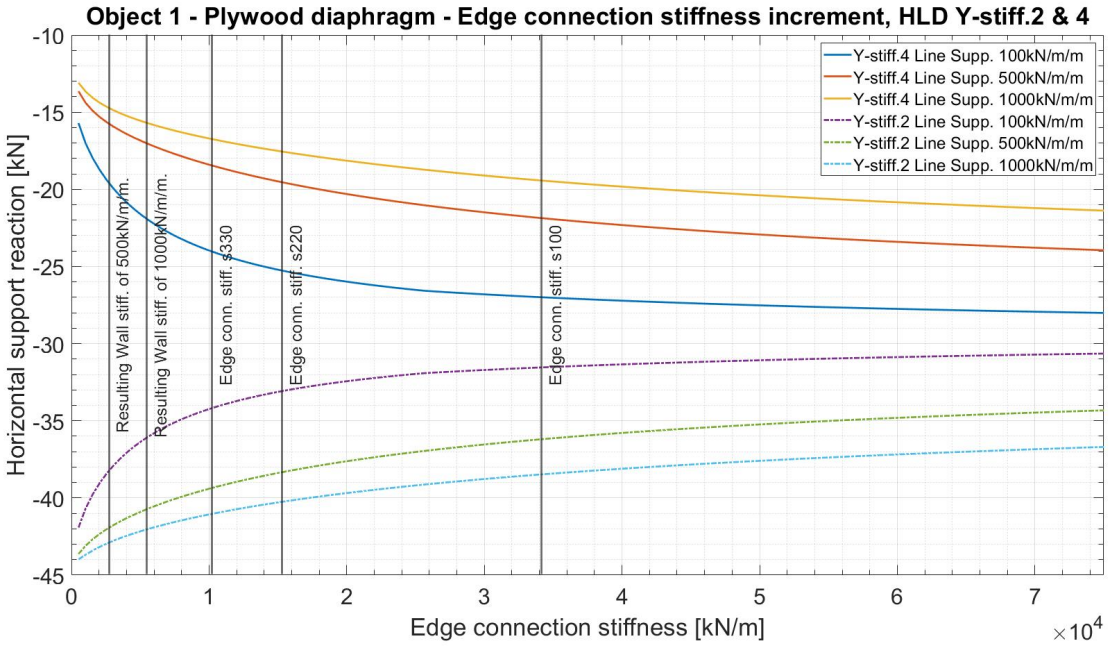

Figure 4.4: Object 1, horizontal load distribution to the line supports y-stiff.2 & 4 of plywood board diaphragm type where the line support stiffness is fixed to; 100/500/1000 kN/m/m, as a function of incremented edge connection stiffness.

4.3.3 CLT panels diaphragm

The CLT diaphragm type is analyzed in two main tracks, where either the line support stiffness is increased for each loop and a fixed stiffness value of the edge connection between adjacent CLT panels. Or, the edge connection between the adjacent panels is increased for each loop, and the line supports (shear walls) have a fixed stiffness value. Results from the analysis are presented in the following subchapters.

4.3.3.1 Diaphragm stiffness

Obtained diaphragm stiffness of the CLT panel diaphragm, with the four different structural joints seen in Section 3.1.3.1, are shown in Table 4.8. The line support stiffness was set to infinitely stiff when the diaphragm stiffness was evaluated.

Table 4.8: Diaphragm stiffness of object 1 with the floor type of CLT panels.

Type of analysis	Span	Deflection (mm)	Stiffness (kN/m)
FEM -	1	0.0635	479950
Inf. stiff.	2	0.1284	442695
	3	0.0545	559210
FEM -	1	0.1123	271390
Cross pair s100	2	0.2761	205875
	3	0.1139	267575
FEM -	1	0.1553	196245
Cross pair s250	2	0.4792	118620
	3	0.1797	169600
FEM -	1	0.1800	169315
Cross pair s350	2	0.6134	92670
	3	0.2216	137530

4.3.3.2 Stiffness increment of line supports

Results obtained from the parametric analysis of the CLT diaphragm, with the four different designs of structural joints see Section 3.1.3.1, and stiffness increment of the line supports are presented in Figure 4.5. Complete results are found in Appendix E.

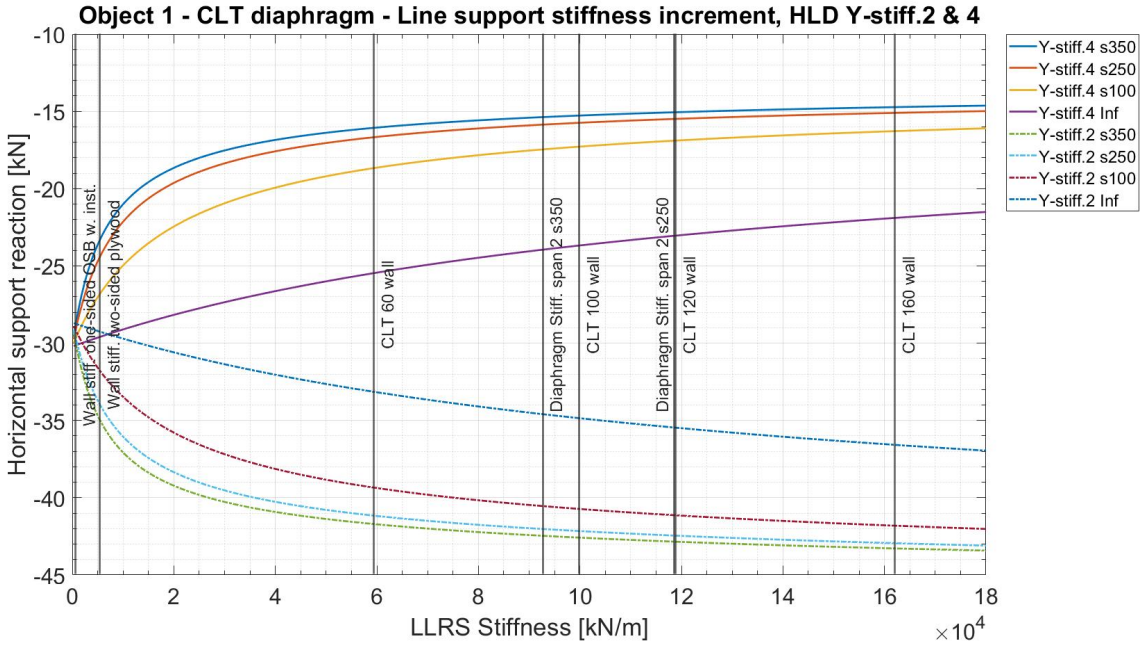

Figure 4.5: Object 1, horizontal load distribution to the line supports y-stiff.2 & 4 of CLT diaphragm type with varying edge connection stiffness as a function of incremented line support stiffness.

4.3.3.3 Stiffness increment of edge connections

Obtained results of the CLT diaphragm type, analyzed in two runs where the lines support stiffness are set to the fixed values of; $500kN/m/m$, and $1000kN/m$ in the respective analysis, while the edge connection stiffness is incremented, are shown in Figure 4.6. Full reports of all analyses can be found in the Appendix E

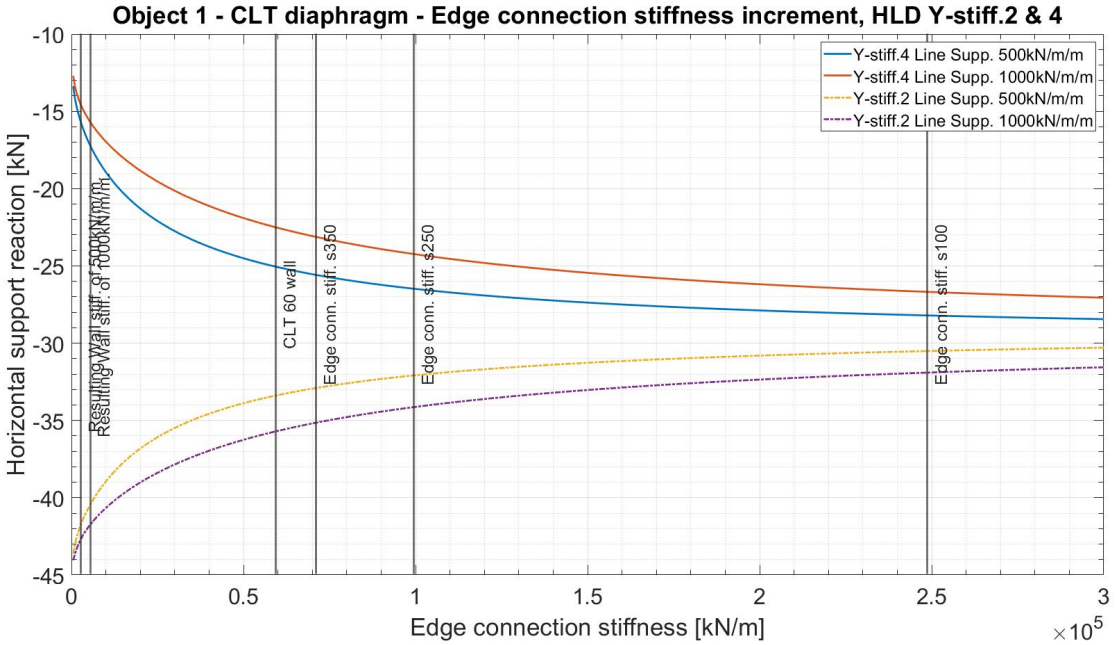

Figure 4.6: Object 1, horizontal load distribution to the line supports y-stiff.2 & 4 of CLT diaphragm where the line support stiffness is fixed to; 500kN/m/m, and 1000kN/m/m, as a function of incremented edge connection stiffness.

4.3.4 TCC panel diaphragm

The TCC diaphragm type of Object 1 is analyzed with the line support stiffness increased for each loop and with a fixed stiffness value of the edge connection between adjacent TCC elements. Results from the analysis are presented in the following subchapters.

4.3.4.1 Diaphragm stiffness

The TCC element diaphragm stiffness is numerically obtained for two different edge connection stiffness types, infinitely stiff, and $50000kN/m$, and the obtained diaphragm stiffness of the TCC diaphragms are shown in Table 4.9. When the diaphragm stiffness was evaluated, the line support stiffness was set to infinitely stiff.

Table 4.9: Diaphragm stiffness of object 1 with the floor type of TCC panels.

Type of analysis	Span	Deflection (mm)	Stiffness (kN/m)
FEM	1	0.0097	3141945
Inf. stiff	2	0.0184	3089230
	3	0.0094	3242220
FEM	1	0.0293	1040170
$50000kN/m$	2	0.0895	635105
	3	0.0354	860930

4.3.4.2 Stiffness increment of line supports

The TCC diaphragm is analyzed in two different sets of line support stiffness increments, where the edge connection stiffness is fixed to; infinitely stiff, and $50000kN/m/m$, where the latter is the obtained shear connection stiffness for grouted concrete joints, see table 4.5. Collected results of the study are shown in Figure 4.7 and full results are found in Appendix E.

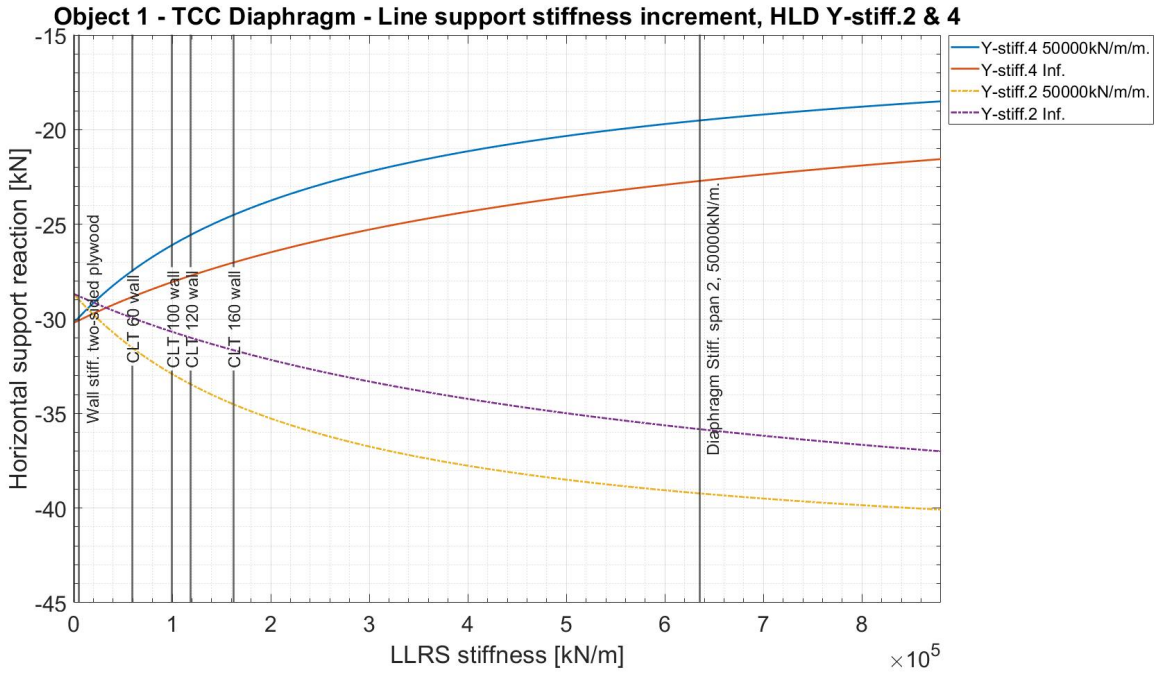

Figure 4.7: Object 1, horizontal load distribution to the line supports y-stiff.2 & 4 of TCC diaphragm type with varying edge connection stiffness as a function of incremented line support stiffness.

4.4 Stiffness relations at 20% redistribution

Extracted stiffness relation of the diaphragm and shear walls at the points of 20% redistribution of the horizontal action, from the either absolute end of rigid or flexible response is the stiffness relation in Table 4.10 obtained.

Table 4.10: Stiffness relation of diaphragm and LLRS for the support *Y-stiff.4* in Object 1, at the redistribution percentages of 20% from rigid and flexible ends.

Diaphragm type	Edge conn. type	Stiffness relation Span 2/ *Y-Stiff.4*		Stiffness relation Span 2/ *Y-Stiff.2*	
		Rigid	Flexible	Rigid	Flexible
Particleboard	-	14.2	1.2	16.9	1.4
TCC	50000	12.8	1.4	14.0	1.6
Plywood	s330	47.6	2.1	48.4	1.7
	s220	43.8	2.1	43.8	1.6
	s100	43.0	2.2	40.7	1.8
CLT	s350	54.5	3.1	50.2	2.4
	s250	52.2	2.9	52.2	2.4
	s100	52.3	3.0	42.6	2.0

4.5 Object 2

Results obtained from the parametric study of Object 2 with the different structural floors are presented in this chapter. Common for upcoming figures are, obtained horizontal reaction force of line supports *y-stiff.1*,*y-stiff.3* and *y-stiff.4* in relation to the shear wall stiffness are presented collected in the figures, for each structural floor with solid, dash-dotted, and dashed colored lines, respectively. Furthermore, vertical stiffness reference lines are shown in the figures, where each line stiffness reference is stated either in the figures or on the legend of the figure. Design horizontal action on Object 2 is $6.376 kN/m$ and derived in Appendix D

Wall stiffness references of Object 2 are calculated with the mean shear wall length of $5.7m$, thus approximated stiffness reference as the shear wall length varies according to Table3.2, multiplied by the obtained shear wall stiffness given in Chapter 4.1. Furthermore, to present the line support stiffness from the FE model in unit kN/m on the x-axis of the figures, the line support stiffness, $kN/m/m$, from FE analysis is also multiplied by the length of $5.7m$ and results in mean stiffness of the shear walls with the stiff direction in the global y-direction. The FE analyses of stiffness increment on edge connections are the edge connection stiffness defined as, $kN/m/m$, which is multiplied by the total depth of the diaphragm, $12.7m$, to obtain the reference in kN/m on the x-axis of figures. Lastly, diaphragm stiffness is presented in each subchapter, diaphragm stiffness, of specific floor diaphragm.

4.5.1 Particleboard diaphragm

Results obtained for object 2 with particleboards are presented in this section.

4.5.1.1 Diaphragm stiffness

The diaphragm stiffness of Object 2 with the floor type of particleboard is shown in Table 4.11, numerical obtained.

Table 4.11: Diaphragm stiffness of object 2 with the floor type of particleboards.

Type of analysis	Span	Deflection (mm)	Stiffness (kN/m)
FEM	1	0.63	72065
	2	0.26	90770
	3	0.67	62690
	4	4.21	12515

4.5.1.2 Stiffness increment of line supports

The resulting horizontal load distribution to the supports, in relation to the stiffness of the line support (shear walls), is presented in Figure 4.8. However, for particleboard, the obtained horizontal reaction forces showed for *Y-stiff.1-4*.

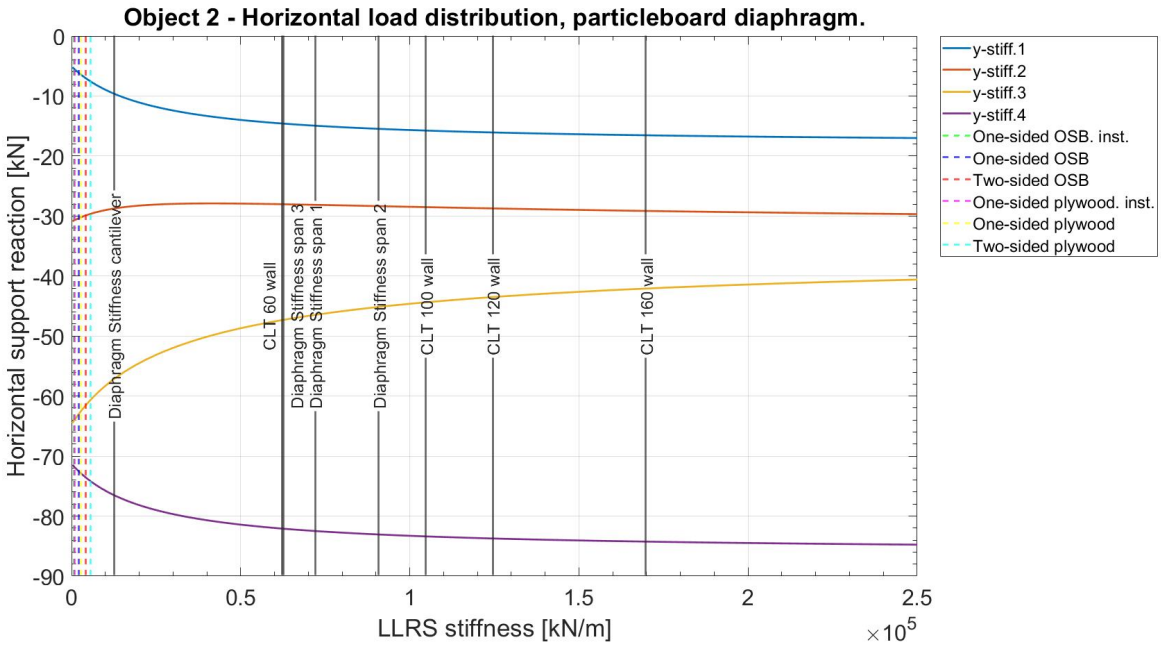

Figure 4.8: Object 2, horizontal load distribution of particleboard diaphragm type with an increment of the line support stiffness.

Moreover, Figure 4.9 presents a zoomed look for wall stiffness up to $15000kN/m$, to ease the interpretation of the horizontal load distribution in the stiffness range of the sheathed framed stud wall types.

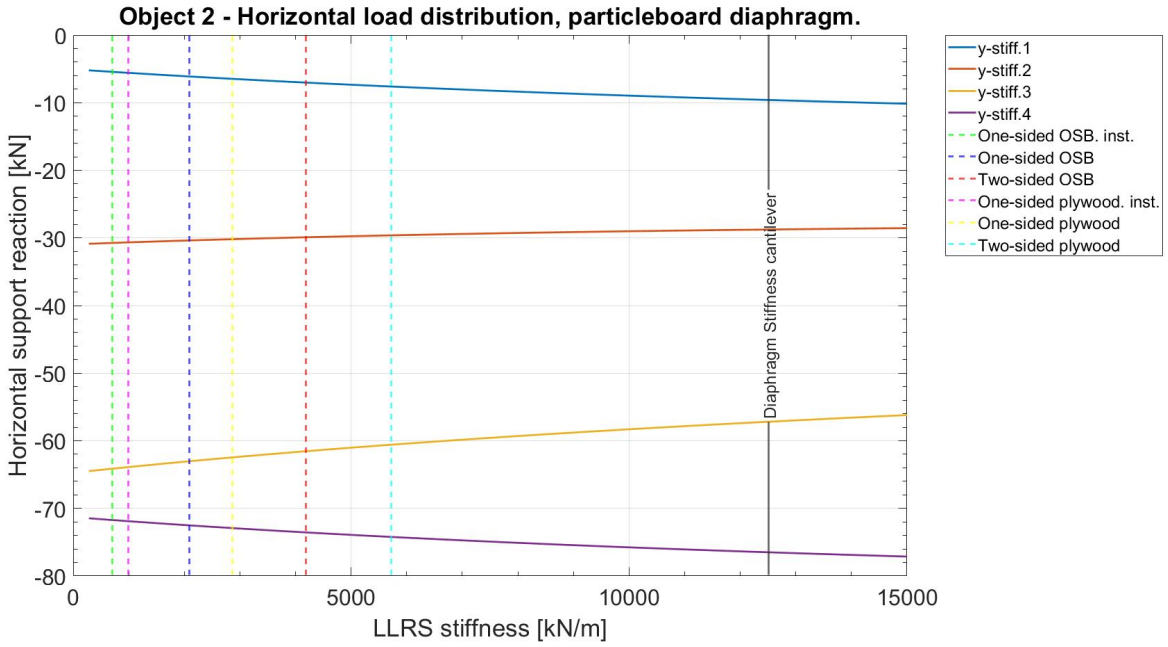

Figure 4.9: Object 2, horizontal load distribution of particleboard diaphragm type with an increment of the line support stiffness. Shear walls stiffness limited to 15k

4.5.2 Plywood panels diaphragm

The plywood diaphragm type for Object 2 is analyzed either with the line support or the edge connection stiffness incremented for each loop in the study. Results from the analysis are presented in the following subchapters.

4.5.2.1 Diaphragm stiffness

The diaphragm stiffness, with the influence of the stiffness of structural joints of the panel-wise plywood board diaphragm type, is presented in Table 4.12. Additionally, the line support stiffness was set to infinitely stiff when the diaphragm stiffness was evaluated.

Table 4.12: Diaphragm stiffness of Object 2 with the floor type of plywood boards with a variation of the edge connection stiffness.

Type of analysis	Span	Deflection (mm)	Stiffness (kN/m)
FEM - inf.	1	0.5304	85600
	2	0.2227	106230
	3	0.8169	51420
	Cantilever	3.9324	13400
FEM - s100	1	1.0529	43120
	2	0.4162	56735
	3	1.7397	24145
	Cantilever	9.2185	5715
FEM - s220	1	1.7414	26075
	2	0.6768	34890
	3	3.0169	13925
	Cantilever	14.3111	3680
FEM - s330	1	2.1607	21015
	2	0.8438	27985
	3	3.8476	10920
	Cantilever	17.3353	3040

4.5.2.2 Stiffness increment of line supports

Results of the analyzes of the panel-wise plywood board diaphragm type are analyzed in four different analyses, see Chapter 3.1.3.1, with an increment of the line supports stiffness are shown in Figure 4.10. A complete compilation of results is found in Appendix E

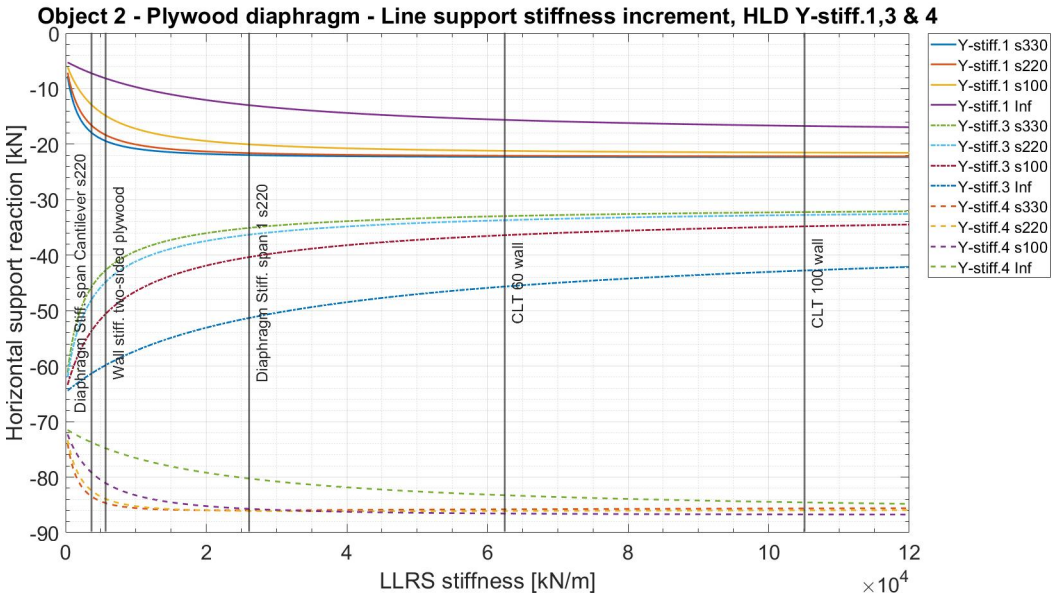

Figure 4.10: Object 2, horizontal load distribution to the line supports y-stiff.1,3 & 4 of plywood board diaphragm type with varying edge connection stiffness as a function of incremented line support stiffness.

4.5.2.3 Stiffness increment of edge connections

Results obtained from plywood board diaphragm floor type are analyzed in three runs where the lines support stiffness set to the fixed values of; $100kN/m/m$ $500kN/m/m$, and $1000kN/m$ respectively in the three analyses, while the edge connection stiffness is incremented for each loop in the analyses, with obtained results shown in Figure 4.11 and full reports of all analyses can be found in the Appendix E

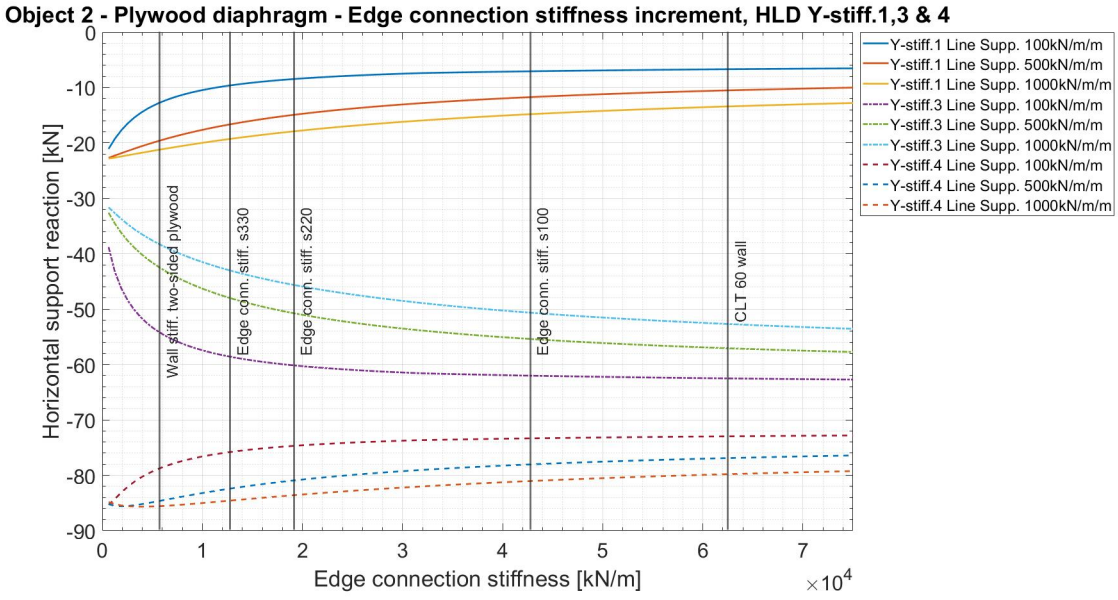

Figure 4.11: Object 2, horizontal load distribution to the line supports y-stiff.1,3 & 4 of plywood board diaphragm type where the line support stiffness is fixed to; 100/500/1000 kN/m/m, as a function of incremented edge connection stiffness.

4.5.3 CLT panels diaphragm

The CLT diaphragm type for Object 2 is analyzed either with the line support or the edge connection stiffness incremented for each loop in the study. Results from the analysis are presented in the following subchapters.

4.5.3.1 Diaphragm stiffness

The obtained results of CLT panel diaphragm stiffness on Object 2 structural floor plan, numerically analyzed with four different edge connection stiffness types stated in Chapter 3.1.3.1, are given in the Table 4.13. When the diaphragm stiffness was evaluated, the line support stiffness was set to infinitely stiff.

Table 4.13: Diaphragm stiffness of object 2 with the floor type of CLT panels.

Type of analysis	Span	Deflection (mm)	Stiffness (kN/m)
FEM - Inf. stiff.	1	0.0870	521880
	2	0.0396	597805
	3	0.1146	365470
	Cantilever	0.4855	108520
FEM - Cross pair s100	1	0.1733	261995
	2	0.0708	334365
	3	0.2620	159860
	Cantilever	1.3128	40135
FEM - Cross pair s250	1	0.2688	168910
	2	0.1111	213080
	3	0.4528	92500
	Cantilever	2.0570	25615
FEM - Cross pair s350	1	0.3248	139790
	2	0.1361	173940
	3	0.5730	73095
	Cantilever	2.4913	21150

4.5.3.2 Stiffness increment of line supports

The horizontal load distribution with the CLT diaphragm, with the structural joints seen in Chapter 3.1.3.1, is shown in Figure 4.12. The complete report of all analyses can be found in the appendix E

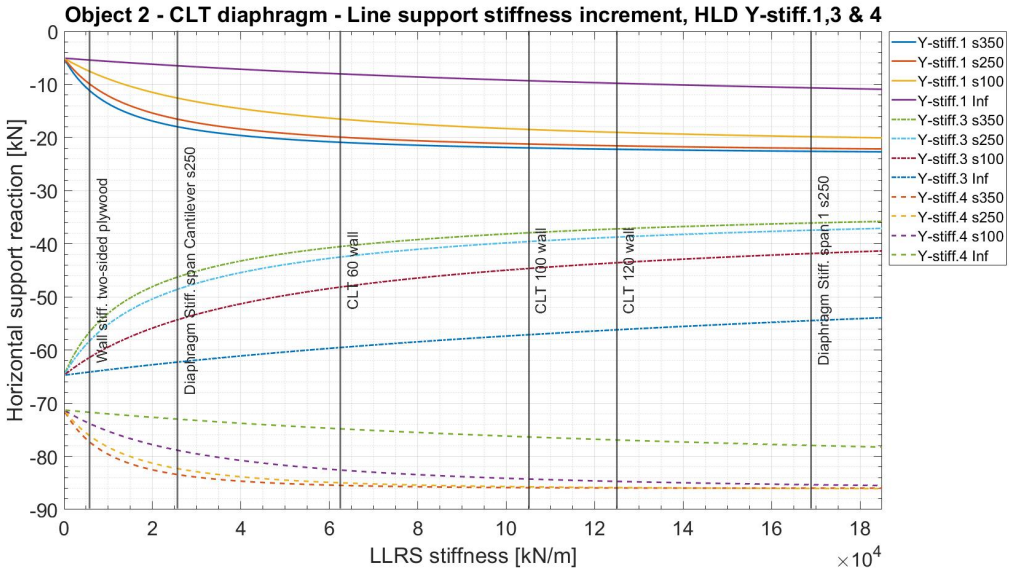

Figure 4.12: Object 2, horizontal load distribution to the line supports y-stiff.1,3 & 4 of CLT panels diaphragm type with varying edge connection stiffness as a function of incremented line support stiffness.

4.5.3.3 Stiffness increment of edge connections

Results obtained from the CLT diaphragm type were analyzed in two runs where the lines support stiffness set to the fixed values of; $500kN/m/m$, and $1000kN/m$ respectively in the two analyses, while the edge connection stiffness is incremented for each loop in the analyses, with obtained results shown in Figure 4.13 and full reports of all analyses can be found in the Appendix E

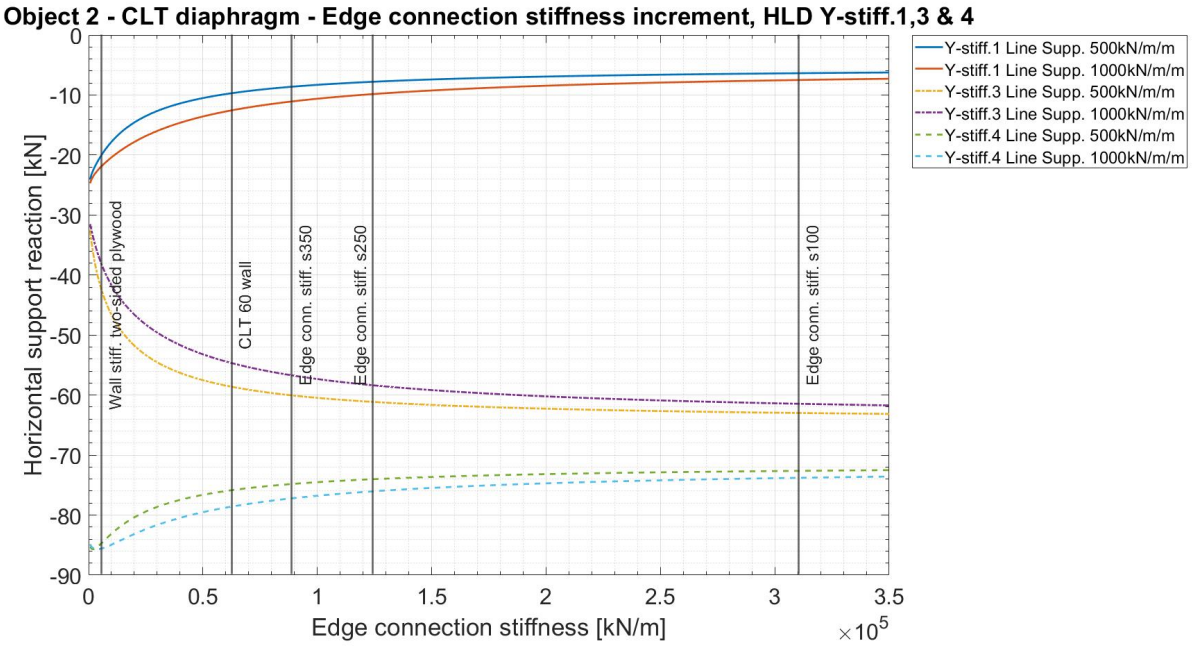

Figure 4.13: Object 2, horizontal load distribution to the line supports y-stiff.1,3 & 4 of CLT panel diaphragm type where the line support stiffness is fixed to; 500/1000 kN/m/m, as a function of incremented edge connection stiffness.

4.5.4 TCC panels diaphragm

The TCC diaphragm type of Object 2 is analyzed with the line support stiffness increased for each loop and with a fixed stiffness value of the edge connection between adjacent TCC elements. Results from the analysis are presented in the following subchapters.

4.5.4.1 Diaphragm stiffness

The TCC element diaphragm stiffness of Object 2 is numerically analyzed for three different edge connection stiffness types, infinitely stiff, $25600kN/m/m$, and $50000kN/m/m$ where the obtained diaphragm stiffness of the TCC diaphragms are shown in table 4.14. When the diaphragm stiffness was evaluated, the line support stiffness was set to infinitely stiff.

Table 4.14: Diaphragm stiffness of Object 2 with the floor type of TCC panels.

Type of analysis	Span	Deflection (mm)	Stiffness (kN/m)
FEM	1	0.0151	3006860
Inf. stiff	2	0.0071	3334225
	3	0.0169	2489060
	Cantilever	0.0859	613360
FEM	1	0.0509	892000
$50000kN/m$	2	0.0234	1011700
	3	0.0786	538300
	Cantilever	0.3693	142500
FEM	1	0.0756	600580
$25600kN/m$	2	0.0357	663110
	3	0.1317	319400
	Cantilever	0.5645	93335

4.5.4.2 Stiffness increment of line supports

Results obtained from the TCC diaphragm analysis on the structural floor plan of Object 2, where edge connection stiffness is set to; infinitely stiff, $25600kN/m/m$, and $50000kN/m/m$, is shown in Figure 4.14. Furthermore, the stiffness of grouted joints are presented in Table 4.5 and complete results of the TCC analyses are found in Appendix E.

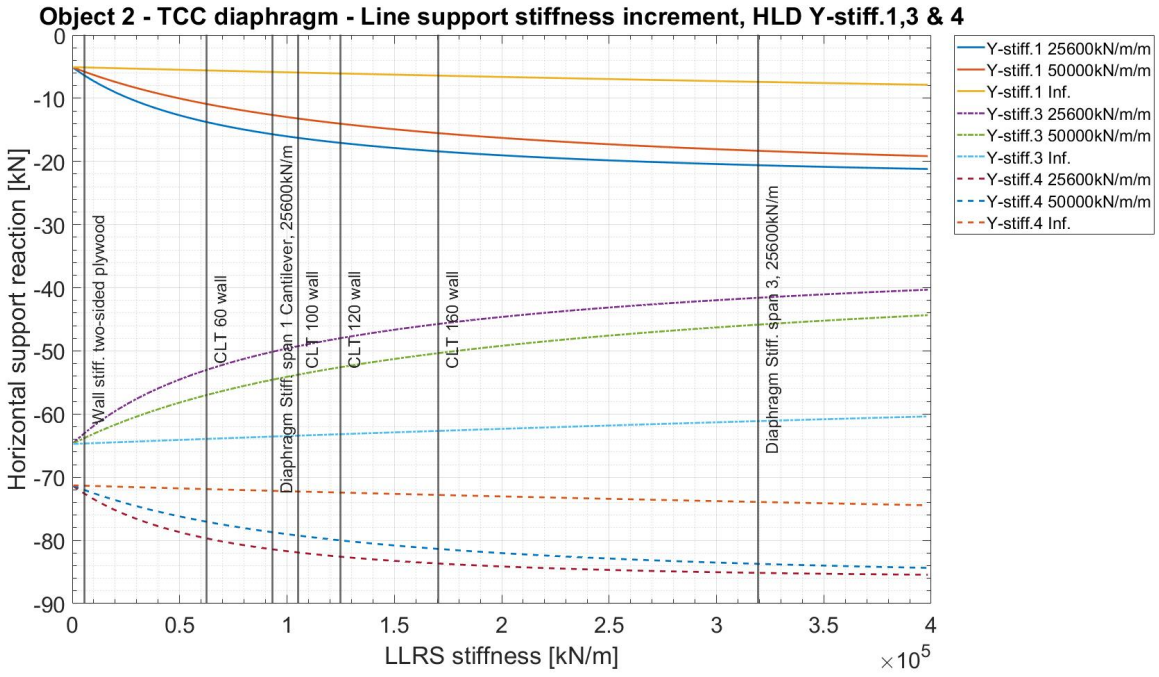

Figure 4.14: Object 2, horizontal load distribution to the line supports y-stiff.1,3 & 4 of TCC diaphragm type with varying edge connection stiffness as a function of incremented line support stiffness.

4.6 Stiffness relations at 20% redistribution

Extracted stiffness relation of the diaphragm and shear walls at the points of 20% redistribution of the horizontal action, from the either absolute end of rigid or flexible response is the stiffness relation in Table 4.15 obtained.

Table 4.15: Stiffness relation of diaphragm and LLRS for the support *Y-stiff.4* in Object 2, at the redistribution percentages of 20% from rigid and flexible ends.

Diaphragm type	Edge conn. type	Stiffness relation Span 1/ *Y-Stiff.1*		Stiffness relation Cantilever/ *Y-Stiff.1*	
		Rigid	Flexible	Rigid	Flexible
Particleboard	-	9.3	0.7	1.6	0.1
TCC	25600	50.9	5.1	7.9	0.8
	50000	41.0	4.0	6.6	0.6
Plywood	s330	38.2	3.4	5.5	0.5
	s100	28.7	2.0	2.1	0.3
CLT	s350	38.0	2.9	5.7	0.4
	s100	22.2	1.5	3.4	0.2
		Span 1/ *Y-Stiff.2/4*		Cantilever/ *Y-Stiff.4*	
Particleboard	-	16.2	1.2	2.8	0.2
TCC	25600	86.8	7.8	14.0	1.2
	50000	67.8	6.3	10.8	1.0
Plywood	s330	84.0	9.4	12.6	1.5
	s100	61.6	6.4	8.2	0.9
CLT	s350	78.4	7.8	11.9	1.2
	s100	49.0	4.7	7.5	0.7
		Span 3/ *Y-Stiff.3*			
Particleboard	-	6.0	0.2		
TCC	25600	21.0	1.6		
	50000	19.0	1.4		
Plywood	s330	17.2	0.7		
	s100	12.7	1.0		
CLT	s350	15.3	0.7		
	s100	10.9	0.6		

5
Discussion

5.1 Analysis of results

Observed for all analyzed floor types is the horizontal load redistribution, when the diaphragm responds from rigid response to flexible, in a non-linear fashion. The majority of the horizontal load redistribution is executed at stiffness ranges closer to the pure rigid response than the pure flexible. In analyzed timber diaphragms, the shear stiffness of a structural joint between two adjacent panels/elements has had a significant impact on the overall diaphragm response. Compared to the stiffer in-plane material plywood, the less stiff in-plane material particleboard obtains a stiffer, and more rigid, membrane behavior when modeled as a solid unit compared to the panel-wise plywood diaphragm. Even with a dense spacing of screws of the plywood diaphragm, the particleboard still shows a more rigid behavior than the panel-wise plywood diaphragm. Additionally, the same tendency of impact by the edge connection stiffness is obtained for the notably in-plane stiffer CLT panel diaphragm, however, the structural joints adjoining CLT panels can be designed stiffer, compare stiffness in Table 4.3 and Table 4.4, thus a reduced effect of the structural joints is obtained, but not significant.

The TCC element diaphragm with an 80 *millimeter* thick precast concrete diaphragm is about 3-4 times stiffer compared to the stiffest timber alternatives, CLT with edge connection of s100 spacing, in this study. Resulting in an overall more rigid response on the structural floor plan of Object 1, seen in Figure 4.7. Moreover, the TCC diaphragm with an edge connections stiffness of $50000kN/m/m$ in a parallel offset manner to the infinitely stiff reference does not show the same accelerated tendencies as the timber diaphragms with structural joints. However, on the structural floor plan of Object 2, isn't the shear stiffness of the grouted joint stiff enough to resist the accelerated transition from rigid to flexible response of the diaphragm, shown in Figure 4.14. Lastly, the analytically obtained stiffness of grouted joints is questionable and further discussed in Section 5.3.

In the analyses with present structural joints influencing the diaphragm response, an accelerated effect in the reform from pure rigid to flexible response of the diaphragm is observed for the more demanding structural floor plan of Object 2, i.e., the cantilever. It could be explained by the rapidly obtained displacement in the edge connections at the cantilever span of Object 2 when the stiffness of the shear wall is increased and starts to semi-lock the diaphragm, thus, interrupting the rigid response of the diaphragm.

Furthermore, by simplifying the calculation model of a diaphragm with present structural joints to a solid diaphragm without structural joints. Or by setting the shear stiffness of structural joints set to infinitely stiff. This will result in an improper load distribution of horizontal actions in the calculations model. For instance, comparing the obtained results of the plywood diaphragm on the structural floor plan of Object 1 with a shear wall stiffness of $5400kN/m$. The obtained horizontal support reaction of line support *Y-stiff.2* is $34kN$ with an edge connection stiffness of $1500kN/m/m$(s220 screw spacing) and $40kN$ if the edge connection is analyzed as infinitely stiff in shear. The deviation is approximately $6kN$ for each storey of the building, and Object 1 is a six-storey building, thus, the horizontal connection force to the foundation, with 6 storeys above, will be underestimated by $36kN$, if the assumption of infinitely stiff edge connections between the plywood panels is incorrect.

5.2 Diaphragm classification

As discussed, the diaphragm transition from rigid to flexible, or vice versa, is in a non-linear fashion for all studied diaphragms. The non-linear behavior adds complexity to analytically classify if the diaphragm response is rigid, semi-rigid, or flexible.
However, with no guidance on diaphragm classification provided by the building regulations, the classification is divided into limits of percentages of redistributed horizontal loads of the difference in the obtained horizontal support reaction between the rigid and flexible diaphragm response. The limit of choice for the redistribution of the horizontal loads, to the classification, is 20-60-20 percent and corresponds to the classifications of rigid, semi-rigid, and flexible response respectively. Thus, the classification of rigid and flexible response is limited to 20% redistribution of the total difference in support reaction obtained between pure rigid or pure flexible diaphragm. Moreover, the limit of 20% is derived from the difference in designing in safety class 1 or 2, in the Eurocodes. If a structural part is designed in safety class 1 the design load is multiplied by a factor of $\gamma_d = 1$, moreover, if it is designed in safety class 2 the design load is multiplied by a factor of $\gamma_d = 0.91$. Thus, with the allowance of 20% redistribution, the difference in support reaction is mostly covered by the difference in safety class design.

Summarized stiffness relation of diaphragm span 2 and LLRS *Y-stiff.2 & 4*, on the structural floor plan of Object 1, at 20% redistribution of horizontal loads, for both rigid and flexible diaphragm, are presented in Table 4.10. Stiffness relations from

the table, show that the particleboard diaphragm and the TCC diaphragm correlate well in the stiffness relations at the boundaries of the classification. Even though the TCC diaphragm comprises structural joints, are the joints stiff enough to prove a more rigid response. Selected values of stiffness relations for particleboard and TCC diaphragms and LLRS are, a classification of rigid if the least stiff diaphragm span is 15 times stiffer or more, and the flexible classification is reached if the diaphragm is 1.5 times stiffer or less. Moreover, stiffness relations of the timber diaphragms plywood and CLT, with structural joints, are also derived from Table 4.10. Plywood diaphragm can be classified as rigid if the diaphragm is about 45 times, or more, stiffer than the LLRs, and a flexible classification of response is if the diaphragm is 2 times stiffer or less than the LLRS. Finally, for Object 1, the CLT diaphragm response is classified as rigid if the CLT diaphragm is 52 times stiffer, or more than the LLRS, and flexible response at a diaphragm stiffness of 2.5 times or less.

Continuing, by studying the stiffness relations of the diaphragm, with the stiffness of *Y.stiff.1,2,3 & 4* of Object 2, at the redistribution degree of 20% for the horizontal loads, from rigid and flexible response, collected in Table 4.15. No correlations or similarities in stiffness relations are observed, which may be the basis for the classification.

In regard to generalized response, no evident correlation between the redistribution of horizontal loads and wall stiffness, for the different joist/slab types, has ocularly been obtained by studying the reference lines in figures. However, it can be generalized that the studied plywood diaphragms response can be classified as semi-rigid at the lowest magnitudes of shear stiffness, and flexible response from a shear stiffness of LLRS corresponding to CLT60 walls, with no regard for shear wall stiffness nor the spacing of the connection. The same generalization can be done for the CLT diaphragm with a sparse spacing of screws, s250, or greater spacing. A final generalization is that the TCC diaphragm is behaving rigidly if the LLRS are sheathed stud shear walls.

5.3 Method and assumptions

5.3.1 Evaluation of structural floor plans

The structural floor plan 1 obtains two end spans and one interior, in the direction of the horizontal loads. Furthermore, the length of the shear wall in the same direction is almost the same, resulting in almost the same stiffness in the line supports during the FE analysis which is beneficial for the interpretation of the results. Furthermore, the staircase and elevator shaft is located at the bottom of the floor plan, and thus, have the least possible impact on the structural joints.

Object 2 on the other hand, has several factors creating unnecessary complexities in the study to determine stiffness relations between the diaphragm and LLRS. E.g., The length of the shear walls, parallel to the load direction and in the global Y-

direction, varies for 3 of 4 shear walls. Furthermore, the cantilever span length is in a longer region and, therefore, obtains a significantly lower stiffness than the other spans. Besides, the placement of the shafts, slightly above the middle in the Y-direction, and towards the periphery of the load attachment giving a local shorter length of edge connection of span 3, had a noticeable impact on span 3, as span 3 obtained a less stiff than for instance span 1, which is a longer span, plus that the cantilever span helps to stiffen up span 3.

5.3.2 Analytical models

The ultimate limit slip modulus, K_u, in Section 3.3.1 is obtained by an analytical model given in Eurocode, in practice, if the screw supplier is known, the manufactures test data can be used that might give a higher value of the slip modulus. Also, the analytical model in Eurocode is only considering the wood density and diameter of the screw, indicating that it may be too simplified for some constellations.

The shear wall stiffness reference in the plotted figures is calculated as independent panels with $1m$ of width, thus if several adjacent sheathed studs walls are rigidly connected and work in unity, a much greater shear stiffness is obtained than the reference in this study, hence, must be considered if comparing against the figures.

Regarding the obtained aggregate inter-locking shear stiffness in Chapter 3.3.2 of the grouted TCC element joints, the used theory behind is evaluated for hollow-core slabs, hence, created and adapted for the hollow-core joints design. However, the TCC joint design reminds of the hollow-core joint in a scaled-down size, and when multi-choice were given, the most conservative choice was used. Also, no shear stiffness contribution of mechanical fasteners was added to the analysis. Hence, the obtained, and used in the parametric study, shear stiffness values of the grouted TCC connection are likely to be conservative.

5.3.3 Numerical analyses

The diaphragms are analyzed in the FE software as pure shell elements with edge connection stiffness properties to adjacent panels, except for the particleboard diaphragm which is seen as a homogeneous shell, and line supports. Furthermore, elements that would have improved the rigidity of the diaphragms, such as timber chords for the joist floors, and mechanical connections in the y' direction of edge connections on CLT and TCC floors are not included in the models. Additional variables had added increased complexity to the FE models, and to the C# script, however, obtained results had probably been closer to the real diaphragm behavior. Moreover, the models were analyzed for pure horizontal loads in a first-order linear elastic theory, eventual influences of buckling/out-of-plane displacements are thus neglected. Also, the degree of trustworthiness of characterizing the particleboard diaphragm as a solid shell, without structural joints, due to it being glue screwed when mounted might be questionable.

6
Conclusion and future work

6.1 Conclusion

The aim of this project was to conclude stiffness relations of common timber/hybrid diaphragms suitable for up to mid-rise structures, furthermore, and examine if generalized guidance of different constellations of diaphragms and LLRS, to ease in the early design phase. The conclusions are as follows:

The parametric stiffness study of Object 1 examined stiffness relations of the diaphragm and LLRS to facilitate the diaphragm response classification. Recommended stiffness relations of the diaphragms and LLRS are;

- Plywood diaphragm can be classified as rigid if the diaphragm is 45 times stiffer, or greater, than the LLRS, and a flexible classification of response is expected if the diaphragm is 2 times stiffer, or less than the LLRS.
- CLT diaphragm response is classified as rigid if the CLT diaphragm is 52 times stiffer, or more than the LLRS, and flexible response at a diaphragm stiffness of 2.5 times or less.
- Particleboard and TCC diaphragms response are rigid if the least stiff diaphragm span is 15 times stiffer or more than LLRS, and a flexible classification is reached if the diaphragm is 1.5 times stiffer or less.

The diaphragm response in the intermediate stiffness relations to rigid and flexible response is considered semi-rigid.

Stiffness relations to classify the diaphragm response on the structural floor plan of Object 2 were not obtained, as stiffness correlations between analyzed diaphragms and the LLRS could not be observed in the parametric study.

Generalized system response to classify the diaphragm response evaluated from results of Object 1 and Object 2;

- Plywood diaphragm response, with present structural joints, can be classified as semi-rigid at the lowest stiffness magnitude of LLRS, and flexible response at stiffness of LLRS corresponding to CLT60 walls.
- TCC diaphragm response can be considered rigid if the stiffness of LLRS is up to two-sided sheathed stud wall.

6.2 Suggestion of future work

Propositions of further work are to examine further structural floor plans, that resemble Object 1, however, with some deviations in the structural floor plan and without a cantilever, to verify the obtained classification boundaries of diaphragm response by stiffness relations of the diaphragm and LLRS for Object 1.

Examine if a more rigid response is obtained in the CLT and TCC diaphragm, with more comprehensive modeling of adding the variable of locally increased stiffness by structural mechanical fasteners added on the diaphragm i.e., perforated flat plate on the CLT diaphragm and steel connections on the TCC diaphragm, which is used in the periphery to resist bending moment.

Lastly, analytical models to obtain the in-plane deformations of the various diaphragm constellations in this study.

Bibliography

[1] About the EN Eurocodes. (2023, January 25). European Comission. https://eurocodes.jrc.ec.europa.eu/en-eurocodes/about-en-eurocodes

[2] Thelandersson, S. (Ed.) (2003). Timber Engineering. John Wiley & Sons Inc.

[3] Blaß, H. J., & Sandhaas, C. (2017). Timber Engineering - Principles for Design. KIT Scientific Publishing. https://doi.org/10.5445/KSP/1000069616

[4] Bell, M., Randy Jensen, William Munyan, Shows Leary, Bill Fenstermacher, Mike Hansen, Dennis Milsten, Kerry DePape, Myron Jonzon, Jim Taylor, & Martin Boutet. (2014). Architectural Woodwork Standards. Edition 2.

[5] Hosker, R. P. (1985). Flow around isolated structures and building clusters: A review.

[6] Elliott, K. S. (2019). Precast Concrete Structures (Second edition). CRC Press. https://doi.org/10.1201/9780367814885

[7] Björn Engström. (n.d.). DISTRIBUTION OF HORIZONTAL LOAD ON BRACING ELEMENTS .

[8] Robert Kliger, Marie Johansson, Roberto Crocetti, Annika Mårtensson, Helena Lidelöw, Bert Norlin, & Anna Pousette. (2022). Design of timber structures Volume 1. Third UK edition.

[9] Gustafsson, A. (2019). The CLT Handbook, CLT structures - facts and planning (E. Borgström & J. Fröbel, Eds.; First edition). Skogsindustrierna.

[10] European Standard. (2010a). Eurocode - Basis of structural design. CEN.

[11] European Standard. (2010b). Eurocode 2: Design of concrete structures - Part 1-1 : General rules and rules for buildings. CEN.

[12] Boverket. (2022). BFS 2022:4 (EKS 12).

[13] European Standard (2022). Eurocode 5: Design of timber structures — Common rules and rules for buildings — Part 1-1: General. Unpublished manuscript.

[14] European Standard (2004). Eurocode 5: Design of timber structures - Part 1-1: General - Common rules and rules for buildings. CEN.

[15] European Standard (2010c). Eurocode 1: Actions on structures - Part 1-4: General actions - Wind actions . CEN.

[16] Schodek, D. L., & Bechthold, M. (2014). Structures (7th ed.). Pearson.

[17] Källsner, B., & Girhammar, U. A. (2009). Horisontalstabilisering av träregelstommar - Plastik dimensionering av väggar med träbaserade skivor.

[18] Ottosen, N., & Petersson, H. (1992). Introduction Finite Element Method. Pearson Education (us).

A

Analytical calculations - Horizontal load distribution

Analytical calculations to obtain horizontal load distribution of a rigid diaphragm on the structural floor plan of Object 1 and 2 is presented in this chapter.

Analytical stiffness distribution of horizontal actions of structural floor plans of Object 1 and Object 2

Structural Floor plan Object 1, shear wall stiffness per meter

Length of shear walls, Object floor plan 1

$SH_{1.1.1} := 1.8\ m$ 2st

$SH1_{1.1.2} := 5.4\ m$ 2st

$SH_{1.1.3} := 2.4\ m$

$SH_{1.2.1} := 3.0\ m$ 2st

$SH_{1.2.2} := 4.6\ m$

$SH_{1.2.3} := 3.6\ m$

$SH_{1.2.4} := 5.2\ m$ 2st

$$h_{1.all} := \begin{bmatrix} 1.8 \\ 5.4 \\ 2.4 \\ 3.0 \\ 4.6 \\ 3.6 \\ 5.2 \end{bmatrix} \cdot m$$

Normalize with length 2.4m. Stiffness is in proportion to total length.

$$s_{normlized} := \frac{h_{1.all}}{h_{1.all_{2,0}}} = \begin{bmatrix} 0.75 \\ 2.25 \\ 1 \\ 1.25 \\ 1.917 \\ 1.5 \\ 2.167 \end{bmatrix}$$

x 2st
y 2st
x
x 2st
x
x
y 2st

$$s_{normlized.full} := \begin{bmatrix} s_{normlized}(0,0) \\ s_{normlized}(0,0) \\ s_{normlized}(1,0) \\ s_{normlized}(1,0) \\ s_{normlized}(2,0) \\ s_{normlized}(3,0) \\ s_{normlized}(3,0) \\ s_{normlized}(4,0) \\ s_{normlized}(5,0) \\ s_{normlized}(6,0) \\ s_{normlized}(6,0) \end{bmatrix} = \begin{bmatrix} 0.75 \\ 0.75 \\ 2.25 \\ 2.25 \\ 1 \\ 1.25 \\ 1.25 \\ 1.917 \\ 1.5 \\ 2.167 \\ 2.167 \end{bmatrix}$$

$Sy\_um := s_{normlized_{1,0}} \cdot 2 + s_{normlized_{6,0}} \cdot 2 = 8.833$

$Sx\_um := s_{normlized_{0,0}} \cdot 2 + s_{normlized_{2,0}} + s_{normlized_{3,0}} \cdot 2 + s_{normlized_{4,0}} + s_{normlized_{5,0}} = 8.417$

Rot center calc, origo at the bottom left corner

$$x_t := \frac{0\ m \cdot s_{normlized_{1,0}} + 19.475\ m \cdot s_{normlized_{1,0}} + 5.04\ m \cdot s_{normlized_{6,0}} + 14.40\ m \cdot s_{normlized_{6,0}}}{Sy\_um}$$

$$y_t := \frac{0\ m \cdot s_{normlized_{0,0}} \cdot 2 + 10.27\ m \cdot s_{normlized_{2,0}} + 6.84\ m \cdot s_{normlized_{3,0}} \cdot 2 + 4.88\ m \cdot s_{normlized_{4,0}} + 4.88\ m \cdot s_{normlized_{5,0}}}{Sx\_um}$$

$x_t = 9.729\ m$

$y_t = 5.233\ m$

Torsional moment

Shear center appears at

$SH := 19.5\ \frac{m}{2} = 9.75\ m$

Total horizontal force

$H := 6.047\ \frac{kN}{m} \cdot 19.5\ m = 117.917\ kN$

Horizontal action acting in negative Y-direction

$T_{neg.Y} := (SH - x_t) \cdot H = 2\ kN \cdot m$

Ortogonal distance in respect of the stiffness direction of the walls to rotational center.

$$sh_{dist} := \begin{bmatrix} -5.233 \\ -5.233 \\ -9.729 \\ 9.729 \\ 5.04 \\ 1.60 \\ 1.60 \\ -0.35 \\ -0.35 \\ -4.69 \\ 4.69 \end{bmatrix} m$$

$$ST_{vector} := \overrightarrow{sh_{dist}{}^{2} \cdot s_{normlized.full}} = \begin{bmatrix} 20.538 \\ 20.538 \\ 212.97 \\ 212.97 \\ 25.402 \\ 3.2 \\ 3.2 \\ 0.235 \\ 0.184 \\ 47.658 \\ 47.658 \end{bmatrix} m^2$$

$$ST := \sum ST_{vector} = 595\ m^2$$

Horizontal force distribution due to rotation

$$H_c := T_{neg.Y} \cdot \frac{\overrightarrow{s_{normlized.full} \cdot sh_{dist}}}{ST} = \begin{bmatrix} -0.016 \\ -0.016 \\ -0.092 \\ 0.092 \\ 0.021 \\ 0.008 \\ 0.008 \\ -0.003 \\ -0.002 \\ -0.042 \\ 0.042 \end{bmatrix} kN$$

Sorting normalization of walls stiffness in the global X and Y direction

$$s_{normlized.x} := \begin{bmatrix} s_{normlized.full}(0,0) \\ s_{normlized.full}(1,0) \\ s_{normlized.full}(4,0) \\ s_{normlized.full}(5,0) \\ s_{normlized.full}(6,0) \\ s_{normlized.full}(7,0) \\ s_{normlized.full}(8,0) \end{bmatrix} = \begin{bmatrix} 0.75 \\ 0.75 \\ 1 \\ 1.25 \\ 1.25 \\ 1.917 \\ 1.5 \end{bmatrix} \qquad s_{normlized.y} := \begin{bmatrix} s_{normlized.full}(2,0) \\ s_{normlized.full}(3,0) \\ s_{normlized.full}(9,0) \\ s_{normlized.full}(10,0) \end{bmatrix} = \begin{bmatrix} 2.25 \\ 2.25 \\ 2.167 \\ 2.167 \end{bmatrix}$$

$s_{norm.x.sum} := \sum s_{normlized.x} = 8.417$ $s_{norm.y.sum} := \sum s_{normlized.y} = 8.833$

Translational distribution of horizontal loads to supports with shear stiffness in Y-direction

$$H_{b.y} := H \cdot \frac{s_{normlized.y}}{s_{norm.y.sum}} = \begin{bmatrix} 30.035 \\ 30.035 \\ 28.923 \\ 28.923 \end{bmatrix} \ kN$$

Rotational distribution of horizontal loads

$$H_c = \begin{bmatrix} -0.016 \\ -0.016 \\ -0.092 \\ 0.092 \\ 0.021 \\ 0.008 \\ 0.008 \\ -0.003 \\ -0.002 \\ -0.042 \\ 0.042 \end{bmatrix} \ kN$$

Total distribution of horizontal loads to the supports of floor plan Object 1

$$H_{final.y.neg.wind.direction} := \begin{bmatrix} H_{b.y}(0,0) + H_c(0,0) \\ H_{b.y}(1,0) + H_c(1,0) \\ H_c(2,0) \\ H_c(3,0) \\ H_c(4,0) \\ H_c(5,0) \\ H_c(6,0) \\ H_c(7,0) \\ H_c(8,0) \\ H_{b.y}(2,0) + H_c(9,0) \\ H_{b.y}(3,0) + H_c(10,0) \end{bmatrix} = \begin{bmatrix} 30.019 \\ 30.019 \\ -0.092 \\ 0.092 \\ 0.021 \\ 0.008 \\ 0.008 \\ -0.003 \\ -0.002 \\ 28.88 \\ 28.965 \end{bmatrix} \ kN$$

y	sh1.1	
x	sh2.1	
x	sh2.2	
x	sh2.3	
x	sh2.4	
y	sh2.5	
y	sh2.6	
y	sh2.7	

Structural Floor plan Object 2, shear wall stiffness per meter

Same type of walls -> constant E

Length of shear walls, floor plan 2

$SH_{2.1.1} := 7.3\ m$ $\quad b := 0.022\ m$

$SH1_{2.2.1} := 12.0\ m$

$SH_{2.2.2} := 12.2\ m$

$SH_{2.2.3} := 3.6\ m$

$SH_{2.2.4} := 3.4\ m$

$SH_{2.2.5} := 4.5\ m$

$SH_{2.2.6} := 6.4\ m$

$SH_{2.2.7} := 4.5\ m$

$$h_{2.all} := \begin{bmatrix} 7.3 \\ 12.0 \\ 12.2 \\ 3.6 \\ 3.4 \\ 4.5 \\ 6.4 \\ 4.5 \end{bmatrix} \cdot m$$

Normalize with length 3.4m. Stiffness is in proportion to total length.

$$s_{normlized} := \frac{h_{2.all}}{h_{2.all_{4,0}}} = \begin{bmatrix} 2.147 \\ 3.529 \\ 3.588 \\ 1.059 \\ 1 \\ 1.324 \\ 1.882 \\ 1.324 \end{bmatrix} \quad \begin{matrix} y \\ x \\ x \\ x \\ x \\ y \\ y \\ y \end{matrix}$$

Summerize total normalized stiffnes

$Sy\_um := s_{normlized_{0,0}} + s_{normlized_{5,0}} + s_{normlized_{6,0}} + s_{normlized_{7,0}} = 6.676$

$Sx\_um := s_{normlized_{1,0}} + s_{normlized_{2,0}} + s_{normlized_{3,0}} + s_{normlized_{4,0}} = 9.176$

Rot center calc, origo at the bottom left corner

$$x_t := \frac{0\ m \cdot s_{normlized_{0,0}} + 7.48\ m \cdot s_{normlized_{5,0}} + 11.375\ m \cdot s_{normlized_{6,0}} + 18.300\ m \cdot s_{normlized_{7,0}}}{Sy\_um}$$

$$y_t := \frac{5.07\ m \cdot s_{normlized_{1,0}} + 5.07\ m \cdot s_{normlized_{2,0}} + 8.265\ m \cdot s_{normlized_{3,0}} + 8.265\ m \cdot s_{normlized_{4,0}}}{Sx\_um}$$

$x_t = 8.318\ m$

$y_t = 5.787\ m$

Torsional moment

Shear center appears at

$SH := 27\ \frac{m}{2} = 13.5\ m$

Total horizontal force

$H := 6.3765\ \frac{kN}{m} \cdot 27\ m = 172.166\ kN$

Horizontal action acting in negative Y-direction

$T_{neg.Y} := (SH - x_t) \cdot H = 892\ kN \cdot m$

Ortogonal distance in respect of the stiffness direction of the walls to rotational center.

$sh_{1.1} := -8.318\ m$ y
$sh_{2.1} := -0.721\ m$ x
$sh_{2.2} := -0.721\ m$ x
$sh_{2.3} := 2.48\ m$ x
$sh_{2.4} := 2.48\ m$ x
$sh_{2.5} := -0.840\ m$ y
$sh_{2.6} := 3.060\ m$ y
$sh_{2.7} := 9.98\ m$ y

$$sh_{dist} := \begin{bmatrix} -8.318 \\ -0.721 \\ -0.721 \\ 2.48 \\ 2.48 \\ -0.840 \\ 3.060 \\ 9.98 \end{bmatrix} m \quad \begin{matrix} \text{y} \\ \text{x} \\ \text{x} \\ \text{x} \\ \text{x} \\ \text{y} \\ \text{y} \\ \text{y} \end{matrix}$$

Torsional stiffness in the system

$$ST_{vector} := \overrightarrow{sh_{dist}{}^{2} \cdot s_{normlized}} = \begin{bmatrix} 148.553 \\ 1.835 \\ 1.865 \\ 6.512 \\ 6.15 \\ 0.934 \\ 17.626 \\ 131.824 \end{bmatrix} m^2$$

y
x
x
x
x
y
y
y

$$ST := \sum ST_{vector} = 315\ m^2$$

Horizontal force distribution due to rotation

$$H_c := T_{neg.Y} \cdot \frac{\overrightarrow{s_{normlized} \cdot sh_{dist}}}{ST} = \begin{bmatrix} -50.538 \\ -7.201 \\ -7.321 \\ 7.431 \\ 7.018 \\ -3.146 \\ 16.3 \\ 37.378 \end{bmatrix} kN$$

sh1.1
sh2.1
sh2.2
sh2.3
sh2.4
sh2.5
sh2.6
sh2.7

Sorting shear walls in global direction of X and Y

$$s_{normlized} = \begin{bmatrix} 2.147 \\ 3.529 \\ 3.588 \\ 1.059 \\ 1 \\ 1.324 \\ 1.882 \\ 1.324 \end{bmatrix}$$

y
x
x
x
x
y
y
y

$$s_{normlized.x} := \begin{bmatrix} s_{normlized}(1,0) \\ s_{normlized}(2,0) \\ s_{normlized}(3,0) \\ s_{normlized}(4,0) \end{bmatrix} = \begin{bmatrix} 3.529 \\ 3.588 \\ 1.059 \\ 1 \end{bmatrix}$$

$$s_{normlized.y} := \begin{bmatrix} s_{normlized}(0,0) \\ s_{normlized}(5,0) \\ s_{normlized}(6,0) \\ s_{normlized}(7,0) \end{bmatrix} = \begin{bmatrix} 2.147 \\ 1.324 \\ 1.882 \\ 1.324 \end{bmatrix}$$

Summation of total stiffness in repsective direction

$s_{norm.x.sum} := \sum s_{normlized.x} = 9.176$ $\quad$ $s_{norm.y.sum} := \sum s_{normlized.y} = 6.676$

Translational load distribution in Y direction

$$H_{b.y} := H \cdot \frac{s_{normlized.y}}{s_{norm.y.sum}} = \begin{bmatrix} 55.366 \\ 34.13 \\ 48.54 \\ 34.13 \end{bmatrix} \ kN$$

$$H_c = \begin{bmatrix} -50.538 \\ -7.201 \\ -7.321 \\ 7.431 \\ 7.018 \\ -3.146 \\ 16.3 \\ 37.378 \end{bmatrix} \ kN$$

sh1.1
sh2.1
sh2.2
sh2.3
sh2.4
sh2.5
sh2.6
sh2.7

Final horizontal load distribution of combined translation and rotation distribution

$$H_{final.y.neg.wind.direction} := \begin{bmatrix} H_{b.y}(0,0) + H_c(0,0) \\ H_c(1,0) \\ H_c(2,0) \\ H_c(3,0) \\ H_c(4,0) \\ H_{b.y}(1,0) + H_c(5,0) \\ H_{b.y}(2,0) + H_c(6,0) \\ H_{b.y}(3,0) + H_c(7,0) \end{bmatrix} = \begin{bmatrix} 4.828 \\ -7.201 \\ -7.321 \\ 7.431 \\ 7.018 \\ 30.984 \\ 64.84 \\ 71.508 \end{bmatrix} \ kN$$

y sh1.1
x sh2.1
x sh2.2
x sh2.3
x sh2.4
y sh2.5
y sh2.6
y sh2.7

B

Analytical calculations - Shear wall stiffness

Analytical calculations to obtain shear wall stiffness of shear walls 1-4 is presented in this chapter.

Shear wall stiffness

Wall stiffness Wall type 1

OSB type 3 board t=12mm

Cantilever

$k_{def.osb3} := 2.25$ Climate class 2

$\psi_{0.2} := 0.3$

$E_{m.osb3} := 4930\ MPa$

$G_{m.osb3} := 1080\ MPa$

$h_1 := 2.580\ m$ Structural storey heig of wall

$P := 10\ kN$ Reference load

$b := 0.012\ m$ OSB board hickness t= 12mm

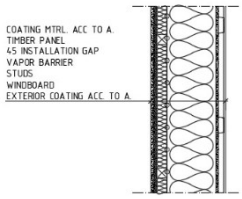

WALL SETUP 1 SCALE 1:10

$H_1 := 1\ m$ Stiffness per unit meter

$H_2 := 0.9\ m$ Stiffness per 0.9 meter.
Standard width of boards

$$I_{h1} := b \cdot \frac{H_1^{\,3}}{12} = 0.001\ m^4$$

$$I_{h2} := b \cdot \frac{H_2^{\,3}}{12} = \left(7.29 \cdot 10^{-4}\right) m^4$$

$A_1 := b \cdot H_1 = 0.012\ m^2$

Table 3.10 Characteristic strength and stiffness properties in MPa and densities in kg/m³ for OSB [1] [2]

Nominal thickness t_{nom} (mm)	OSB/2, OSB/3 [4]			OSB/4 [4]		
	> 6 – 10	> 10 – 18	> 18 – 25	> 6 – 10	> 10 – 18	> 18 – 25
Strength values						
Bending $f_{c,0}$ parallel to the strands // [3]	18,0	16,4	14,8	24,5	23,0	21,0
Bending $f_{c,90}$ perpendicular to the strands ⊥ [3]	9,0	8,2	7,4	13,0	12,2	11,4
Tension $f_{t,0}$ parallel to the strands // [3]	9,9	9,4	9,0	11,9	11,4	10,9
Tension $f_{t,90}$ perpendicular to the strands ⊥ [3]	7,2	7,0	6,8	8,5	8,2	8,0
Compression $f_{c,0}$ parallel to the strands // [3]	15,9	15,4	14,8	18,1	17,6	17,0
Compression $f_{c,90}$ perpendicular to the strands ⊥ [3]	12,9	12,7	12,4	14,3	14,0	13,7
Panel shear f_v	6,8	6,8	6,8	6,9	6,9	6,9
Planar shear f_r	1,0	1,0	1,0	1,1	1,1	1,1
Mean stiffness values [5]						
Bending $E_{c,0}$ parallel to the strands // [3]	4 930	4 930	4 930	6 780	6 780	6 780
Bending $E_{c,90}$ perpendicular to the strands ⊥ [3]	1 980	1 980	1 980	2 680	2 680	2 680
Tension $E_{t,0}$ parallel to the strands // [3]	3 800	3 800	3 800	4 300	4 300	4 300
Tension $E_{t,90}$ perpendicular to the strands ⊥ [3]	3 000	3 000	3 000	3 200	3 200	3 200
Compression $E_{c,0}$ parallel to the strands // [3]	3 800	3 800	3 800	4 300	4 300	4 300
Compression $E_{c,90}$ perpendicular to the strands ⊥ [3]	3 000	3 000	3 000	3 200	3 200	3 200
Panel shear G_v	1 080	1 080	1 080	1 090	1 090	1 090
Planar shear G_r	50	50	50	60	60	60
Density						
Density ρ_k	550	550	550	550	550	550

[1] The values shall be modified by k_{mod} or k_{def} according to *table 3.2, page 8,* and *table 9.1, page 32.* OSB/2 may only be used in service class 1. OSB/3 and OSB/4 may be used also in service class 2.
[2] Parallel to the strands in the outer layer.
[3] Perpendicular to the strands in the outer layer.
[4] Oriented strand boards are classified in types OSB/2–OSB/4, according to EN 300.
[5] 5/6th percentile values are determined as 0.85 times the mean values.
[6] The availability of board types and board thicknesses should be checked with the board manufacturers or board suppliers before design is made.

Source: Table according to EN 12369–1:2001.

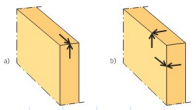

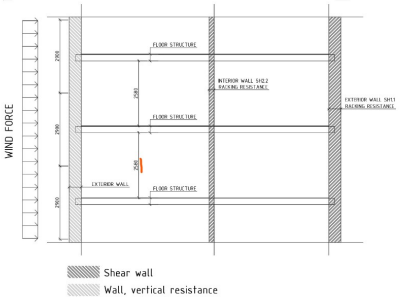

Figure 3.8: Section of reference *Object*1

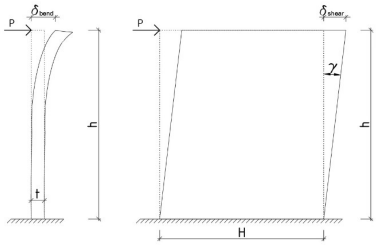

Figure 3.12: Bending and shear deflection of a cantilever wall (beam) subjected to point load, P, at the top

$A_2 := b \cdot H_2 = 0.011\ m^2$

$\rho_{m1} := 550\ \frac{kg}{m^3}$ Mean density timber material 1, mean density of OSB

$\rho_{m2} := 350\ \frac{kg}{m^3}$ Mean density timber material 2, mean density of c14. Safe approach.

$d := 3.9$ Diameter of the screw, 3.9-4.2mm

$unit\_corecc := \frac{1}{\frac{kg^{\frac{3}{2}}}{m^{\frac{9}{2}}}}$

Stiffness of 1m length:

$k_{ser} := \left(\sqrt{\rho_{m1} \cdot \rho_{m2}}\right)^{1.5} \cdot \frac{d}{23} \cdot unit\_corecc \cdot \frac{N}{mm} = 1558.331\ \frac{N}{mm}$

$k_u := \frac{2}{3} \cdot k_{ser} = 1038.888\ \frac{N}{mm}$

Final Youngs, Shear and Slip modulus

$k_{ser.osb3.fin} := \frac{k_u}{1 + \psi_{0.2} \cdot k_{def.osb3}} = 620.231\ \frac{N}{mm}$

$G_{mean.osb3.final} := \frac{G_{m.osb3}}{1 + \psi_{0.2} \cdot k_{def.osb3}} = \left(6.448 \cdot 10^8\right)\ Pa$

$E_{mean.osb3.final} := \frac{E_{m.osb3}}{1 + \psi_{0.2} \cdot k_{def.osb3}} = \left(2.943 \cdot 10^9\right)\ Pa$

$s_{nail\_spaceing} := 100\ mm$

$\delta_{nails} := 4.5 \cdot \frac{s_{nail\_spaceing}}{1000\ mm} \cdot \frac{P}{k_{ser.osb3.fin}} = 7.255\ mm$

$\delta_{h1.osb} := \frac{P \cdot {h_1}^3}{3 \cdot E_{mean.osb3.final} \cdot I_{h1}} + \frac{P \cdot h_1}{A_1 \cdot G_{mean.osb3.final}} + 4.5 \cdot \frac{s_{nail\_spaceing}}{1000\ mm} \cdot \frac{P}{k_u} = 27.11543\ mm$

$k_{1.osb} := \frac{P}{\delta_{h1.osb}} = 368.794\ \frac{kN}{m}$

From Gyproc "Handbok 7", stud framed walls with installation area has a stiffness of 34% of it origin.

$$k_{1\_installation.osb} := 0.34 \cdot k_{1.osb} = 125.39 \ \frac{kN}{m}$$

Stiffness of 0.9m length:

$$\delta_{h0.9.osb} := \frac{P \cdot {h_1}^3}{3 \cdot E_{mean.osb3.final} \cdot I_{h2}} + \frac{P \cdot h_1}{A_2 \cdot G_{mean.osb3.final}} + 4.5 \cdot \frac{s_{nail\_spaceing}}{900 \ mm} \cdot \frac{P}{k_{ser.osb3.fin}} = 0.03845 \ m$$

$$k_{0.9.osb} := \frac{P}{\delta_{h0.9.osb}} = 260.105 \ \frac{kN}{m}$$

$$k_{0.9\_installation.osb} := 0.34 \cdot k_{0.9.osb} = 88.436 \ \frac{kN}{m}$$

Wall stiffness Wall type 1
Plywood board t=12mm, "Moelven oputsad Vänerply"

Cantilever

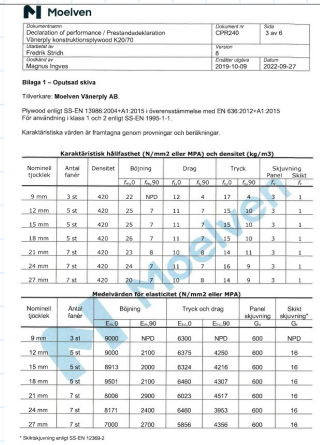
Moelven

Declaration of performance / Prestandadeklaration
Vänerply konstruktionsplywood K20/70

Bilaga 1 – Oputsad skiva

Tillverkare: **Moelven Vänerply AB**

Plywood enligt SS-EN 13986:2004+A1:2015 i överensstämmelse med EN 636:2012+A1:2015
För användning i klass 1 och 2 enligt SS-EN 1995-1-1.

Karaktäristiska värden är framtagna genom provningar och beräkningar.

Karaktäristisk hållfasthet (N/mm2 eller MPA) och densitet (kg/m3)

Nominell tjocklek	Antal fanér	Densitet	Böjning		Drag		Tryck		Skjuvning Panel	Skiva
			$f_{m,0}$	$f_{m,90}$	$f_{t,0}$	$f_{t,90}$	$f_{c,0}$	$f_{c,90}$	f_v	f_v
9 mm	3 st	420	22	NPD	12	4	17	4	3	1
12 mm	5 st	420	25	7	11	7	15	10	3	1
15 mm	5 st	420	25	7	11	7	15	10	3	1
18 mm	5 st	420	26	7	11	7	15	10	3	1
21 mm	7 st	420	23	8	10	8	14	11	3	1
24 mm	7 st	420	24	7	11	7	16	9	3	1
27 mm	7 st	420	20	7	10	8	14	9	3	1

Medelvärden för elasticitet (N/mm2 eller MPA)

Nominell tjocklek	Antal fanér	Böjning		Tryck och drag		Panel skjuvning	Skiva skjuvning*
		$E_{m,0}$	$E_{m,90}$	$E_{t,0}$	$E_{t,90}$	G_v	G_v
9 mm	3 st	9000	NPD	6300	NPD	600	NPD
12 mm	5 st	9000	2100	6375	4250	600	16
15 mm	5 st	8913	2000	6324	4216	600	16
18 mm	5 st	9501	2100	6460	4307	600	16
21 mm	7 st	8006	2900	6023	4517	600	16
24 mm	7 st	8171	2400	6460	3953	600	16
27 mm	7 st	7000	2700	5856	4396	600	16

* Skiktskjuvning enligt SS-EN 12369-2

$E_{m.ply} := 9000\ MPa$ $k_{def.ply} := 1$

$G_{m.ply} := 600\ MPa$

$h_1 := 2.580\ m$ Structural storey heig of wall

$P := 10\ kN$ Reference load

$b := 0.012\ m$ OSB board thickness t= 12mm

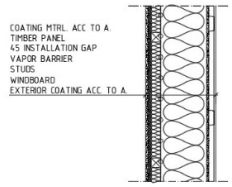

WALL SETUP 1 SCALE 1:10

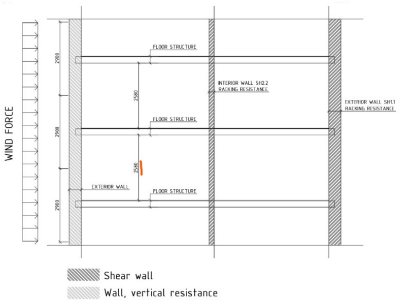

Figure 3.8: Section of reference *Object*1

$H_1 := 1\ m$ Stiffness per unit meter

$H_2 := 0.9\ m$ Stiffness per 0.9 meter.
Standard width of boards

$$I_{h1} := b \cdot \frac{H_1^{\,3}}{12} = 0.001\ m^4$$

$$I_{h2} := b \cdot \frac{H_2^{\,3}}{12} = \left(7.29 \cdot 10^{-4}\right) m^4$$

$A_1 := b \cdot H_1 = 0.012\ m^2$

$A_2 := b \cdot H_2 = 0.011\ m^2$

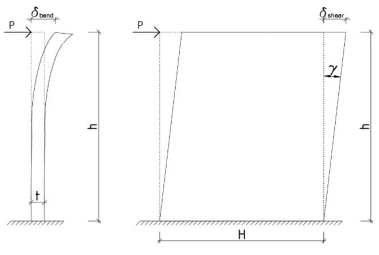

Figure 3.12: Bending and shear deflection of a cantilever wall (beam) subjected to point load, P, at the top

$\rho_{m1} := 420 \ \frac{kg}{m^3}$ Mean density timber material 1, mean density of plywood

$\rho_{m2} := 350 \ \frac{kg}{m^3}$ Mean density timber material 2, mean density of c14. Safe approach.

$d := 3.9$ Diameter of the screw, 3.9-4.2mm

$unit\_corecc := \frac{1}{\frac{kg^{\frac{3}{2}}}{m^{\frac{9}{2}}}}$

Stiffness of 1m length:

$k_{ser} := \left(\sqrt{\rho_{m1} \cdot \rho_{m2}}\right)^{1.5} \cdot \frac{d}{23} \cdot unit\_corecc \cdot \frac{N}{mm} = 1272.989 \ \frac{N}{mm}$

$k_u := \frac{2}{3} \cdot k_{ser} = 848.66 \ \frac{N}{mm}$

Final youngs, shear and slip modulus

$k_{ser.ply.fin} := \frac{k_u}{1 + \psi_{0.2} \cdot k_{def.ply}} = 652.815 \ \frac{N}{mm}$

$G_{mean.ply.final} := \frac{G_{m.ply}}{1 + \psi_{0.2} \cdot k_{def.ply}} = \left(4.615 \cdot 10^8\right) \ Pa$

$E_{mean.ply.final} := \frac{E_{m.ply}}{1 + \psi_{0.2} \cdot k_{def.ply}} = \left(6.923 \cdot 10^9\right) \ Pa$

$s_{nail\_spaceing} := 100 \ mm$

$\delta_{nails} := 4.5 \cdot \frac{s_{nail\_spaceing}}{1000 \ mm} \cdot \frac{P}{k_{ser.ply.fin}} = 6.893 \ mm$

$\delta_{h1} := \frac{P \cdot {h_1}^3}{3 \cdot E_{mean.ply.final} \cdot I_{h1}} + \frac{P \cdot h_1}{A_1 \cdot G_{mean.ply.final}} + \delta_{nails} = 0.01982 \ m$

$k_{1.ply} := \frac{P}{\delta_{h1}} = 504.534 \ \frac{kN}{m}$

From Gyproc "Handbok 7", stud framed walls with installation area has a stiffness of 34% of it origin.

$$k_{1\_installation.ply} := 0.34 \cdot k_{1.ply} = 171.541 \ \frac{kN}{m}$$

$$\delta_{h2} := \frac{P \cdot {h_1}^3}{3 \cdot E_{mean.ply.final} \cdot I_{h2}} + \frac{P \cdot h_1}{A_2 \cdot G_{mean.ply.final}} + \delta_{nails} = 0.02341 \ m$$

$$k_{0.9.ply} := \frac{P}{\delta_{h2}} = 427.137 \ \frac{kN}{m}$$

$$k_{0.9\_installation.ply} := 0.34 \cdot k_{0.9.ply} = 145.226 \ \frac{kN}{m}$$

Wall stiffness Wall type 2
OSB board t=12mm

Cantilever

$k_{def.osb3} := 2.25$ Climate class 2

$\psi_{0.2} := 0.3$

$E_{m.osb3} := 4930\ MPa$

$G_{m.osb3} := 1080\ MPa$

$h_1 := 2.580\ m$ Structural storey heig of wall

$P := 10\ kN$ Reference load

$b := 0.012 \cdot 2\ m$ OSB board hickness t= 12mm

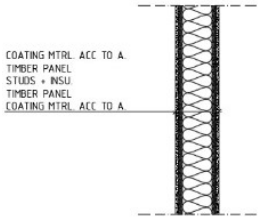

WALL SETUP 2 SCALE 1:10

$H_1 := 1\ m$ Stiffness per unit meter

$H_2 := 0.9\ m$ Stiffness per 0.9 meter.
Standard width of boards

$$I_{h1} := b \cdot \frac{H_1^{\,3}}{12} = 0.002\ m^4$$

$$I_{h2} := b \cdot \frac{H_2^{\,3}}{12} = 0.001\ m^4$$

$A_1 := b \cdot H_1 = 0.024\ m^2$

$A_2 := b \cdot H_2 = 0.022\ m^2$

Table 3.10 Characteristic strength and stiffness properties in MPa and densities in kg/m³ for OSB [1] [6]

Nominal thickness t_{nom} (mm)	OSB/2, OSB/3 [4]			OSB/4 [4]		
	> 6 – 10	> 10 – 18	> 18 – 25	> 6 – 10	> 10 – 18	> 18 – 25
Strength values						
Bending $f_{m,k}$ parallel to the strands // [2]	18,0	16,4	14,8	24,5	23,0	21,0
Bending $f_{m,k}$ perpendicular to the strands ⊥ [3]	9,0	8,2	7,4	13,0	12,2	11,4
Tension $f_{t,k}$ parallel to the strands // [2]	9,9	9,4	9,0	11,9	11,4	10,9
Tension $f_{t,k}$ perpendicular to the strands ⊥ [3]	7,2	7,0	6,8	8,5	8,2	8,0
Compression $f_{c,k}$ parallel to the strands // [2]	15,9	15,4	14,8	18,1	17,6	17,0
Compression $f_{c,k}$ perpendicular to the strands ⊥ [3]	12,9	12,7	12,4	14,3	14,0	13,7
Panel shear $f_{v,k}$	6,8	6,8	6,8	6,9	6,9	6,9
Planar shear $f_{r,k}$	1,0	1,0	1,0	1,1	1,1	1,1
Mean stiffness values [5]						
Bending $E_{0,m}$ parallel to the strands // [2]	4 930	4 930	4 930	6 780	6 780	6 780
Bending $E_{90,m}$ perpendicular to the strands ⊥ [3]	1 980	1 980	1 980	2 680	2 680	2 680
Tension $E_{t,0,m}$ parallel to the strands // [2]	3 800	3 800	3 800	4 300	4 300	4 300
Tension $E_{t,90,m}$ perpendicular to the strands ⊥ [3]	3 000	3 000	3 000	3 200	3 200	3 200
Compression $E_{c,0,m}$ parallel to the strands // [2]	3 800	3 800	3 800	4 300	4 300	4 300
Compression $E_{c,90,m}$ perpendicular to the strands ⊥ [3]	3 000	3 000	3 000	3 200	3 200	3 200
Panel shear $G_{v,m}$	1 080	1 080	1 080	1 090	1 090	1 090
Planar shear $G_{r,m}$	50	50	50	60	60	60
Density						
Density ρ_k	550	550	550	550	550	550

[1] The values shall be modified by k_{mod} or k_{def} according to *table 3.2, page 8,* and *table 9.1, page 32.* OSB/2 may only be used in service class 1. OSB/3 and OSB/4 may be used also in service class 2.
[2] Parallel to the strands in the outer layer.
[3] Perpendicular to the strands in the outer layer.
[4] Oriented strand boards are classified in types OSB/2- OSB/4, according to EN 300.
[5] 5th percentile values are determined as 0,85 times the mean values.
[6] The availability of board types and board thicknesses should be checked with the board manufacturers or board suppliers before design is made.
Source: Table according to EN 12369-1:2001.

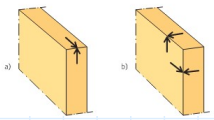

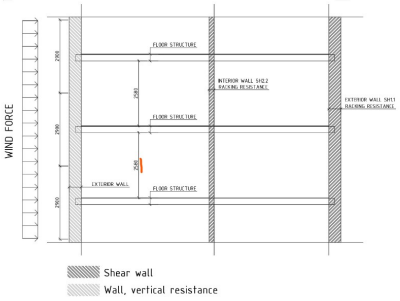

Figure 3.8: Section of reference *Object*1

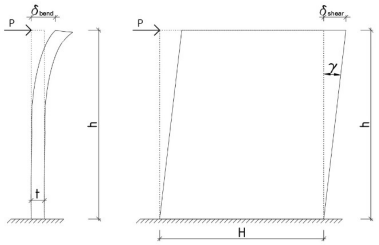

Figure 3.12: Bending and shear deflection of a cantilever wall (beam) subjected to point load, P, at the top

$\rho_{m1} := 550 \ \frac{kg}{m^3}$ Mean density timber material 1, mean density of OSB

$\rho_{m2} := 350 \ \frac{kg}{m^3}$ Mean density timber material 2, mean density of c14. Safe approach.

$d := 3.9$ Diameter of the screw, 3.9-4.2mm

$unit\_corecc := \frac{1}{\frac{kg^{\frac{3}{2}}}{m^{\frac{9}{2}}}}$

Stiffness of 1m length:

$k_{ser} := \left(\sqrt{\rho_{m1} \cdot \rho_{m2}}\right)^{1.5} \cdot \frac{d}{23} \cdot unit\_corecc \cdot \frac{N}{mm} = 1558.331 \ \frac{N}{mm}$

$k_u := \frac{2}{3} \cdot k_{ser} = 1038.888 \ \frac{N}{mm}$

Final youngs, shear and slip modulus

$k_{ser.osb3.fin} := \frac{k_u}{1 + \psi_{0.2} \cdot k_{def.osb3}} = 620.231 \ \frac{N}{mm}$

$G_{mean.osb3.final} := \frac{G_{m.osb3}}{1 + \psi_{0.2} \cdot k_{def.osb3}} = \left(6.448 \cdot 10^8\right) \ Pa$

$E_{mean.osb3.final} := \frac{E_{m.osb3}}{1 + \psi_{0.2} \cdot k_{def.osb3}} = \left(2.943 \cdot 10^9\right) \ Pa$

$s_{nail\_spaceing} := 50 \ mm$

HALF SPACING FOR TWOSIDED?

$\delta_{nails} := 4.5 \cdot \frac{s_{nail\_spaceing}}{1000 \ mm} \cdot \frac{P}{k_{ser.osb3.fin}} = 3.628 \ mm$

$\delta_{h1.osb} := \frac{P \cdot {h_1}^3}{3 \cdot E_{mean.osb3.final} \cdot I_{h1}} + \frac{P \cdot h_1}{A_1 \cdot G_{mean.osb3.final}} + 4.5 \cdot \frac{s_{nail\_spaceing}}{1000 \ mm} \cdot \frac{P}{k_u} = 13.55771 \ mm$

$k_{1.osb} := \frac{P}{\delta_{h1.osb}} = 0.738 \ \frac{kN}{mm}$

From Gyproc "Handbok 7", stud framed walls with installation area has a stiffness of 34% of it origin.

$$k_{1\_installation.osb} := 0.34 \cdot k_{1.osb} = 250.78 \ \frac{kN}{m}$$

Stiffness of 0.9m length:

$$\delta_{h0.9.osb} := \frac{P \cdot {h_1}^3}{3 \cdot E_{mean.osb3.final} \cdot I_{h2}} + \frac{P \cdot h_1}{A_2 \cdot G_{mean.osb3.final}} + 4.5 \cdot \frac{s_{nail\_spaceing}}{900 \ mm} \cdot \frac{P}{k_{ser.osb3.fin}} = 0.01922 \ m$$

$$k_{0.9.osb} := \frac{P}{\delta_{h0.9.osb}} = 520.21 \ \frac{kN}{m}$$

$$k_{0.9\_installation.osb} := 0.34 \cdot k_{0.9.osb} = 176.871 \ \frac{kN}{m}$$

Wall stiffness Wall type 2
Plywood board t=12mm

Cantilever

$E_{m.ply} := 9000\ MPa$ $k_{def.ply} := 1$

$G_{m.ply} := 600\ MPa$

$h_1 := 2.580\ m$ Structural storey heig of wall

$P := 10\ kN$ Reference load

$b := 0.012 \cdot 2\ m$ OSB board thickness t= 12mm

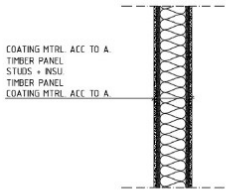

WALL SETUP 2 SCALE 1:10

$H_1 := 1\ m$ Stiffness per unit meter

$H_2 := 0.9\ m$ Stiffness per 0.9 meter.
Standard width of boards

$$I_{h1} := b \cdot \frac{H_1^{\,3}}{12} = 0.002\ m^4$$

$$I_{h2} := b \cdot \frac{H_2^{\,3}}{12} = 0.001\ m^4$$

$A_1 := b \cdot H_1 = 0.024\ m^2$

$A_2 := b \cdot H_2 = 0.022\ m^2$

Moelven

Dokumentnamn	Dokument nr	Sida
Declaration of performance / Prestandadeklaration Vänerply konstruktionsplywood K20/70	CPR240	3 av 6
Utarbetad av: Fredrik Stridh	Version: 8	
Godkänd av: Magnus Ingves	Ersätter utgåva: 2019-10-09	Datum: 2022-09-27

Bilaga 1 – Oputsad skiva

Tillverkare: **Moelven Vänerply AB**.

Plywood enligt SS-EN 13986:2004+A1:2015 i överensstämmelse med EN 636:2012+A1:2015
För användning i klass 1 och 2 enligt SS-EN 1995-1-1.

Karaktäristiska värden är framtagna genom provningar och beräkningar.

Karaktäristisk hållfasthet (N/mm2 eller MPA) och densitet (kg/m3)

Nominell tjocklek	Antal fanér	Densitet	Böjning		Drag		Tryck		Skjuvning Panel	Skjuvning Skikt
			$f_{m,0}$	$f_{m,90}$	$f_{t,0}$	$f_{t,90}$	$f_{c,0}$	$f_{c,90}$	f_v	f_r
9 mm	3 st	420	22	NPD	12	4	17	4	3	1
12 mm	5 st	420	25	7	11	7	15	10	3	1
15 mm	5 st	420	25	7	11	7	15	10	3	1
18 mm	5 st	420	26	7	11	7	15	10	3	1
21 mm	7 st	420	23	8	10	8	14	11	3	1
24 mm	7 st	420	24	7	11	7	16	9	3	1
27 mm	7 st	420	20	7	10	8	14	9	3	1

Medelvärden för elasticitet (N/mm2 eller MPA)

Nominell tjocklek	Antal fanér	Böjning		Tryck och drag		Panel skjuvning	Skikt skjuvning*
		$E_{m,0}$	$E_{m,90}$	$E_{c,0}$	$E_{c,90}$	G_v	G_r
9 mm	3 st	9000	NPD	6300	NPD	600	NPD
12 mm	5 st	9000	2100	6375	4250	600	16
15 mm	5 st	8913	2000	6324	4216	600	16
18 mm	5 st	9501	2100	6460	4307	600	16
21 mm	7 st	8006	2900	6023	4517	600	16
24 mm	7 st	8171	2400	6460	3953	600	16
27 mm	7 st	7000	2700	5856	4356	600	16

* Skiktskjuvning enligt SS-EN 12369-2

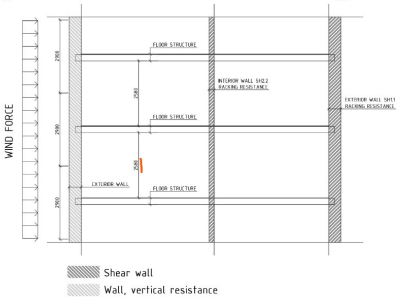

Figure 3.8: Section of reference *Object*1

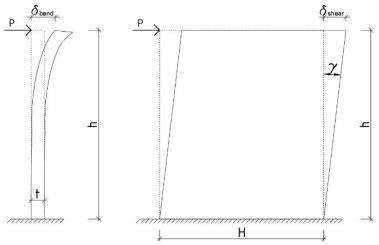

Figure 3.12: Bending and shear deflection of a cantilever wall (beam) subjected to point load, P, at the top

$\rho_{m1} := 420 \ \frac{kg}{m^3}$ Mean density timber material 1, mean density of plywood

$\rho_{m2} := 350 \ \frac{kg}{m^3}$ Mean density timber material 2, mean density of c14. Safe approach.

$d := 3.9$ Diameter of the screw, 3.9-4.2mm

$unit\_corecc := \frac{1}{\frac{kg^{\frac{3}{2}}}{m^{\frac{9}{2}}}}$

Stiffness of 1m length:

$k_{ser} := \left(\sqrt{\rho_{m1} \cdot \rho_{m2}}\right)^{1.5} \cdot \frac{d}{23} \cdot unit\_corecc \cdot \frac{N}{mm} = 1272.989 \ \frac{N}{mm}$

$k_u := \frac{2}{3} \cdot k_{ser} = 848.66 \ \frac{N}{mm}$

Final youngs, shear and slip modulus

$k_{ser.ply.fin} := \frac{k_u}{1 + \psi_{0.2} \cdot k_{def.ply}} = 652.815 \ \frac{N}{mm}$

$G_{mean.ply.final} := \frac{G_{m.ply}}{1 + \psi_{0.2} \cdot k_{def.ply}} = \left(4.615 \cdot 10^8\right) \ Pa$

$E_{mean.ply.final} := \frac{E_{m.ply}}{1 + \psi_{0.2} \cdot k_{def.ply}} = \left(6.923 \cdot 10^9\right) \ Pa$

$s_{nail\_spaceing} := 50 \ mm$

TWO SIDED SHEATING S100 > CALC AS ONE SIDE WITH S50

$\delta_{nails} := 4.5 \cdot \frac{s_{nail\_spaceing}}{1000 \ mm} \cdot \frac{P}{k_{ser.ply.fin}} = 3.447 \ mm$

$\delta_{h1} := \frac{P \cdot {h_1}^3}{3 \cdot E_{mean.ply.final} \cdot I_{h1}} + \frac{P \cdot h_1}{A_1 \cdot G_{mean.ply.final}} + \delta_{nails} = 0.00991 \ m$

$k_{1.ply} := \frac{P}{\delta_{h1}} = 1009.067 \ \frac{kN}{m}$

From Gyproc "Handbok 7", stud framed walls with installation area has a stiffness of 34% of it origin.

$$k_{1\_installation.ply} := 0.34 \cdot k_{1.ply} = 343.083 \ \frac{kN}{m}$$

$$\delta_{h2} := \frac{P \cdot {h_1}^3}{3 \cdot E_{mean.ply.final} \cdot I_{h2}} + \frac{P \cdot h_1}{A_2 \cdot G_{mean.ply.final}} + \delta_{nails} = 0.01171 \ m$$

$$k_{0.9.ply} := \frac{P}{\delta_{h2}} = 854.273 \ \frac{kN}{m}$$

$$k_{0.9\_installation.ply} := 0.34 \cdot k_{0.9.ply} = 290.453 \ \frac{kN}{m}$$

Wall stiffness Wall type 3 and 4 (same stiffness properties)
CLT

Indata CLT sections

$P := 10\ kN$

C panels
The grain direction of the cover layers is always parallel to the production widths.

Thickness [mm]	Panel type [–]	Layers [–]	Panel design [mm]						
			C***	L	C***	L	C***	L	C***
60	C3s	3	20	20	20				
80	C3s	3	20	40	20				
90	C3s	3	30	30	30				
100	C3s	3	30	40	30				
120	C3s	3	40	40	40				
100	C5s	5	20	20	20	20	20		
120	C5s	5	30	20	20	20	30		
140	C5s	5	40	20	20	20	40		
160	C5s	5	40	20	40	20	40		

Thickness of layers

$t_{20} := 20\ mm$

$t_{30} := 30\ mm$

$t_{40} := 40\ mm$

Total thickness of layers in the cross section ("C")

Material values:
E_0 = 11,000 MPa for timber in strength class C24 = E_{ref}
E_0 = 8,000 MPa for C16,
E_{90} = 0 MPa, G_{090} = 650 MPa and G_{9090} = 50 MPa.

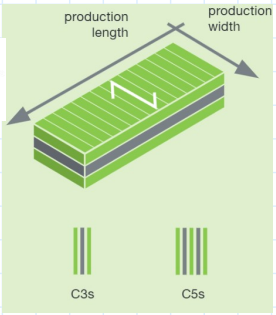

$clt_{60} := 2 \cdot t_{20} = 0.04\ m$

$clt_{100} := 2 \cdot t_{30} = 0.06\ m$

$clt_{120.3lay} := 2 \cdot t_{40} = 0.08\ m$

$clt_{120.5lay} := 2 \cdot t_{30} + t_{20} = 0.08\ m$

$clt_{160.5lay} := 3 \cdot t_{40} = 0.12\ m$

$E_{mean.c24} := 11000\ MPa$ $E_{mean.c16} := 8000\ MPa$ $G_{mena.c24} := 690\ MPa$

$h_1 = 2.58\ m$ Structural storey heig of wall

Length of shear walls, floor plan 1

$SH_{1.1.1} := 1.8\ m$

$SH1_{1.1.2} := 5.4\ m$

$SH_{1.1.3} := 2.4\ m$

$SH_{1.2.1} := 3.0\ m$

Length of shear walls, floor plan 2

$SH_{2.1.1} := 7.3\ m$

$SH1_{2.2.1} := 12.0\ m$

$SH_{2.2.2} := 12.2\ m$

$SH_{2.2.3} := 3.6\ m$

$SH_{1.2.2} := 4.6\ m$

$SH_{1.2.3} := 3.6\ m$

$SH_{1.2.4} := 5.2\ m$

$SH_{2.2.4} := 3.4\ m$

$SH_{2.2.5} := 4.5\ m$

$SH_{2.2.6} := 6.4\ m$

$SH_{2.2.7} := 4.5\ m$

$$h_{1.all} := \begin{bmatrix} 1.8 \\ 5.4 \\ 2.4 \\ 3.0 \\ 4.6 \\ 3.6 \\ 5.2 \end{bmatrix} \cdot m \qquad h_{2.all} := \begin{bmatrix} 7.3 \\ 12.0 \\ 12.2 \\ 3.6 \\ 3.4 \\ 4.5 \\ 6.4 \\ 4.5 \end{bmatrix} \cdot m$$

$$I_{clt.60} := clt_{60} \cdot \frac{h_{1.all}^{3}}{12} = \begin{bmatrix} 0.019 \\ 0.525 \\ 0.046 \\ 0.09 \\ 0.324 \\ 0.156 \\ 0.469 \end{bmatrix} m^4 \qquad I_{clt.100} := clt_{100} \cdot \frac{h_{1.all}^{3}}{12} = \begin{bmatrix} 0.029 \\ 0.787 \\ 0.069 \\ 0.135 \\ 0.487 \\ 0.233 \\ 0.703 \end{bmatrix} m^4$$

CLT 120 3 and 5 layer has the same moment of intertia.

$$I_{clt.120} := clt_{120.3lay} \cdot \frac{h_{1.all}^{3}}{12} = \begin{bmatrix} 0.039 \\ 1.05 \\ 0.092 \\ 0.18 \\ 0.649 \\ 0.311 \\ 0.937 \end{bmatrix} m^4 \qquad I_{clt.120.5lay} := clt_{120.5lay} \cdot \frac{h_{1.all}^{3}}{12} = \begin{bmatrix} 0.039 \\ 1.05 \\ 0.092 \\ 0.18 \\ 0.649 \\ 0.311 \\ 0.937 \end{bmatrix} m^4$$

$$I_{clt.160} := clt_{160.5lay} \cdot \frac{h_{1.all}^{3}}{12} = \begin{bmatrix} 0.058 \\ 1.575 \\ 0.138 \\ 0.27 \\ 0.973 \\ 0.467 \\ 1.406 \end{bmatrix} m^4$$

$k_{def.clt} := 1.1$

$$G_{mean.clt.final} := \frac{G_{mena.c24}}{1 + \psi_{0.2} \cdot k_{def.clt}} = \left(5.188 \cdot 10^{8}\right) Pa$$

$$E_{mean.clt.final} := \frac{E_{mean.c24}}{1+\psi_{0.2}\cdot k_{def.clt}} = \left(8.271\cdot 10^{9}\right)\ Pa$$

$t_{clt60} := 60\ mm$ $t_{clt100} := 100\ mm$ $t_{clt120} := 120\ mm$ $t_{clt160} := 160\ mm$

$$A_{clt.60} := h_{1.all}\cdot t_{clt60} = \begin{bmatrix} 0.108 \\ 0.324 \\ 0.144 \\ 0.18 \\ 0.276 \\ 0.216 \\ 0.312 \end{bmatrix} m^2 \qquad A_{clt.100} := h_{1.all}\cdot t_{clt100} = \begin{bmatrix} 0.18 \\ 0.54 \\ 0.24 \\ 0.3 \\ 0.46 \\ 0.36 \\ 0.52 \end{bmatrix} m^2$$

$$A_{clt.120} := h_{1.all}\cdot t_{clt120} = \begin{bmatrix} 0.216 \\ 0.648 \\ 0.288 \\ 0.36 \\ 0.552 \\ 0.432 \\ 0.624 \end{bmatrix} m^2 \qquad A_{clt.160} := h_{1.all}\cdot t_{clt160} = \begin{bmatrix} 0.288 \\ 0.864 \\ 0.384 \\ 0.48 \\ 0.736 \\ 0.576 \\ 0.832 \end{bmatrix} m^2$$

$$\delta_{clt60.1} := \frac{P\cdot {h_1}^3}{3\cdot E_{mean.clt.final}\cdot I_{clt.60}} + \frac{P\cdot h_1}{A_{clt.60}\cdot G_{mean.clt.final}} = \begin{bmatrix} 0.81651 \\ 0.16668 \\ 0.49556 \\ 0.35319 \\ 0.20152 \\ 0.27474 \\ 0.17416 \end{bmatrix} mm$$

$$\delta_{clt100.1} := \frac{P\cdot {h_1}^3}{3\cdot E_{mean.clt.final}\cdot I_{clt.100}} + \frac{P\cdot h_1}{A_{clt.100}\cdot G_{mean.clt.final}} = \begin{bmatrix} 0.51364 \\ 0.10088 \\ 0.30735 \\ 0.21704 \\ 0.12233 \\ 0.16781 \\ 0.10548 \end{bmatrix} mm$$

120 CLT with 3 or 5-layers has the same sectional data for moment of inertia and shear area, thus, same deflection.

$$\delta_{clt120.1} := \frac{P \cdot {h_1}^3}{3 \cdot E_{mean.clt.final} \cdot I_{clt.120}} + \frac{P \cdot h_1}{A_{clt.120} \cdot G_{mean.clt.final}} = \begin{bmatrix} 0.40825 \\ 0.08334 \\ 0.24778 \\ 0.17659 \\ 0.10076 \\ 0.13737 \\ 0.08708 \end{bmatrix} \ mm$$

$$\delta_{clt160.1} := \frac{P \cdot {h_1}^3}{3 \cdot E_{mean.clt.final} \cdot I_{clt.160}} + \frac{P \cdot h_1}{A_{clt.160} \cdot G_{mean.clt.final}} = \begin{bmatrix} 0.29136 \\ 0.06195 \\ 0.17957 \\ 0.12924 \\ 0.07468 \\ 0.10117 \\ 0.06469 \end{bmatrix} \ mm$$

Stiffness of CLT walls Floor plan 1.

$$k_{clt60} := \frac{P}{\delta_{clt60.1}} = \begin{bmatrix} 12247 \\ 59997 \\ 20179 \\ 28314 \\ 49624 \\ 36398 \\ 57418 \end{bmatrix} \frac{kN}{m} \qquad k_{clt100} := \frac{P}{\delta_{clt100.1}} = \begin{bmatrix} 19469 \\ 99123 \\ 32537 \\ 46075 \\ 81745 \\ 59591 \\ 94804 \end{bmatrix} \frac{kN}{m}$$

$$k_{clt120} := \frac{P}{\delta_{clt120.1}} = \begin{bmatrix} 24495 \\ 119993 \\ 40359 \\ 56628 \\ 99248 \\ 72796 \\ 114837 \end{bmatrix} \frac{kN}{m} \qquad k_{clt160} := \frac{P}{\delta_{clt160.1}} = \begin{bmatrix} 34322 \\ 161410 \\ 55687 \\ 77375 \\ 133906 \\ 98841 \\ 154572 \end{bmatrix} \frac{kN}{m}$$

Calculations to obtain stiffness of the CLT shear walls in floor plan 2.

$$I_{clt.60.2} := clt_{60} \cdot \frac{h_{2.all}{}^3}{12} = \begin{bmatrix} 1.297 \\ 5.76 \\ 6.053 \\ 0.156 \\ 0.131 \\ 0.304 \\ 0.874 \\ 0.304 \end{bmatrix} m^4 \qquad I_{clt.100.2} := clt_{100} \cdot \frac{h_{2.all}{}^3}{12} = \begin{bmatrix} 1.945 \\ 8.64 \\ 9.079 \\ 0.233 \\ 0.197 \\ 0.456 \\ 1.311 \\ 0.456 \end{bmatrix} m^4$$

CLT 120 3 and 5 layer has
the same moment of intertia.

$$I_{clt.120.2} := clt_{120.3lay} \cdot \frac{h_{2.all}{}^3}{12} = \begin{bmatrix} 2.593 \\ 11.52 \\ 12.106 \\ 0.311 \\ 0.262 \\ 0.608 \\ 1.748 \\ 0.608 \end{bmatrix} m^4 \quad I_{clt.120.5lay.2} := clt_{120.5lay} \cdot \frac{h_{2.all}{}^3}{12} = \begin{bmatrix} 2.593 \\ 11.52 \\ 12.106 \\ 0.311 \\ 0.262 \\ 0.608 \\ 1.748 \\ 0.608 \end{bmatrix} m^4$$

$$I_{clt.160.2} := clt_{160.5lay} \cdot \frac{h_{2.all}{}^3}{12} = \begin{bmatrix} 3.89 \\ 17.28 \\ 18.158 \\ 0.467 \\ 0.393 \\ 0.911 \\ 2.621 \\ 0.911 \end{bmatrix} m^4$$

$G_{mean.clt.final} = \langle 5.19 \cdot 10^8 \rangle \ Pa$ $\qquad k_{def.clt} = 1.1$

$E_{mean.clt.final} = \langle 8.27 \cdot 10^9 \rangle \ Pa$

$t_{clt60} = 0.06 \ m$ $\qquad t_{clt100} = 0.1 \ m$ $\qquad t_{clt120} = 0.12 \ m$ $\qquad t_{clt160} = 0.16 \ m$

$$A_{clt.60.2} := h_{2.all} \cdot t_{clt60} = \begin{bmatrix} 0.438 \\ 0.72 \\ 0.732 \\ 0.216 \\ 0.204 \\ 0.27 \\ 0.384 \\ 0.27 \end{bmatrix} m^2 \qquad A_{clt.100.2} := h_{2.all} \cdot t_{clt100} = \begin{bmatrix} 0.73 \\ 1.2 \\ 1.22 \\ 0.36 \\ 0.34 \\ 0.45 \\ 0.64 \\ 0.45 \end{bmatrix} m^2$$

$$A_{clt.120.2} := h_{2.all} \cdot t_{clt120} = \begin{bmatrix} 0.876 \\ 1.44 \\ 1.464 \\ 0.432 \\ 0.408 \\ 0.54 \\ 0.768 \\ 0.54 \end{bmatrix} m^2 \qquad A_{clt.160.2} := h_{2.all} \cdot t_{clt160} = \begin{bmatrix} 1.168 \\ 1.92 \\ 1.952 \\ 0.576 \\ 0.544 \\ 0.72 \\ 1.024 \\ 0.72 \end{bmatrix} m^2$$

$$\delta_{clt60.2} := \frac{P \cdot {h_1}^3}{3 \cdot E_{mean.clt.final} \cdot I_{clt.60.2}} + \frac{P \cdot h_1}{A_{clt.60.2} \cdot G_{mean.clt.final}} = \begin{bmatrix} 0.11888 \\ 0.07027 \\ 0.06908 \\ 0.27474 \\ 0.29661 \\ 0.20697 \\ 0.13743 \\ 0.20697 \end{bmatrix} mm$$

$$\delta_{clt100.2} := \frac{P \cdot {h_1}^3}{3 \cdot E_{mean.clt.final} \cdot I_{clt.100.2}} + \frac{P \cdot h_1}{A_{clt.100.2} \cdot G_{mean.clt.final}} = \begin{bmatrix} 0.07168 \\ 0.04224 \\ 0.04152 \\ 0.16781 \\ 0.18149 \\ 0.1257 \\ 0.08298 \\ 0.1257 \end{bmatrix} mm$$

120 CLT with 3 or 5-layers has the same sectional data for moment of inertia and shear area, thus, same deflection.

$$\delta_{clt120.2} := \frac{P \cdot {h_1}^3}{3 \cdot E_{mean.clt.final} \cdot I_{clt.120.2}} + \frac{P \cdot h_1}{A_{clt.120.2} \cdot G_{mean.clt.final}} = \begin{bmatrix} 0.05944 \\ 0.03514 \\ 0.03454 \\ 0.13737 \\ 0.1483 \\ 0.10349 \\ 0.06871 \\ 0.10349 \end{bmatrix} mm$$

$$\delta_{clt160.2} := \frac{P \cdot {h_1}^3}{3 \cdot E_{mean.clt.final} \cdot I_{clt.160.2}} + \frac{P \cdot h_1}{A_{clt.160.2} \cdot G_{mean.clt.final}} = \begin{bmatrix} 0.04436 \\ 0.0263 \\ 0.02586 \\ 0.10117 \\ 0.10903 \\ 0.07667 \\ 0.05121 \\ 0.07667 \end{bmatrix} mm$$

Stiffness of CLT walls Floor plan 2.

$$k_{clt60.2} := \frac{P}{\delta_{clt60.2}} = \begin{bmatrix} 84120 \\ 142305 \\ 144757 \\ 36398 \\ 33715 \\ 48315 \\ 72766 \\ 48315 \end{bmatrix} \frac{kN}{m} \qquad k_{clt100.2} := \frac{P}{\delta_{clt100.2}} = \begin{bmatrix} 139504 \\ 236725 \\ 240819 \\ 59591 \\ 55101 \\ 79552 \\ 120505 \\ 79552 \end{bmatrix} \frac{kN}{m}$$

$$k_{clt120.2} := \frac{P}{\delta_{clt120.2}} = \begin{bmatrix} 168240 \\ 284610 \\ 289514 \\ 72796 \\ 67429 \\ 96631 \\ 145531 \\ 96631 \end{bmatrix} \frac{kN}{m} \qquad k_{clt160.2} := \frac{P}{\delta_{clt160.2}} = \begin{bmatrix} 225445 \\ 380202 \\ 386730 \\ 98841 \\ 91721 \\ 130437 \\ 195293 \\ 130437 \end{bmatrix} \frac{kN}{m}$$

Obtain stiffness properties of unit length, m, along the wall section. Floor plan 1

$$k_{clt60.1.meter} := \frac{k_{clt60}}{h_{1.all}} = \begin{bmatrix} 6804 \\ 11111 \\ 8408 \\ 9438 \\ 10788 \\ 10111 \\ 11042 \end{bmatrix} \frac{\left(\frac{kN}{m}\right)}{m} \qquad k_{clt100.1.meter} := \frac{k_{clt100}}{h_{1.all}} = \begin{bmatrix} 10816 \\ 18356 \\ 13557 \\ 15358 \\ 17771 \\ 16553 \\ 18232 \end{bmatrix} \frac{\left(\frac{kN}{m}\right)}{m}$$

$$k_{clt120.1.meter} := \frac{k_{clt120}}{h_{1.all}} = \begin{bmatrix} 13608 \\ 22221 \\ 16816 \\ 18876 \\ 21576 \\ 20221 \\ 22084 \end{bmatrix} \frac{\left(\frac{kN}{m}\right)}{m} \qquad k_{clt160.1.meter} := \frac{k_{clt160}}{h_{1.all}} = \begin{bmatrix} 19068 \\ 29891 \\ 23203 \\ 25792 \\ 29110 \\ 27456 \\ 29725 \end{bmatrix} \frac{\left(\frac{kN}{m}\right)}{m}$$

Obtain stiffness properties of unit length, m, along the wall section. Floor plan 2

$$k_{clt60\_2.1.meter} := \frac{k_{clt60.2}}{h_{2.all}} = \begin{bmatrix} 11523 \\ 11859 \\ 11865 \\ 10111 \\ 9916 \\ 10737 \\ 11370 \\ 10737 \end{bmatrix} \frac{\left(\frac{kN}{m}\right)}{m} \qquad k_{clt100\_2.1.meter} := \frac{k_{clt100.2}}{h_{2.all}} = \begin{bmatrix} 19110 \\ 19727 \\ 19739 \\ 16553 \\ 16206 \\ 17678 \\ 18829 \\ 17678 \end{bmatrix} \frac{\left(\frac{kN}{m}\right)}{m}$$

$$k_{clt120\_2.1.meter} := \frac{k_{clt120.2}}{h_{2.all}} = \begin{bmatrix} 23047 \\ 23717 \\ 23731 \\ 20221 \\ 19832 \\ 21474 \\ 22739 \\ 21474 \end{bmatrix} \frac{\left(\frac{kN}{m}\right)}{m} \qquad k_{clt160\_2.1.meter} := \frac{k_{clt160.2}}{h_{2.all}} = \begin{bmatrix} 30883 \\ 31683 \\ 31699 \\ 27456 \\ 26977 \\ 28986 \\ 30514 \\ 28986 \end{bmatrix} \frac{\left(\frac{kN}{m}\right)}{m}$$

C

Analytical calculations - Stiffness of structural joints

Analytical calculations of obtained shear stiffness of timber and TCC joints are presented in this appendix.

Stiffness of mechanical fastened timber joints

$\psi_{0.2} := 0.3$ $k_{def.osb3} := 2.25$ $k_{def.ply} := 1$ $k_{def.clt} := 1.1$

Stiffness of fastener CLT

$\rho_{m1} := 420 \ \frac{kg}{m^3}$ Mean density timber material 1, mean density of clt c24

$\rho_{m2} := 420 \ \frac{kg}{m^3}$ Mean density timber material 2, mean density of clt c24.

$d := 6.5$ Diameter of the screw. [mm]

$$unit\_corecc := \frac{1}{\frac{kg^{\frac{3}{2}}}{m^{\frac{9}{2}}}}$$

$$k_{ser} := \left(\sqrt{\rho_{m1} \cdot \rho_{m2}}\right)^{1.5} \cdot \frac{d}{23} \cdot unit\_corecc \cdot \frac{N}{mm} = 2432.537 \ \frac{N}{mm}$$

$$k_u := \frac{2}{3} \cdot k_{ser} = 1621.691 \ \frac{N}{mm} \qquad k_u = 1.622 \ \frac{kN}{mm}$$

$$k_{ser.clt.fin} := \frac{k_u}{1 + \psi_{0.2} \cdot k_{def.clt}} = \left(1.219 \cdot 10^3\right) \ \frac{kN}{m}$$

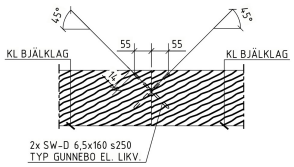

Two screws spacing s350mm
resulting with kN/m/m

$$k_{ser.clt.spacing350} := \frac{2 \cdot k_{ser.clt.fin}}{0.35 \ m} = 6968 \ \frac{\left(\frac{kN}{m}\right)}{m}$$

Two screws spacing s250mm
resulting with kN/m/m

$$k_{ser.clt.spacing250} := \frac{2 \cdot k_{ser.clt.fin}}{0.25 \ m} = 9755 \ \frac{\left(\frac{kN}{m}\right)}{m}$$

Two screws spacing s100mm
resulting with kN/m/m

$$k_{ser.clt.spacing100} := \frac{2 \cdot k_{ser.clt.fin}}{0.10 \ m} = 24386 \ \frac{\left(\frac{kN}{m}\right)}{m}$$

Fastener Plywood/C24 Joist

$\rho_{m1} := 350 \ \frac{kg}{m^3}$ Mean density timber material 1, mean density of joist c14 (safe approach)

$\rho_{m2} := 420 \ \frac{kg}{m^3}$ Mean density timber material 2, mean density of clt c24.

$d := 4.0$ Diameter of the screw. [mm]

$unit\_corecc := \frac{1}{\frac{kg^{\frac{3}{2}}}{m^{\frac{9}{2}}}}$

$k_{ser} := \left(\sqrt{\rho_{m1} \cdot \rho_{m2}}\right)^{1.5} \cdot \frac{d}{23} \cdot unit\_corecc \cdot \frac{N}{mm} = 1305.63 \ \frac{kN}{m}$

$k_u := \frac{2}{3} \cdot k_{ser} = 870.42 \ \frac{N}{mm}$ $k_u = 0.87 \ \frac{kN}{mm}$

$k_{ser.ply.fin} := \frac{k_u}{1 + \psi_{0.2} \cdot k_{def.ply}} = 669.554 \ \frac{kN}{m}$

If screws on both sides to connect -> twice the deformations, thus, half the stiffness.

Two screws with a spacing s330mm

$k_{ser.ply.spacing330} := \frac{k_{ser.ply.fin}}{0.33 \ m} = 2029 \ \frac{\left(\frac{kN}{m}\right)}{m}$

$k_{ser.ply.double.side.conn.330} := \frac{k_{ser.ply.spacing330}}{2} = 1014.476 \ \frac{\left(\frac{kN}{m}\right)}{m}$

Two screws with a spacing s220mm

$k_{ser.ply.spacing220} := \frac{k_{ser.ply.fin}}{0.22 \ m} = 3043 \ \frac{\left(\frac{kN}{m}\right)}{m}$

$k_{ser.ply.double.side.conn.220} := \frac{k_{ser.ply.spacing220}}{2} = 1521.713 \ \frac{\left(\frac{kN}{m}\right)}{m}$

Two screws with a spacing s100mm

$k_{ser.ply.spacing100} := \frac{k_{ser.ply.fin}}{0.100 \ m} = 6696 \ \frac{\left(\frac{kN}{m}\right)}{m}$

$k_{ser.ply.double.side.conn.100} := \frac{k_{ser.ply.spacing100}}{2} = 3347.77 \ \frac{\left(\frac{kN}{m}\right)}{m}$

Shear stiffness in grouted joint

Shear stiffness for mid span (worst case) of object 1

Design horizontal line load

$q := 6.05\ \frac{kN}{m}$

Span length

$l := 9.4\ m$

$M_b := \frac{q \cdot l^2}{8} = 66.822\ kN \cdot m$ $V := q \cdot \frac{l}{2} = 28.435\ kN$

Aspect ratio of the geometry

$B := 8.3\ m$

$L := 9.4\ m$

Internal leverarm

If B/L 0.5 < 1.0 -> Z=0.8*B

$\frac{B}{L} = 0.883$

$z := 0.8 \cdot B = 6.64\ m$

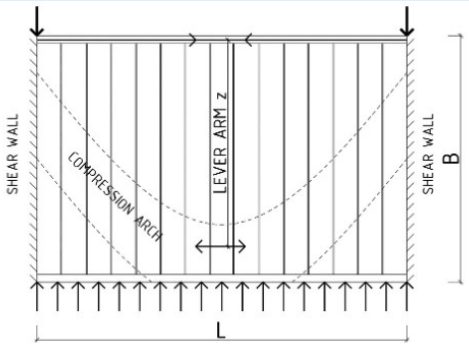

Force in tie

$T := \frac{M_b}{z} = 10.064\ kN$

Steel yield limit 500MPa

$f_{yk} := 500\ MPa$

Partial factor rebar steel

$\gamma_s := 1.15$

$f_{yd} := \frac{f_{yk}}{\gamma_s} = 435\ MPa$

Area rebar diameter 10mm

$A_{\phi 10} := \left(10\ \frac{mm}{2}\right)^2 \cdot \pi = 79\ mm^2$

Area rebar diameter 8mm

$A_{\phi 8} := \left(8\ \frac{mm}{2}\right)^2 \cdot \pi = 50\ mm^2$

Area rebar diameter 12mm

$A_{\phi 12} := \left(12\ \frac{mm}{2}\right)^2 \cdot \pi = 113\ mm^2$

$$A_{sh.calc} := \frac{T}{f_{yd}} = 23.146\ mm^2$$

$$A_{sh.prov} := 2 \cdot A_{\phi 8} = 100.531\ mm^2$$

$W := 2.4\ m$ Width of the precasted element

$$30 \cdot 8\ mm \cdot \frac{A_{sh.calc}}{A_{sh.prov}} = 55.258\ mm$$

$$0.8 \cdot W = 1920\ mm$$

$$L_s := min\left(30 \cdot 8\ mm \cdot \frac{A_{sh.calc}}{A_{sh.prov}}, 0.8 \cdot W\right) = 55.258\ mm$$

Rebar steel Young's modulus

$E_s := 200\ GPa$

$$\delta_{bar} := \frac{T \cdot L_s}{A_{sh.prov} \cdot E_s} = 0.028\ mm$$

Delta_ti is obtained from table on RHS

$\delta_{ti} := 0.150\ mm$ 28days, width of precast element 1200mm
joint width of 50mm.

Elastic elonggation of the rebars

$l_s := \delta_{bar} + \delta_{ti} = 0.178\ mm$ ok if l_s < 0.5mm, if not -> increase rebar area

Table 3.6: Initial crack widths in prefabricated concrete elements with grouted joints

Age of precast unit when joint is filled (days)	Width of precast unit (mm)	Width of longitudinal joint (mm)	Initial crack width δ_{ti}(mm)
<7	1200	25	0.215
	1200	50	0.230
	600	25	0.115
	600	50	0.130
28	1200	25	0.135
	1200	50	0.150
	600	25	0.075
	600	50	0.090
>90	1200	25	0.095
	1200	50	0.110
	600	25	0.055
	600	50	0.070

Totalt slip in a longitudinal grouted joint of adjacent elements

$$\delta_s := \frac{\ln\left(\frac{l_s}{\delta_{ti}}\right)}{3} \cdot mm = 0.056\ mm$$

$$K_s := \frac{V}{\delta_s} = 504\ \frac{kN}{mm} \qquad K_s = 504098\ \frac{kN}{m}$$

Joint length

$$l_{joint} := B = 8.3\ m$$

Stiffness per unit length of joint

$$K_{s.joint} := \frac{K_s}{l_{joint}} = 60735\ \frac{\left(\frac{kN}{m}\right)}{m}$$

Shear stiffness for mid span (worst case) of object 2

Design horizontal line load

$q := 6.38\ \frac{kN}{m}$

Span length

$l := 8.68\ m$

$M_b := \frac{q \cdot l^2}{2} = 240.342\ kN \cdot m$ $V := q \cdot l = 55.378\ kN$

Aspect ratio of the geometry

$B := 12.3\ m$

$L := 8.68\ m$

Internal leverarm

If B/L > 1.0 -> T=0.5*V/(B/L)

$\frac{B}{L} = 1.417$

$z := 0.8 \cdot B = 9.84\ m$

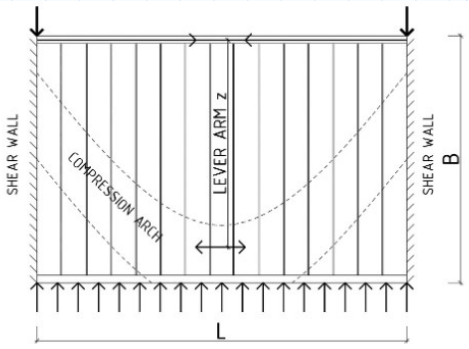

Force in tie

$T := \frac{0.5 \cdot V}{\left(\frac{B}{L}\right)} = 19.54\ kN$

Steel yield limit 500MPa

$f_{yk} := 500\ MPa$

Partial factor rebar steel

$\gamma_s := 1.15$

$f_{yd} := \frac{f_{yk}}{\gamma_s} = 435\ MPa$

Area rebar diameter 8mm

Area rebar diameter 10mm

$A_{\phi 10} := \left(10\ \frac{mm}{2}\right)^2 \cdot \pi = 79\ mm^2$

Area rebar diameter 12mm

$A_{\phi 8} := \left(8\ \frac{mm}{2}\right)^2 \cdot \pi = 50\ mm^2$ $A_{\phi 12} := \left(12\ \frac{mm}{2}\right)^2 \cdot \pi = 113\ mm^2$

$A_{sh.calc} := \frac{T}{f_{yd}} = 44.942\ mm^2$

$A_{sh.prov} := 2 \cdot A_{\phi 8} = 100.531\ mm^2$

$W := 2.4\ m$ Width of the precasted element

$30 \cdot 8\ mm \cdot \frac{A_{sh.calc}}{A_{sh.prov}} = 107.291\ mm$

$0.8 \cdot W = 1920\ mm$

$L_s := min\left(30 \cdot 8\ mm \cdot \frac{A_{sh.calc}}{A_{sh.prov}}, 0.8 \cdot W\right) = 107.291\ mm$

Rebar steel Young's modulus

$E_s := 200\ GPa$

$\delta_{bar} := \frac{T \cdot L_s}{A_{sh.prov} \cdot E_s} = 0.104\ mm$

Delta_ti is obtained from table on RHS

$\delta_{ti} := 0.150\ mm$ 28days, width of precast element 1200mm joint width of 50mm.

Table 3.6: Initial crack widths in prefabricated concrete elements with grouted joints

Age of precast unit when joint is filled (days)	Width of precast unit (mm)	Width of longitudinal joint (mm)	Initial crack width δ_{ti}(mm)
<7	1200	25	0.215
	1200	50	0.230
	600	25	0.115
	600	50	0.130
28	1200	25	0.135
	1200	50	0.150
	600	25	0.075
	600	50	0.090
>90	1200	25	0.095
	1200	50	0.110
	600	25	0.055
	600	50	0.070

Elastic elonggation of the rebars

$l_s := \delta_{bar} + \delta_{ti} = 0.254\ mm$ ok if l_s < 0.5mm, if not -> increase rebar area

Totalt slip in a longitudinal grouted joint of adjacent elements

$$\delta_s := \frac{\ln\left(\frac{l_s}{\delta_{ti}}\right)}{3} \cdot mm = 0.176\ mm$$

$$K_s := \frac{V}{\delta_s} = 315\ \frac{kN}{mm}$$

$$K_s = 314792\ \frac{kN}{m}$$

Joint length

$l_{joint} := B = 12.3\ m$

Stiffness per unit length of joint

$$K_{s.joint} := \frac{K_s}{l_{joint}} = 25593\ \frac{\left(\frac{kN}{m}\right)}{m}$$

D

Analytical calculations - Horizontal actions

Analytical calculations of horizontal actions of Object 1 and Object 2.

Horizontal actions

Unintended inclination floor 1

$\theta_0 := \frac{1}{200}$

$l := 2.5$ The storey height, in meters, of the vertical load-carrying members. Note, use no unit in equation.

$m := 25$ The number of vertical load-carrying elements on analyzed floor

$G_{k.floor} := 440\ kN$ g=2kn/m2, tot area = 220m2

$Q_{k.floor} := 440\ kN$ q=2kn/m2

$N_a := 5 \cdot \left(G_{k.floor} + Q_{k.floor}\right) = 4400\ kN$ Accumulated vertical force from all storeys above [kN].

$N_b := G_{k.floor} + Q_{k.floor} = 880\ kN$ Vertical force from studied floor level [kN].

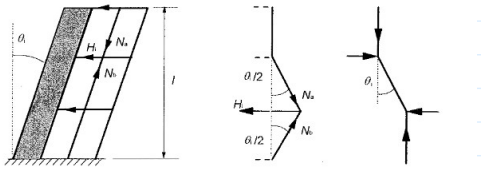

Figure 5.1: Examples of the effect of geometric imperfections

$\alpha_h := \frac{2}{\sqrt{l}} = 1.265$

$\alpha_h := \left\| \begin{array}{l} \text{if } \alpha_h < \frac{2}{3} \\ \quad \left\| \text{return } \frac{2}{3} \right. \\ \text{else if } \alpha_h > 1 \\ \quad \left\| \text{return } 1 \right. \\ \text{else} \\ \quad \left\| \text{return } \alpha_h \right. \end{array} \right.$

$uf := 2$

$\alpha_h = 1$

$\alpha_m := \sqrt{0.5 \cdot \left(1 + \frac{1}{m}\right)}$

$$\theta_i := \theta_0 \cdot \alpha_h \cdot \alpha_m = 0.004$$

$$H_{diaphragm.un.incl} := \theta_i \cdot \frac{\left(N_b + N_a\right)}{2} = 9.519\ \boldsymbol{kN}$$

$$q_{un.inc} := \frac{H_{diaphragm.un.incl}}{20\ \boldsymbol{m}} = 0.476\ \frac{\boldsymbol{kN}}{\boldsymbol{m}}$$

Wind load floor plan 1

$h_{facade} := 2.9\ \boldsymbol{m}$ Storey facade height

$z := 25\ \boldsymbol{m}$ Height of the building

$d := 10\ \boldsymbol{m}$ The length of the cross-side of the structure

$\nu_b := 25\ \frac{\boldsymbol{m}}{\boldsymbol{s}}$ Basic wind velocity of the location where the structure is situated

Terrain category		z_0 m	z_{min} m
0	Sea or coastal area exposed to the open sea	0.003	1
I	Lakes or flat and horizontal area with negligible vegetation and without obstacles	0.01	1
II	Area with low vegetation such as grass and isolated obstacles (trees, buildings) with separations of at least 20 obstacle heights	0.05	2
III	Area with regular cover of vegetation or buildings or with isolated obstacles with separations of maximum 20 obstacle heights (such as villages, suburban terrain, permanent forest)	0.3	5
IV	Area in which at least 15 % of the surface is covered with buildings and their average height exceeds 15 m	1.0	10
NOTE:	The terrain categories are illustrated in A.1.		

Terrain type III

$z_0 := 0.3\ \boldsymbol{m}$ Value are specific for terrain type

$z_{0.paralell} := 0.05\ \boldsymbol{m}$ Reference value, shall not be changed

$$k_r := 0.19 \cdot \left(\frac{z_0}{z_{0.paralell}}\right)^{0.07} = 0.215$$

$$C_e\left(z_{.var}\right) := \left[k_r \cdot \ln\left(\frac{z_{.var}}{z_0}\right)\right]^2 \cdot \left[1 + \frac{7}{\ln\left(\frac{z_{.var}}{z_0}\right)}\right]$$

$$C_e(z) = 2.344$$

$$\rho := 1.25\ \frac{\boldsymbol{kg}}{\boldsymbol{m}^3}$$

$$q_{b1} := \frac{1}{2} \cdot \rho \cdot {\nu_b}^2 = 390.625\ Pa$$

$$q_{p1} := C_e(z) \cdot q_{b1} = 0.916\ \frac{kN}{m^2}$$

$$\frac{z}{d} = 2.5$$

$$c_{pe.10.zoneD} := 0.8$$

Table 3.4: Values of c_{pe} given in Eurocode

Zone	D		E	
h/d	$c_{pe,10}$	$c_{pe,1}$	$c_{pe,10}$	$c_{pe,1}$
5	+0.8	+1.0	-0.7	
1	+0.8	+1.0	-0.5	
≤ 0.25	+0.7	+1.0	-0.3	

Interpolation zone E

$$c_{pe.10.zoneE} := -0.5 + \left((-0.7) - (-0.5)\right) \cdot \left(\frac{\left(\frac{z}{d}\right) - 1}{5 - 1}\right) = -0.575$$

$$c_{pe.fin} := \left|c_{pe.10.zoneD}\right| + \left|c_{pe.10.zoneE}\right| = 1.375$$

$$w := c_{pe.fin} \cdot q_{p1} = 1.259\ \frac{kN}{m^2}$$

The line load on diaphragm

$$q_{wind} := w \cdot h_{facade} = 3.651\ \frac{kN}{m}$$

Final line load Object 1

$$q_{diaphragm} := q_{un.inc} \cdot 1.2 + q_{wind} \cdot 1.5 = 6.047\ \frac{kN}{m}$$

Unintended inclination floor 2

$\theta_0 := \frac{1}{200}$

$l := 2.5$ The storey height, in meters, of the vertical load-carrying members. Note, use no unit in equation.

$m := 16$ The number of vertical load-carrying elements on analyzed floor

$G_{k.floor} := 686\ kN$ g=2kn/m2, tot area = 27*12.7=343m2

$Q_{k.floor} := 686\ kN$ q=2kn/m2

$N_a := 5 \cdot \left(G_{k.floor} + Q_{k.floor}\right) = 6860\ kN$ Accumulated vertical force from all storeys above [kN].

$N_b := G_{k.floor} + Q_{k.floor} = 1372\ kN$ Vertical force from studied floor level [kN].

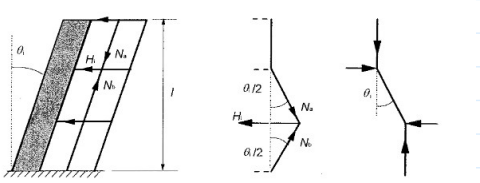

Figure 5.1: Examples of the effect of geometric imperfections

$\alpha_h := \frac{2}{\sqrt{l}} = 1.265$

$\alpha_h :=$ if $\alpha_h < \frac{2}{3}$ return $\frac{2}{3}$ else if $\alpha_h > 1$ return 1 else return α_h

$\alpha_h = 1$

$\alpha_m := \sqrt{0.5 \cdot \left(1 + \frac{1}{m}\right)}$

$\theta_i := \theta_0 \cdot \alpha_h \cdot \alpha_m = 0.004$

$uf := 2$

$$H_{diaphragm.un.incl} := \theta_i \cdot \frac{(N_b + N_a)}{2} = 15\ kN$$

$$q_{un.inc} := \frac{H_{diaphragm.un.incl}}{20\ m} = 0.75\ \frac{kN}{m}$$

Final line load floor plan 2

$$q_{diaphragm.2} := q_{un.inc} \cdot 1.2 + q_{wind} \cdot 1.5 = 6.376\ \frac{kN}{m}$$

E

Complete results of parametric study

Object 1

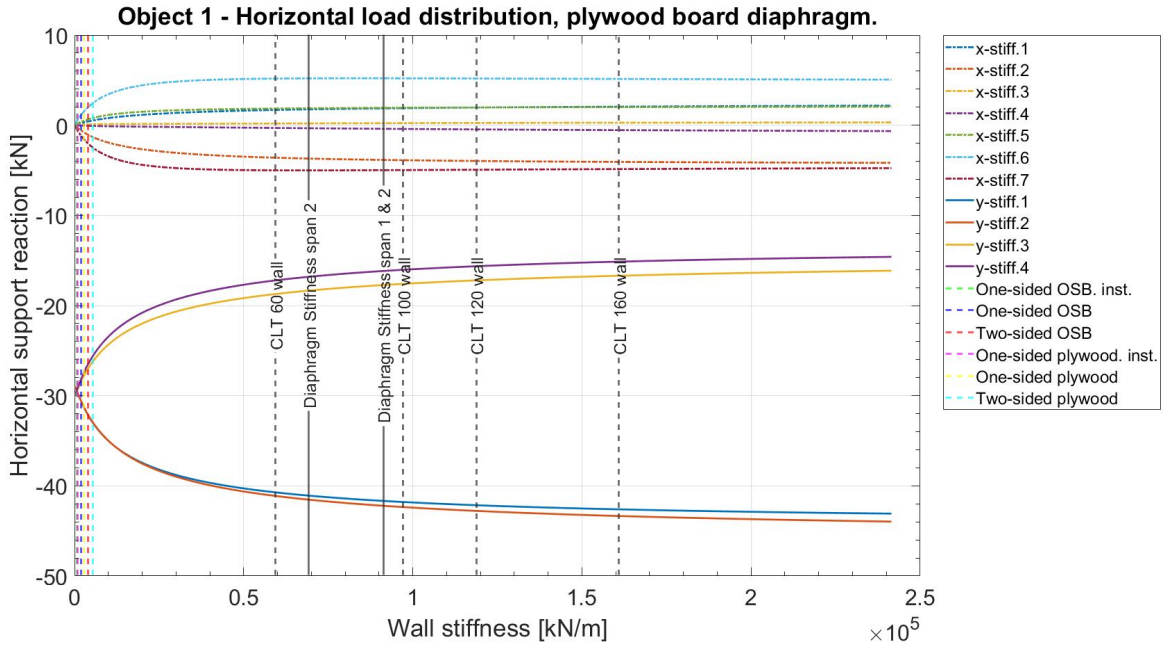

*

Object 1, horizontal load distribution of plywood board diaphragm setup with an increment of the line support stiffness and infinitely stiff edge connection.

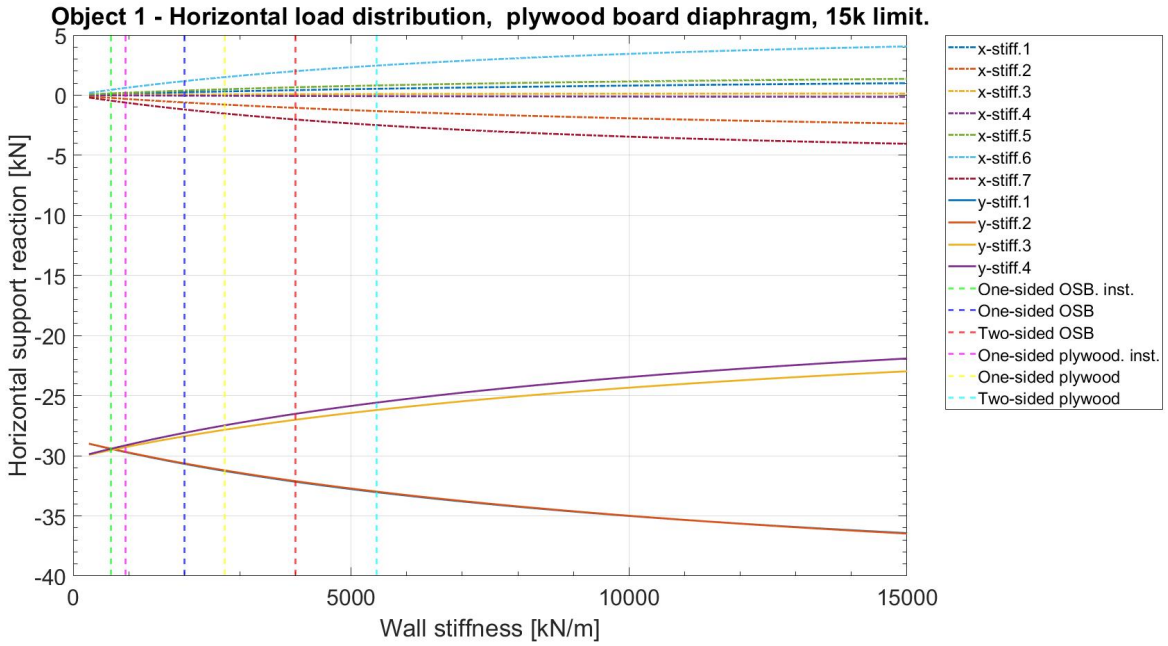

*

Object 1, horizontal load distribution of plywood board diaphragm setup with an increment of the line support stiffness and infinitely stiff edge connection. X-axis 15k limit.

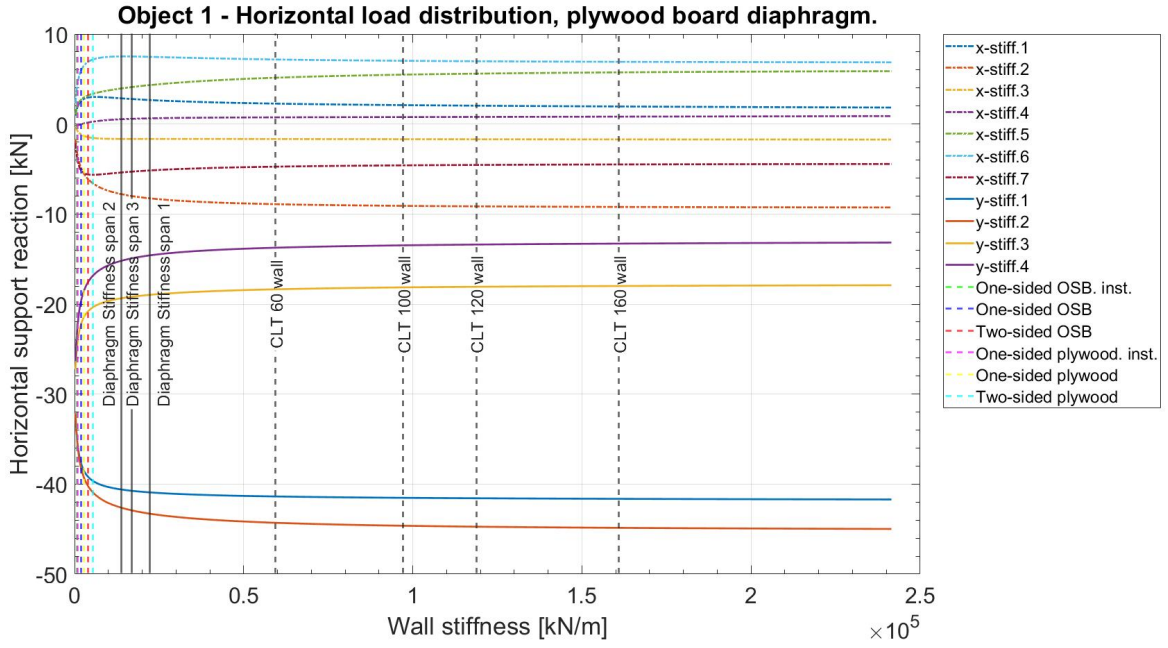

*

Object 1, horizontal load distribution of plywood board diaphragm setup with an increment of the line support stiffness and constant edge connection stiffness 1000kN/m/m.

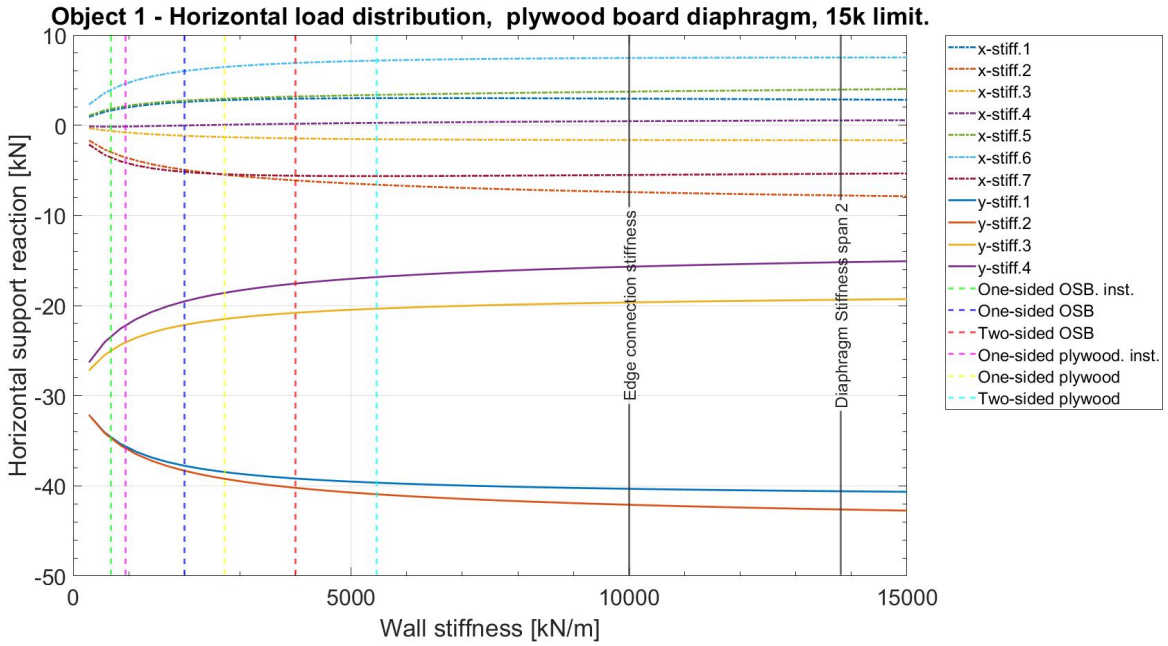

Object 1, horizontal load distribution of plywood board diaphragm setup with an increment of the line support stiffness and constant edge connection stiffness 1000kN/m/m. X-axis limited to 15k.

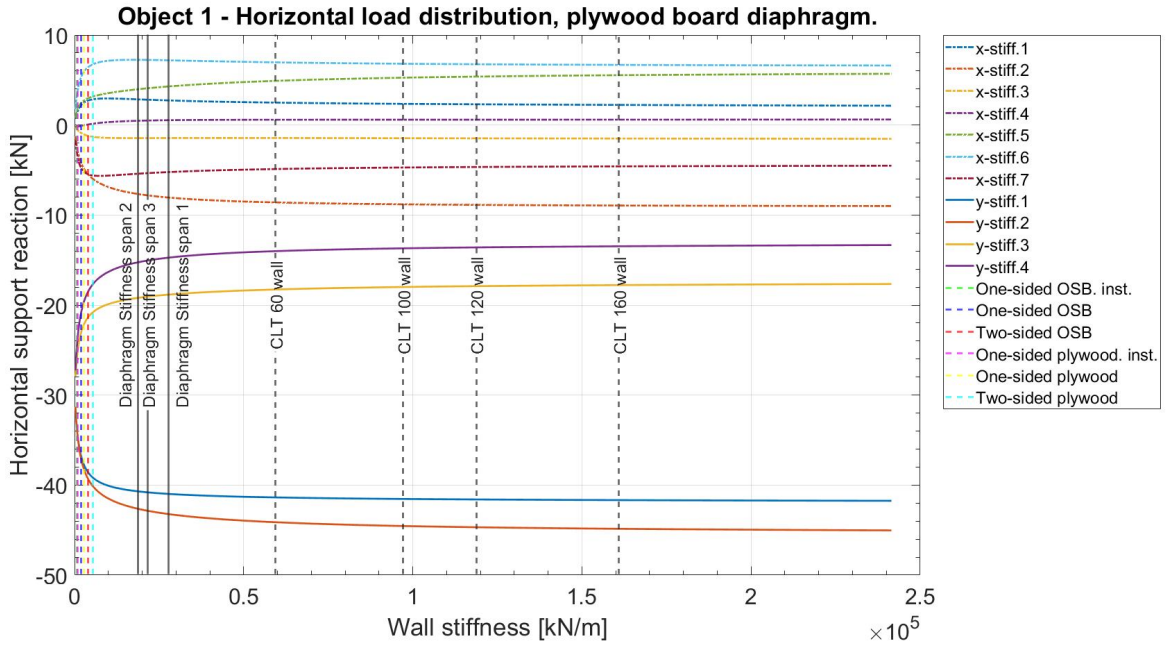

Object 1, horizontal load distribution of plywood board diaphragm setup with an increment of the line support stiffness and constant edge connection stiffness 1500kN/m/m.

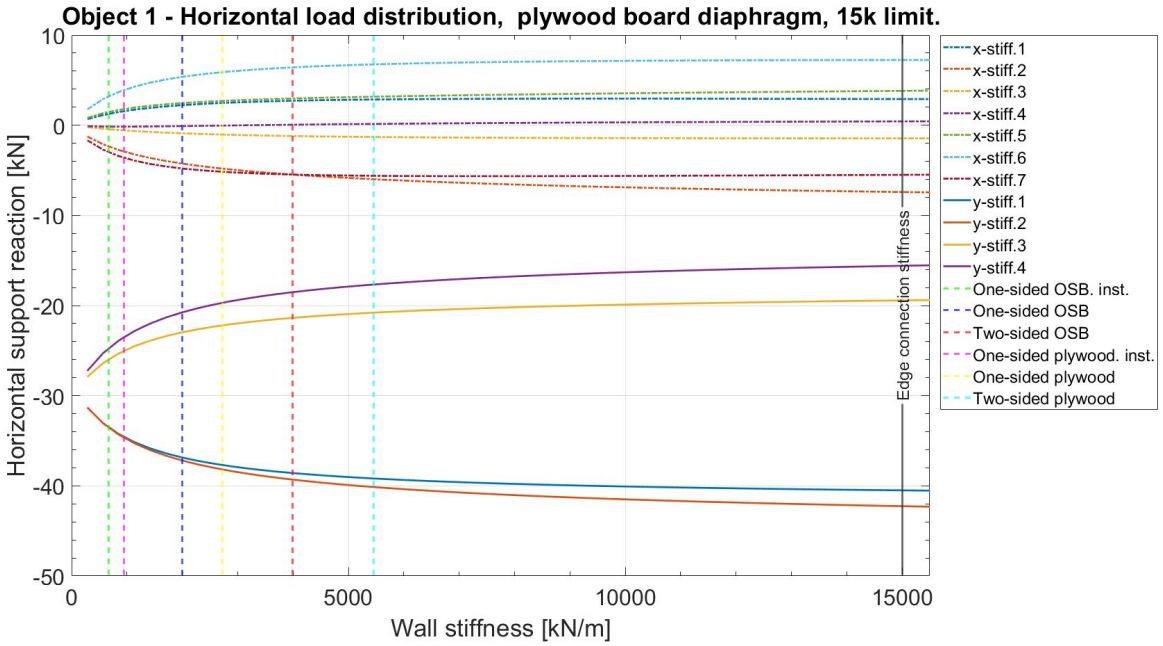

Object 1, horizontal load distribution of plywood board diaphragm setup with an increment of the line support stiffness and constant edge connection stiffness 1500kN/m/m. X-axis limited to 15k.

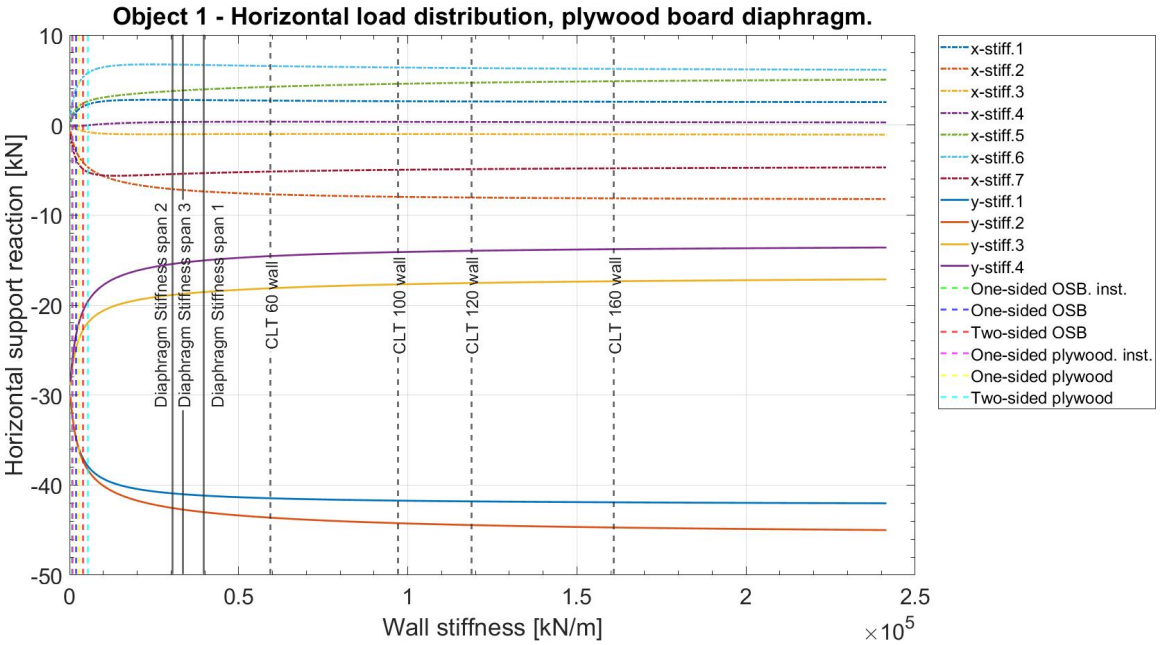

Object 1, horizontal load distribution of plywood board diaphragm setup with an increment of the line support stiffness and constant edge connection stiffness 3350kN/m/m.

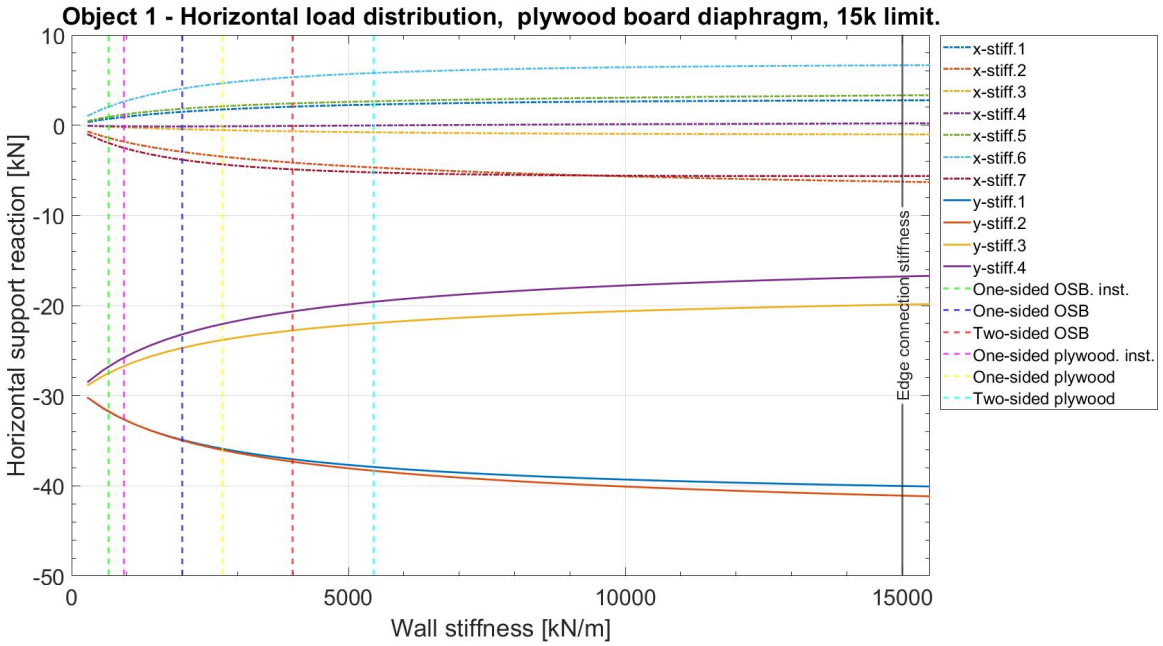

Object 1, horizontal load distribution of plywood board diaphragm setup with an increment of the line support stiffness and constant edge connection stiffness 3350kN/m/m. X-axis limited to 15k.

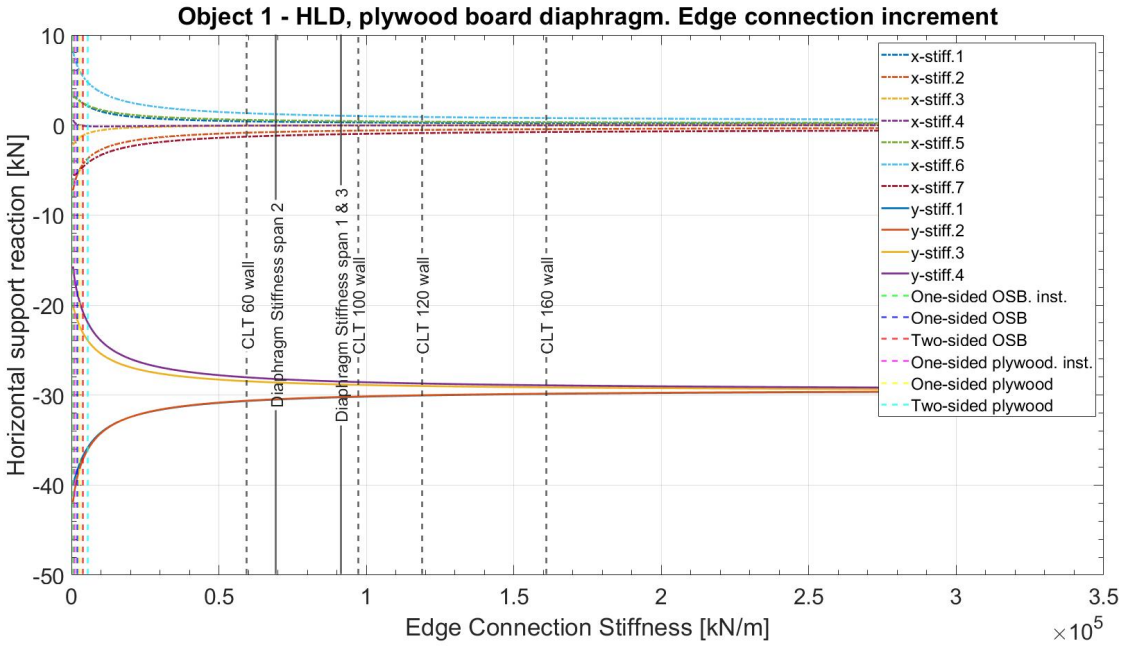

Object 1, horizontal load distribution of plywood board diaphragm setup with an increment of the edge connection stiffness and a constant line support stiffness of 100kN/m/m.

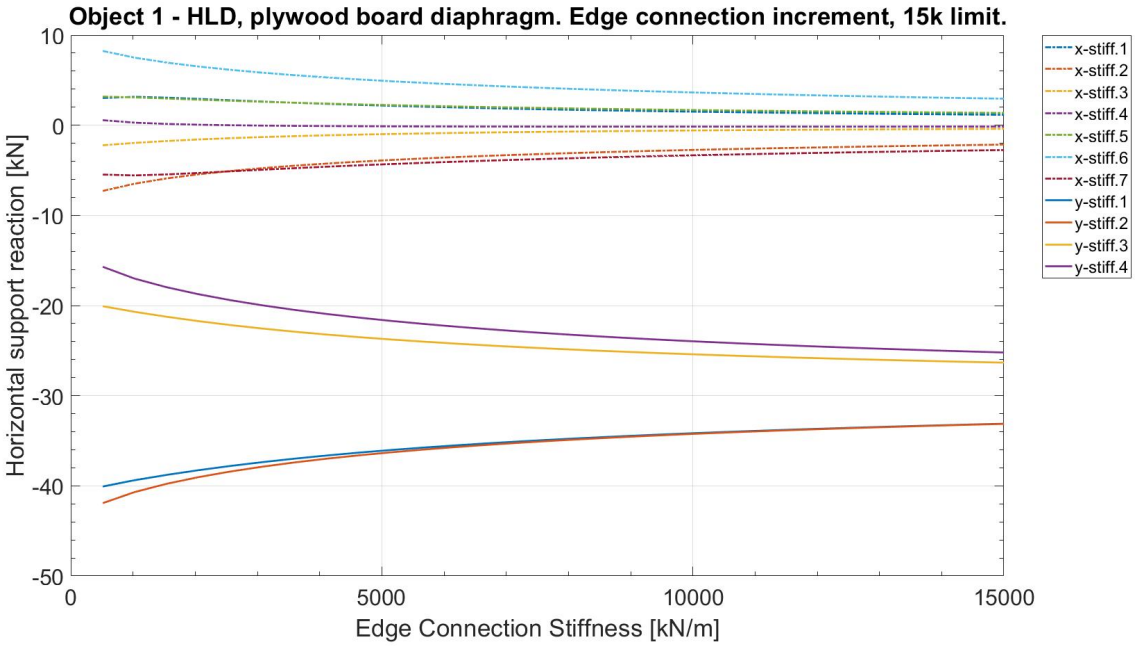

Object 1, horizontal load distribution of plywood board diaphragm setup with an increment of the edge connection stiffness and a constant line support stiffness of 100kN/m/m. X-axis limited to 15k.

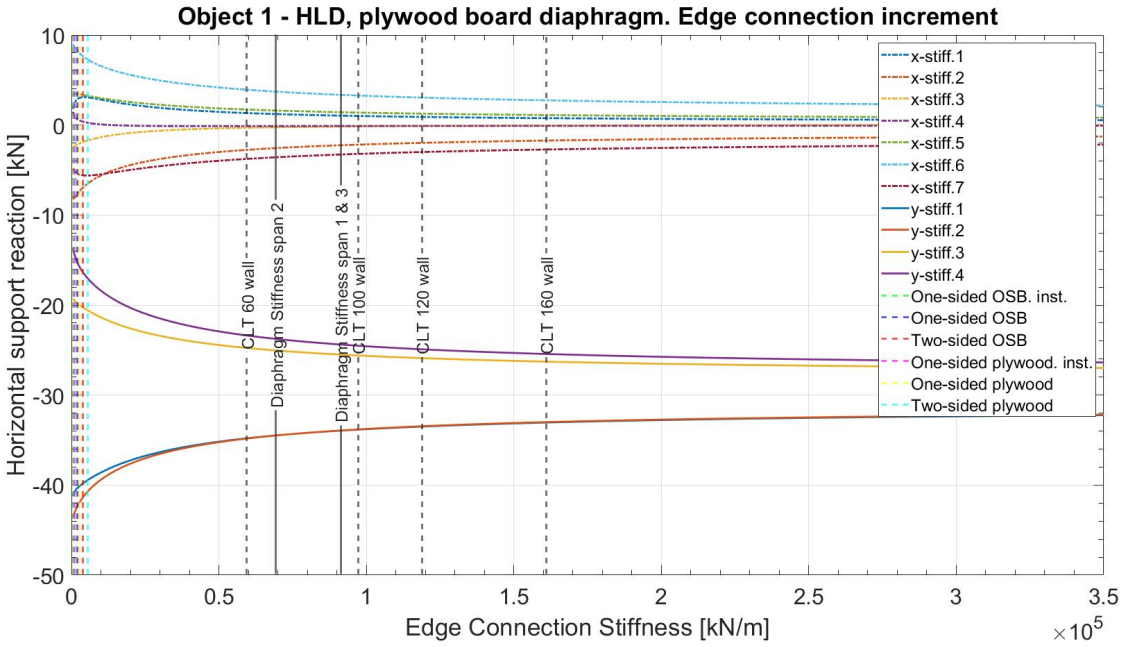

Object 1, horizontal load distribution of plywood board diaphragm setup with an increment of the edge connection stiffness and a constant line support stiffness of 500kN/m/m

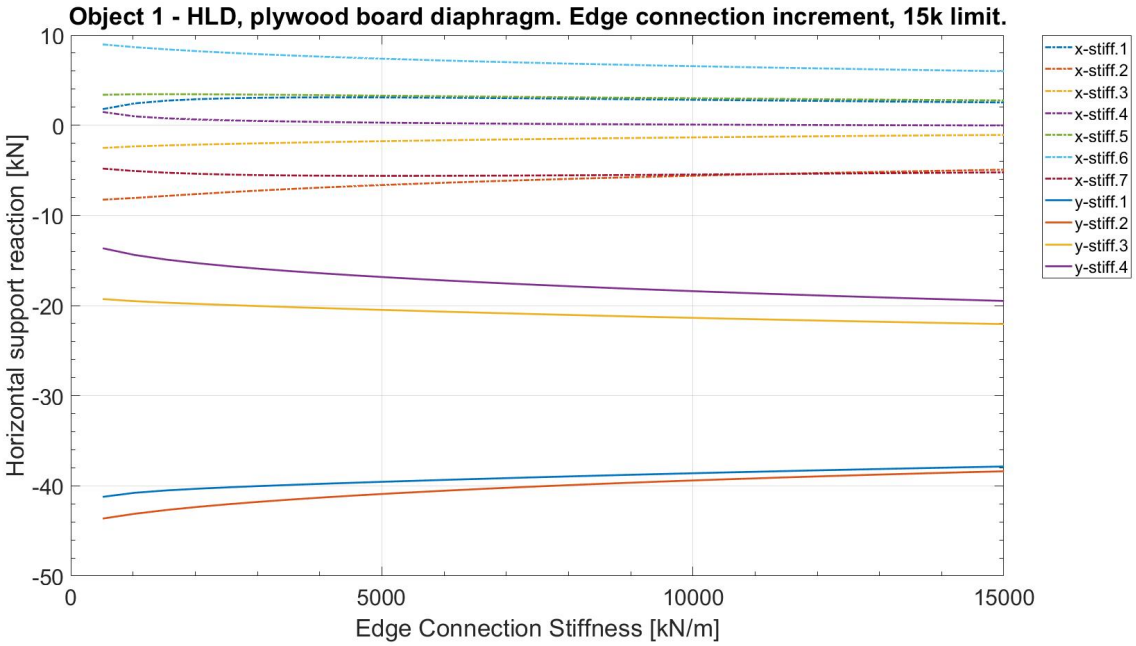

Object 1, horizontal load distribution of plywood board diaphragm setup with an increment of the edge connection stiffness and a constant line support stiffness of 500kN/m/m. X-axis limited to 15k.

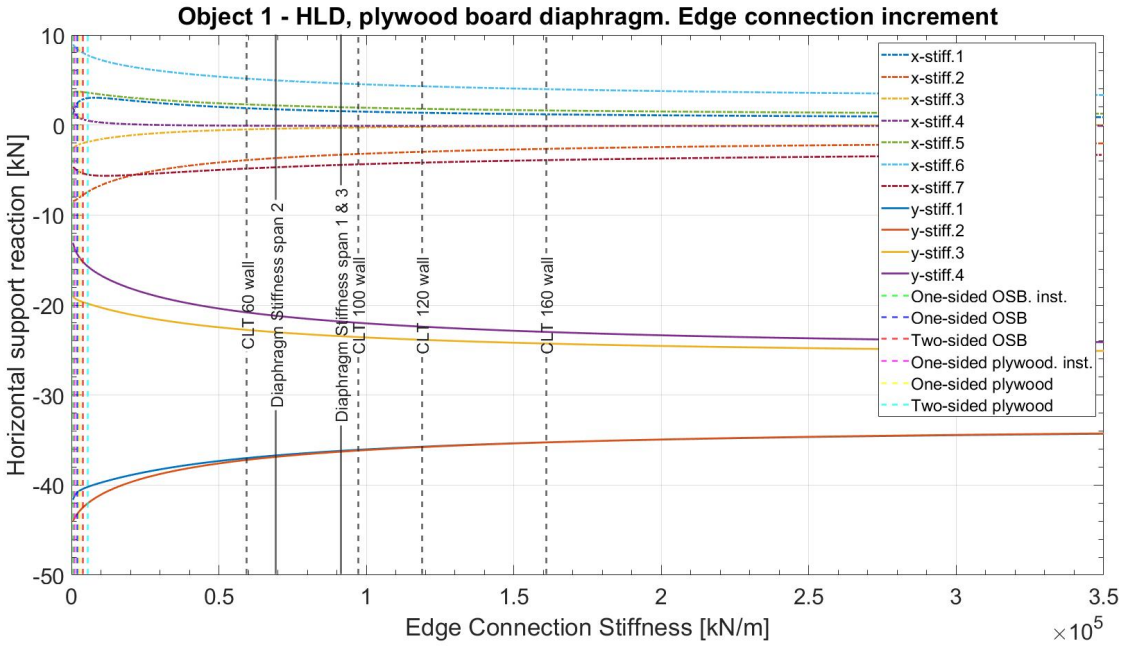

Object 1, horizontal load distribution of plywood board diaphragm setup with an increment of the edge connection stiffness and a constant line support stiffness of 1000kN/m/m

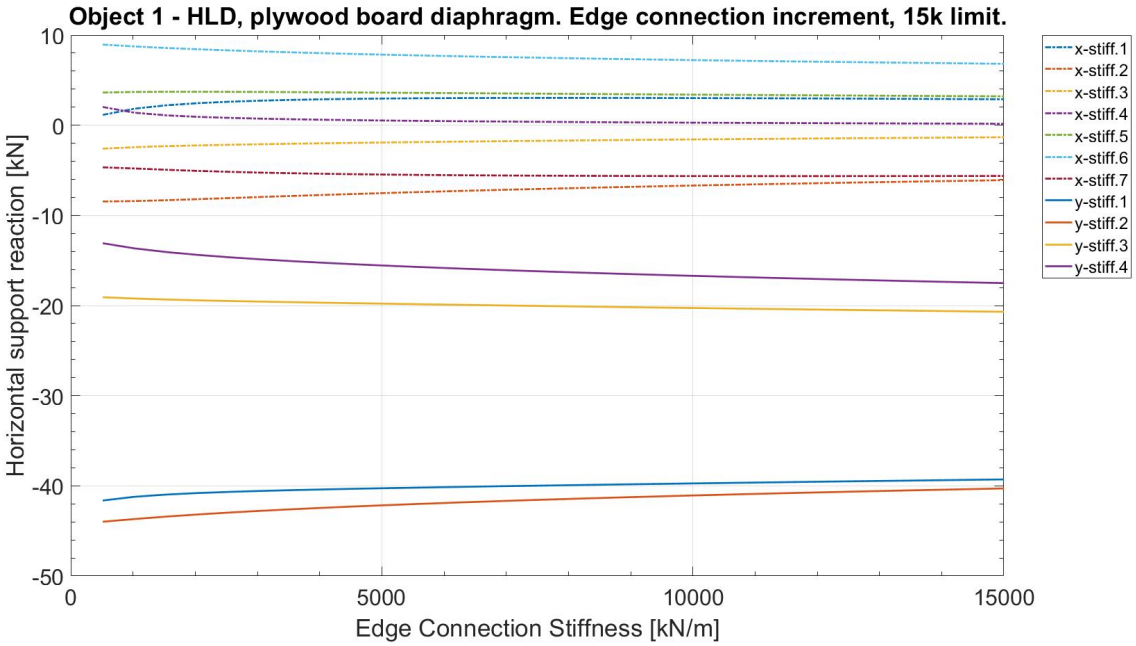

Object 1, horizontal load distribution of plywood board diaphragm setup with an increment of the edge connection stiffness and a constant line support stiffness of 1000kN/m/m. X-axis limited to 15k.

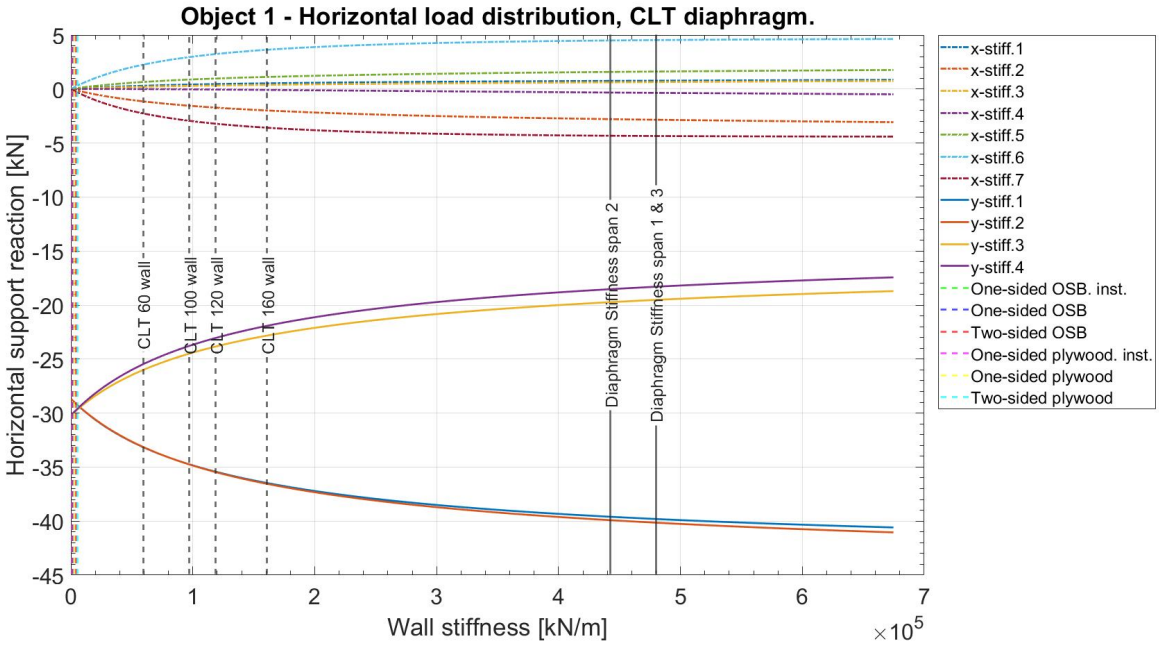

Object 1, horizontal load distribution of CLT panels diaphragm setup with an increment of the line support stiffness and infinitely stiff edge connection.

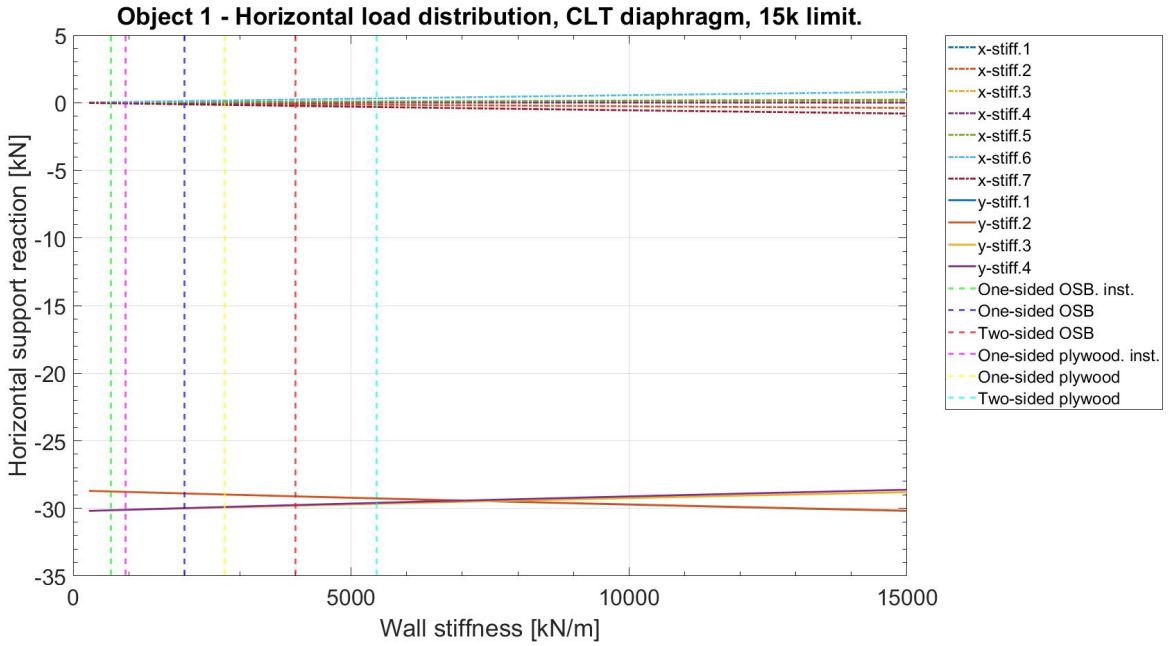

Object 1, horizontal load distribution of CLT panels diaphragm setup with an increment of the line support stiffness and infinitely stiff edge connection. X-axis limited to 15k.

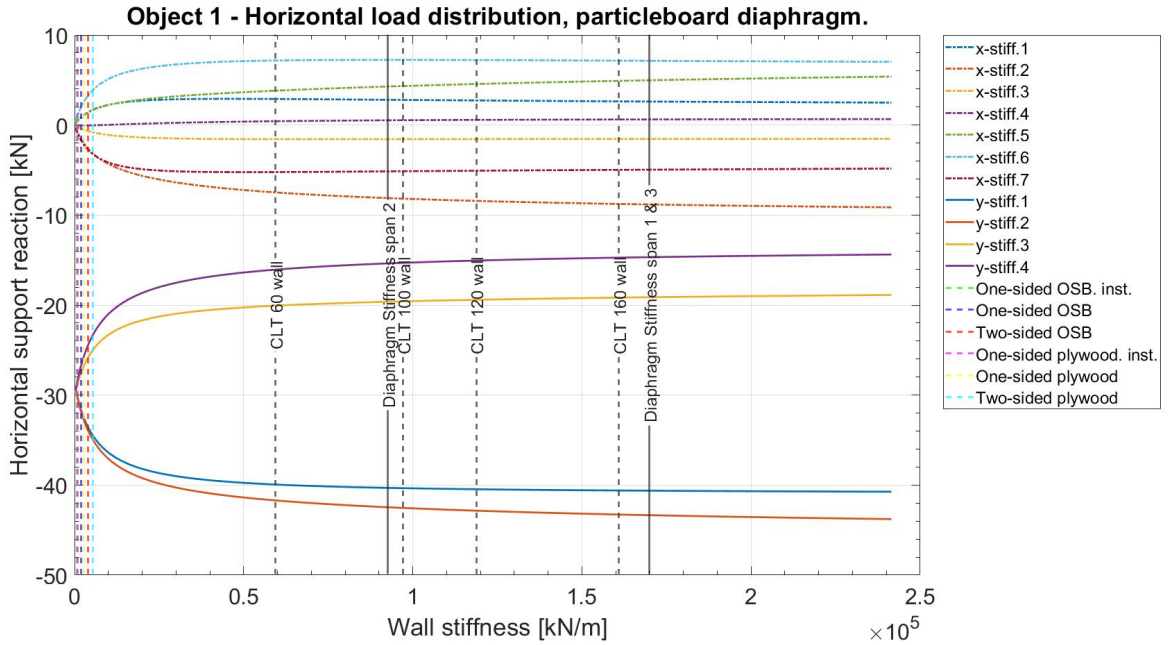

Object 1, horizontal load distribution of CLT panels diaphragm setup with an increment of the line support stiffness and a constant edge connection stiffness of 6968kN/m/m.

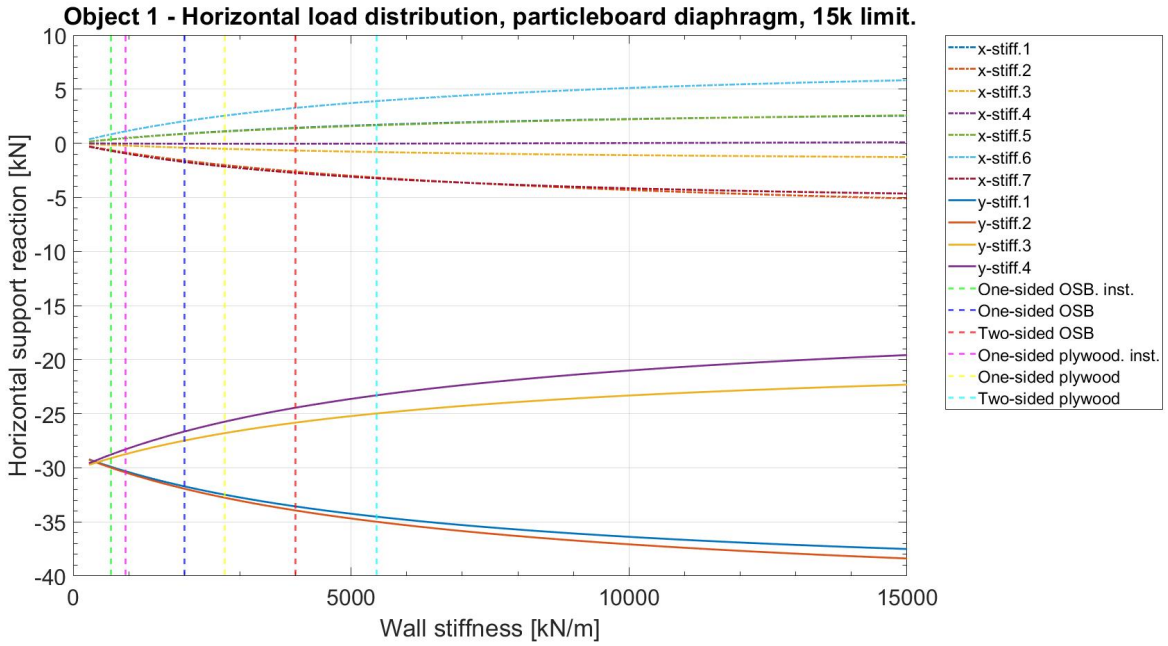

Object 1, horizontal load distribution of CLT panels diaphragm setup with an increment of the line support stiffness and a constant edge connection stiffness of 6968kN/m/m. X-axis limited to 15k.

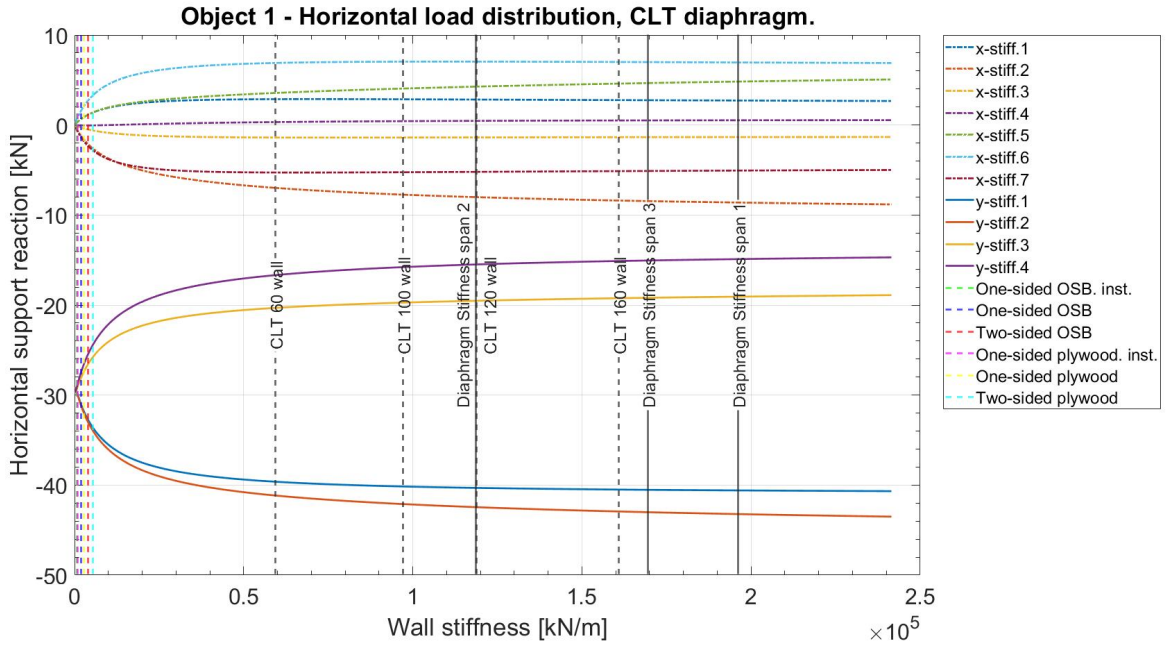

Object 1, horizontal load distribution of CLT panels diaphragm setup with an increment of the line support stiffness and a constant edge connection stiffness of 9755kN/m/m.

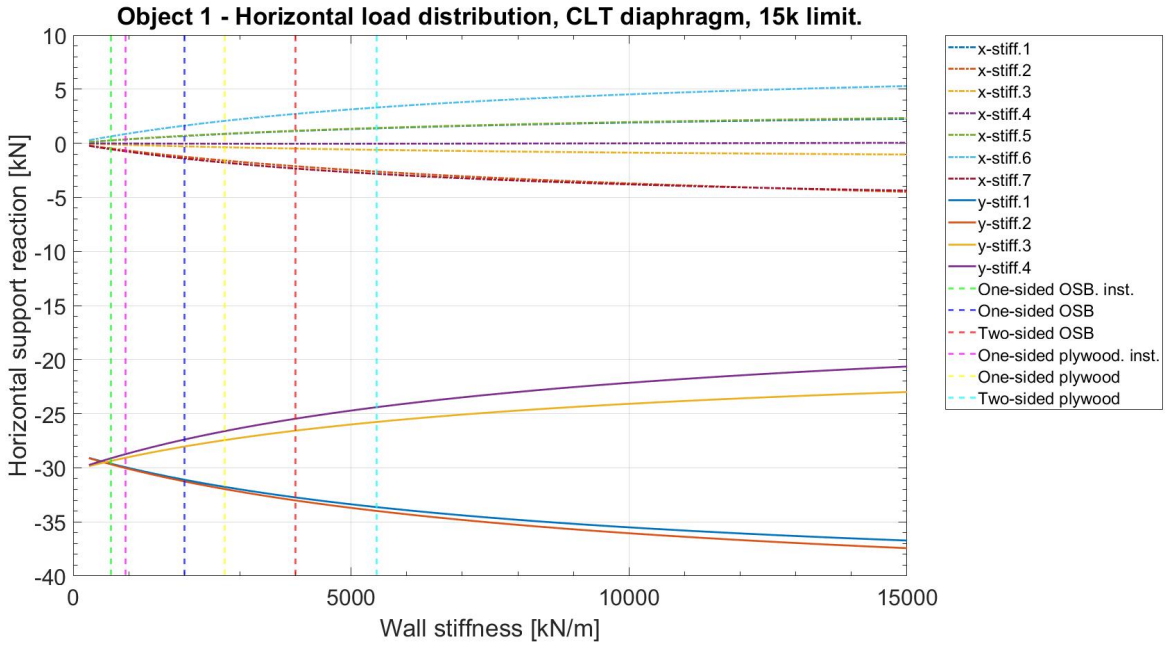

Object 1, horizontal load distribution of CLT panels diaphragm setup with an increment of the line support stiffness and a constant edge connection stiffness of 9755kN/m/m. X-axis limited to 15k.

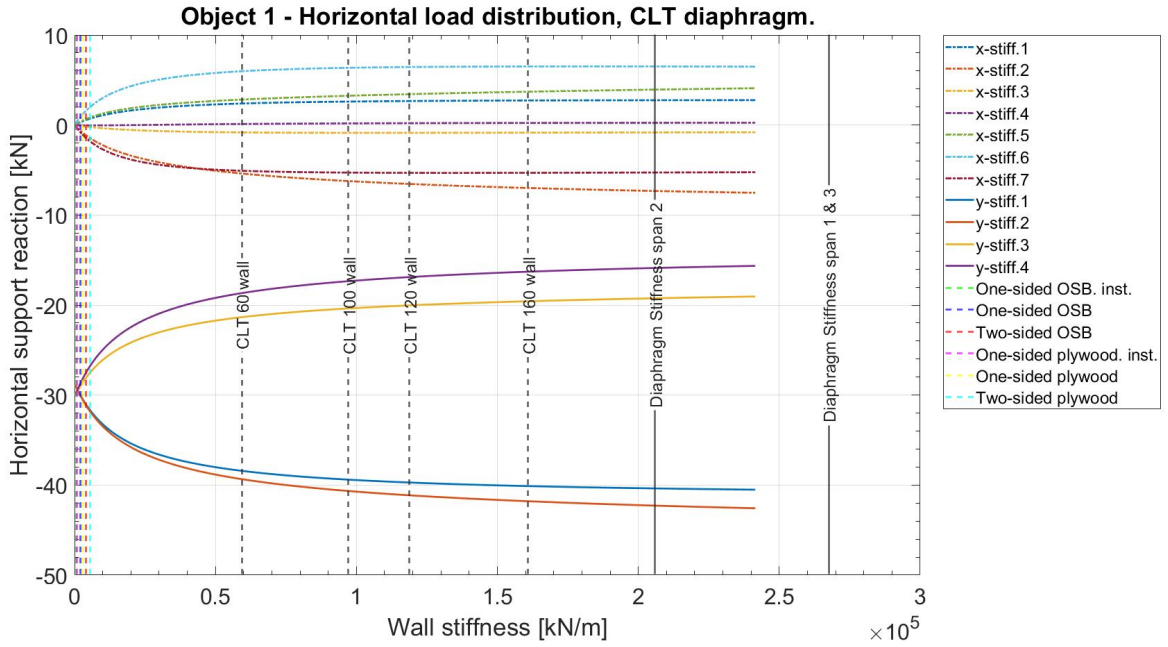

Object 1, horizontal load distribution of CLT panels diaphragm setup with an increment of the line support stiffness and a constant edge connection stiffness of 24386kN/m/m.

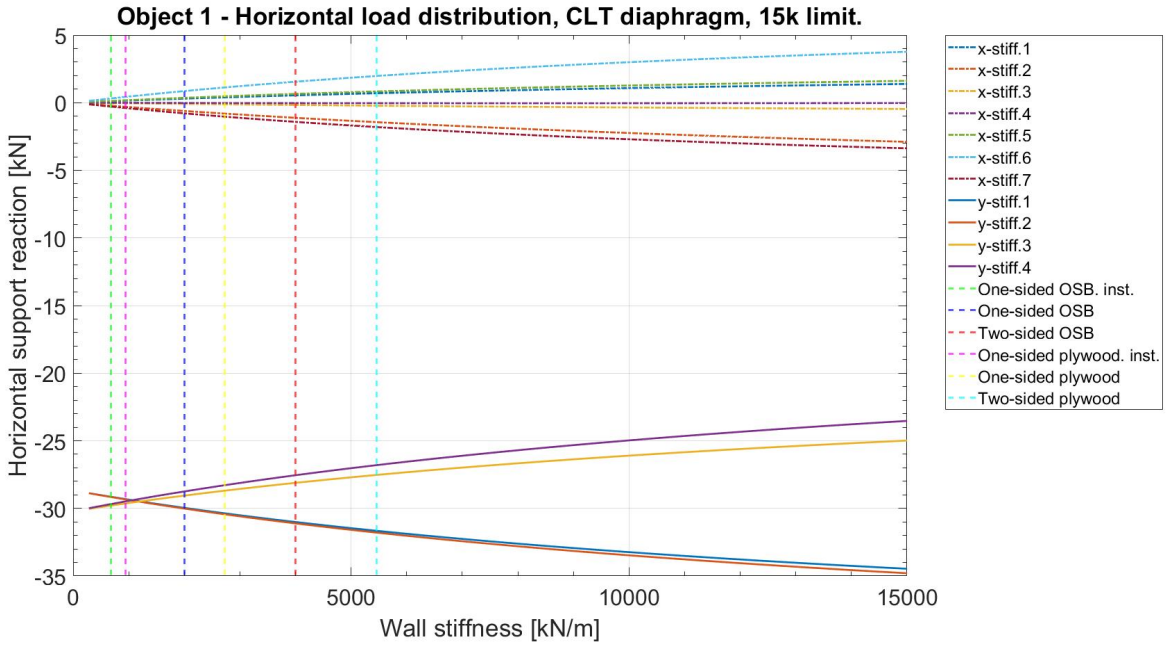

Object 1, horizontal load distribution of CLT panels diaphragm setup with an increment of the line support stiffness and a constant edge connection stiffness of 24386kN/m/m. X-axis limited to 15k.

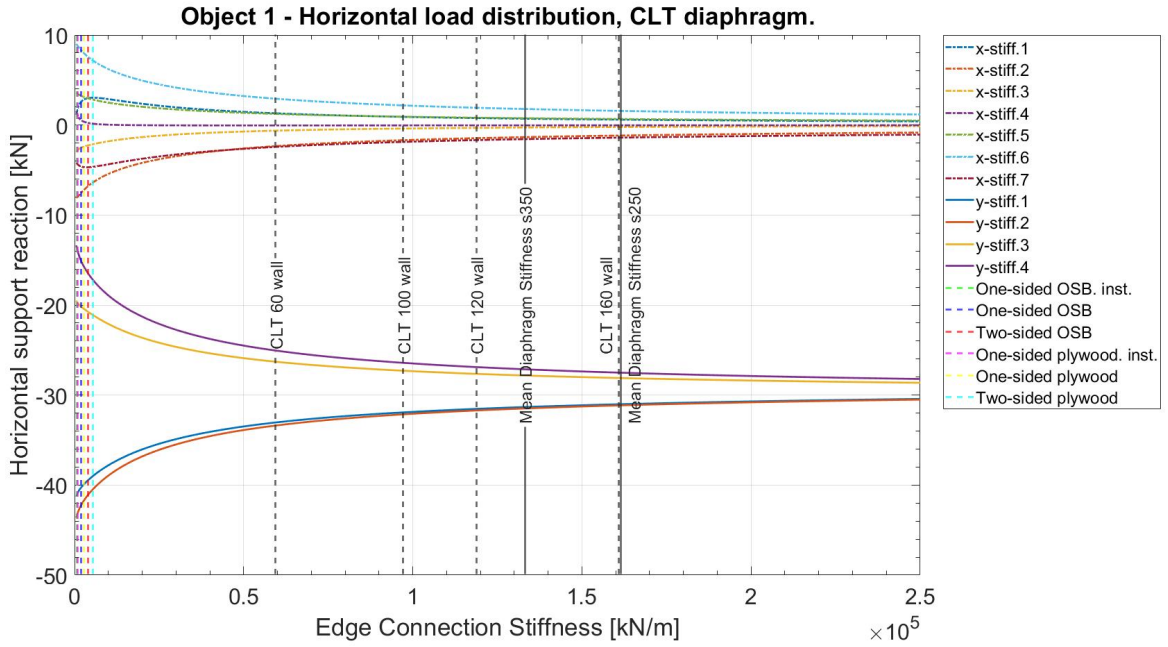

Object 1, horizontal load distribution of CLT panels diaphragm setup with an increment of the edge connection stiffness and a constant line support stiffness of 500kN/m/m

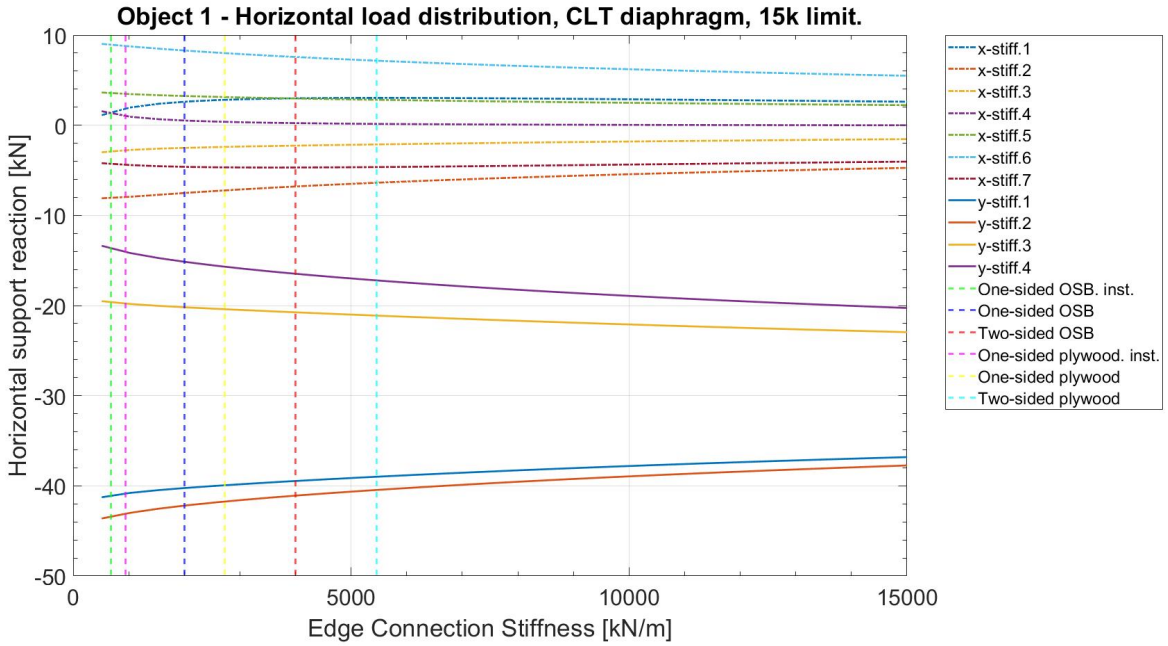

Object 1, horizontal load distribution of CLT panels diaphragm setup with an increment of the edge connection stiffness and a constant line support stiffness of 500kN/m/m. X-axis limited to 15k.

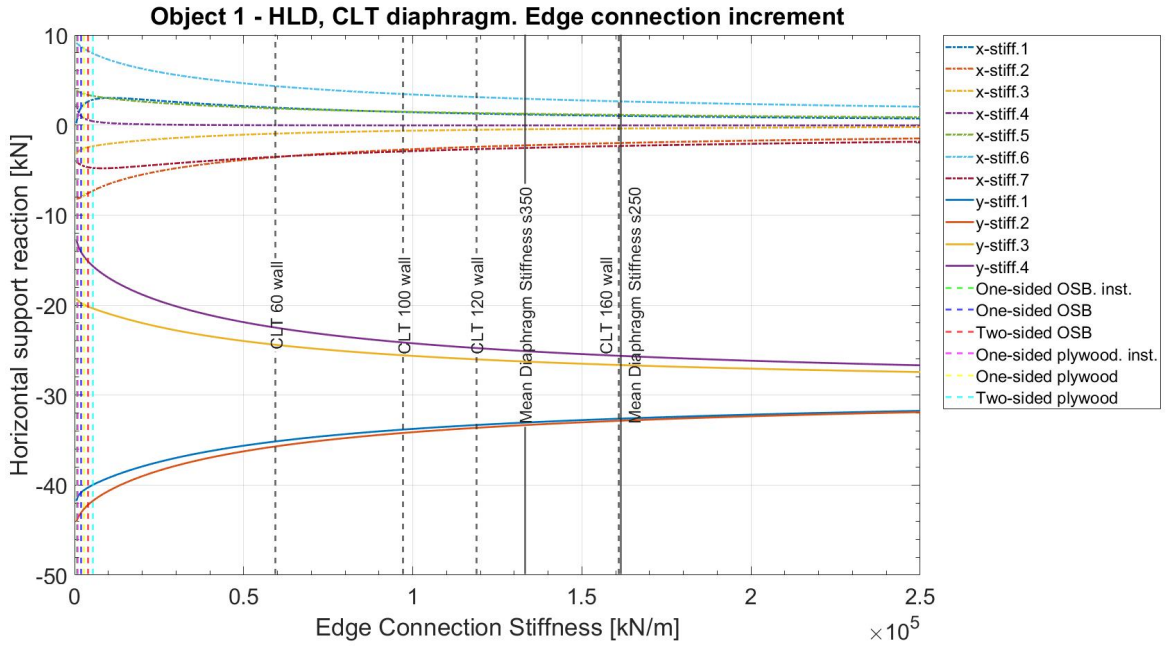

Object 1, horizontal load distribution of CLT panels diaphragm setup with an increment of the edge connection stiffness and a constant line support stiffness of 1000kN/m/m

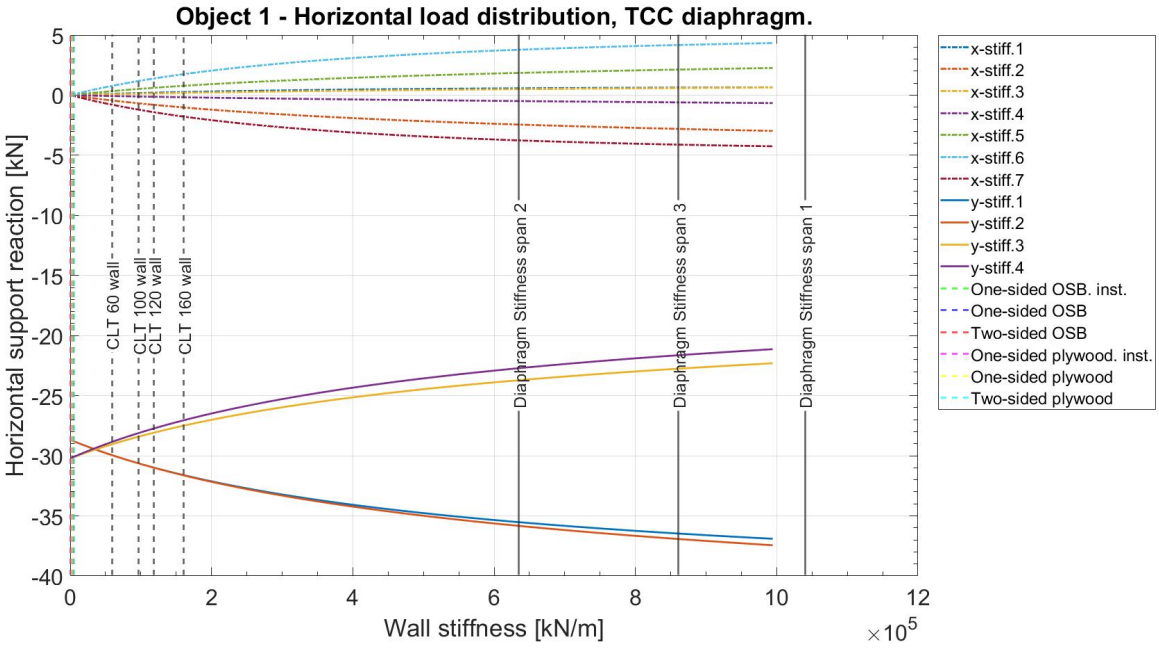

Object 1, horizontal load distribution of TCC panels diaphragm setup with an increment of the line support stiffness and a constant infinitely stiff edge connection.

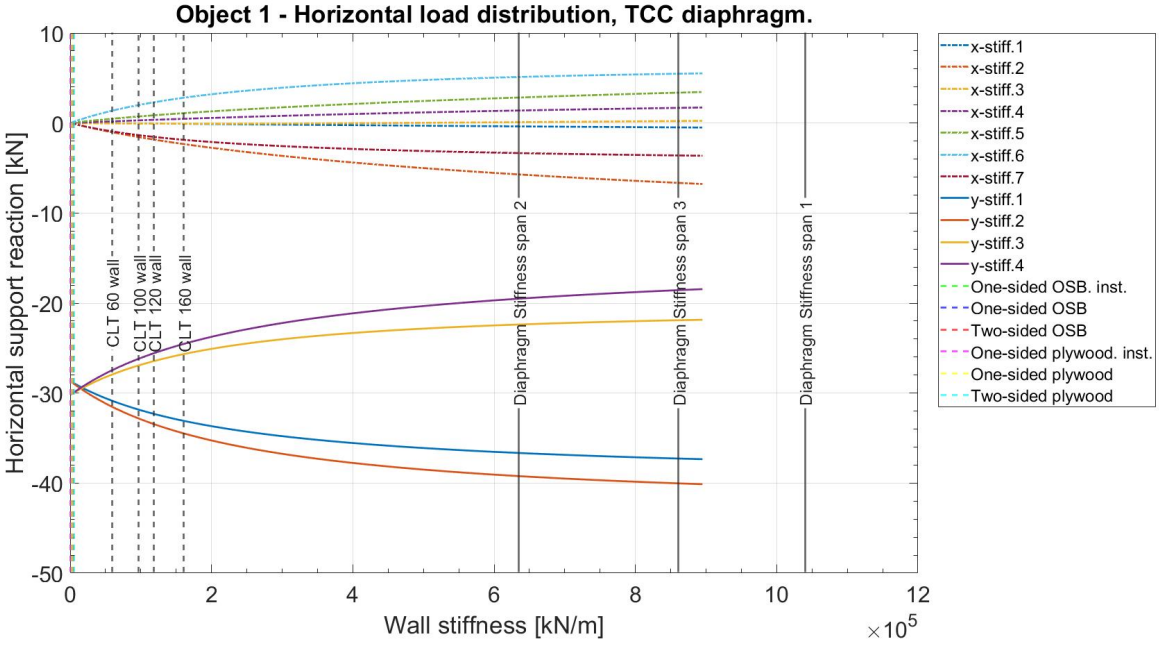

Object 1, horizontal load distribution of TCC panels diaphragm setup with an increment of the line support stiffness and a constant edge connection stiffness of 50000kN/m/m.

Object 2

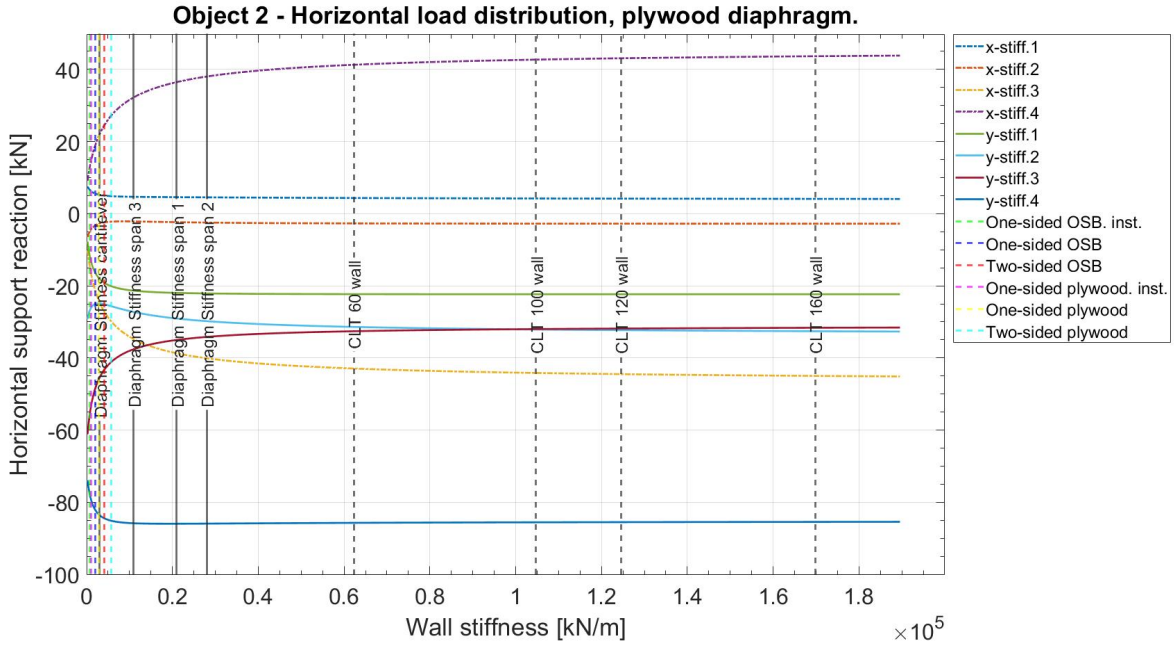

Object 2, horizontal load distribution of plywood board diaphragm setup with an increment of the line support stiffness and constant edge connection stiffness 1000kN/m/m.

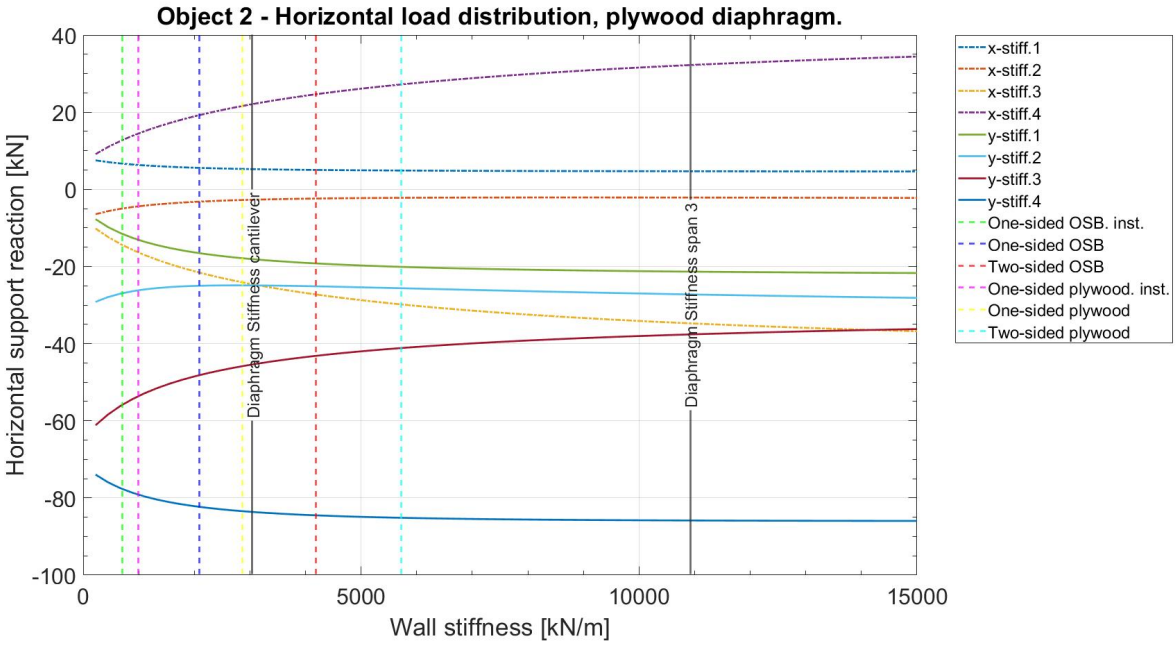

Object 2, horizontal load distribution of plywood board diaphragm setup with an increment of the line support stiffness and constant edge connection stiffness 1000kN/m/m. X-axis limited to 15k.

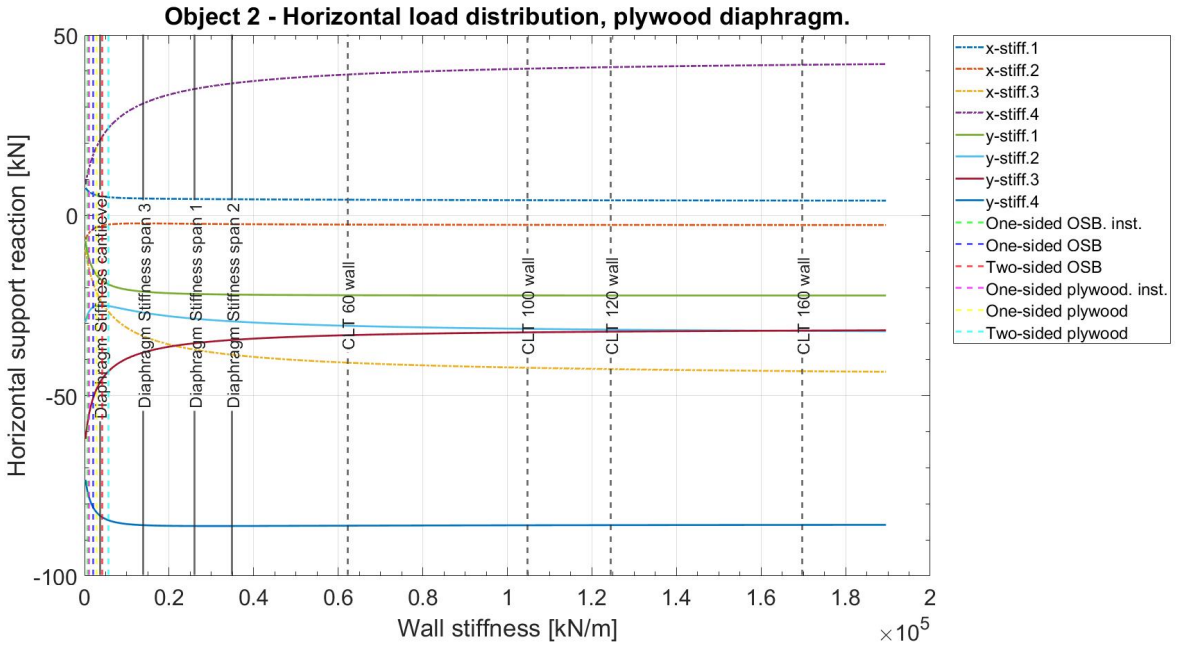

Object 2, horizontal load distribution of plywood panels diaphragm setup with an increment of the edge connection stiffness and a constant line support stiffness of 1340kN/m/m

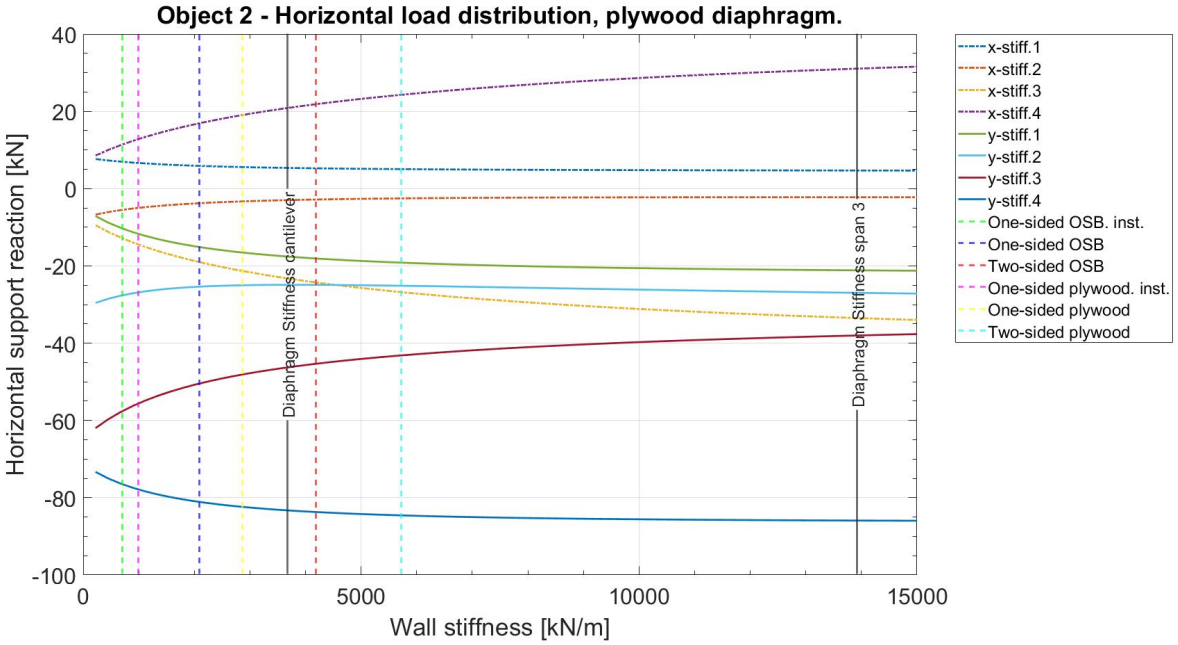

Object 2, horizontal load distribution of plywood panels diaphragm setup with an increment of the edge connection stiffness and a constant line support stiffness of 1340kN/m/m. X-axis limited to 15k.

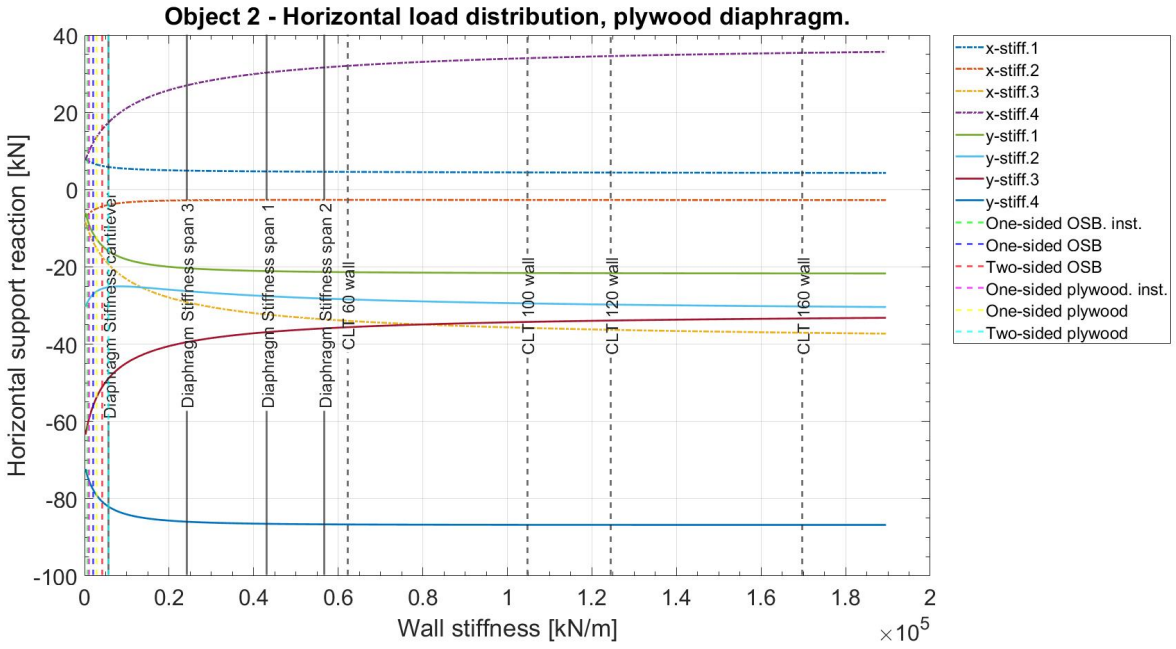

Object 2, horizontal load distribution of plywood panels diaphragm setup with an increment of the edge connection stiffness and a constant line support stiffness of 3350kN/m/m

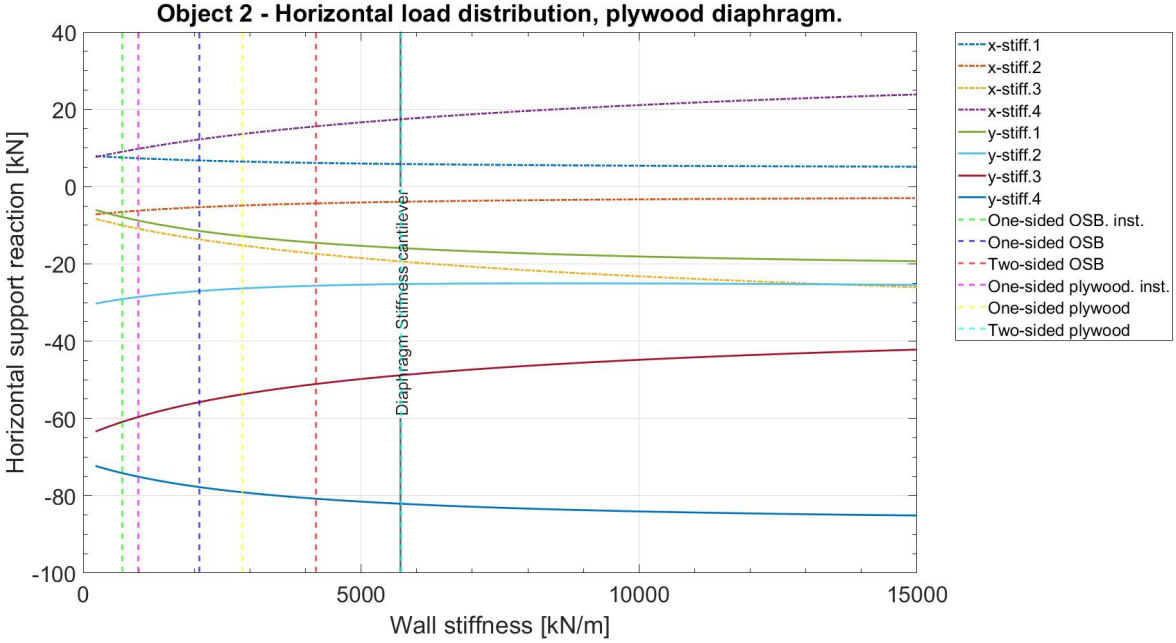

Object 2, horizontal load distribution of plywood panels diaphragm setup with an increment of the edge connection stiffness and a constant line support stiffness of 3350kN/m/m. X-axis limited to 15k.

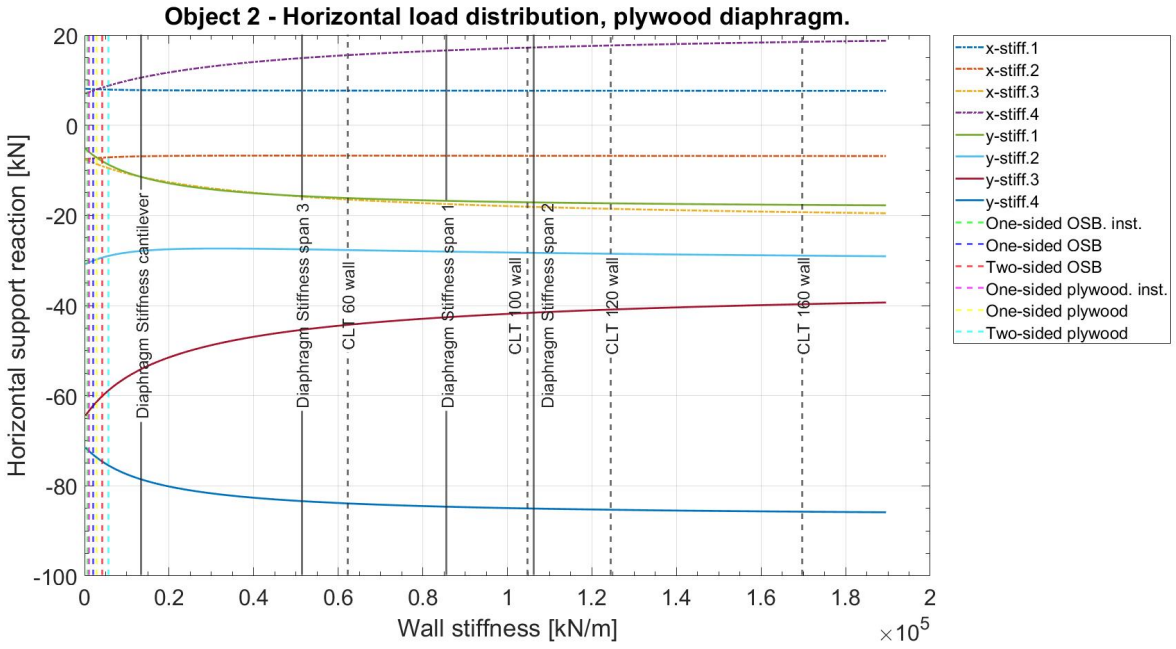

Object 2, horizontal load distribution of plywood panels diaphragm setup with an increment of the line support stiffness and a constant infinitely stiff edge connection.

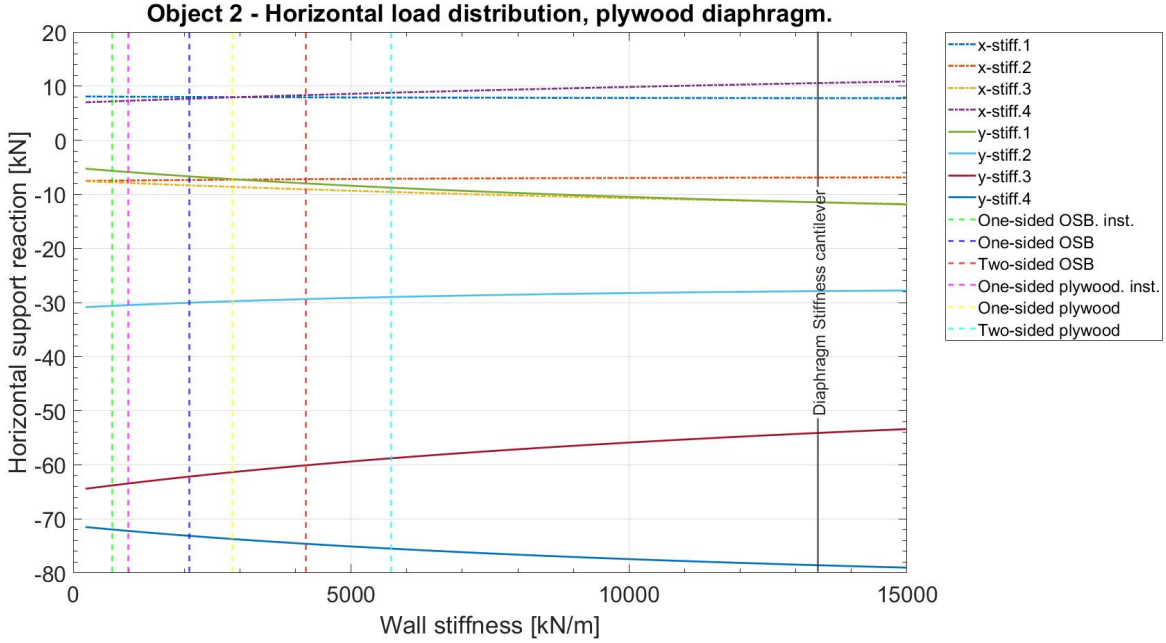

Object 2, horizontal load distribution of plywood panels diaphragm setup with an increment of the line support stiffness and a constant infinitely stiff edge connection. X-axis limited to 15k.

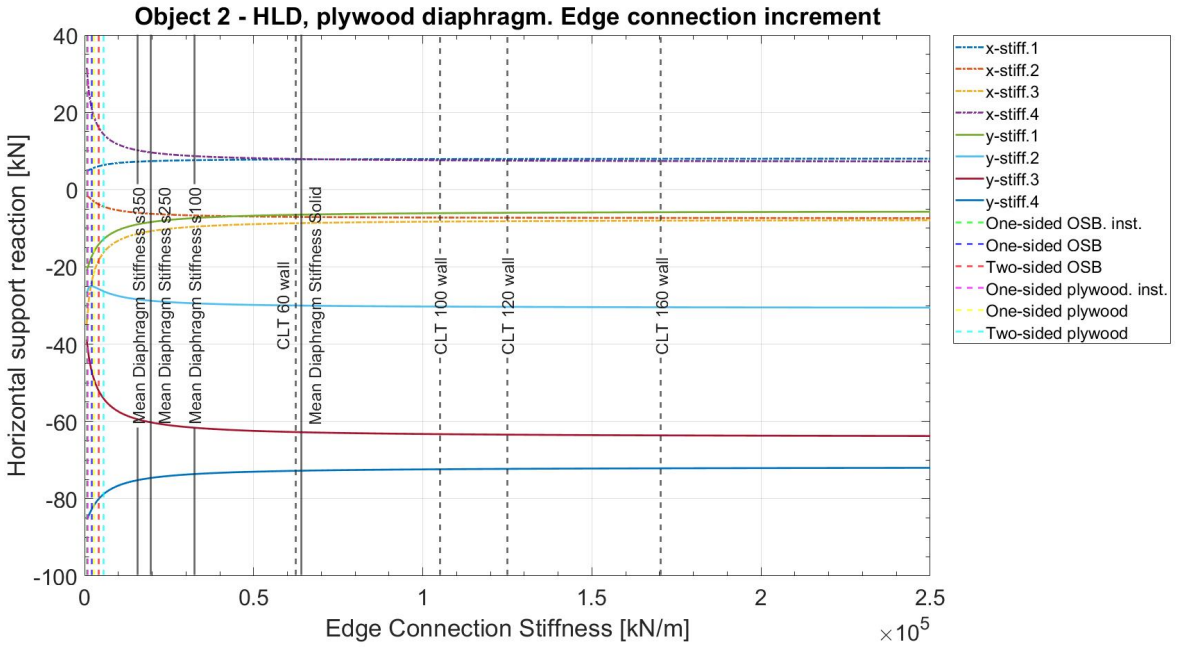

Object 2, horizontal load distribution of plywood panels diaphragm setup with an increment of the edge connection stiffness and a constant line support stiffness of 100kN/m/m

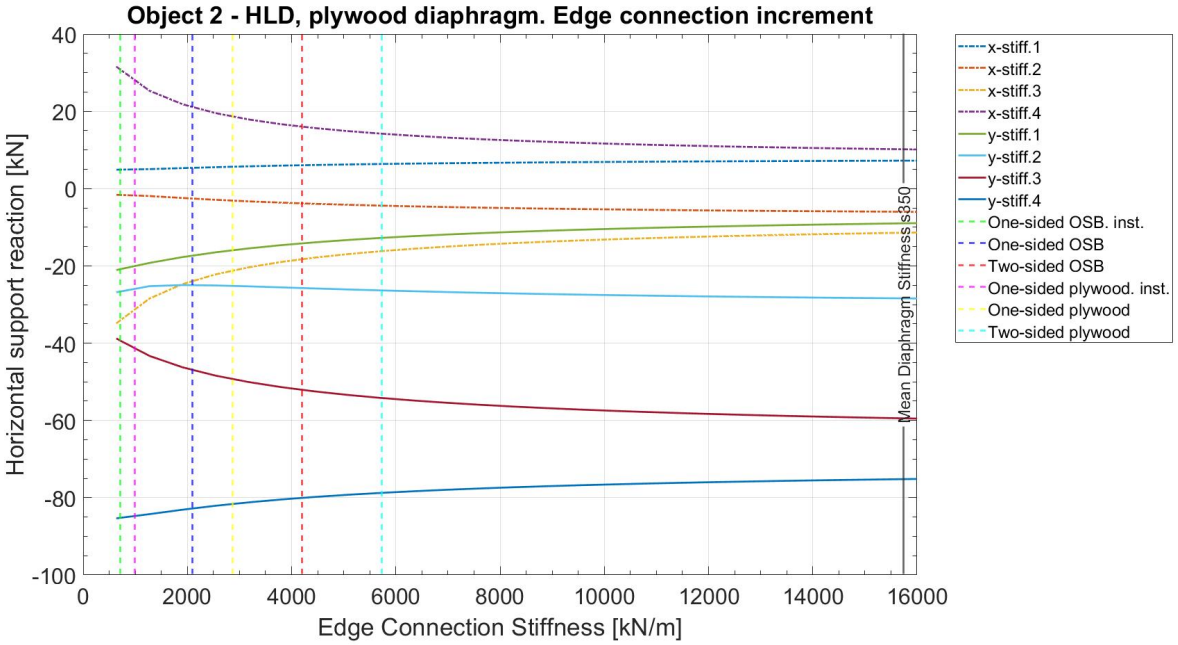

Object 2, horizontal load distribution of plywood panels diaphragm setup with an increment of the edge connection stiffness and a constant line support stiffness of 100kN/m/m. X-axis limited to 16k.

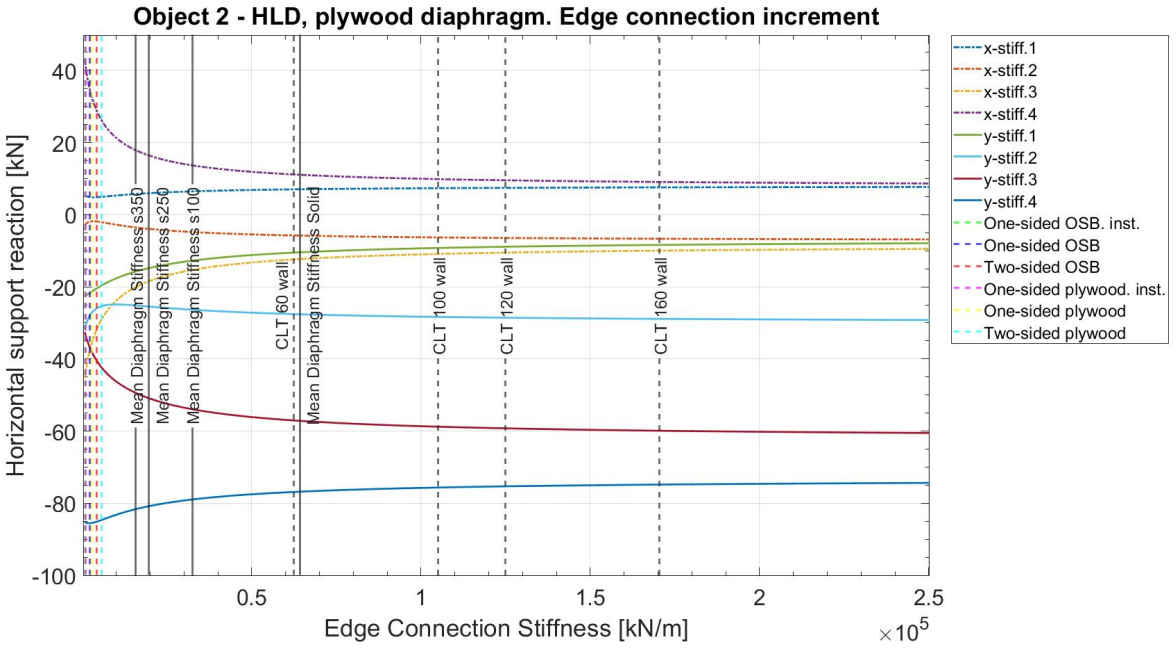

Object 2, horizontal load distribution of plywood panels diaphragm setup with an increment of the edge connection stiffness and a constant line support stiffness of 500kN/m/m

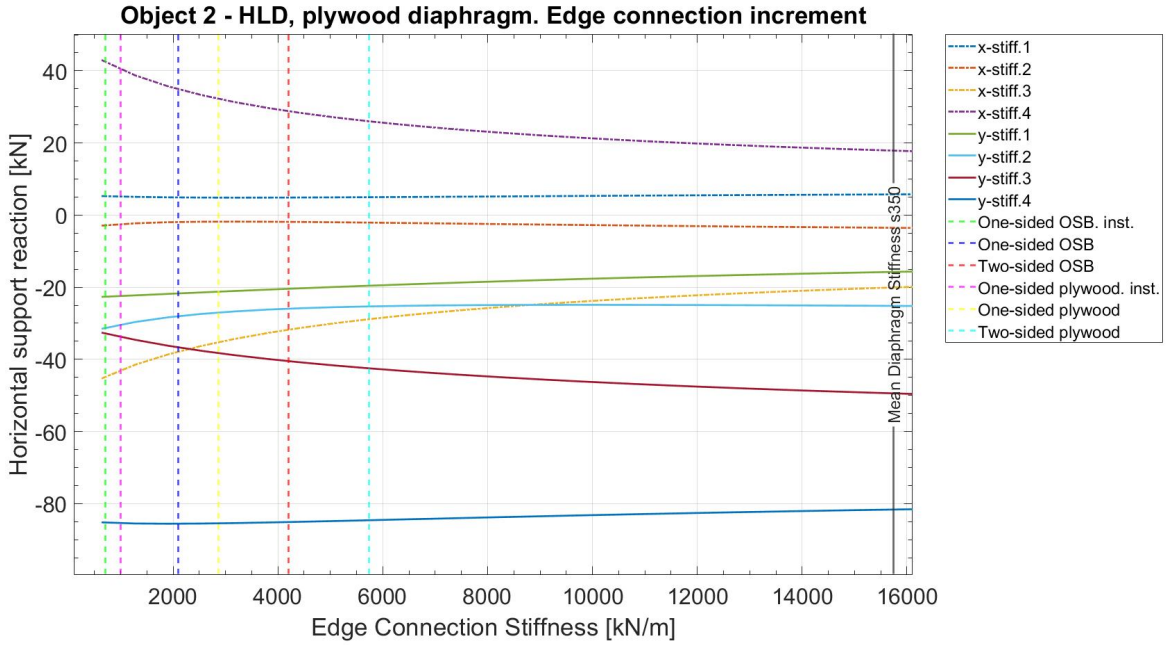

Object 2, horizontal load distribution of plywood panels diaphragm setup with an increment of the edge connection stiffness and a constant line support stiffness of 500kN/m/m. X-axis limited to 16k.

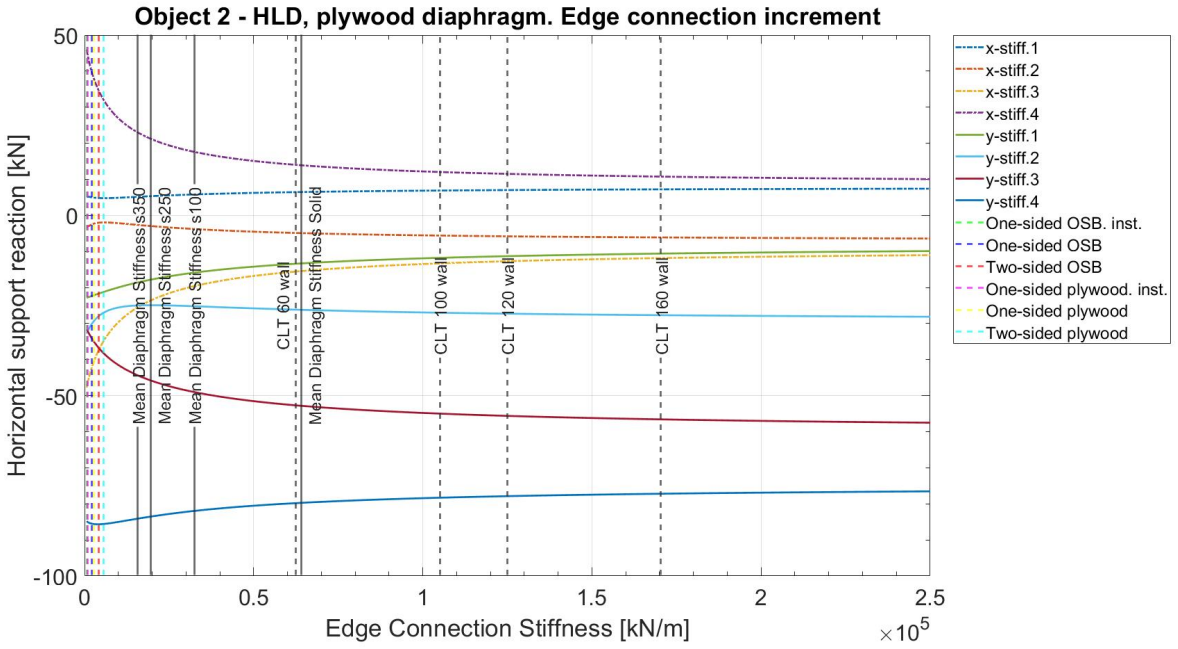

Object 2, horizontal load distribution of plywood panels diaphragm setup with an increment of the edge connection stiffness and a constant line support stiffness of 1000kN/m/m

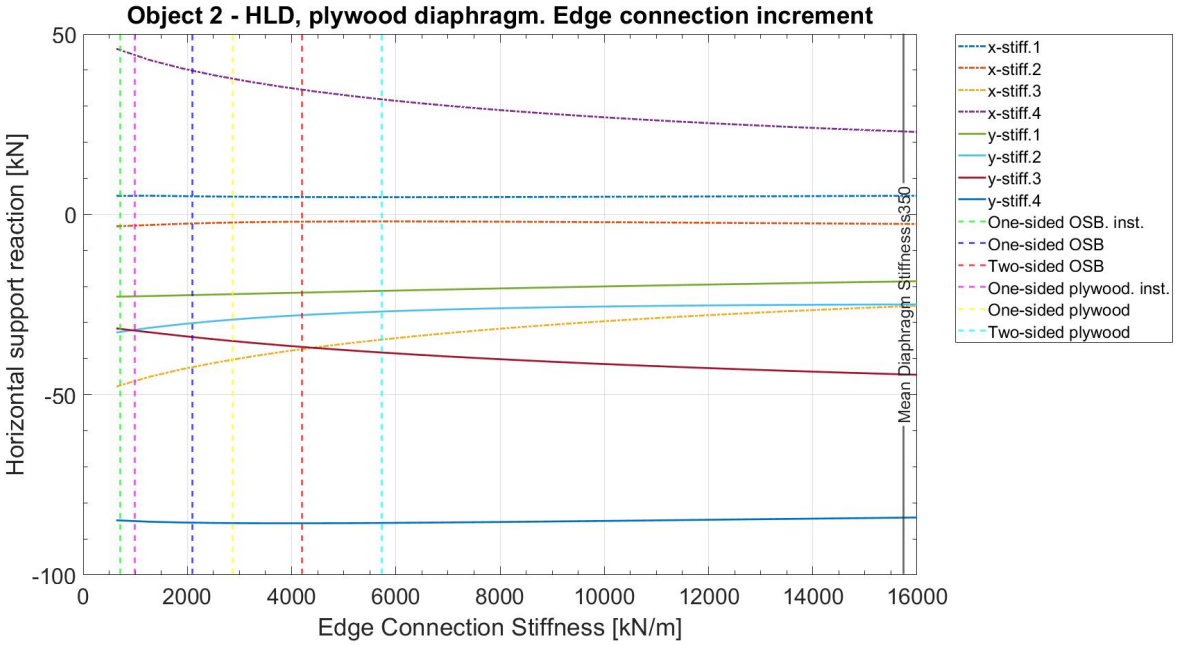

Object 2, horizontal load distribution of plywood panels diaphragm setup with an increment of the edge connection stiffness and a constant line support stiffness of 1000kN/m/m. X-axis limited to 16k.

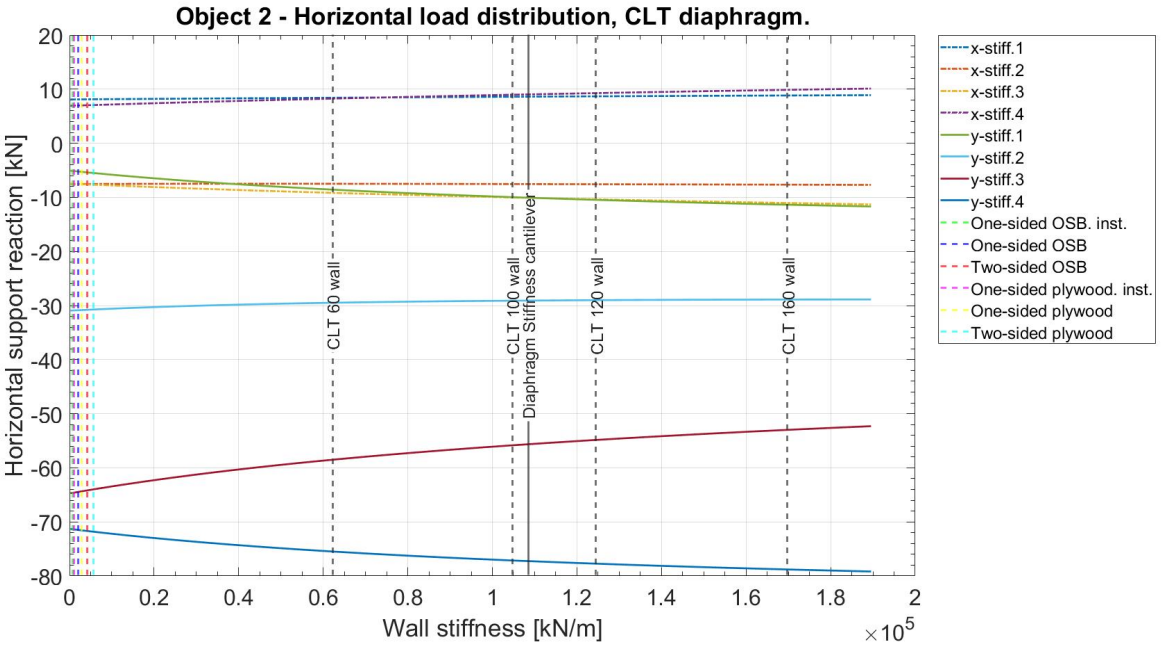

Object 2, horizontal load distribution of CLT panels diaphragm setup with an increment of the line support stiffness and infinitely stiff edge connection.

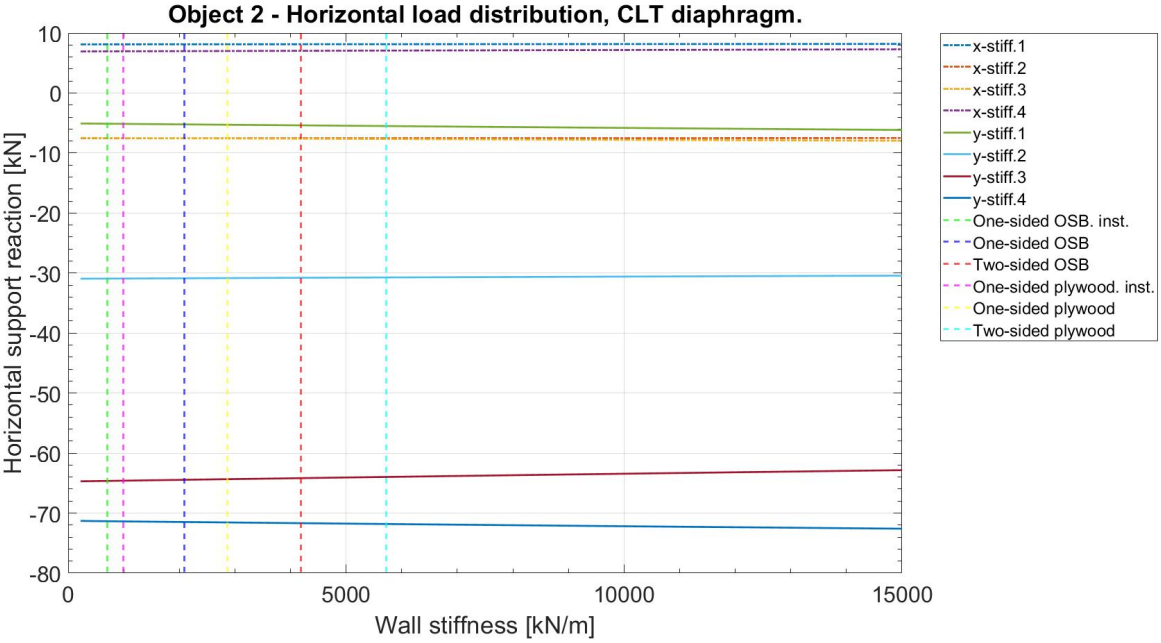

Object 2, horizontal load distribution of CLT panels diaphragm setup with an increment of the line support stiffness and infinitely stiff edge connection. X-axis limited to 15k.

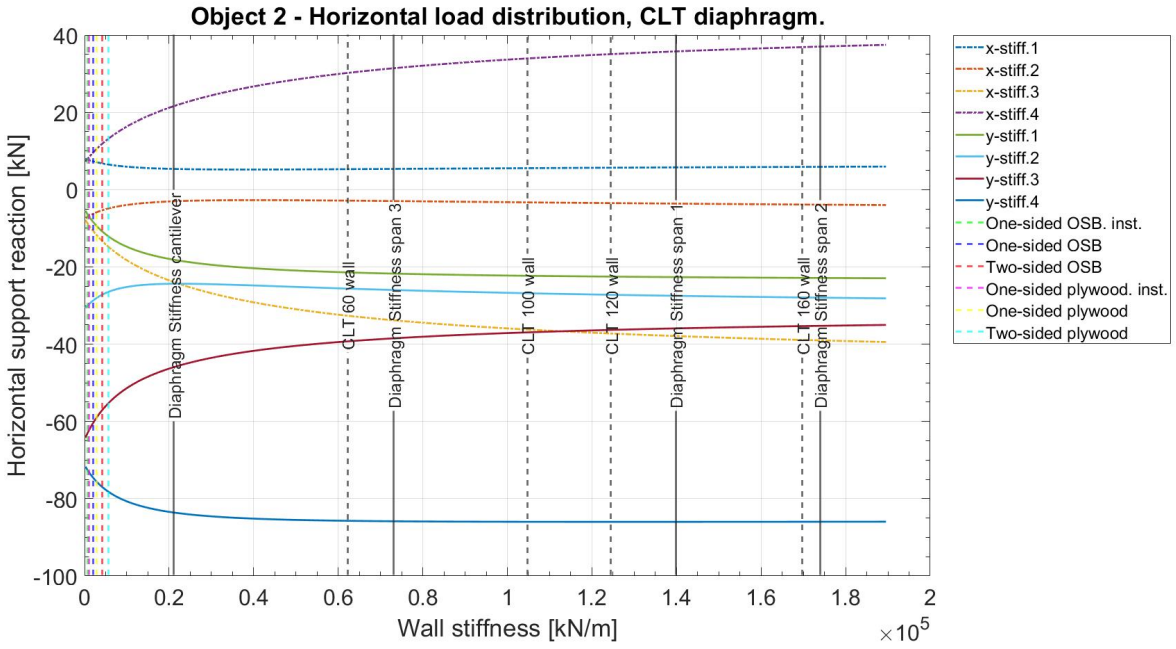

Object 2, horizontal load distribution of CLT panels diaphragm setup with an increment of the line support stiffness and a constant edge connection stiffness of 6968kN/m/m.

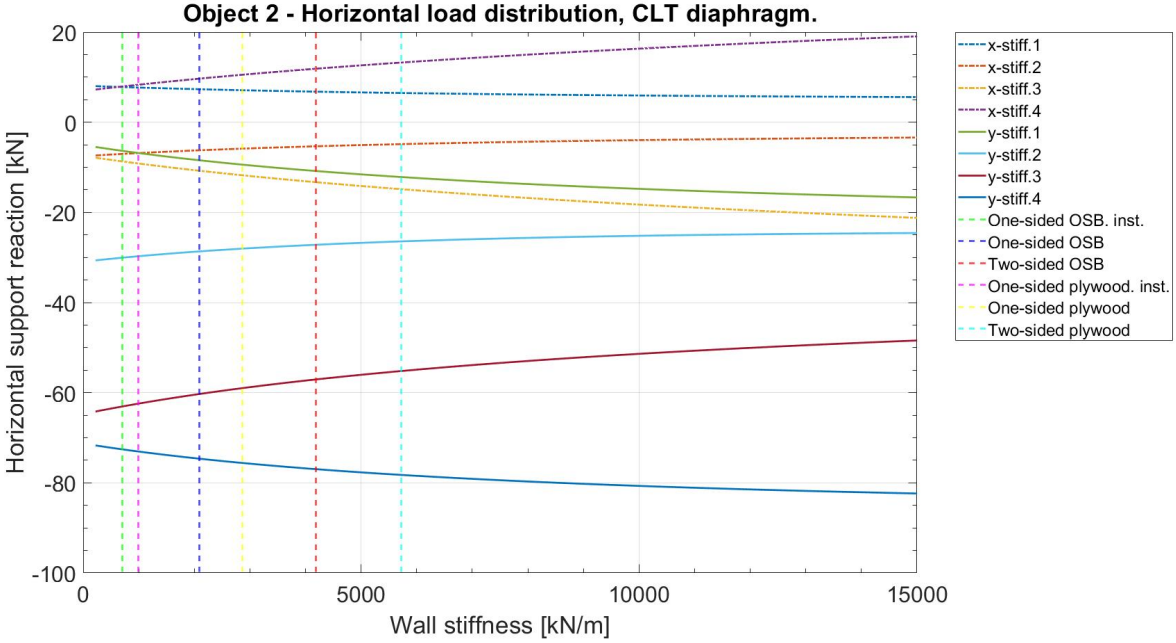

Object 2, horizontal load distribution of CLT panels diaphragm setup with an increment of the line support stiffness and a constant edge connection stiffness of 6968kN/m/m. X-axis limited to 15k.

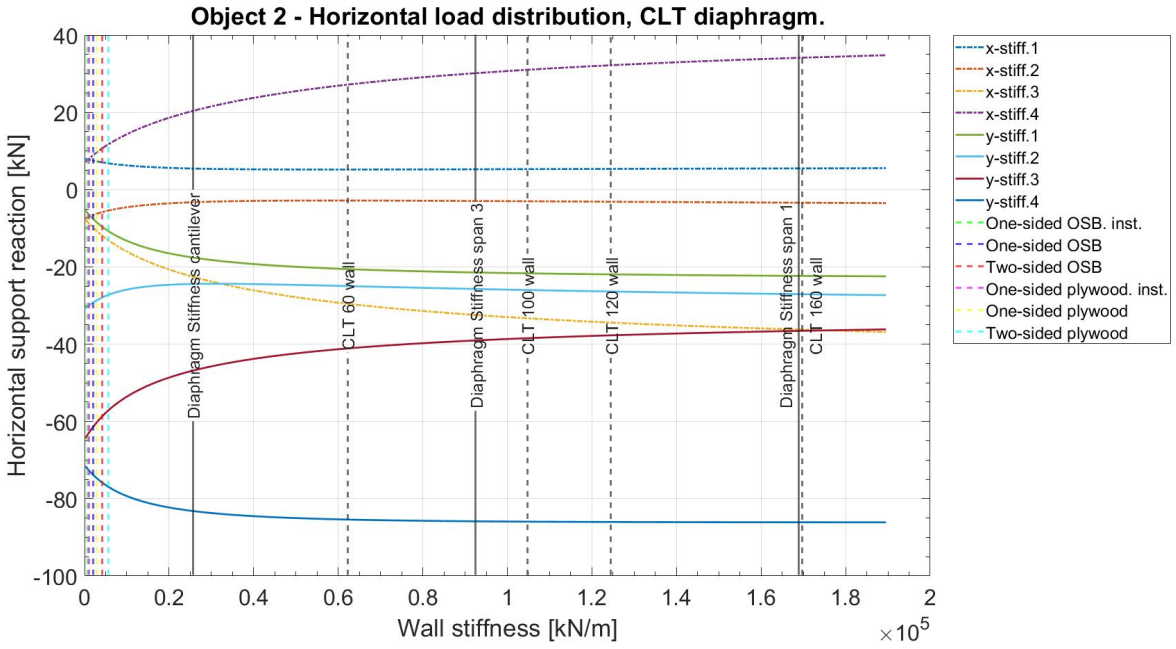

Object 2, horizontal load distribution of CLT panels diaphragm setup with an increment of the line support stiffness and a constant edge connection stiffness of 9755kN/m/m.

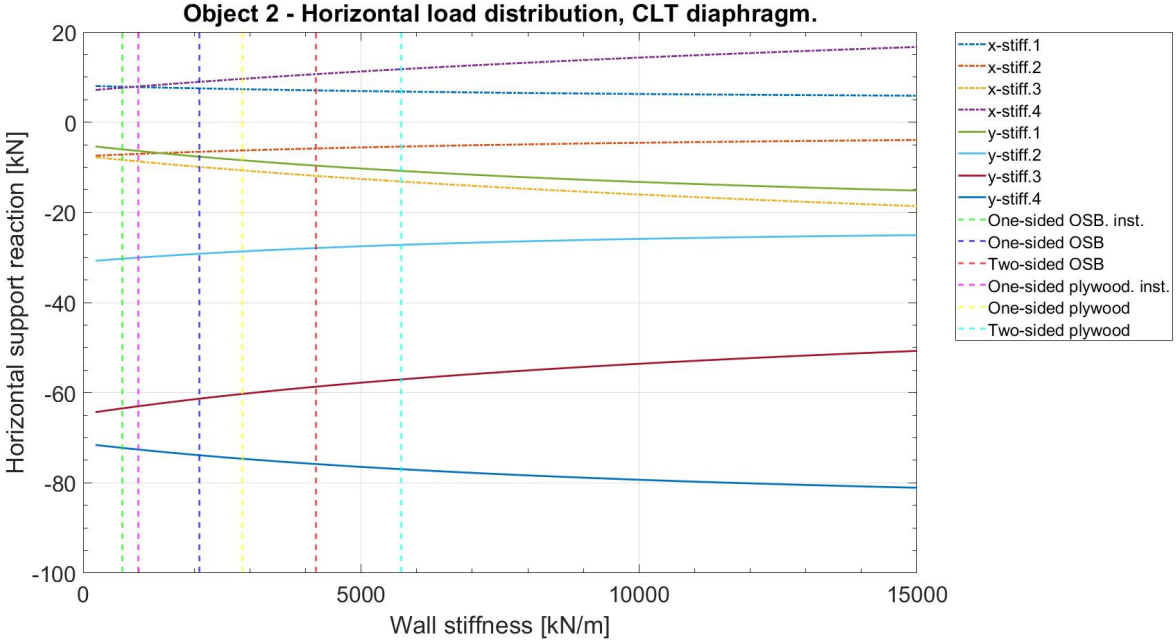

Object 2, horizontal load distribution of CLT panels diaphragm setup with an increment of the line support stiffness and a constant edge connection stiffness of 9755kN/m/m. X-axis limited to 15k.

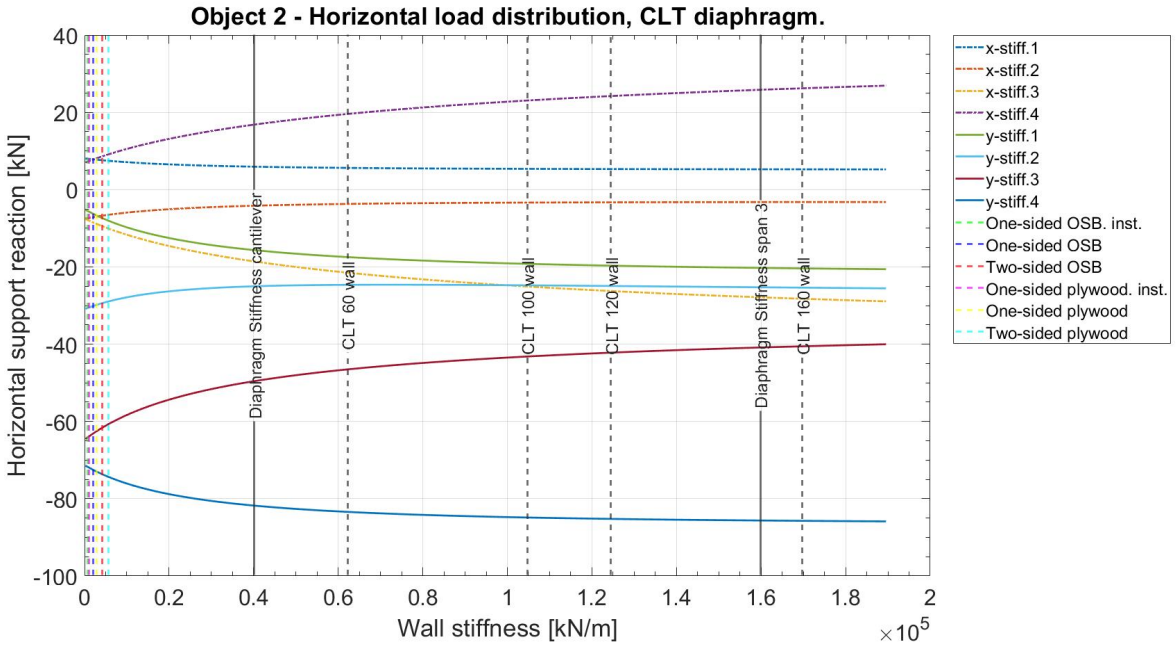

Object 2, horizontal load distribution of CLT panels diaphragm setup with an increment of the line support stiffness and a constant edge connection stiffness of 24390kN/m/m.

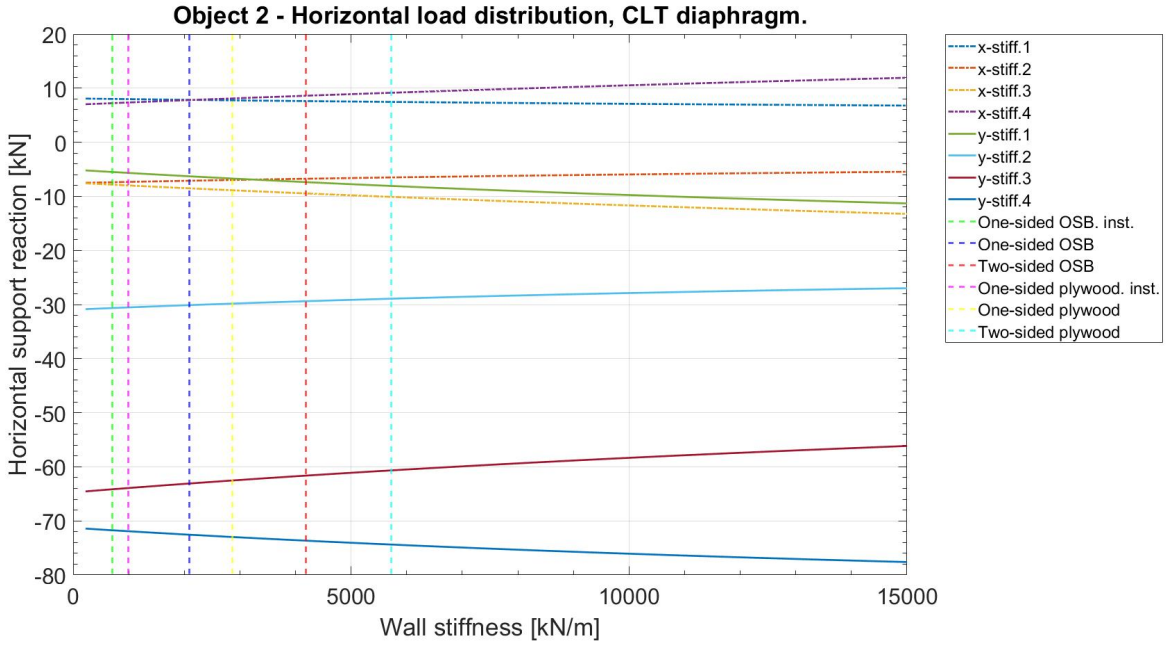

Object 2, horizontal load distribution of CLT panels diaphragm setup with an increment of the line support stiffness and a constant edge connection stiffness of 24390kN/m/m. X-axis limited to 15k.

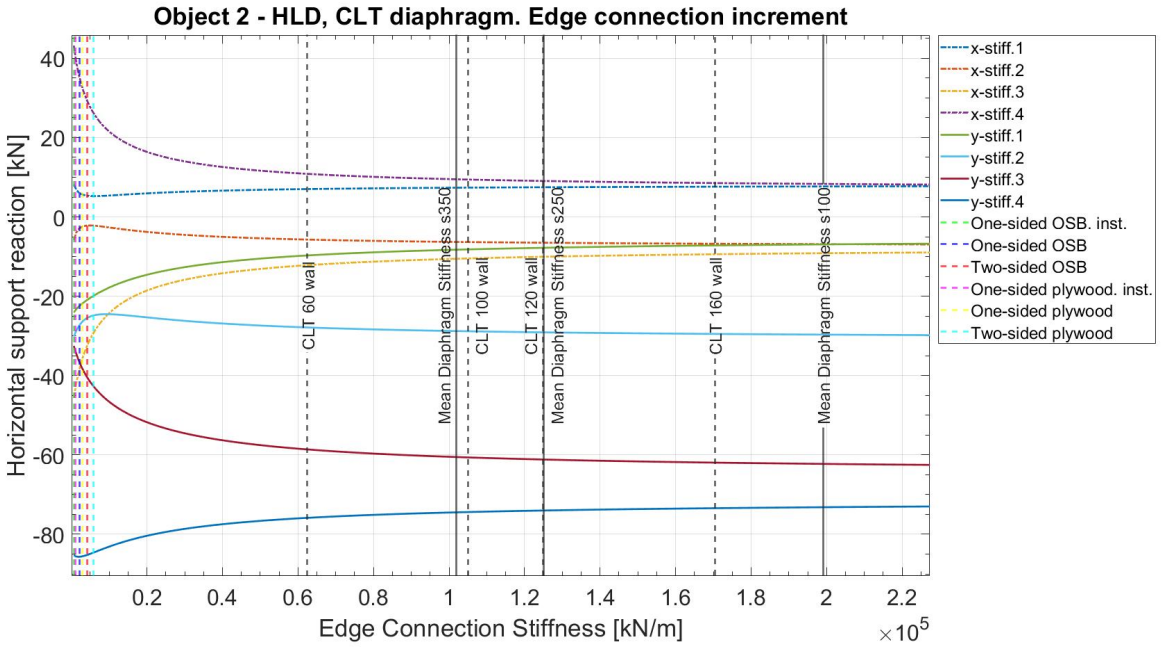

Object 2, horizontal load distribution of CLT panels diaphragm setup with an increment of the edge connection stiffness and a constant line support stiffness of 500kN/m/m

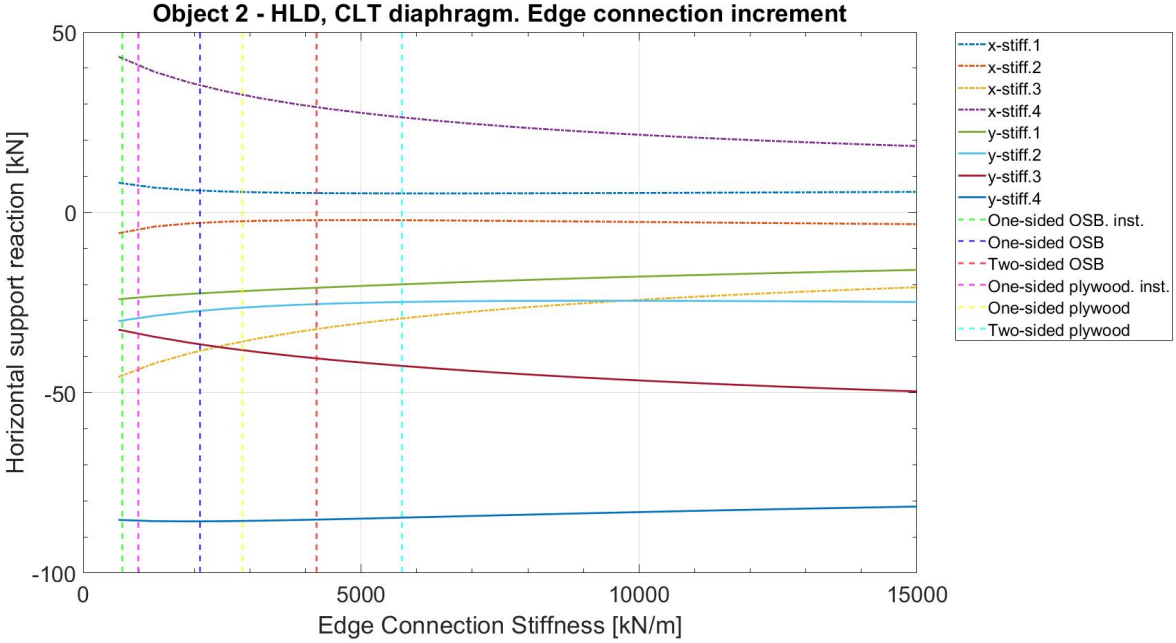

Object 2, horizontal load distribution of CLT panels diaphragm setup with an increment of the edge connection stiffness and a constant line support stiffness of 500kN/m/m. X-axis limited to 15k.

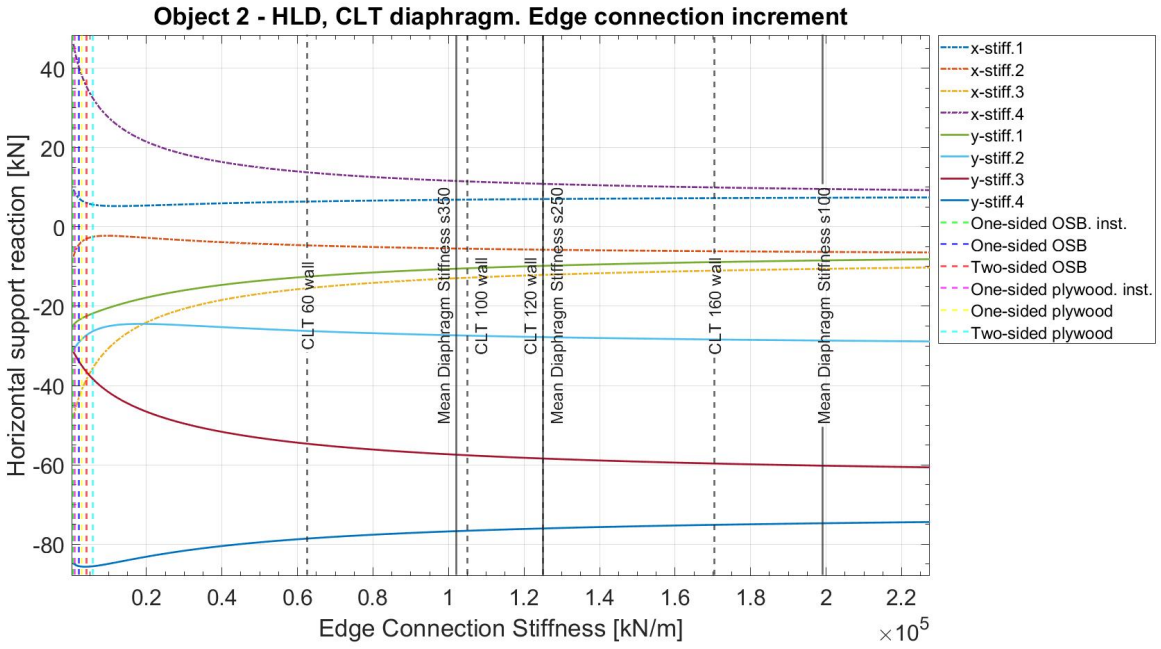

Object 2, horizontal load distribution of CLT panels diaphragm setup with an increment of the edge connection stiffness and a constant line support stiffness of 1000kN/m/m

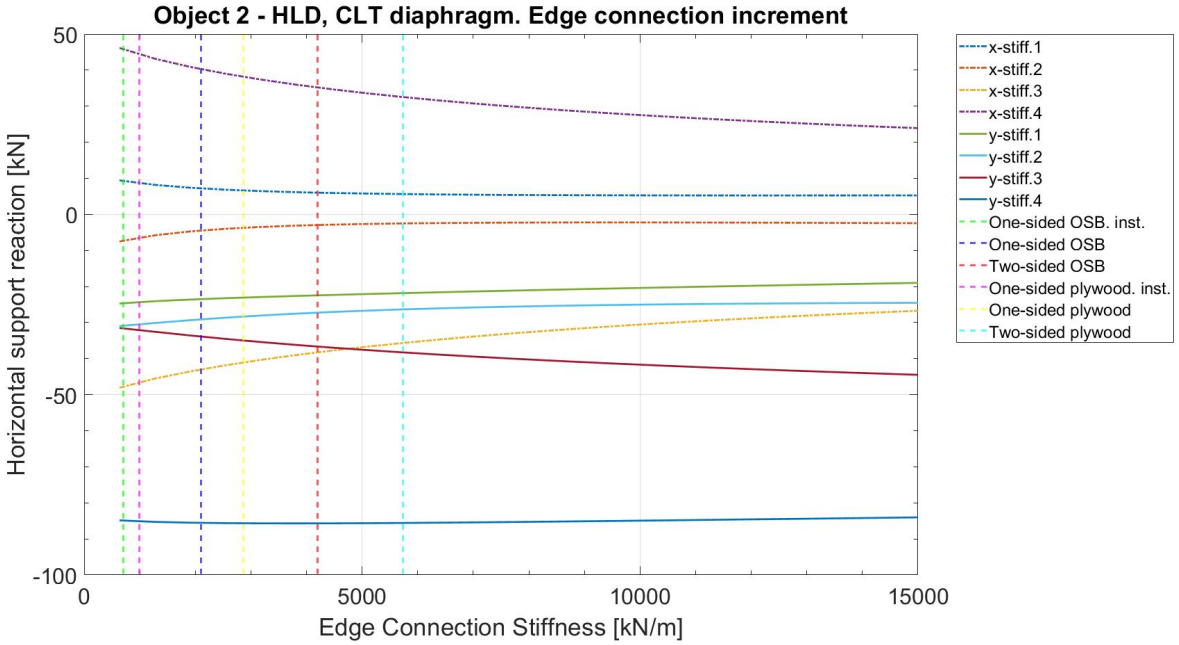

Object 2, horizontal load distribution of plywood panels diaphragm setup with an increment of the edge connection stiffness and a constant line support stiffness of 1000kN/m/m. X-axis limited to 15k.

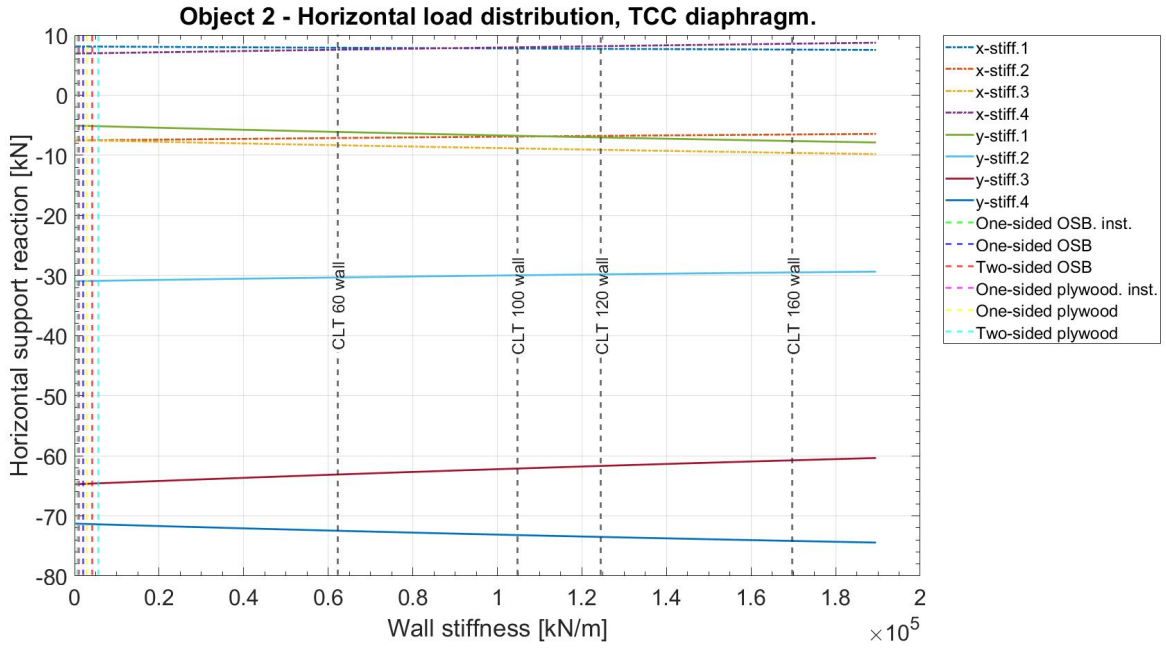

Object 2, horizontal load distribution of TCC panels diaphragm setup with an increment of the line support stiffness and a constant infinitely stiff edge connection.

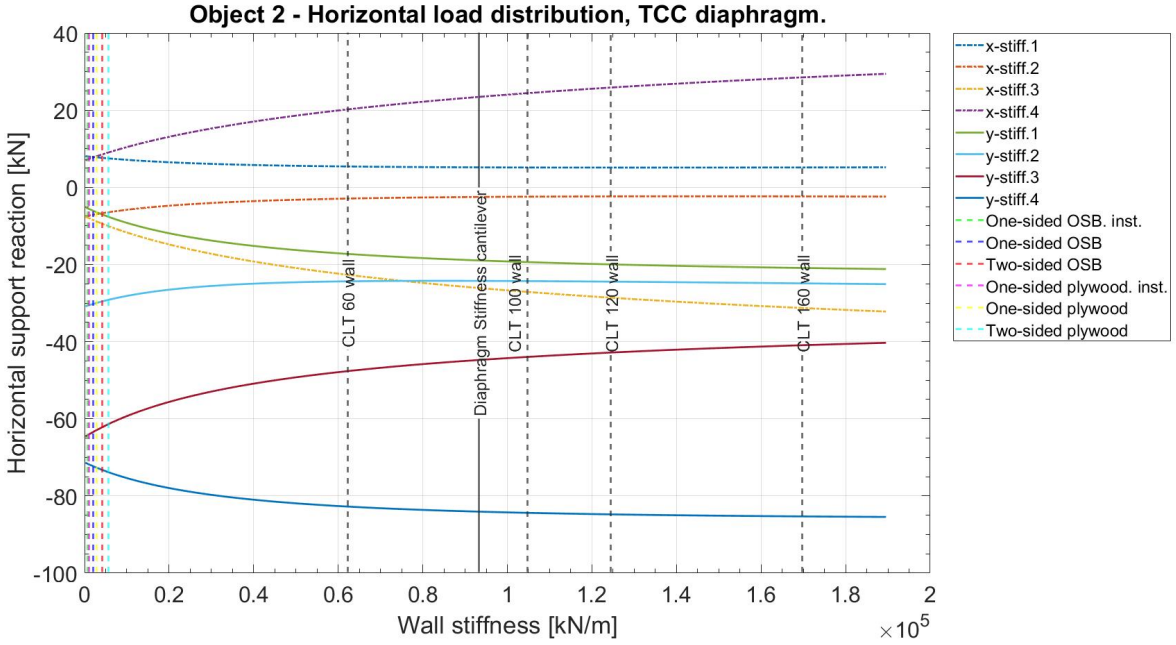

Object 2, horizontal load distribution of TCC panels diaphragm setup with an increment of the line support stiffness and a constant edge connection stiffness of 25600kN/m/m.

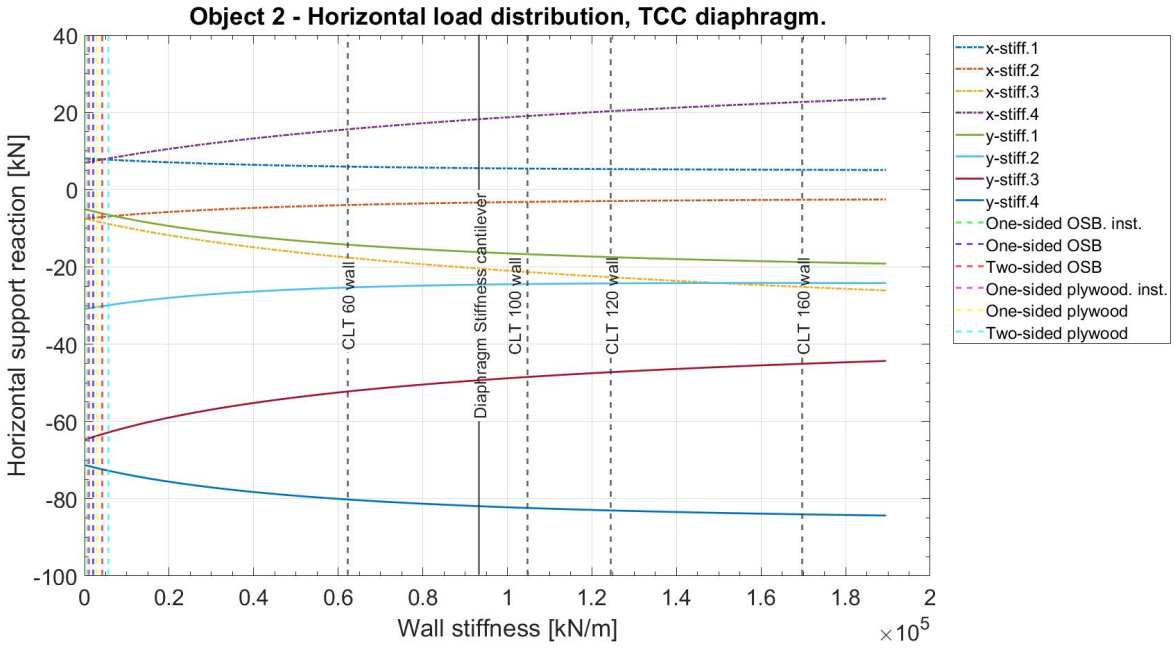

Object 2, horizontal load distribution of TCC panels diaphragm setup with an increment of the line support stiffness and a constant edge connection stiffness of 50000kN/m/m.

F

C# Script

Listing F.1: C# script

```
using System;
using System.IO;
using System.Collections.Generic;
using System.Linq;
using System.Text;
using System.Threading.Tasks;
using System.Xml.Linq;
using FemDesign;
using FemDesign.Calculate;
using FemDesign.Materials;
using FemDesign.Results;
using FemDesign.Shells;
using FemDesign.Supports;
using StruSoft.Interop.StruXml.Data;
using static System.Net.Mime.MediaTypeNames;
using System.Diagnostics.Metrics;
using FemDesign.Releases;
using System.Collections.Generic;
using System.Collections.ObjectModel;
using System.ComponentModel.Design;
using CsvHelper;
using System.Globalization;
using System.Runtime.CompilerServices;
using System.Security.AccessControl;
using FemDesign.Geometry;
using Microsoft.VisualBasic;


namespace FemDesign.Floor1
{
    internal class Program
    {
        static void Main()
        {
            // READ MODEL  . For some unknown reason just typing "model_1.struxml" dosent work.
            string struxmlPath = "C:\\femdesign-api-master\\Parametric.Study\\models\\model_2_tcc.struxml";
            var model = Model.DeserializeFromFilePath(struxmlPath);

            string resultsPath = "C:\\femdesign-api-master\\Test.2\\Results";
            string tempPath = "C:\\femdesign-api-master\\Parametric.Study\\temp";
            string bscPath = "C:\\femdesign-api-master\\Test.2\\batch.bsc";
            List<string> bscPaths = new List<string>();
            bscPaths.Add(bscPath);
            //Create a directory called struxml if it dosent exist. .struxml files from each run will be saved in folder.
            Directory.CreateDirectory("C:\\femdesign-api-master\\Parametric.Study\\Ber\\struxml\\");

            //Identify if any edge connection exist that are to be parametric studied.
            //Edge connections must be named 'elem.conn' to be found by the script.
            var rigidtyList = new List<Motions>();
            var elemLength = new List<double>();

            using (StreamWriter writerScript = new StreamWriter("C:\\femdesign-api-master\\Parametric.Study\\Ber\\Edge_Connections_Length.csv"))
            {
                //NB! FOR TIMBER PANELS!

                foreach (var listPanels in model.Entities.Panels)
                {
                    foreach (var edges in listPanels.InternalPanels.IntPanels[0].Region.Contours[0].Edges)
                    //foreach (var edges in listPanels.Region.Contours[0].Edges)
                    {
                        if (edges.EdgeConnection != null && edges.EdgeConnection.Name.Contains("elem.conn"))
                        {
                            rigidtyList.Add(edges.EdgeConnection.Rigidity.Motions);
                            elemLength.Add(edges.Length);
                            writerScript.WriteLine(edges.Length);
```

```
66                          }
67                      }
68                  }
69
70
71
72                  //NB! CODE FIND CONCRETE SLABS IN MODEL WITH ITS EDGE CONNECTION.
73                  foreach (var slabSections in model.Entities.Slabs)
74                  {
75                      foreach (var edges in slabSections.SlabPart.Region.Contours[0].Edges)
76
77                      {
78                          if (edges.EdgeConnection != null && edges.EdgeConnection.Name.
                                Contains("elem.conn"))
79                          {
80                              rigidtyList.Add(edges.EdgeConnection.Rigidity.Motions);
81                              elemLength.Add(edges.Length);
82                              writerScript.WriteLine(edges.Length);
83                          }
84                      }
85                  }
86
87
88                  //NB! CODE FIND FICTITIOUS SHELLS IN MODEL WITH ITS EDGE CONNECTION.
89                  foreach (var shellSections in model.Entities.AdvancedFem.FictitiousShells)
90                  {
91                      foreach (var edges in shellSections.Region.Contours[0].Edges)
92
93                      {
94                          if (edges.EdgeConnection != null && edges.EdgeConnection.Name.
                                Contains("elem.conn"))
95                          {
96                              rigidtyList.Add(edges.EdgeConnection.Rigidity.Motions);
97                              elemLength.Add(edges.Length);
98                              writerScript.WriteLine(edges.Length);
99                          }
100                     }
101                 }
102
103
104
105             }
106
107             //Number of iteration
108             int itterations = 200;
109
110             //Analysis, state that the load combination is to use. If cases -> see calcCase
111             var analysis = new Analysis(calcComb: true);
112
113             //Units
114             var units = UnitResults.Default();
115             units.Displacement = Results.Displacement.mm;
116             var increment = 1;
117
118             //Increment variable
119             var incri = 0;
120
121             using (var femDesign = new FemDesignConnection(minimized: false))
122
123                 //For loop that initiate the run.
124                 for (int i = 1; i <= itterations; i++)
125                 {
126
127                     if (i <= 50)
128                     {
129                         //Increment of stiffness each run
130                         ////[kN/m/m]
131                         increment = 50;
132                     }
133
134                     else if (i > 50 && i <= 150)
135                     {
136                        //Increment of stiffness each run
137                        //increment = 150; //[kN/m/m]
138                        increment = 150; //[kN/m/m]
139                     }
140                     else if (i > 150 && i <= 175)
141                     {
142                        //Increment of stiffness each run
143                        //increment = 250; //[kN/m/m]
144                        increment = 250; //[kN/m/m]
145                     }
146                     else
147                     {
148                         increment = 750;
149                     }
150
151                     incri = incri + increment;
152
153                 //Finds line supports with the longitudinal stiffness in the x-direction
154                 var lineSupportsIDX_stiff = model.Entities.Supports.LineSupport.Where(x
                        => x.Name.Contains("x-stiff")).ToList();
155                 var lineSupportsIDY_stiff = model.Entities.Supports.LineSupport.Where(x
                        => x.Name.Contains("y-stiff")).ToList();
156
```

```
157
158                     // TO SET THE INITIAL STIFFNESS PROPERTIES OF THE LINE SUPPORTS
159
160                     using (StreamWriter writerScript = new StreamWriter("C:\\femdesign-api-
                            master\\Parametric.Study\\Ber\\stiffness_line_support_x_dir_" + i +
                            ".csv"))
161                     {
162                         foreach (var line_x in lineSupportsIDX_stiff)
163                         {
164                             // Start value of the X-direction stiffness
165
166                             line_x.Motions.XNeg = incri;
167                             line_x.Motions.XPos = incri;
168
169                             //If wanna fix the stiffness values of a line support.
170                             //line_x.Motions.XNeg = 100; //Math.Pow(10, 5);
171                             //line_x.Motions.XPos = 100; //Math.Pow(10, 5);
172
173
174                             Console.WriteLine("Line supports with stiffness in x-direction: "
                                    + line_x.Motions.XPos + "/" + line_x.Motions.XNeg);
175                             writerScript.WriteLine(line_x.Motions.XPos);
176                         }
177                     }
178
179                     using (StreamWriter writerScript = new StreamWriter("C:\\femdesign-api-
                            master\\Parametric.Study\\Ber\\stiffness_line_support_y_dir_" + i +
                            ".csv"))
180                     {
181
182                         foreach (var line_y in lineSupportsIDY_stiff)
183                         {
184                             // Start value of the global Y-direction stiffness NB! Local
                                    coordinate system of the line supports, thus, stiffness in
                                    the x-direction.
185
186                            line_y.Motions.XPos = incri;
187                            line_y.Motions.XNeg = incri;
188
189                             //If wanna fix the stiffness values of a line support.
190                             //line_y.Motions.XNeg = 100; //Math.Pow(10, 5);
191                             //line_y.Motions.XPos = 100;//Math.Pow(10, 5);
192
193                             Console.WriteLine("Line supports with stiffness in y-direction: "
                                    + line_y.Motions.XPos + "/" + line_y.Motions.XNeg);
194                             writerScript.WriteLine(line_y.Motions.XPos);
195                         }
196
197                     }
198
199                     //Change the stiffness of the edge connection between timber panels.
200                     // NB! Edge connections that are to be changed must be named 'elem.conn'
                            in FEM settings to be found by the script.
201                     // Furthermore, xpos -> stiffness parallel the edge connection.
202                     using (StreamWriter writerScript = new StreamWriter("C:\\femdesign-api-
                            master\\Parametric.Study\\Ber\\stiffness_edge_connection_x_dir_" + i
                             + ".csv"))
203                     {
204                         foreach (var motions in rigidtyList)
205                         {
206                             motions.XPos = 50000;  //[kN/m/m]  //incri
207                             motions.XNeg = 50000;  //[kN/m/m]
208                             motions.YPos = 50000; //Math.Pow(10, 7);  //[kN/m/m]
209                             motions.YNeg = 50000; //Math.Pow(10, 7);  //[kN/m/m]
210                             Console.WriteLine("Edge connection stiffness parallel to the
                                    joint: " + motions.XPos + "/" + motions.XNeg);
211                             writerScript.WriteLine(motions.XPos);
212                         }
213                     }
214
215
216                     //Saving struxml for each run
217                     string outPathIndividual = "C:\\femdesign-api-master\\Parametric.Study\\
                            Ber\\struxml\\run_" + i + "_.struxml";
218                     model.SerializeModel(outPathIndividual);
219
220
221                     //Start analysis
222                     femDesign.RunAnalysis(model, analysis);
223
224                     //Get the Line support resultants
225                     var lineSupportReaction = femDesign.GetResults<LineSupportResultant>();
226                     var nodalDisp = femDesign.GetResults<NodalDisplacement>(units);
227
228                      // Print results
229                      Console.WriteLine();
230                      Console.WriteLine("Id          | Reaction  ");
231
232                      foreach (var reaction in lineSupportReaction)
233                      {
234                          if (reaction.CaseIdentifier == "LC2ULS")
235                          {
236                              Console.WriteLine($"{reaction.Id,10} | {reaction.Fx,10}");
237
238                          }
```

```
239                         }
240
241                         using (StreamWriter writerScript = new StreamWriter("C:\\femdesign-api-
                                master\\Parametric.Study\\Ber\\reactions_values_run_" + i + ".csv")
                                )
242                         {
243                             foreach (var reaction in lineSupportReaction)
244                             {
245                                     if (reaction.CaseIdentifier == "LC2ULS")
246                                     {
247                                         writerScript.WriteLine(reaction.Fx);
248                                     }
249                             }
250                         }
251
252                         if (i == 1)
253                         {
254                             using (StreamWriter writerScript = new StreamWriter("C:\\femdesign-
                                    api-master\\Parametric.Study\\Ber\\reactions_id_run.csv"))
255                             {
256                                 foreach (var reaction in lineSupportReaction)
257                                 {
258                                     if (reaction.CaseIdentifier == "LC2ULS")
259                                     {
260                                         writerScript.WriteLine(reaction.Id);
261                                     }
262                                 }
263                             }
264
265                             using (StreamWriter writerScript = new StreamWriter("C:\\femdesign-
                                    api-master\\Parametric.Study\\Ber\\reactions_id_length.csv"))
266
267                             {
268                                 foreach (var reaction in lineSupportReaction)
269                                 {
270                                     if (reaction.CaseIdentifier == "LC2ULS")
271                                     {
272                                         writerScript.WriteLine(reaction.HalfLength * 2);
273
274                                     }
275                                 }
276                             }
277
278                             using (StreamWriter writerScript = new StreamWriter("C:\\femdesign-
                                    api-master\\Parametric.Study\\Ber\\nodal_disp_run_id.csv"))
279                             {
280                                 foreach (var nodal in nodalDisp)
281                                 {
282                                     writerScript.WriteLine(nodal.NodeId);
283                                 }
284                             }
285                         }
286
287                         using (StreamWriter writerScript = new StreamWriter("C:\\femdesign-api-
                                master\\Parametric.Study\\Ber\\nodal_disp_run_Ex" + i + ".csv"))
288                         {
289                             foreach (var nodal in nodalDisp)
290                             {
291                                 writerScript.WriteLine(nodal.Ex);
292                             }
293                         }
294                         using (StreamWriter writerScript = new StreamWriter("C:\\femdesign-api-
                                master\\Parametric.Study\\Ber\\nodal_disp_run_Ey" + i + ".csv"))
295                         {
296                             foreach (var nodal in nodalDisp)
297                             {
298                                 writerScript.WriteLine(nodal.Ey);
299                             }
300                         }
301
302                         Console.WriteLine("End of run: " + i);
303
304                     }
305             }
306         }
307 }
```